UNIVERSIDADE ESTADUAL PAULISTA
"JÚLIO DE MESQUITA FILHO"

Nucleus of Bioassays, Biosynthesis and Ecophysiology of natural products
(NuBBE)

DENISE MEDEIROS SELEGATO

METABOLOMIC STUDIES OF PLANT-ASSOCIATED FUNGI – METHOD DEVELOPMENT FOR THE INCREASED PRODUCTION AND IDENTIFICATION OF MICROBIAL BIOACTIVE SECONDARY METABOLITES

Thesis submitted to the Chemistry Institute São Paulo University - UNESP as a requirement for obtaining the title of Doctor in Philosophy (Chemistry).

Supervisor: Prof. Dr. Ian Castro-Gamboa
Co-supervisor: Dr. Rafael Teixeira Freire

Araraquara, 2019.

UNIVERSIDADE ESTADUAL PAULISTA
"JÚLIO DE MESQUITA FILHO"

Núcleo de Bioensaio, Biossíntese e Ecofisiologia de produtos naturais (NuBBE)

DENISE MEDEIROS SELEGATO

ESTUDOS METABOLÔMICOS DE FUNGOS ASSOCIADOS A PLANTAS – DESENVOLVIMENTO DE MÉTODOS PARA O AUMENTO DA PRODUÇÃO E IDENTIFICAÇÃO DE METABÓLITOS SECUNDÁRIOS BIOATIVOS MICROBIANOS

Tese apresentada ao Instituto de Química, Universidade Estadual Paulista, como parte dos requisitos para obtenção do título de Doutor em Química.

Orientador: Prof. Dr. Ian Castro-Gamboa
Co-orientador: Dr. Rafael Teixeira Freire

Araraquara, 2019.

FICHA CATALOGRÁFICA

Selegato, Denise Medeiros

S464m Metabolomic studies of plant-associated fungi: method development for the increased production and identification of microbial bioactive metabolites / Denise Medeiros Selegato. – Araraquara: [s.n.], 2019

286 p.: il.

Thesis (doctor) – Universidade Estadual Paulista, Instituto de Química

Advisor: Ian Castro-Gamboa

Co-advisor: Rafael Teixeira Freire

1. Metabolomics. 2. Natural products. 3. Coculture technique. 4. Microbiology. 5. Chemometrics. I. Title.

Elaboração: Seção Técnica de Aquisição e Tratamento da Informação
Biblioteca do Instituto de Química, Unesp, câmpus de Araraquara

unesp

UNIVERSIDADE ESTADUAL PAULISTA

Câmpus de Araraquara

CERTIFICADO DE APROVAÇÃO

TÍTULO DA TESE: "Metabolomic studies of plant-associated fungi - method development for the increased production and identification of microbial bioactive secondary metabolites"

AUTORA: DENISE MEDEIROS SELEGATO
ORIENTADOR: IAN CASTRO GAMBOA
COORIENTADOR: RAFAEL TEIXEIRA FREIRE

Aprovada como parte das exigências para obtenção do Título de Doutora em QUÍMICA, pela Comissão Examinadora:

Prof. Dr. IAN CASTRO GAMBOA
Departamento de Química Orgânica / Instituto de Química - UNESP - Araraquara

Prof. Dr. ALBERTO JOSÉ CAVALHEIRO
Departamento de Química Orgânica / Instituto de Química - UNESP - Araraquara

Profª. Drª. LETÍCIA VERAS COSTA LOTUFO
Departamento de Farmacologia / Instituto de Ciências Biomédicas - USP - São Paulo

Dr. LUIZ ALBERTO COLNAGO
Embrapa Instrumentação / Empresa Brasileira de Pesquisa Agropecuária - São Carlos

Prof. Dr. CRISTIANO SOLEO DE FUNARI
Departamento de Bioprocessos e Biotecnologia / Faculdade de Ciências Agronômicas - UNESP - Botucatu

Araraquara, 29 de março de 2019

CURRICULUM VITAE

1. PROFESSIONAL INFORMATION

Address: Nucleus of Bioassays, Biosynthesis, and Ecophysiology of Natural Products (NuBBE), Organic Chemistry Department, Institute of Chemistry, São Paulo State University (UNESP). Rua Professor Francisco Degni, 55 - CEP: 14800-900, Araraquara, SP, Brazil.

E-mail: denisemselegato@gmail.com.

2. EDUCATION

2014-2019 PhD Candidate in Chemistry

Institute of Chemistry, São Paulo State University (UNESP), Araraquara, Brazil

Title: Metabolomic Studies of Plant-associated Fungi – Method Development for the Increased Production and Identification of Microbial Bioactive Secondary Metabolites

Supervisor: Prof. Dr. Ian Castro-Gamboa (Co-supervisor: Dr. Rafael Teixeira Freire)

Scholarship: Fundação de Amparo à Pesquisa do Estado de São Paulo (FAPESP), Process number. 2014/05935-0

2017-2018 Research Internship (Guest PhD Candidate)

Institute of Biology, Leiden University, Leiden, The Netherlands

Title: Metabolomics of endophytic and rhizospheric fungi by Nuclear Magnetic Resonance (NMR) and High-performance thin-layer chromatography (HPTLC)

Supervisor: Prof. Dr. Young Hae Choi

Scholarship: FAPESP, Process number 2017/06466-2

2008-2013 Bachelor in Pharmacy and Biochemistry

School of Pharmaceutical Sciences (FCF), São Paulo State University (UNESP), Araraquara, Brazil

Title: Proposing a new vaccine for bovine brucellosis using a biotechnological approach

Supervisor: Prof. Dra. Rosemeire Cristina Linhari Rodrigues Pietro

Internship: Ourofino Animal Health (Pharmaceutical Industry) - Biotechnology Research and Development Department (R&D) – 1 year (2012-2013).

3. PUBLISHED ARTICLES TO INDEXED JOURNALS

3.1. (PUBLISHED) SELEGATO, DM.; FREIRE, R.T.; TANNÚS, A.; CASTRO-GAMBOA, I. New dereplication methods applied to NMR-based metabolomics of different *Fusarium* species isolated from *Senna spectabilis*'s rhizosphere. *Journal of the Brazilian Chemical Society. Natural Products Special Issue.* **2016**, *27* (8), 1421.

3.2. (PUBLISHED) CARNEVALE, F.C.; PILON, A.C.; SELEGATO, D.M.; GU, H.; FREIRE, R.T.; RAFTERY, D.; LOPES, N.P.; CASTRO-GAMBOA, I. Dereplication of natural products using GC-TOF Mass Spectrometry: improved metabolite identification by spectral deconvolution ratio analysis. *Frontiers in Molecular Biosciences,* **2016**, *3*, 59-72.

3.3. (PUBLISHED) SELEGATO, D.M.; MONTEIRO, A. F.; VIEIRA, N.C.; CARDOSO, P.; PAVANI, V.D.; BOLZANI, V.S.; CASTRO-GAMBOA, I. Update: Biological and Chemical Aspects of *Senna spectabilis. Journal of the Brazilian Chemical Society*, **2017,** *28* (3), 415-426.

3.4. (PUBLISHED) FREIRE, R.T.; BERO, J., BEAUFAY, C., SELEGATO, D.M., CHOI, Y.C., QUENTIN-LECLERCQ, J. Metabolomic analysis of *Keetia* species – targeted identification of antiplasmodial triterpenes. *Metabolomics,* **2019**, *15* (3), 15-27.

3.5. (PUBLISHED) PAVARINI, D.P.; SELEGATO, D.M.; CASTRO-GAMBOA, I.; SACRAMENTO, L.V.; FURLAN, M. Ecological insights to track cytotoxic compounds among *Maytenus ilicifolia* living individuals and clones of *ex situ* collection. *Molecules,* **2019,** *24*, 1160.

3.6. (ACCEPTED) SELEGATO, D.M.; FREIRE, R.T.; PILON, A.C.; BIASSETO, C.R.; OLIVEIRA, H.C.; ABREU, L.M.; ARAÚJO, A.R.; BOLZANI, V.S.; CASTRO-GAMBOA, I. Improvement of Bioactive Metabolite Production in Microbial Cultures - A systems approach by OSMAC and ^{1}HqNMR. *Magnetic Resonance in Chemistry (MRC),* **2019.** doi.org/10.1002/mrc.4874.

3.7. (ACCEPTED) SELEGATO, D.M.; PILON, A.C.; CARNEVALE-NETO, F. Book Chapter: Plant metabolomics using NMR spectroscopy. In: NMR in metabolomics – Methods and Protocols. Springer Protocols, **2019**.

4. SUBMITTED ARTICLES TO INDEXED JOURNALS

4.1. (SUBMITTED) SELEGATO, D.M.; PILON, A.C.; FERNANDES, R.P.; PINHO, D.R.; CARNEVALE-NETO, F.; FREIRE, R.T.; CASTRO-GAMBOA, I.; BOLZANI, V.S.; LOPES, N.P. Metabolômica De Plantas: Um Tutorial. *Química Nova*, **2019 (review)**.

4.2. (SUBMITTED) SELEGATO, D.M., CASTRO-GAMBOA, I., KIM, H.K., CHOI, Y.C. Exploitation of Co-culture for the Enhancement of Microbial Chemical Diversity. *Applied Microbiology and Biotechnology*, **2019 (review).**

5. LONG-TERM COURSES (OVER 100 HOURS)

5.1. Mass Spectrometry – Principles and Applications. 12 credits. Lecturer: Prof. Dr. Humberto Milagre (UNESP/Brazil). **Grade A.**

5.2. Advanced Organic Chemistry. 12 credits. Lecturer: Profa. Dra. Cintia Duarte de Freitas Milagre and Profa. Dra. Angela Regina Araújo (UNESP/Brazil). **Grade A.**

5.3. Qualitative Analysis on Complex Mixtures. 12 credits. Lecturer: Prof. Dr. Alberto Jose Cavalheiro and Prof. Dr. Ian Castro-Gamboa (UNESP/Brazil). **Grade A.**

5.4. Theory and Methodology for the Separation, Isolation and Purification of Organic Compounds. 12 credits. Lecturer: Prof. Dr. Alberto José Cavalheiro (UNESP/Brazil). **Grade A.**

5.5. Spectrometric Methods. 12 credits. Lecturer: Profa. Dra. Lourdes Campaner dos Santos (UNESP/Brazil). **Grade A.**

5.6. Chemometrics I-III. 12 credits. Lecturer: Profa. Dra. Fabíola Manhas Verbi Pereira. **Grade A.**

5.7. Analysis of Organic Compounds by ^{13}C and 2D-Nuclear Magnetic Resonance (NMR). 8 credits. Lecturer: Prof. Hidetake Imasato (São Paulo University – USP/Brazil). **Grade A.**

5.8. NMR of Natural Products. 8 credits. Lecturer: Prof. Dr. Ian Castro-Gamboa (UNESP/Brazil). **Grade A.**

5.9. Special Topic: Basic Aspects in Chemical Ecology: Incorporating Metabolomics and Multiway Analysis. 2 credits. Lecturer: Prof. Dr. Christopher Jeffrey (University of Nevada). **Grade A.**

5.10. Special Topic: Introduction to NMR and Metabolomics. 2 credits. Lecturer: Prof. Dr. Arthur S. Edison (Georgia University). **Grade A.**

5.11. Special Topic: Introduction to Metabolomics and Chemometrics applied to natural product chemistry. 2 credits. Lecturer: Prof. Dr. Emerson F. Queiroz. **Grade A.**

Total: 94 credits.

6. SHORT-TERM COURSES

6.1. (2014) Liquid NMR – Principles and Applications. 40 hours. Lecturer: Prof. Dr. Antonio Gilberto Ferreira. Federal University of São Carlos, UFSCAR, São Carlos, Brazil.

6.2. (2015) 8th International Workshop on Metabolomics. 40 hours. Leiden University, Leiden, Netherlands.

6.3. (2015) Understanding NMR Spectroscopy. 40 hours. Lecturer: Prof. Dr. James Keeler (University of Cambridge), Belo Horizonte, Brazil.

6.4. (2019) Workshop on Sequencing Data Analysis. 16 hours. University of Campinas (UNICAMP), Campinas, Brazil.

7. SCIENTIFIC WORK PRESENTED ON CONFERENCE PROCEEDINGS (POSTER PRESENTATION)

7.1. (2015) SELEGATO, D.M.; VIEIRA, N.C.; FREIRE, R.T., PAVANI, V.D.; CASTRO-GAMBOA, I. Metabolomic Studies of Fungi Isolated from the Rhizosphere of *Senna spectabilis*. First Brazilian Workshop on Bioinformatics/Chemometrics for Metabolomics, 2015, Ribeirão Preto, Brazil.

7.2. (2015) SELEGATO, D.M. CASTRO-GAMBOA, I. Metabolomic Screening of Fungi isolated from *Senna spectabilis* by Design of Experiments (DoE) and Principal Component Analysis (PCA). II Winter School of Chemometrics, 2015, Campinas, Brazil.

7.3. (2015) FREIRE, R.T.; PILON, A.C.; SELEGATO, D.M.; BOLZANI, V.S.; CASTRO-GAMBOA, I.; TANNÚS, A. Development of a Pattern Recognition and Dereplication Software applied to NMR Spectroscopy. 5th Brazilian Conference on Natural Products (BCNP) and XXXI Annual Meeting on Micromolecular Evolution, Systematics and Ecology (RESEM). 2015, Atibaia, Brazil.

7.4. (2015) MURAKAMI, C. NASTRI, J.P.; SELEGATO, D.M.; FRAIGE, K.; LIMA, M.E.L.; BORALLE, N. BOLZANI, V.S.; MORENO, P.R.H.; YOUNG, M.C.M. Principal Component Analysis (PCA) of ^{1}HNMR and antifungal assay of *Hedyosmum brasiliense* male and female extracts from Cerrado and Atlantic Forest. 5th BCNP and XXXI RESEM. 2015, Atibaia, Brazil.

7.5. (2016) FREIRE, R.T.; SELEGATO, D.M.; PILON, A.C.; CASTRO-GAMBOA, I.; TANNÚS, A. Molecular Networking on NMR - Identification of Compounds Classes using ^{1}H, ^{13}C e ^{13}C-HSQC. 32th Joint Meeting of the International Society of Chemical Ecology (ISCE), 2016, Foz do Iguaçu, Brazil.

7.6. (2016) SELEGATO, D.M.; FREIRE, R.T.; CASTRO-GAMBOA, I. NMR quantification in complex mixtures – OSMAC methodology for metabolites evaluation from *Fusarium oxysporum* isolated from *Senna spectabilis*'s rizhosphere. III Congress of the Brazilian Association of Pharmaceutical Sciences (ABCF), 2016, Porto Alegre, Brazil.

7.7. (2017) SELEGATO, D.M.; FREIRE, R.T.; PILON, A.C.; BIASSETO, C.R.; OLIVEIRA, H.C.; ABREU, L.M.; ARAÚJO, A.R.; BOLZANI, V.S.; CASTRO-GAMBOA, I. Microbe Metabolic Monitoring – systematic analysis of secondary metabolites by One Strain Many Compounds (OSMAC) methodology and ^{1}H-qNMR of complex mixtures. XI Brazilian Symposium of Pharmacognosy and XVI Latin America Symposium of Pharmacobotany, 2017, Curitiba, Brazil.

7.8. (2018) SELEGATO, D.M.; FREIRE, R.T.; PILON, A.C.; CASTRO-GAMBOA, I. A systems approach using OSMAC and ^{1}HqNMR - Improvement of Bioactive Metabolite Production in Microbial Cultures. Metabolomics Symposium Hogeschool, Leiden, Netherlands.

7.9. (2018) SELEGATO, D.M.; FREIRE, R.T.; PILON, A.C.; CASTRO-GAMBOA, I. A systems approach using OSMAC and ^{1}HqNMR - Improvement of Bioactive Metabolite Production in Microbial Cultures. European Magnetic Resonance Meeting (EUROMAR), Nantes, France.

7.10. (2018) SELEGATO, D.M.; BLOMBERG, N.; ROL, S.; FREITAS, T.R.; EROL, O.; PIVATTO, M.; DANUELLO, A.; CASTRO-GAMBOA, I., CHOI, Y.H. Chemical Response of *Fusarium oxysporum* to Toxic Plant-metabolites - Evaluation of the Defense Mechanisms of Rhizospheric Fungus against Piperidine Alkaloids by HPTLC-metabolomics. 3rd Latin America Metabolic Profile Symposium (LAMPS), Rio de Janeiro, Brazil.

8. LECTURES IN INTERNATIONAL CONFERENCES (ORAL PRESENTATION)

8.1. (2018) Conference: 3rd Latin America Metabolic Profiling Symposium (LAMPS), Rio de Janeiro, Brazil. Lecture: Enhancement of microbial chemical diversity – Inducing cryptic antimicrobial secondary metabolites by co-culture.

8.2. (2017) Conference: 46th World Chemistry Congress and 49th IUPAC General Assembly, São Paulo, Brazil. Lecture: Integration of ^{1}HNMR-dereplication algorithm and MS/MS Molecular Networking for the identification of secondary metabolites.

8.3. (2016) Conference: 2nd Latin American Metabolic Profiling Symposium (LAMPS), Rosario, Argentina. Lecture: Metabolic profile analysis of different *Fusarium* species – integration of ^{1}HNMR-dereplication algorithm and MS/MS Molecular Networking for the identification of secondary metabolites.

8.4. (2016) Conference: 32th Joint Meeting of the International Society of Chemical Ecology (ISCE), Foz do Iguaçu, Brazil. Lecture: MS/MS Molecular Networking as a Dereplication Strategy applied to *Fusarium* sp extracts isolated from *Senna spectabilis*'s rhizosphere.

8.5. (2015) Conference: 5th Brazilian Conference on Natural Products - BCNP and XXXI Annual Meeting on Micromolecular Evolution, Systematics and Ecology, Atibaia, Brazil. Lecture: A new computational dereplication method applied to NMR-based metabolomic study on different *Fusarium* species isolated from the rhizosphere of *Senna spectabilis*.

9. SCIENTIFIC DAILY SUPERVISION

9.1. Students: Sanne Rol e Niek Blomberg (Hogeschool, Leiden, Netherlands).
Research title: Metabolomic application to monitor biotransformation processes: Piperidine alkaloids bio-effect on *Fusarium*. Supervisor: Prof. Dr. Young Hae Choi.

9.2. Student: Lígia Louro (School of Pharmaceutical Sciences, UNESP, Araraquara, Brazil).
Research title: Study of fungi isolated from *Senna spectabilis*'s fungi aiming the identification of bioactive secondary metabolites. Supervisor: Prof. Dr. Ian Castro-Gamboa.

9.3. Student: Lucas Paulino (School of Pharmaceutical Sciences, UNESP, Araraquara, Brazil).
Research title: Study of fungi isolated from *Senna spectabilis*'s fungi aiming the identification of bioactive secondary metabolites with anticholinesterase activity. Supervisor: Prof. Dr. Ian Castro-Gamboa.

10. TEACHING TRAINING

Organic Chemistry II for the undergraduate in Chemical Engineer (IQ-UNESP).
Supervisor: Prof. Dr. Ian Castro-Gamboa. Lecture: (1) carboxylic acid and derivatives reaction, (2) introduction to amines and (3) arenediazonium salt reactions.

11. PRESENTATION OF MANDATORY SEMINAR

Title: Chemical Ecology – General Aspects and New Strategies To Semiochemical Identification (40 minute-seminar). Presented on 08/04/2016 at 14:30hrs.

12. AWARDS

12.1. (2018) Best Oral Presentation Award. Lecture: Enhancement of microbial chemical diversity: Inducing cryptic antimicrobial secondary metabolites by co-culture. Conference: 3rd Latin America Metabolic Profile Symposium (LAMPS), Rio de Janeiro, Brazil.

12.2. (2017 and 2018) Travel Stipend Scholarship for the Sanibel Conference 2017 (American Society of Mass Spectrometry) and Small Molecule NMR Conference (SMASH), 2018, USA.

12.3. (2015) Best Poster Award. Poster: A new computational dereplication method applied to NMR-based metabolomic study on different *Fusarium* species isolated from the rhizosphere of *Senna spectabilis*. Conference: 5th Brazilian Conference on Natural Products (BCNP) and XXXI Annual Meeting on Micromolecular Evolution, Systematics and Ecology (RESEM), 2015. Atibaia, Brazil.

12.4. (2015) Best Poster Award. Poster: Patent PCT/BR2015/000075 - Development of a Pattern Recognition and Dereplication Software applied to Nuclear Magnetic Resonance Spectroscopy. Conference: 5th Brazilian Conference on Natural Products (BCNP) and XXXI Annual Meeting on Micromolecular Evolution, Systematics and Ecology (RESEM), 2015. Atibaia, Brazil.

I dedicate this thesis to my parents, for their sincere love and their ever-present support in my personal and professional endeavors. You are the reason and motivation for everything I achieve in life.

ACKNOWLEDGEMENTS

I would like to express my appreciation and thanks to (in Portuguese):

Ao professor Dr. Ian Castro-Gamboa, companheiro de caminhada, pelo apoio, compreensão e amizade.

Ao professor Dr. Young Hae Choi, pelo aceite durante o estágio de doutorado sanduíche, toda paciência na orientação e incentivo que tornaram possível a conclusão desta tese.

Ao Dr. Rafael Teixeira Freire, companheiro de vida e co-orientador, pelo apoio incondicional.

Aos meus pais Sérgio e Regina e aos meus irmãos Marcos, Sérgio e Lucas, que não mediram esforços para que eu chegasse até aqui. Não só pela motivação diária, mas pelo amor, dedicação e muita paciência. Vocês são a razão de todas as minhas conquistas.

Aos profissionais e doutores Bianca Ferreira, Nivaldo Boralle, José Carlos Tomaz, Juliana Rodrigues, João Bronzel e Lucinéia Marconcini, que muito mais do que análises, me ensinaram sobre química e dedicaram seu tempo durante a execução desse trabalho.

Agradeço ao grupo *Natural Products Laboratory* (NPL) e os colaboradores da Universidade de Leiden: Luis Salome, Lina Bayona, Yanhui Ge, Martine Huberty, Alisa Hunter, Gerardo Jiménez, Wim Oomen, Melina Videnova, Laura Arnesano, Barbora Pomerancova, Thomas van der Toorn, Sanne Rol, Niek Blomberg, Pieter Jansen, Yangan Chen, Yingjie Zhou, Martijn Jansen pela ajuda, parceria e discussão durante a execução do trabalho.

Agradeço aos Professores Ângela R. Araújo, Maísa Furlan, Vanderlan da Silva Bolzani, Alberto J. Cavelheiro, Dulce Helena S. Silva, Letícia V. C. Lotufo, Ilana L. B. C. Camargo, Cristiano S. Funari, Luiz Alberto Colnago, Isabele R. Nascimento e Norberto P. Lopes por todo o ensinamento transmitido nessa árdua jornada científica. Obrigada pela orientação, conselhos e todas as ideias que me impulsionaram a fazer mais e melhor.

Agradeço aos colaboradores Profa. Dr. Ana Marisa Fusco Almeida, Dr. Haroldo César de Oliveira, Profa. Dra. Ilana L. B. da C. Camargo, Dr. Rafaela Fernandes, Bsc. Gabriela Righetto, Profa. Dra. Maria Claudia M. Young, Cynthia Murakami, Profa. Dra. Letícia

Lotufo, Prof. Dr. Norberto P. Lopes, José Carlos Tomaz e Izabel Cristina Casanova Turatti pelos resultados obtidos e por toda a parceria ao longo dos anos. A contribuição de vocês engrandeceu o trabalho e foi fundamental em todas as etapas da tese.

Agradeço aos amigos do NuBBE, que foram tão importantes na minha vida acadêmica. A amizade de vocês enriqueceram não só meu trabalho científico como também minha conscientização humana, cultural e social.

Aos colaboradores, conselheiros e, acima de tudo, amigos Fernando Medeiros, Isabel Coutinho, Luiz Dutra, Cláudia Seidl, Gabriel Mazzi, Daniel Fonseca, Thais Guaraldo, Daniel Pavarini, Alan Pilon, Mônica Pienegonda, Fausto Carnevale Neto, Paula Bueno e Camila Capel que me incentivaram todos os dias e ofereceram apoio nos momentos mais difíceis. Sou eternamente grata a vocês.

A minha família, em especial meus avós Hilda (*in memoriam*), Dorothy e Octacílio e pelo carinho e incentivo em todos os momentos.

Ao Instituto de Química e programa de pós-graduação em Química pela oportunidade de realização do doutorado.

Às agências de fomento CAPES e FAPESP pelo auxílio financeiro na bolsa de doutorado no Brasil e doutorado sanduíche.

“...the sea's only gifts are harsh blows and, occasionally, the chance to feel strong. Now, I don't know much about the sea, but I do know that that's the way it is here. And I also know how important it is in life not necessarily to be strong but to feel strong, to measure yourself at least once, to find yourself at least once in the most ancient of human conditions, facing blind, deaf stone alone, with nothing to help you but your own hands and your own head...”

— Primo Levi

ABSTRACT

The discovery of new drug leads from natural sources has decreased over the last decades, emerging the use of new and uncommon matrices for the screening of bioactive secondary metabolites. Among those, the plant microbiota and marine microorganisms have demonstrated a great potential to provide new pharmaceutical leads, producing a high diversity of chemical structures encountered in little-explored and extensive microbial population. Conventionally, microbial metabolite screening is performed in monocultures, in the absence of biotic and abiotic interactions. However, the lack of these communications commonly found in nature seriously limit the chemical diversity that can be obtained by one single strain, remaining silenced many other genes encoded for new secondary metabolites. Over the last decade, several methods have been developed aiming to understand the conditions under which biosynthetic cryptic genes are activated. Among those, the post genomic strategies have revealed widespread potential for the enhancement of chemical diversity, modifying different levels of the cellular machinery for a comprehensive regulation of the microbial metabolome. These strategies include co-cultivation, biotransformation and One Strain Many Compounds (OSMAC) and have been successfully used as a fast and inexpensive alternative for the induction of new bioactive compounds. Notwithstanding these strategies for the expansion of the microbial metabolome, in the screening of these complex matrices, the large dynamic range and diversity of metabolites still hamper their identification and biological correlation. These analytical obstacles require increasingly robust techniques and the use of algorithms for a more accurate and multivariate analysis of the chemical data. In this work, we present an integrative strategy for the enhancement of the identification and detection of secondary metabolites in plant-associated microbes. For this, we have applied different post-genomic strategies and computational tools to accurately elucidate known and novel bioactive metabolites in crude extracts. Results showed that post genomic strategies provided a significant increase in the chemical diversity of all selected fungi, in which co-culture resulted in the highest and more diverse metabolic induction. Moreover, the application of Nuclear Magnetic Resonance (NMR) and Mass Spectrometry (MS)-dereplication methodologies, combined with deconvolution-based ^{1}HNMR quantification and MS/MS Molecular Networking, enabled the extraction of a broader chemical data, accurate biological correlation and the identification of several secondary metabolites never reported for the targeted species. Overall, microbes have demonstrated a multitude of biosynthetic pathways. Hence, the activation of cryptic genes led not only to the identification of novel biologically promising leads, but also a better understanding of how the biotic and abiotic interactions can interfere on these fungal metabolomes.

Keywords: fungi, microbial metabolomics, dereplication, development of computational algorithms, post-genetic strategies, co-culture, OSMAC.

RESUMO

A descoberta de novos alvos farmacêuticos derivados de fontes naturais vem diminuindo ao longo das últimas décadas, impulsionando o uso de matrizes naturais novas e incomuns para a busca de metabólitos secundários bioativos. Dentre essas, a microbiota de plantas e os microrganismos marinhos demonstraram um grande potencial para fornecer novos metabólitos biologicamente ativos, produzindo uma alta diversidade de estruturas químicas encontradas em populações microbianas extensas e pouco exploradas. Convencionalmente, a triagem de metabólitos microbianos é realizada em monoculturas, na ausência de interações bióticas e abióticas. No entanto, a falta dessas interações encontradas na natureza limita a diversidade química que pode ser obtida por uma única cepa, permanecendo silenciadas diversos outros genes que codificam novos metabólitos secundários. Durante a última década, vários métodos têm sido desenvolvidos para compreender as condições sob as quais os genes cripticos são ativados. Dentre elas, as estratégias pós-genômicas revelaram um amplo potencial para o aumento da diversidade química, modificando diferentes níveis da maquinaria celular para uma regulação holística do metaboloma microbiano. Estas estratégias incluem co-cultivo, alimentação por metabólitos e *One Strain Many Compounds* (OSMAC) e têm sido utilizados com sucesso como uma alternativa rápida e barata para a indução de novos metabólitos. Apesar da eficácia das estratégias pós-genômicas na expansão do metaboloma microbiano, durante a avaliação dessas matrizes complexas, a grande dinâmica e diversidade química ainda dificulta sua identificação e correlação biológica dos metabólitos secundários. Como consequência, esses obstáculos analíticos exigem o uso de técnicas cada vez mais robustas e aplicação de algoritmos para uma análise mais precisa e multivariada dos dados. O presente trabalho descreve a integração de estratégias biológicas e analíticas para a aumento da identificação e detecção de metabólitos secundários produzidos por fungus associados à plantas. Para tanto, diferentes estratégias pós-genômicas e ferramentas computacionais foram incorporadas para identificar metabólitos conhecidos e inéditos diretamente em extratos brutos. Os resultados mostraram que as estratégias pós-genômicas proporcionaram um aumento significativo na diversidade química de todos os fungos selecionados, em que a co-cultura resultou na maior e mais ampla indução metabólica. Adicionalmente, a aplicação das metodologias de desreplicação por ressonância magnética nuclear (RMN) e espectrometria de massas (MS), alinhado ao uso de ferramentas de deconvolução e análise de redes de interações moleculares, permitiram a extração de dados químicos confiáveis e a identificação de diversos metabólitos secundários nunca relatados para as espécies estudadas. De maneira geral, os micro-organismos demonstraram possuir uma infinidade de caminhos biossintéticos. Sendo assim, a ativação dos genes cripticos levaram não apenas à identificação de moléculas promissoras, mas também a um melhor entendimento das interações bióticas e abióticas dessas espécies de fungos e do ambiente que habitam.

Palavras-chave: micro-organismos, metabolômica, desreplicação, desenvolvimento de algoritmos computacionais, estratégias pós-genéticas, co-cultura, OSMAC.

SUMÁRIO

RESUMO EXPANDIDO

Plantas e micro-organismos possuem papel fundamental na descoberta de novas substâncias bioativas (NEWMAN; CRAGG, 2016). Em sua mais recente revisão, Newman e Cragg (2016) mostraram que mais de 50% dos fármacos comercializados atualmente possuem origem natural (NP), encontrados na sua forma pura ou como base para produção de compostos derivados, análogos ou semissintetizados, demonstrando o vasto potencial que essas matrizes naturais têm na produção de moléculas com potencialidades terapêuticas (NEWMAN; CRAGG, 2016).

Apesar de expressivo, ao longo das últimas décadas, a descoberta de novos metabólitos bioativos naturais tem caído consideravelmente. Os principais fatores deste declínio são o constante re-isolamento dos principais quimiotipos, os desafios da abordagens uni-variadas, a introdução da química combinatória e as dificuldades no desenvolvimento de métodos que permitam a triagem rápida de matrizes complexas, limitando a interpretação e bioprospecção desses dados (MUSHTAQ et al., 2014).

Dentro desta perspectiva, a química de produtos naturais tem buscado o desenvolvimento de novas estratégias para a obtenção de uma visão mais holística do sistema biológico. Nos últimos anos, essas estratégias tem sido fundamentais para a bioprospecção das fontes naturais e incorporam quatro principais abordagens: **(i)** biologia de sistemas, que estuda patologias e mecanismos terapêuticos de maneira integrada e multivariável; a **(ii)** quimiometria, que permite a análise e interpretação da variação química em processos multifatoriais; a **(iii)** metabolômica, que avalia perfis químicos buscando intepretações e correlações relevantes na variação dinâmica do sistema; e a **(iv)** desreplicação, que integra e compara dados químicos de moléculas conhecidas, simplificando o processo analítico de elucidação estrutural (FUNARI et al., 2013; KELL, 2004; NICHOLSON; LINDON, 2008; WORLEY; POWERS, 2013).

Especificamente, a metabolômica pode ser entendida como o estudo quantitativo e qualitativo de toda a resposta metabólica de um organismo sujeito à diferentes rotinas de vida, estímulos ambientais ou modulações genéticas (NICHOLSON; LINDON, 2008; OLIVER et al., 1998; WAGNER; SEFKOW; KOPKA, 2003) e têm sido utilizada na química de produtos naturais (PN) para a caracterização de amostras ou substâncias (COUTINHO et al., 2016; GUIZELLINI et al., 2018), controle de qualidade (FRAIGE et al., 2015), melhoramento de plantações (PRADO et al., 2018), desenvolvimento de

medicamentos (CARDOSO et al., 2017), ecologia-química (PILATTI et al., 2017), distribuição e evolução taxonômica (DOS SANTOS et al., 2017) e no entendimento de funções bioquímicas (SCHAKER et al., 2017). Ainda que considerado a muitos anos como uma ciência viável, a aplicação da abordagem metabolômica em PN aconteceu apenas recentemente devido à combinação de fatores tecnológicos, dentre os quais podemos destacar: os avanços na miniaturização e análises em *high-throughput* tanto em separação quanto detecção, o desenvolvimento computacional (processadores e memórias capazes de alocar e calcular grandes volumes de dados) e a adequação de métodos estatísticos e de reconhecimento de padrões, incialmente desenvolvidos para o campo da economia e, posteriormente adaptados para a aquisição, análise e tratamento de conjuntos de dados em sistemas biológicos (HONG et al., 2016; JORGE et al., 2016).

Para o melhor entendimento da metabolômica dentro da química de produtos naturais, uma revisão extensa foi escrita pela doutoranda e está em processo de submissão. O propósito deste trabalho foi incentivar e auxiliar a pesquisa em metabolômica de plantas no Brasil e em outras comunidades científicas. Para tanto, delineamos sistematicamente um tutorial incluindo todas as etapas que envolvem a aplicação de um estudo metabolômico em plantas, destacando os benefícios e ao mesmo tempo apontando os principais desafios relativos a escolha no processo de planejamento, coleta, aquisição, análise e tratamento de dados.

Complementarmente às abordagens holísticas desenvolvidas para análise dos perfis químicos, estudos recentes têm focado a busca de compostos bioativos em fontes exóticas, como a rizosfera e seus micro-organismos associados, micro-organismos endofíticos e organismos marinhos, visando a bioprospecção de rotas biosintéticas pouco exploradas. Atualmente, mesmo com os obstáculos relacionados à genes silenciados e cepas incultiváveis, metabólitos derivados de micro-organismos são considerados o futuro dos programas de bioprospecção, produzindo uma alta diversidade estrutural e biológica (BERTRAND et al., 2014a; NEWMAN; CRAGG, 2016). Ademais, sequenciamento do genoma de fungos e bactérias vêm mostrando que o potencial de matrizes microbianas para produzir compostos bioativos é consideravelmente subestimado, o que significa que uma gama muito mais ampla de metabólitos poderia ser produzida se os genes silenciosos fossem induzidos por quaisquer métodos (BERTRAND et al., 2013a; CHIANG et al., 2008; GALAGAN et al., 2005; MOODY, 2014; SCHROECKH et al., 2009).

Convencionalmente, a triagem de metabólitos de micro-organismos é realizada em monoculturas, na ausência de interações biótica e abiótica comumente encontradas na natureza. Entretanto, a falta de interações limita a diversidade química que pode ser obtida por uma única cepa e resulta no constante re-isolamento de metabólitos secundários já conhecidos e na diminuição do isolamento de novos compostos (MARMANN et al., 2014; PETTIT, 2009). Durante a última década, vários métodos foram desenvolvidos com o objetivo de entender e otimizar as condições sob as quais os genes crípticos que codificam rotas biosintéticas são ativados, visando maximizar a diversidade química obtida a partir de espécies microbianas (SCHROECKH et al., 2009; WAKEFIELD et al., 2017).

Dentre as abordagens para expansão do metaboloma microbiano, os métodos genéticos, como a engenharia metabólica, epigenética e mutasíntese, são os mais utilizados para ativação de genes em estudos de monocultura. No entanto, seus protocolos normalmente requerem instrumentações de alto custo para a otimização da produção de metabólitos com potencial biológico, além de um conhecimento prévio do genoma microbiano (AGHCHEH; KUBICEK, 2015; BERGMANN et al., 2007).

Mais recentemente, o aumento da resistência de micro-organismos patogênicos impulsionou a busca de métodos rápidos e baratos para a indução de compostos ativos em matrizes microbianas. Nesse sentido, estratégias pós-genômicas (do inglês *post-genomic strategies*) surgiram como uma alternativa para o aprimoramento da diversidade química, regulando de maneira abrangente os metabólitos secundários (BERTRAND et al., 2014a; HERTWECK, 2009; WAKEFIELD et al., 2017). Esses métodos incluem *One Strain, Many Compounds* (OSMAC) (BODE et al., 2002; WEI et al., 2010), co-cultura (MARMANN et al., 2014; PETTIT, 2009), biotransformação (HEGAZY et al., 2015; VENISETTY; CIDDI, 2003) e alimentação metabólica (AHMAD et al., 2014; BAYDOUN et al., 2013; HEGAZY et al., 2015) e modificam diferentes níveis da maquinaria celular para a modulação da biossíntese de fungos e bactérias.

Em monoculturas, OSMAC e alimentação de metabólicos no meio são duas das estratégias pós-genômicas mais usadas para a ativação de rotas biosintéticas e envolvem a variação de parâmetros de crescimento microbiano, como a introdução de metabólitos exógenos (*metabolic feeding*) (AHMAD et al., 2014; BAYDOUN et al., 2013; HEGAZY et al., 2015) ou composição do meio de cultura (temperatura, agitação e luminosidade) (BODE et al., 2002; WEI et al., 2010), na tentativa de estimular, em quantidade e diversidade, a produção de metabólitos a partir de uma única fonte microbiana. Em geral,

OSMAC usa o design de experimentos (DoE) para avaliar sistematicamente o efeito das diferentes variáveis, otimizando as condições para a melhor produção dos metabólitos alvo (BRACARENSE; TAKAHASHI, 2014; OOIJKAAS et al., 1999; PIMENTA et al., 2010).

Já a co-cultura envolve o cultivo de dois ou mais microrganismos no mesmo ambiente e é considerada uma das maneiras mais eficientes de induzir rotas biosintéticas crípticas. Na fermentação mista, os microrganismos metabolizam o substrato do meio de cultura juntos, imitando o ambiente microbiano competitivo da natureza para a produção e regulação de metabólitos secundários (RATEB et al., 2013; WAKEFIELD et al., 2017). Em experimentos de co-cultura, a comunicação microbiana ocorre através de compostos voláteis ou por sinalização física e leva à secreção de metabólitos secundários como um resultado direto da ativação de genes biosintéticos silenciados, embora seu mecanismo de indução, no contexto genético, biológico e ecológico, permaneça amplamente desconhecido (PETTIT, 2011a; RATEB et al., 2013; SCHROECKH et al., 2009). Em termos práticos, a co-cultura não requer nenhum conhecimento prévio do mecanismo de sinalização, nem qualquer instrumentação especial para o cultivo e interpretação de dados (MOODY, 2014), diminuindo consideravelmente o custo do experimento. No Capítulo 04 desta tese, discutimos em detalhes todo o fluxo experimental de co-cultura, avaliando como os parâmetros bióticos podem ser otimizados para aumentar a diversidade química. Particularmente, nós interpretamos todas as principais publicações de fermentação mista de 1978 a 2019, mostrando os diferentes tipos de induções metabólicas, comunicação microbiana e como essas interações alteram o resultado biológico na análise metabólica direcionada e não direcionada.

O presente trabalho visa o desenvolvimento de métodos para o aumento da produção e detecção de metabólitos secundários microbianos. Para tanto, diferentes estratégias pós-genômicas foram integradas com ferramentas computacionais visando aumentar a diversidade do metaboloma, a interpretação química e a correlação biológica desses dados. Através da metabolômica, esta tese visa a aplicação de métodos para superação dos principais desafios analíticos e microbiológicos na identificação de metabólitos microbianos diretamente em matrizes complexas, garantindo uma exploração racional e abrangente dos perfis químicos de fungos associados a plantas.

Este trabalho está dividido em seis capítulos para melhor compreensão do conteúdo (Fluxograma 1). Os três primeiros detalham o desenvolvimento e aplicação de ferramentas computacionais em desreplicação para superação dos desafios analíticos da

metabolômica microbiana, enquanto os três últimos descrevem o uso de métodos pós-genômicos para o aumento da diversidade química destes fungos.

Para superação dos desafios analíticos, o primeiro capítulo descreve o desenvolvimento de um algoritmo de desreplicação baseado em Ressonância Magnética Nuclear (RMN) de hidrogênio para facilitar a identificação dos metabólitos majoritários em matrizes fúngicas. Já o segundo capítulo traz a análise exploratória dessas mesma matrizes por espectrometria de massas, realizadas para confirmar os metabólitos previamente identificados por RMN, bem como identificar diversas outras classes metabólicas destas fontes orgânica. Por fim, no terceiro capítulo, os extratos das espécies selecionadas são submetidos à microfracionamento, ensaios biológicos e análise pela rede de interações moleculares permitindo a avaliação da distribuição metabólica dessas amostras e a elucidação de metabólitos com potencial terapêutico promissor.

Já para a ativação dos genes silenciados e expansão do metaboloma, os três últimos capítulos mostram a integração de estratégias pós-genômicas com ferramentas aplicadas à metabolômica para maximizar a produção, identificação e detecção de metabólitos, bem como gerar uma abordagem racional para o estudo da coexistência química entre microrganismos e seu meio ambiente. No capítulo 04, iniciamos o estudo das estratégias pós-genômicas com uma revisão em co-cultura. Em seguida, no capítulo 05, nós apresentamos uma estratégia em co-cultura para a seleção e avaliação de cultivos mistos com potencial antimicrobiano. Por fim, o capítulo 06 descreve uma estratégia integrativa entre OSMAC e um método de deconvolução e quantificação por ^{1}HNMR para otimização e monitoramento de compostos bioativos em fungos endofíticos e rizosféricos.

Fluxograma 1. Descrição dos capítulos deste trabalho, divididos em seis tópicos para melhor compreensão do conteúdo.

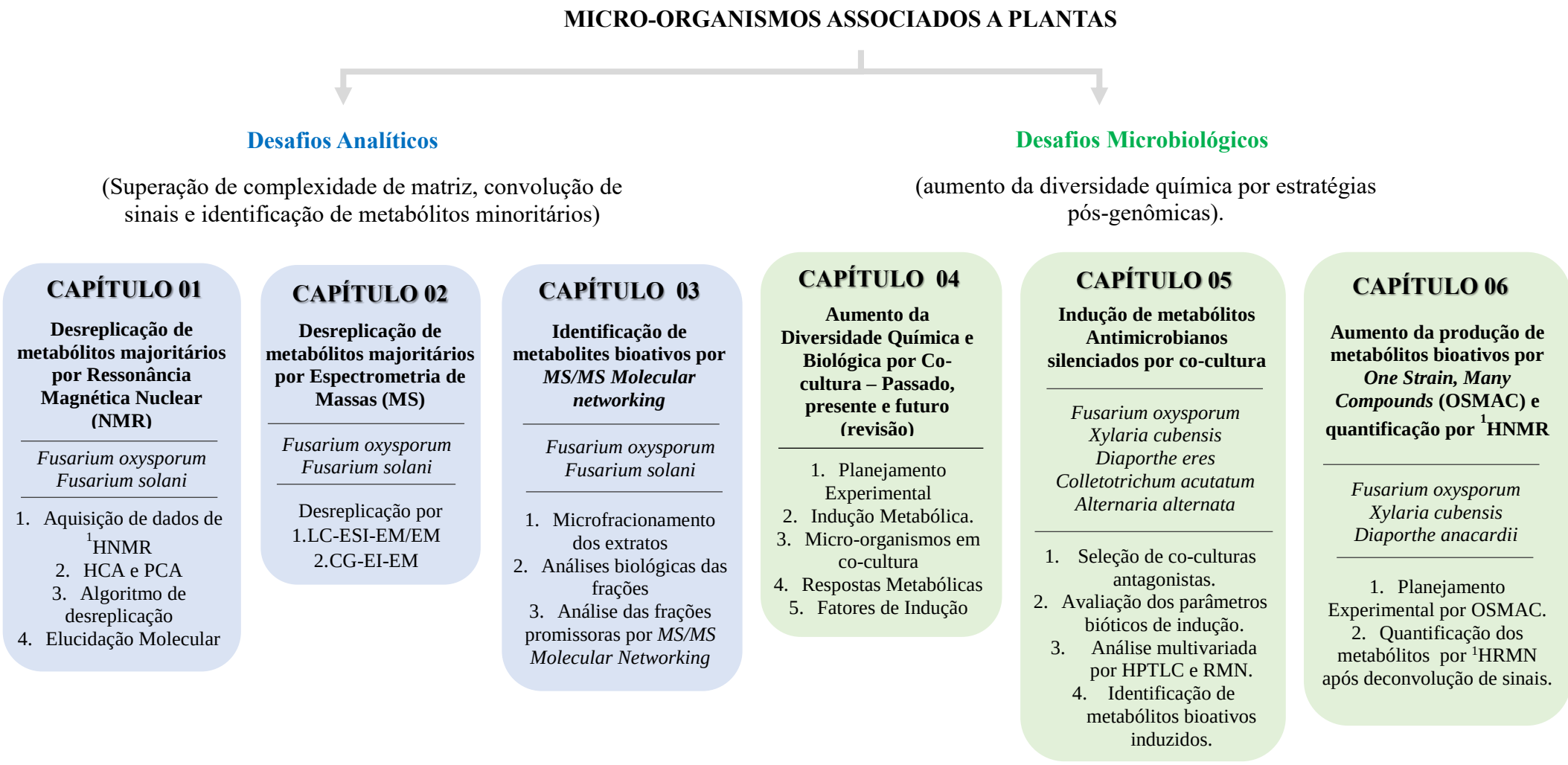

No primeiro capítulo desta tese, nós objetivamos a identificação de metabólitos majoritários pela desreplicação em RMN através da criação de um novo método para a seleção e extração de deslocamentos químicos de interesse em dados de *Fusarium solani* e *F. oxysporum* isolados da rizosfera de *Senna spectabilis.* O algoritmo desenvolvido utiliza os valores de *loading* da componente principal que melhor separou as espécies de *Fusarium* na Análise de Componentes Principais (PCA) para extração de sinais importantes que distinguem ambas as espécies. Esses deslocamentos químicos foram elucidados pela análise uni e bidimensionais de RMN e confirmados pela comparação destes dados experimentais com informações de um banco de dados desenvolvidos para metabólitos de *Fusarium*. Em *F. oxysporum*, a metodologia identificou o ácido fusárico (I) e o depsipeptídeo da família eniantina denominada beauvericina (II) enquanto para *F. solani*, o metabólito identificado foi depsipeptídeo HA23 (III). De maneira geral, o uso dessa estratégia mostrou-se capaz de desreplicar diferentes micotoxinas produzidas em alta abundância por ambos os fungos, permitindo a identificação de metabólitos secundários, mesmo em perfis altamente semelhantes.

No segundo capítulo, os mesmos extratos em monocultura de *F. oxysporum* e *F. solani* foram submetidos à desreplicação por espectrometria de massas, visando identificar outros quimiotipos majoritários que não foram elucidados por RMN. Para tanto, os extratos foram analisados por cromatografia líquida (LC-DAD-ESI(+)-EMAR e LC-DAD-ESI-EM/EM) e gasosa (CG-EI-EM) hifenadas à espectrometria de massas, seguida da comparação desses dados experimentais com aqueles de moléculas conhecidas presentes em bancos de dados consolidados na literatura. Os resultados mostram que a desreplicação por EM, associada a diferentes técnicas de separação, garantiu uma visão abrangente da produção metabólica, identificando 16 diferentes metabólitos. A desreplicação por LC-EM identificou sete compostos, incluindo a beauvericina, para ambas as espécies de *Fusarium*, alcalóides da família da camptotecina, para *F. solani*, e análogos do ácido picolinico para *F. oxysporum*. Já a análise por CG-EM utilizou amostras derivatizadas e foi capaz de identificar dez compostos diferentes, destacando o ácido fusárico e análogos para *F. oxysporum*, além de metabólitos primários de ambas as espécies, como álcoois e ácidos orgânicos.

No terceiro capítulo, os mesmos extratos fúngicos de *F. oxysporum* e *F. solani* foram submetidos à fracionamento em micro-escala seguido da avaliação da atividade biológica, visando a identificação de metabólitos secundários bioativos. Estes testes biológicos incluíram ensaios antifúngicos, antibacterianos, antibiofilme e de inibição da

enzima acetilcolinesterase. A elucidação dos metabólitos das frações promissoras foi realizada inicialmente pela avaliação da rede de interações moleculares de dados de massas sequenciais (do inglês *MS/MS Molecular Networking*), em que dados de fragmentação são agrupados de acordo com a similaridade química. Em seguida, os metabólitos propostos pela análise de fragmentação foram confirmados pela avaliação do erro da massa de alta resolução, bem como proposição dos fragmentos e seus mecanismos de fragmentação. A rede de interações moleculares contribuiu para a análise quimiotaxonômica dessas espécies e revelou que, para cada grupo formado, havia pelo menos um nódulo de cada espécie de *Fusarium,* sugerindo um denominador genético comum. Além disso, os resultados mostraram que o fracionamento reduziu a complexidade da matriz e permitiu a seleção de frações que possuem bioativas promissoras. Todas as amostras bioativas pertencem exclusivamente à *F. oxysporum*. As frações polares de ambas as variedades de *F. oxysporum* (CSP-19b e R18) apresentaram atividade antifúngica contra *Cladosporium*, atividade antibiofilme contra *Staphylococcus epidermidis*, atividade bacteriostática frente a *Enterococcus faecalis* e forte inibição da enzima acetilcolinesterase. Já as frações apolares da cepa CSP-19b também foram selecionadas como biopromissoras e exibiram alta erradicação do biofilme e forte potencial antibacteriano. A desreplicação dos compostos das frações bioativas foi realizada separadamente de acordo com a polaridade da fração. A análise das frações apolares levou à identificação da beauvericina e 6 análogos nunca relatados para esta espécie: os compostos conhecidos beauvericinas A, G1 e G2, e os compostos inéditos denominados FOxy 01, 02 e 03. Estes compostos pertencem à família da eniantina e exibem forte atividade antimicrobiana e antitumoral. Já a análise das frações polares revelou a presença de ácido fusárico e desidrofusárico, previamente elucidados no Capítulo 2, juntamente com dois análogos minoritários que nunca foram relatados para esta espécie. No geral, a combinação de atividade biológica, fracionamento e rede de interações moleculares foi uma estratégia eficiente para a identificação de compostos e permitiu a elucidação de diferentes micotoxinas bioativas, superando desafios da complexidade de matriz e da identificação de compostos minoritárias diretamente em matrizes complexas.

Após a aplicação de diferentes estratégias de desreplicação para superar os principais problemas analíticos na metabolômica microbiana, a segunda parte desta tese foi a expansão do metaboloma microbiano por estratégias pós-genômicas. Dentre as estratégias empregadas, a co-cultura têm sido uma metodologia de sucesso para a ativação

de genes crípticos e não requer conhecimento prévio do genoma e das vias biossintéticas, nem equipamentos especiais para o cultivo e interpretação de dados. Na literatura, diversas revisões mostraram o potencial do co-cultivo para a indução de metabólitos com potencial biológico. No entanto, estas revisões são limitadas para a descrição de resultados químicos relevantes relatados na literatura. No capítulo quatro, para a melhor condução desses experimentos, realizamos uma revisão que contém todo o fluxo experimental de co-cultura, contribuindo para o desenvolvimento de métodos padronizados e compatíveis com procedimentos analíticos de alto rendimento (do inglês *high-throughput analytical procedures*). Particularmente, interpretamos todas as principais publicações de cultivo misto de 1978 a 2019, mostrando o que foi relatado até o momento sobre os diferentes tipos de co-cultura, induções metabólicas, interações microbianas, e como estas interações podem ser otimizadas para aumentar a diversidade química e biológica de fungos e bactérias.

Após a revisão de co-cultura, no capítulo cinco, mostramos o desenvolvimento de uma estratégia para aumentar a diversidade química e o potencial antimicrobiano usando co-cultura em meio sólido. Especificamente, nós cultivamos os fungos associados à plantas das espécies de *Diaporthe eres*, *Fusarium oxysporum*, *Alternaria alternata*, *Colletotrichum acutatum* e *Xylaria cubensis*, em pares, para selecionar co-culturas que apresentam interações antagônicas e induções metabólicas promissoras. As co-culturas selecionadas foram avaliadas frente a diferentes aspectos bióticos da indução química por análise por cromatografia de camada fina de alto performace (HPTLC), que inclui a determinação da variedade fúngica indutora e o melhor período de incubação. Além disso, análises quimiométricas utilizando dados de HPTLC e RMN foram realizadas para a identificação desses compostos induzidos e a correlação destes com a atividade antimicrobiana. Os resultados mostram que cada espécie fúngica apresentou diferentes respostas morfológicas, químicas e biológicas na presença de linhagens competidoras. A avaliação das co-culturas selecionadas no seu ambiente biótico ótimo de indução metabólica mostrou um aumento não apenas na diversidade química, mas também na atividade antimicrobiana. A análise multivariada dos dados revelou que o potencial antimicrobiano foi correlacionado aos metabólitos secundários de *F. oxysporum* e *D. eres*. De um lado, co-cultura de *F. oxysporum* aumentou a produção de beauvericina em 3 vezes, um depsipeptídeo que apresenta forte atividade antifúngica contra *C. acutatum*, além de forte atividade antibacteriana contra *S. aureus*, *P. fluorences* e *E. coli*. Por outro lado, co-culturas de *Diaporthe* revelaram a indução de um metabólito inédito da família

da bisantraquinona, um composto não produzido em culturas axênicas que exibe atividade antifúngica moderada contra *F. oxysporum*, atividade antibacteriana forte contra *Bacillus cereus* e atividade antibacteriana moderada contra *S. aureus*.

Por último, no capítulo final desta tese, apresentamos uma estratégia para a otimização e monitoramento de compostos bioativos em fontes microbianas usando uma estratégia integrativa por OSMAC-Design de Experimentos (DoE) e quantificação por RMN de hidrogênio através de valores de área deconvoluídos por algoritimo GSD (MestreNova). Para tanto, monitoramos e quantificamos os compostos bioativos ácido fusárico, citocalasina D e ácido 3-nitropropiônico, produzidos respectivamente, por *F. oxysporum*, *X. cubensis* e *Diaporthe anacardii*, seguindo uma estratégia OSMAC-DoE para a avaliação sistemática da agitação, temperatura e luminosidade. O planejamento OSMAC-DoE foi realizado visando verificar em quais parâmetros abióticos a produção dos metabólitos alvo era maior e foi calculado usando duas respostas diferentes. A primeira utilizou os valores de massa total dos extratos brutos obtidos em cada experimento OSMAC e continha informações sobre o crescimento fúngico e a regulação da produção metabólica global. Já a segunda resposta empregou os valores do percentual de pureza (teor) dos metabólitos bioativos alvo de cada experimento OSMAC e continha informações sobre a regulação desses compostos, independentemente do crescimento dos fungos. Para a segunda resposta, todos os deslocamentos químicos dos metabólitos alvo nos spectros de hidrogênio foram submetidos à deconvolução por GSD e os valores de área deste algoritmo foram utilizados para quantificação por RMN, em comparação com um padrão interno. Os resultados mostraram que o planejamento OSMAC-DoE aumentou a produção dos metabólitos alvo em até 33% usando apenas 8 experimentos. Além disso, o uso de GSD foi capaz de extrair automaticamente valores de área precisos nos espectros de hidrogênio, mesmo quando os deslocamentos químicos estavam altamente convoluídos com outras ressonâncias. Além disso, a quantificação por ^{1}HNMR usando valores de área do GSD foi reprodutível para todas as espécies e apresentou resultados de validação que foram muitas vezes mais seletivos e precisos do que métodos comparativos, garantindo uma quantificação robusta diretamente em matrizes complexas.

No geral, os metabólitos secundários microbiano mostraram-se ser o futuro para o descobrimento de novos medicamentos. Mesmo com os problemas relacionados a genomas silenciados e linhagens inculturáveis, os micro-organismos foram capazes de produzir estruturas químicas extremamente diversas encontradas em populações

microbianas ainda pouco exploradas, tornando-se uma fonte quase ilimitada de estruturas complexas e biologicamente ativas.

Apesar de vantajosas, algumas dificuldades analíticas e microbiológicas dificultaram a interpretação química e biológica dos dados. Para superação desses desafios, esta tese mostrou a combinação de estratégias pós-genômicas, técnicas analíticas e o uso de ferramentas computacionais e estatísticas para uma análise abrangente do metaboloma microbiano. A seleção destas metodologias deve sempre ser baseada em uma avaliação cuidadosa do perfil químico, além de uma pesquisa bibliográfica sobre as informações químicas, genômicas e biológicas disponíveis para espécies selecionadas. Muitas vezes, somente através da combinação de química orgânica, química analítica, microbiologia e análises estatísticas, os resultados foram suficientemente abrangentes, sendo usadas quase sem distinção de uma maneira única e integrada.

INTRODUCTION

Microbial secondary metabolites, resulted from several million years of evolutionary biosynthetic optimization, have tremendous potential to provide new therapeutic agents (PETTIT, 2009). In a recent review, Newman and Cragg have shown that, even with the challenges related to unlocked genomes and unculturable strains, microbial bioactive compounds are the future for drug discovery programs (NEWMAN; CRAGG, 2016), accounting for over 42 thousand natural compounds already reported from different microbial families (LAATSCH, 2012).

The potential of these microbial secondary metabolites comes not only from an extremely diverse chemical structures but also from an extensive and still little studied microbial population. Indeed, recent whole-genome sequencing of several fungi and bacteria shows that the potential of microbial matrices to produce secondary metabolites is fairly underestimated, meaning that a much broader range of compounds could be produced if the silent genes are induced by whatever methods (BERGMANN et al., 2007; CHIANG et al., 2008; GALAGAN et al., 2005; HIBBING et al., 2010; SCHROECKH et al., 2009).

Conventionally, in the fields of microbiology, single-strain cultivation has been the standard method for the screening of secondary metabolites. However, owing to the absence of biotic and abiotic interactions, the growth conditions in monocultures are significantly different from those encountered in the natural environment (ONAKA et al., 2011; PETTIT, 2009). In nature, microbial metabolic pathways are often regulated by complex cascades, in which their chemical profiles are controlled by genes and influenced by biotic communication with external factors. For example, on competitive environments, microbial species engage in constant interactions with their neighbors, competitors and hosts, resulting in ecological effects that ensures survival and shapes the community (MOODY, 2014).

The absence of biotic and abiotic incentive is the biggest limitation of axenic cultures and limits the chemical diversity that can be obtained by one single strain. In fact, monoculture screening often provides a still increasing rate of redundancy, resulting in chemically poorer profiles and the frequent re-isolation of known secondary metabolites (HONG et al., 2009; MARMANN et al., 2014). In the last decade, several methods have been developed to eventually embody the physiological conditions under which cryptic genes are activated, in an attempt to stimulate their biosynthetic pathways and elicit the

production of hitherto unexpressed chemical diversity (SCHROECKH et al., 2009; WAKEFIELD et al., 2017). Overall, these strategies have been successfully applied for the genomic activation, simultaneously modifying different levels of the cellular machinery to regulate the production of different classes of secondary metabolites (BERTRAND et al., 2014a; HERTWECK, 2009; WAKEFIELD et al., 2017).

Among those, genetic-dependent approaches, such as mutasynthesis, heterologous expression and metabolic engineering (BERGMANN et al., 2007), have been used as one of the most effective methodologies for gene activation. However, these procedures are mostly applied for known structures and require both expensive instrumentation and a previous knowledge of the microbial genome.

More recently, the increase in microbial resistance to conventional therapy has urged the development of fast and cheap methodologies to enhance the microbial diversity. In this sense, the cultivation-dependent methodologies (or post-genomic strategies) have emerged as a viable alternative, modifying different levels of the cellular machinery for a more holistic regulation of secondary metabolites. These strategies includes substrate feeding (DE BOER; SCHMIDT-DANNERT, 2003), co-culture and One Strain, Many Compounds (OSMAC) (BODE et al., 2002; RATEB et al., 2011; ROMANO et al., 2018; WEI et al., 2010) and do not require any prior knowledge of the genome and biosynthetic pathways, nor any special equipment for the cultivation and data interpretation.

Microbial co-culture involves the cultivation of two or more microorganisms in the same confined environment and has been considered to be a golden strategy to induce cryptic pathways. In mixed fermentation, microorganisms metabolize the media substrate together, mimicking the competitive microbial environment for the production and regulation of constitutively molecules (RATEB et al., 2013; WAKEFIELD et al., 2017). On these experiments, microbial communication occurs either by volatiles or *in-loco* signaling and leads to the regulation of secondary metabolites, even if the detailed inducing mechanism, in the biological and ecological context, remain largely unknown (PETTIT, 2011a; RATEB et al., 2013; SCHROECKH et al., 2009).

One Strain, Many Compounds (OSMAC) is one of the most used post-genomic strategies and involves the manipulation of culture parameters, such as media composition, temperature, agitation and luminosity, in an attempt to stimulate, in quantity and diversity, the production of secondary metabolites from a single microbial source (BODE et al., 2002; HUSSAIN et al., 2017; ROMANO et al., 2018; WEI et al., 2010). Usually, OSMAC uses Design of Experiments (DoE) to systematically evaluate the effect

of different growth parameters, estimating the optimized conditions for the production of new metabolites, as well as the regulation of known compounds (BRACARENSE; TAKAHASHI, 2014; OOIJKAAS et al., 1999; PIMENTA et al., 2010).

Although post-genomic strategies represent successful methodological advances in the expansion of the microbial metabolome, analytical issues related to the identification and quantification of metabolites in complex matrices remain a cornerstone in microbial natural products research. Some examples of difficulties encountered in microbial metabolic analysis include the constant re-isolation of inactive or known chemotypes, the polarity-related structural complexity and the wide metabolic dynamics, requiring highly sensitive and robust analytical methods (ITO; MASUBUCHI, 2014). Moreover, combined with state-of-the-art analytical techniques, recent studies have also incorporated the use of computational tools that perform deconvolution, pattern recognition and multivariate data analysis, facilitating the statistical, chemical and biological interpretation of these complex natural matrices.

OBJETIVES

In this sense, the main goal of this work is to present an integrative strategy for the enhancement of identification and detection of secondary metabolites in microbial matrices, overcoming the major analytical and microbiological challenges in microbial metabolomics. In this context, we aim to:

1. Overcome analytical challenges in microbial metabolomics, such as matrix complexity, signal convolution and the identification of minor metabolites, by:
    - Exploration of the chemical fingerprinting of plan-associated fungi by untargeted and multi-technique dereplication approaches.
    - Generation of a rational strategy to identify, quantify and monitor the production of secondary metabolites in complex matrices.
    - Integration of computational tools and multivariate data analysis to facilitate metabolite identification, quantification and correlation to biological activity.

2. Overcome microbiological challenges in microbial metabolomics by the application of different post-genomic strategies:
    - Expansion of the microbial metabolome by the activation of silent genes coded for known and novel secondary metabolites.

CHAPTER 1. DEREPLICATION OF MAJOR SECONDARY METABOLITES BY NUCLEAR MAGNETIC RESONANCE (NMR)

Article title: New dereplication methods applied to NMR-based metabolomics on different *Fusarium* species isolated from *Senna spectabilis*'s rhizosphere (http://dx.doi.org/10.5935/0103-5053.20160139).

Journal: Journal of the Brazilian Chemical Society (JBCS).

Status: Published.

Authors: Denise M. Selegato[a], Rafael T. Freire[b], Alberto Tannús[b], Ian Castro-Gamboa[a*]

Affiliations:

[a] Nuclei of Bioassays, Ecophysiology and Biosynthesis of Natural Products (NuBBE), Institute of Chemistry (ICAr) – São Paulo State University (UNESP) – Araraquara, SP**,** Brazil.

[b] Centro de Imagens e Espectroscopia in vivo por Ressonância Magnética (CIERMag), Instituto de Física de São Carlos (IFSC) – University of São Paulo (USP) – São Carlos, SP**,** Brazil.

Justification:

This chapter aimed to identify the major secondary metabolites produced by the fungi isolated from the rhizosphere of *S. spectabilis* by incorporating chemometric analysis into proton NMR data from the crude extracts of *Fusarium* species. Specifically, this work showed the selection of fungi, their genetic identification and all stages of the new computational method developed for the analysis of ^{1}HNMR data, enabling the selection and extraction of important metabolic signals, later elucidated by one and two-dimensional NMR. All the content described in this chapter was published in the *Journal of the Brazilian Chemical Society*, in 2016, in an article entitled "New Dereplication Method Applied to NMR-Based Metabolomics on Different *Fusarium* Species Isolated from Rhizosphere of *Senna Spectabilis"*.

Abstract

The search for new bioactive natural products steadily increased the use of bioinformatic tools that enabled efficient analysis of complex matrices. In this context, dereplication methods has emerged as a fast way of identifying known compounds, accelerating sample selection and the identification of interesting chemotypes. Conventionally, for a comprehensiveview of the chemical profile, dereplication is performed by a multitude of analytical techniques, including mass spectrometry and nuclear magnetic resonance. However, ^{1}HNMR still presents high spectral complexity, due to the difficulty to be hyphenated with chromatographic introductory systems and low-sensitivity, hindering both biological assesment and metabolite identification. This work aimed to create a new computational method that analyses ^{1}HNMR data from *F. solani* and *F. oxysporum* isolated from *S. spectabilis's* rizhosphere by combining multivariate data analysis and bioinformatics. The developped algorithm uses Principal Component Analysis (PCA) loading values to select and extract important chemical shifts that distingish both species, allowing the identification of important biomarkers even in highly similar profiles. As a result, the method, associated with other NMR experiments and information from an *in-house Fusarium*'s metabolite library, was able to dereplicate different mycotoxins produced in high abundance by both fungi, identifying fusaric acid (I) and beauvericin (II) for *F. oxysporum* and the depsipeptide HA 23 (III) from *F. solani*.

Keywords: Dereplication method, *Fusarium*, PCA, NMR-based metabolomics, *Senna spectabilis*

1. Introduction

The holistic view of natural product (NP) chemistry has a key role in the discovery of novel bioactive metabolites. Using state of the art analytical techniques, a broader view of the chemical composition allows a fast evaluation of the complex matrices and further understanding of both synergistic and antagonistic relationships in natural sources (NEWMAN; CRAGG, 2016).

Recently, in order to achieve an accurate chemical response, the development of computational tools has become of fundamental importance in the current dereplication programs, aiming mainly to decrease complexity and facilitate the identification of new potential compounds (NG et al., 2009; WOLFENDER et al., 2009). In this context, dereplication has emerged as a rapid way of identifying known compounds in crude extracts, facilitating the detection of bioactive chemotypes and decreasing the redundant isolation of known compounds (NEWMAN; CRAGG, 2016; WOLFENDER et al., 2015). When compared to the univariate approaches, dereplication has been considered a fast and cheaper alternative, decreasing the cost and the use of organic solvents (NG et al., 2009; WOLFENDER et al., 2009).

Classically, dereplication methods combine biological screening with data obtained by hyphenated protocols, such as LC-DAD/HRMS and LC-DAD/RMN, LC-DAD/MS/MS (GAUDÊNCIO; PEREIRA, 2015; JARUSSOPHON et al., 2009; NIELSEN et al., 2011; WILLIAMS et al., 2015; WOLFENDER et al., 2015). In those experiments, data interpretation and molecule identification are commonly achieved by comparison with robust databases containing spectroscopic and spectrometric data of previously reported compounds. More recently, several other tools have been developed to achieve efficient and more factual paths for metabolite elucidation (GAUDÊNCIO; PEREIRA, 2015). Among the enhancements in the dereplication process, we highlight the use of 2D/^{13}CNMR, signal deconvolution (BLAISE et al., 2010; COBAS; SEOANE; SÝKORA, 2008), bioinformatics, molecular networking applied to the omics sciences (genomics, proteomics, metabolomics) (WANG et al., 2016; YANG et al., 2013), the use of taxonomic filters and unsupervised multivariate data analysis (FUNARI et al., 2012; GAUDÊNCIO; PEREIRA, 2015; NIELSEN; LARSEN, 2015; WILLIAMS et al., 2015; WOLFENDER; QUEIROZ; HOSTETTMANN, 2006).

In parallel to the development of new dereplication tools, microorganisms, especially those isolated from unstudied NP matrices, such as plant's rhizosphere and

marine organisms, have emerged as an interesting source of new active compounds, mainly due to their high molecular complexity and potential to produce heterogeneous secondary metabolites. Furthermore, recent whole genome evaluation has shown that their potential to produced secondary metabolites is fairly underestimated due to the presence of silent genes, enabling the production of different active metabolites in a single strain (ALY et al., 2010; ALY; DEBBAB; PROKSCH, 2011; VANDERMOLEN et al., 2013).

In order to rationally explore the chemical composition of the selected microorganisms, in this work, we have analyzed complex fungi extracts isolated from *S. spectabilis*, aiming to dereplicate important chemical shifts in ^{1}HNMR data that differentiate *Fusarium* species. For this, we have developed an algorithm that uses PCA loading values to rapidly extract chemical shifts that distinguished the fungi metabolic profiles, enabling the selection and extraction of important signals directly from the complex data. Further, through comparison with an *in house* ^{1}HNMR library and online databases, this work showed the elucidation of these selected chemical shifts even in highly overlapped data, providing metabolite identification in crude extracts and the determination of the most abundant secondary metabolites and possible biomarkers for these species.

2. Materials and Methods

2.1. *Selection of Filamentous Fungi Isolated from S. spectabilis*

The fungi selection was based on the preliminary studies of *Senna spectabilis*'s rhizosphere reported by Dr. Patrícia Cardoso, a researcher associated with NuBBE, in which 180 microorganisms were isolated, including 127 fungi and 53 bacteria (CARDOSO, 2015). The fungi were isolated from a healthy rizhospheric region according to reported isolation methods (CARDOSO, 2015; PARKINSON; THOMAS, 1965).

In order to avoid the random selection of these filamentous fungi, these microbes were chosen by both biological and chemical screening. For that, all 127 fungi were inoculated in Czapek and incubated for 10 days, at room temperature and in the absence of light. The viable cultures (*i.e.* the cultures that grew well on this selected media) had their metabolites extracted and submitted to biological assay and metabolic fingerprinting. The biological analysis included antifungal against *Cladosporium* species,

acetylcholinesterase inhibition and colorectal antitumor assays and aimed the selection of extracts with promising therapeutic potential (protocols described in Chapter 3). Moreover, the chemical analysis of the bioactive fungi was performed by metabolic footprinting (*i.e.* metabolic profile of the culture medium supernatant) by ^{1}HNMR for the selection of species that displayed different chemotypes.

For all the Chapters of this thesis, Czapek was established as the standard culture medium due to its low nutrient compostition. This restriction not only decreases the signal convolution in ^{1}HNMR anaysis but also mimics the competitive rhizospheric environment, maximizing microbial stress for the induction of silenced secondary metabolites (BERTRAND et al., 2014b).

Microbial screening results allowed the selection of three fungi isolated from the rhizosphere, encoded as CSP-19b, CSP-R18 and CSP-5b. CSP-5b showed strong antifungal activity against *C. cladosporioides* and *C. sphaerospermum* and an expressive inhibition of the acetylcholinesterase enzyme, while CSP-R18 and CSP-19b displayed also promising antitumor potential in addition to high antifungal and anti-acetylcholinesterase activities. Furthermore, Principal Component Analysis (PCA) of ^{1}HNMR data showed that CSP-5b, CPS-R18 and CSP-19b are placed three opposite coordinates in the score plot, evidencing also a different metabolic production. All results of the biological assays are available in Table SM1 and Figure SM1 of the Supplementary Material.

2.2. *Genetic Identification of Filamentous Fungi Isolated from S. spectabilis*

Genetic identification of all three selected fungi was carried out in the Laboratory of Clinical Mycology and Proteomic Nucleus at the Faculty of Pharmaceutical Sciences, UNESP, Araraquara, in collaboration with Profa. Dr. Ana Marisa Fusco Almeida and Dr. Haroldo César de Oliveira.

Genetic analysis was done through Internal Transcribed Spacer region (ITS) using primers ITS1 (5´-CTTGGTCATTTAGAGGAAGTAA-3´) and ITS4 (5´-TCCTCCGCTTATTGATATGC-3´). The DNA-ITS region consists of interspecifically highly conserved sequences that are slightly variable among different species. Thus, nucleotide sequencing of the ITS1-5.8S-ITS2 region of isolated fungi rRNA allows the identification of phylogenetic relationships beyond species distinction.

DNA extraction, ITS amplification by polymerase chain reaction (PCR) and PCR

products sequencing protocols were based on Sanger method (SANGER; NICKLEN; COULSON, 1977), and the sequences obtained by sequencing PCR were analysed by Basic Local Alignment Search Tool (BLASTn) (ALTSCHUL et al., 1997), available on http://blast.ncbi.nlm.nih.gov/Blast.cgi and deposited at GenBank under access number JX435189.1 (CSP-5b), KP230811.1 (CSP-R18) and LC055797.1 (CSP-19b).

2.3.*Fermentation and Extraction*

The selected fungi were initially preserved by inoculation of the pre-culture plugs in Czapek-agar at neutral pH ($NaNO_3$, 1.5 g L^{-1}; KH_2PO_4, 0.5 g L^{-1}; $MgSO_4$, 0.25 g L^{-1}; $FeSO_4$. $7H_2O$, 0.025 g L^{-1}; KCl, 2.5 g L^{-1}; D-glucose, 30.0 g L^{-1} and agar 20.0 g L^{-1}) and incubation for 12 days at room temperature and in the dark. After incubation, 0.5 cm^2 plugs of these starting cultures were added to vials containing 1000 µl of 50% glycerol, previously sterilized in a vertical autoclave for 20 minutes at 121 °C, and stored at -80 °C. The preserved fungi were used in all the chapters of these thesis to avoid random mutagenesis along time.

For the analysis of the chemical profiles and genetic identification, the preserved fungi were activated in Czapek-agar and incubated for 10 days at 25 °C and the absence of light. Following, the plugs of active filamentous fungi were inoculated into 3.2 L of Czapek-broth and incubated for 28 days at room temperature and in static mode. After the growing period, the cultures were vacuum filtered and divided into two parts: (1) the mycelium, which was frozen in liquid nitrogen and submitted to genetic identification and (2) the supernatant, which was extracted for the metabolomic analysis. All cultivations were performed in triplicates, in which the same inoculated petri dish was used for all three erlenmeyer sets.

The aqueous solution obtained after filtration of the liquid culture was extracted with three portions of ethyl acetate (EtOAc ACS 99.5%, Sigma-Aldrich). The organic extract was then dehydrated with 30g of anhydrous sodium sulfate ($NaSO_4$, 99%, Sigma-Aldrich) and dried on a rotary evaporator under vacuum at 40°C and 240 mbar to remove the extractive solvent. For the removal of polar interferents and suspended particles, the organic extracts were resolubilized in methanol-HPLC, filtered with a 0.22 µm membrane filtration, to remove suspended particles and subjected to solid-phase extraction (SPE). to remove highly non-polar compounds. For this clean-up procedure, the C18 SPE-columns were first activated with 10 volumes of column of methanol HPLC-grade

(Sigma-Aldrich) and the ethyl-acetate extracts were eluted using 10 volumes of column of the same methanolic solution.

2.4. *NMR Analysis*

Each sample triplicate was prepared in instrumental duplicate using 3 mg ± 0.1 of extract (after clean-up) re-suspended in 750 μL of deuterated methanol, using volumetric pipette. All samples were solubilized in an ultrasonic bath for 3 minutes (temperature of 25°C and 35,000 oscillations per second), centrifuged for 15 minutes at 6000 rpm, to remove any suspended particles, and transferred to a 5 mm-NMR tube. NMR spectra were recorded on Bruker Ascend (14.1 T) Cryoprobe spectrometer (Billerica, Massachusetts, USA) using non-deuterated residual signal as reference.

For ^{1}HNMR acquisition (600 MHz), analysis parameters were: number of points (TD) 65k; number of scans (NS) 64; relaxation delay (d1) 1.00 s, spectral width (SW) 13 ppm, temperature 295.2 K and acquisition time of 2 minutes and 38 seconds. Saturation on the residual water signal, at δ4.90, was performed by presaturation pulse sequence using composite pulse (Bruker sequence, zgcppr).

For molecule confirmation after dereplication algorithm, two-dimensional experiments gradient-selected Heteronuclear Single Quantum Coherence (HSQC) and gradient-selected Heteronuclear Multiple Bond Correlation (HMBC), as well as unidimensional Total Correlation Spectroscopy (1D-TOCSY) and Nuclear Overhauser Effect spectroscopy (1D-NOESY) were performed on all extracts of *F. oxysporum* and *F. solani*. Pulse sequences used on 2D NMR analysis were (a) ^{13}CHSQC: phase-sensitive ge-2D multiplicity-edited HSQC using PEP and adiabatic pulses with gradients in back-inept (hsqcedetgpsisp2.4, Bruker) and (b) ^{13}CHMBC: phase-sensitive ge-2D HMBC using a two-fold low-pass *J*-filter (hmbcetgpl3nd 2D, Bruker). 1D-NOESY was performed using selnogpzs, which minimizes artifacts in NOESY spectra arising from to the evolution of zero-quantum coherence of *J*-coupled spins during the mixing time. 1D-TOCSY was obtained using seldigpzs, in which a selective echo refocuses the selected spin and is then transferred down the spin system by the DIPSI-II isotropic mixing sequence.

For HMBC and HSQC acquisition, analysis parameters were, respectively for ^{1}H (f2) and ^{13}C (f1), spectrometer frequency 600.13/150.91 MHz, time domain (TD) 512/512, spectral width (SW) 13/230 ppm, number of scans (NS) 32; relaxation delay

(d1) 1.50 s and temperature 295.2 K. For 1D-TOCSY and 1D-NOESY acquisition, analysis parameters were time domain (TD) 65k, number of scans (NS) 512; relaxation delay (d1) 1.00 s, spectral width (SW) 13 ppm and temperature 295.2 K.

2.5. *^{1}HNMR Data Pre-processing*

No preprocessing functions were applied on the Free Induction Decays (FIDs). After Fourier Transformation (FT), spectra were referenced, phased and exported in American Standard Code for Information Interchange (ASCII) format files using MestReNova 10.0.2 software (MestreLab Research SL, Santiago de Compostela, Spain) (WILLCOTT, 2009). The text files were inserted as tables on MATLAB R2015a software (Infometrix, Mathworks, Natick, Massachusetts, USA) for further matrix pre-processing, chemometric and computational analysis.

Only NMR information from δ-0.5 to 11.0 was selected for pre-processing treatments. Additionally, NMR information from δ3.00 to 4.17, which comprises sugars components from Czapek-broth, was removed. The start and end points of each integral region were forced to zero amplitude using airPLS baseline correction algorithm (ZHANG; CHEN; LIANG, 2010) and then normalized to total area. Alignment was performed using ICOSHIFT algorithm (SAVORANI; TOMASI; ENGELSEN, 2010) and no data reduction by bucketing or binning was performed.

2.6. *^{1}HNMR Multivariate Data Analysis and Dereplication algorithm*

Unsupervised chemometric analysis was acquired using MATLAB R2015a software (Infometrix, Mathworks, Natick, Massachusetts, USA). Hierarchical Clustering Analysis (HCA) was calculated using Euclidean distance as the pairwise distance and ward as linkage. For mean-centered PCA, NIPALS algorithm (Nonlinear Iterative Partial Least Squares) was applied at a 95% of confidence interval (ANDRECUT, 2008). The dereplication algorithm was entirely written in MATLAB R2018a language and the input data was the loading values of principal component 2 (PC2) obtained by PCA of *F. oxysporum* and *F. solani* ^{1}HNMR data.

2.7. *In house Metabolic database*

In order to compare the selected chemical shifts from the dereplication algorithm,

a *in-house* database was compiled with chemical shifts reported for the major metabolites found in all three selected species. The database included ^{1}HNMR data of 47 secondary metabolites from *F. oxysporum* and 32 secondary metabolites from *F. solani*; including jasmonates, tricothecenes, enniatins, naphthoquinones, and others. The structures were drawn using ChemDraw Ultra 12.0 (PerkinElmer Informatics, Massachusetts, USA) and ^{1}HNMR prediction in $CDCl_3$ was made using MestReNova 10.0.2 (Metrelab Research SL, Santiago de Compostela, Spain).

2.8. *Confirmatory LC-DAD-ESI-HRMS/MS Analysis*

High-resolution mass spectra were measured for all replicates on a LC–DAD-HRMS-QTOF Micromass spectrometer using electrospray ionization (ESI) in the positive mode and Quadrupole-time of flight (q-TOF) analyzer. For the LC analysis, we have used UV SPD detector system and Kinetex C18 100R column (5 µm particles size, dimensions 150 x 4.60 mm). For MS analysis, the parameters were: cone voltage 4500 kV, desolvation temperature 450 °C, nebulizing gas 10 psi and collision energy 25 eV.

For tandem MS in the automated mode, a MS (MS1) was acquired, selecting the major ions of each retention times followed by a real time fragmentation experiment. All LC-MS/AutoMS experiments were done in AmaZon speed (Bruker Corporation, Massachusetts, EUA), using electrospray ionization (ESI) in the positive mode and ion trap analyzer at the following parameters: nebulizer pressure 70 psi, drying gas flow 12 L min^{-1} and drying gas temperature of 350 °C.

3. Results and Discussion

3.1. Fungi genetic identification and metabolite extraction

Senna spectabilis bellows to the Fabaceae family and refers to a plant widely used in folk herbal medicine and extensively studied towards their chemical diversity. The selection of this plant as the object of study comes from the well-known cytotoxic activity of its rhizosphere, attributed mainly to the biotic and abiotic interactions between the plant and the microbes that inhabit this competitive environment (CARDOSO, 2015). In 2017, a major revision has been published by this author with an updated of all chemical and biological data of this species, which includes the presence of bioactive piperidine alkaloids, pentacyclic triterpenes and anthraquinones (SELEGATO et al., 2017).

Genetic identification of the selected fungi from the rhizosphere showed that all three strains belong to *Fusarium*, the major genus found in this region of *S. spectabilis* (Figure 1.1). DNA extraction of *F. solani* yielded 21.8 ng μL^{-1} at a 1.8 purity and 98 % identity, while *F. oxysporum* yielded doble (50.6 ng μL^{-1}) at a 1.9 purity and 99 % identity. These filamentous fungi are commonly found in soil and live both symbiotically and as a pathogen in several Leguminosae, producing a variety of bioactive secondary metabolites, including jasmonates and mycotoxins such as picolinic acid derivatives, depsipeptides and naphthoquinones (MICHIELSE; REP, 2009).

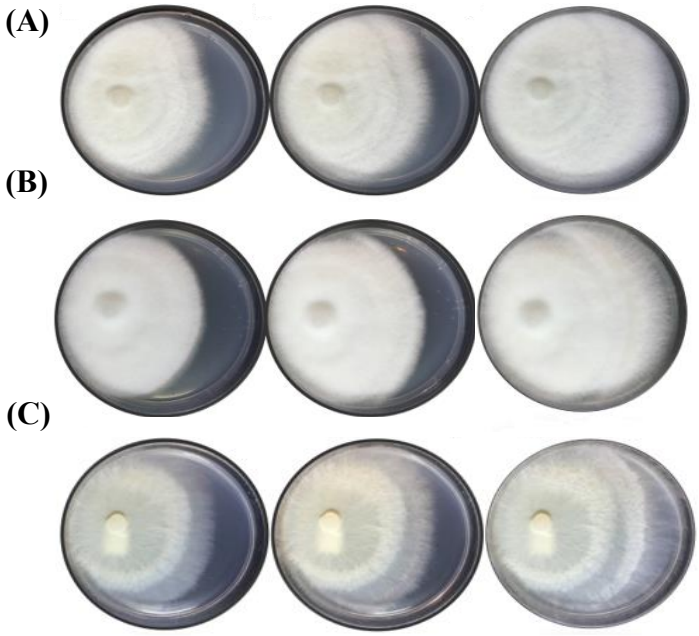

Figure 1.1. Petri dishes of selected fungi after growth on solid media (Czapek) for 9, 10 and 13 days; (A) *F. solani* CSP-5b, (B) *F. oxysporum* CSP-19b and (C) *F. oxysporum* CSP-R18.

After metabolite extraction and clean-up process, each sample replicate was weighted, showing that the higher DNA density in *F. oxysporum* led to an extraction 6 times higher than *F. solani*. Once *F. oxysporum* produced 112.61 mg (replicate a), 128.45 mg (replicate b) and 136 mg (replicate c) of EtOAc extract, *F. solani* only displayed 16.18 mg (replicate a), 22.76 mg (replicate b) and 26.43 mg (replicate c).

3.2.Chemical Profile of Analysis of F. solani and F. oxysporum

The preprocessed ^{1}HNMR spectra of *F. oxysporum* (CSP-19b and CSP-R18) and *F. solani* (CSP-5b) revealed the high complexicity of both metabolic profiles (Figure 1.2).

Spectra of both species present high overall similary, with small differences only in the aromatic and aliphatic regions, highlighting the necessity of an algorithm that recognizes important chemical shifts from complex data.

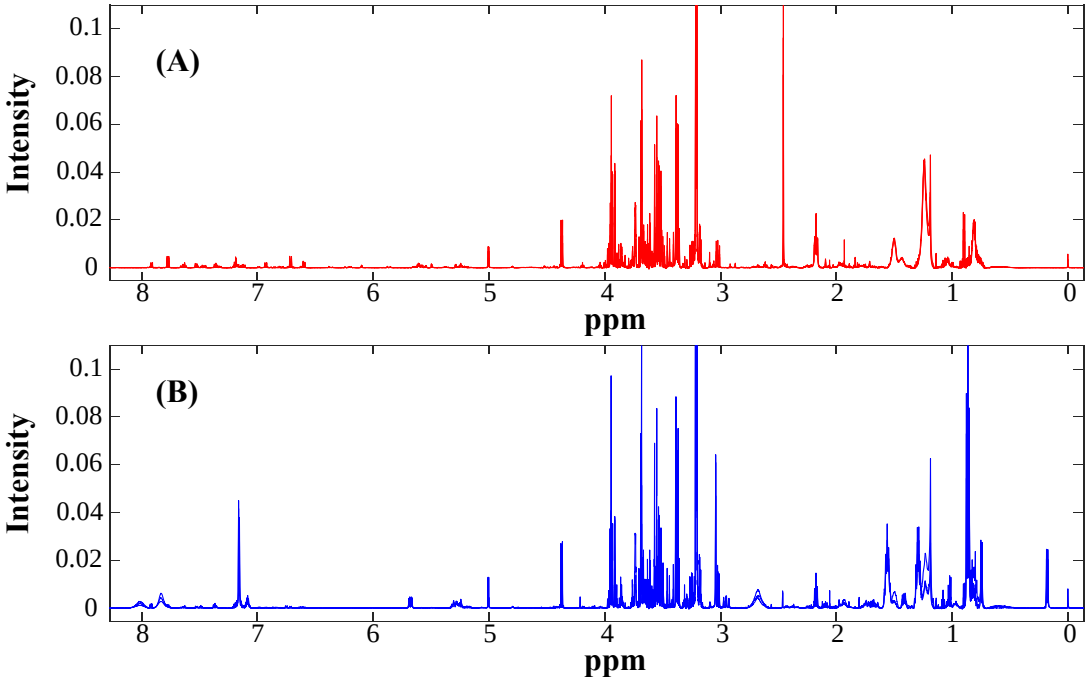

Figure 1.2. ^{1}HNMR spectra of fungal replicates before preprocessing treatment. For the multivariate data analysis, region from 3 to 4 ppm was removed. **(A)** Overlap of 7 spectra from *F. solani*'s replicates. **(B)** Overlap of 6 spectra from *F. oxysporum*'s replicates.

Primarily, hierarchical clustering was applied as the first unsupervised chemometric analysis, employed to check the similarity on the chemical data and to assure that the ^{1}HNMR replicates of both fungi were similar among themselves and reliable for comparison among each other. HCA results, abridged as a dendrogram (Figure 1.3), shows two major clusters, each related to one *Fusarium* species, illustrating the statistical difference between them, further explored on PCA. Moreover, all sample and instrumental replicates presented very high similarity among themselves, indicating low standard deviation and, consequently, little difference on metabolite production.

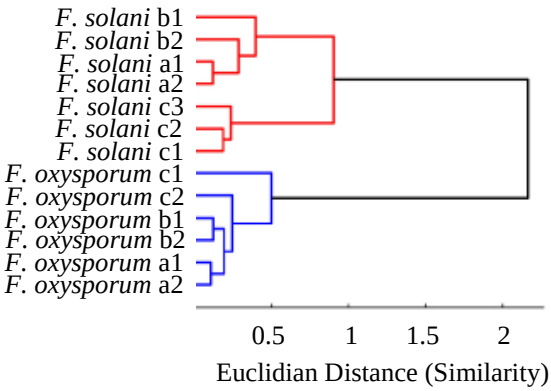

Figure 1.3. HCA dendrogram of ^{1}HNMR spectra of *F. solani* and *F. oxysporum* extracts. Samples replicates are represented by letters (a, b and c) and experimental replicates are represented by numbers (1 and 2).

Following the HCA analysis, ^{1}HNMR data was submitted to Principal Component Analysis (PCA). When conducting PCA without binning the data, it is possible to observe the projection of a real NMR peak shape, expressed on the loading values of the respected principal component (PC). On this unsupervised analysis, chemical composition from metabolic profiles influences the PCs, enabling the separation of samples in a multidimensional space, observed on the PCA score plots. In general, different PCs comprise different loading values, which means that each loading component could have one or more chemical substances that are responsible to organize the samples in a multidimensional space (BRO; SMILDE, 2014; CANDES et al., 2011; JOLLIFFE, 2002).

The grouping pattern observed on HCA was repeated on PCA, with two distinguished groups easily observed on the score plot for PC1 and PC2 values (total variance of 93%). Principal component 2 was the PC that best chemically differentiates both fungi, with *F. oxysporum* samples arranged in the positive values and *F. solani* samples placed in the negative PC2 values (Figure 1.4 A). Analysis of the PC2 loading plot clearly revealed that the positive values were highly similar to the original ^{1}HNMR spectra of *F. oxysporum*, while the negative values were remarkably close to *F. solani*'s (Figure 1.4 B). Hence, at the end of the chemometric analysis, PCA was a reliable tool for species discrimination and the selection of important chemical shifts that will be further analyzed by the dereplication algorithm.

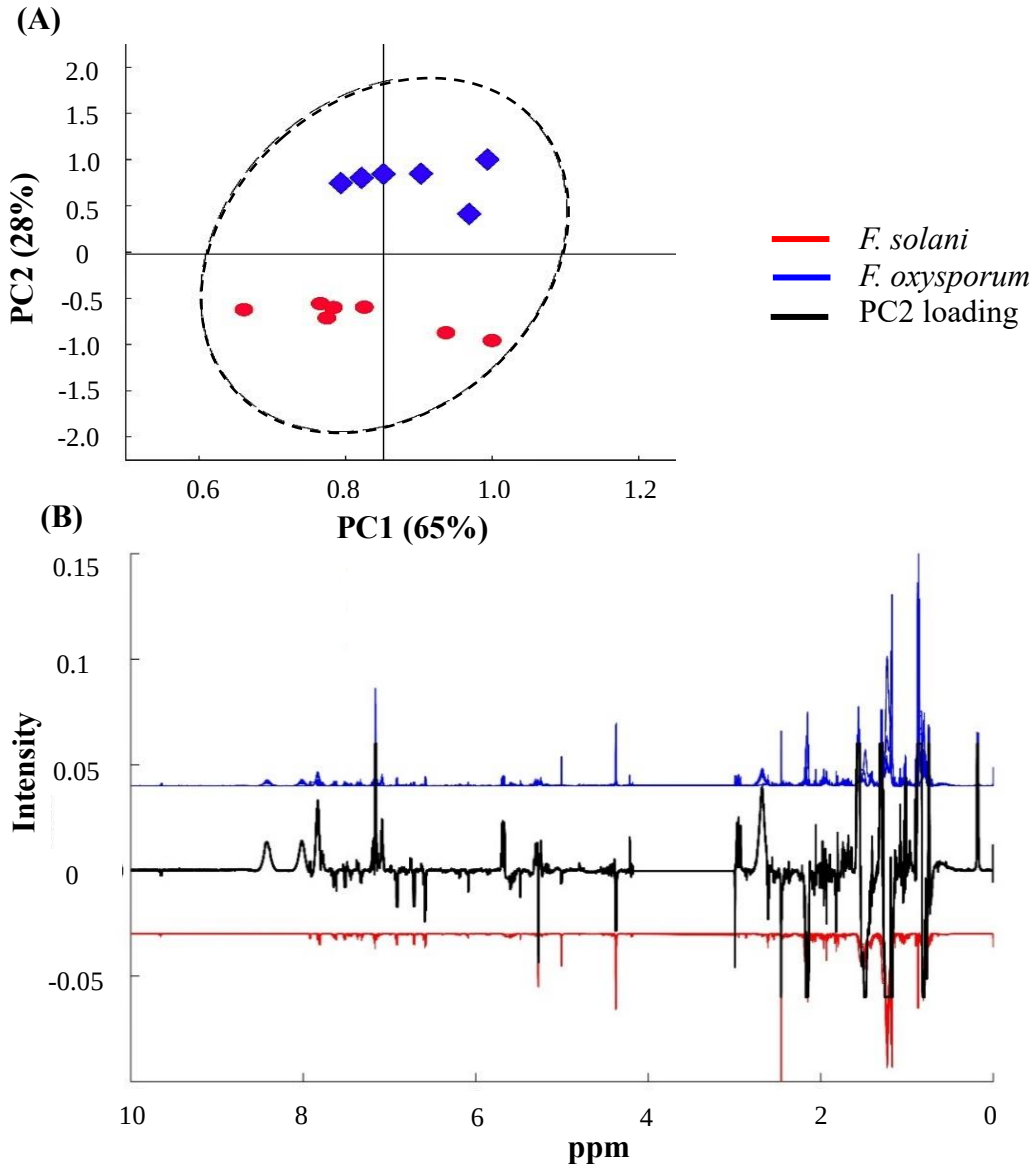

Figure 1.4. (A) PCA score plots of ^{1}HNMR spectra of *F. solani* and *F. oxysporum* extracts (PC1 x PC2, Total variance of 93%); 95% of confidence interval. **(B)** PCA C2 loadings plot of ^{1}H NMR spectra of *F. solani* and *F. oxysporum* matrices (total variance of 28%), in black; ^{1}HNMR spectra of replicates from *F. oxysporum* (blue, both strains CSP-R18 and CSP-19b) and *F. solani* (red and inverted, strain CSP-5b) after preprocessing treatment.

3.3. Dereplication Algorithm Description

The dereplication method can use as input data the loading values of PCA or PLS-DA analysis. For this particular example, loading values of PC2 best separated both *Fusarium* species and were used for further computational analysis.

(1) The first step of the algorithm is to make a cut on the positive and negative loading values of the selected PC based on the threshold cut. This threshold cut is made to avoid the selection of noise and minor signals, targeting only possible chemical shifts from compounds that best chemically separate the samples at a particular PC. The pre-selected threshold can be optimized for each analysis according to the purpose of study and the number of spectral regions you wish to select. Since the threshold could be any value between the minimum and the maximum intensity of the respective loadings, different tests can be performed to obtain an optimum cut that comprises the most intense signals. For PC2 loading, threshold cuts were performed at 20% of the maximum, for positive values, and 8% of the minimum, for negative ones (Figure 1.5).

(2) The second step was to identify the maximum and minimum values in the selected regions after the threshold cut, which are used in the algorithm to create ppm blocks (binning). The maximum values determine the number of peaks (signal multiplicity) in the selected region, while the minimum values identify the starting and the ending point of each ppm block. Figure 1.5 shows the selected chemical shits from the positive (green diamond) and negative (pink circle) PC2 loading values and the threshold cut (red dashed line) used for both parts. The maximum difference between peaks to create the signal blocks was 0.05 ppm, totaling six regions from positive values and 12 regions from negative numbers, which are evaluated on step 3.

(3) The third step is crucial for the dereplication analysis and consists in extracting, from the entire ^{1}HNMR spectra, the exact chemical shift region of each ppm block identified on the previous step. For this, the intensities of these extracted blocks are individually correlated with the fungi ^{1}HNMR spectra that have the same chemical shift values. As expected, all six regions from the positive loading values were highly correlated to *F. oxysporum* ^{1}HNMR spectra (Figure 1.6 a-f), while all 12 regions from the negative PC2 loading values were highly correlate to *F. solani* ^{1}HNMR spectra (Figure 1.6 g-r). Only four of the twelve regions selected from the negative values were used for further evaluation, since regions that corresponds to signals from Czapek-broth (identified by comparison with Czapek blank spectrum) were excluded from the analysis.

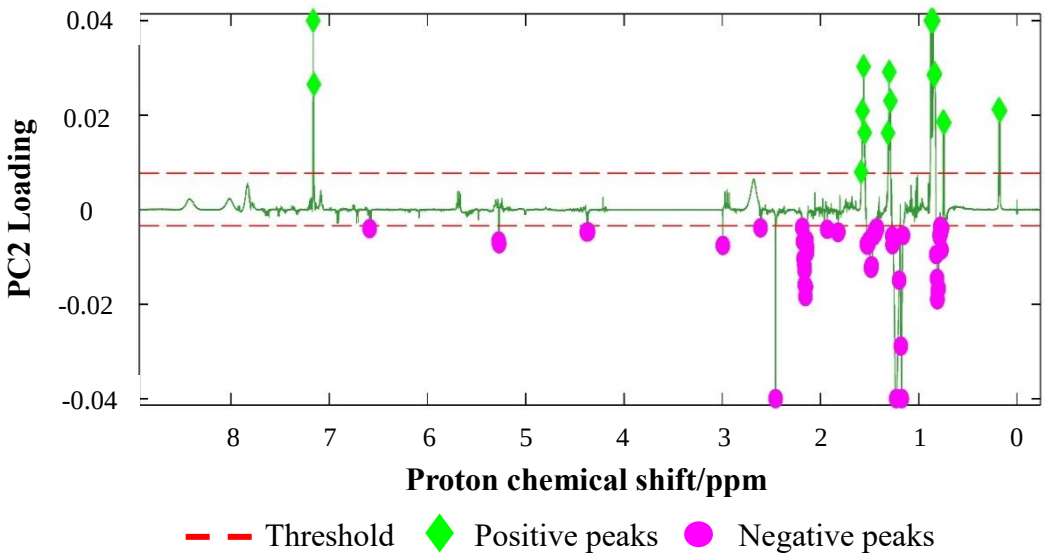

Figure 1.5. PCA loading plot for principal component 2 (PC2); Threshold cut for positive and negative are shown as red dashed line. The peaks that were used to create the chemical shift blocks are shown in green diamond, for the positive part, and magenta circle, for the negative part.

(4) Lastly, once the correlations values between loadings and ^{1}HNMR spectra are established, the ppm blocks are separated in two groups: highly and poorly correlated to the loading regions. The correlation to stipulate highly and poorly correlated groups is set in the algorithm input and can be optimized according to the matrix complexity. The correlation threshold between the PC2 loadings blocks and the samples blocks was 75% and 71% to the positive and negatives loading values, respectively. Highly correlated from positive and negative loading analysis can be observed in Figure 1.7 (a – f) and Figure 1.7 (g-j), respectively.

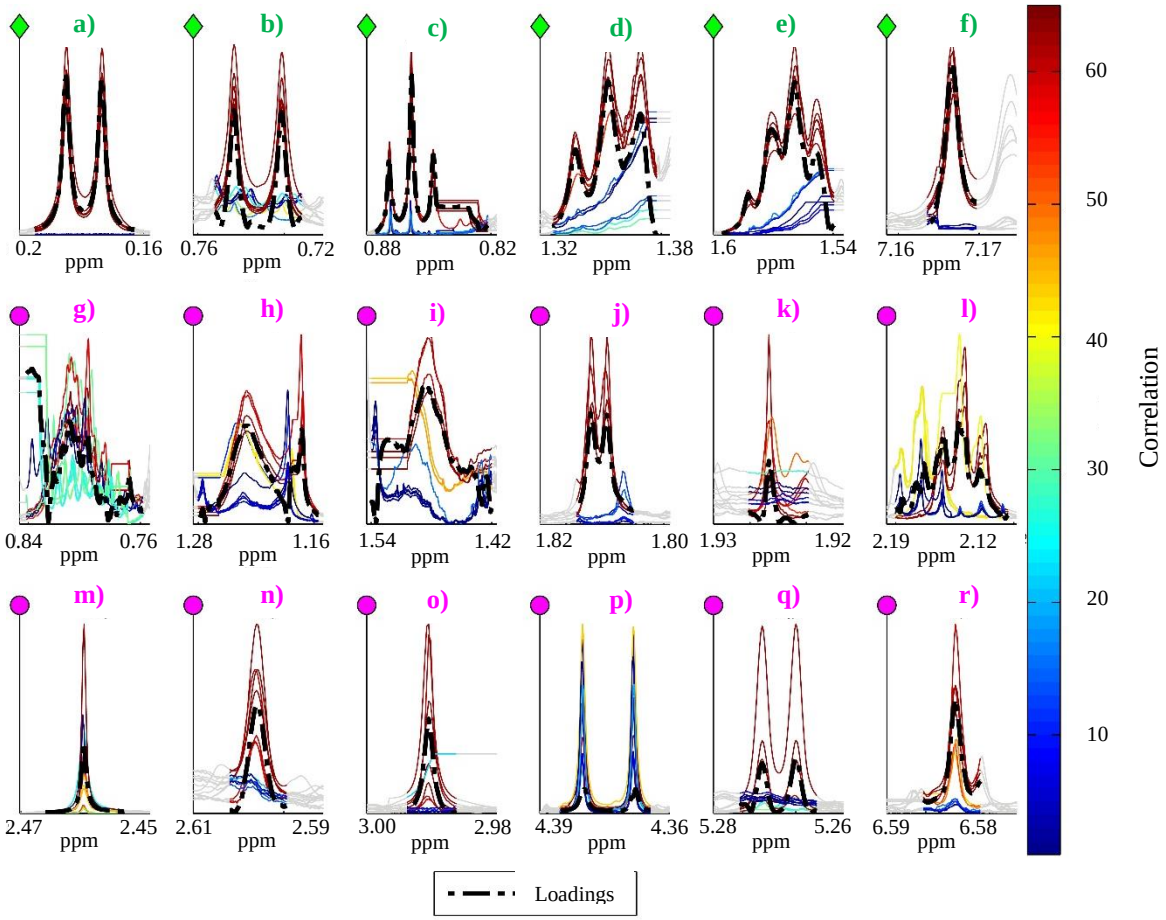

Figure 1.6. In color, the [1]HNMR chemical shift blocks identified and extracted from spectra matrix (gray). The colors from blue to red, in a jet scale, represent the correlation values between spectra regions and PC2 loadings region in percentage values. From a) to f) are the chemical shift regions identified by the positive part of the PC2 loadings and from g) to r) are the chemical shift regions identified by the negative part of the PC2 loading.

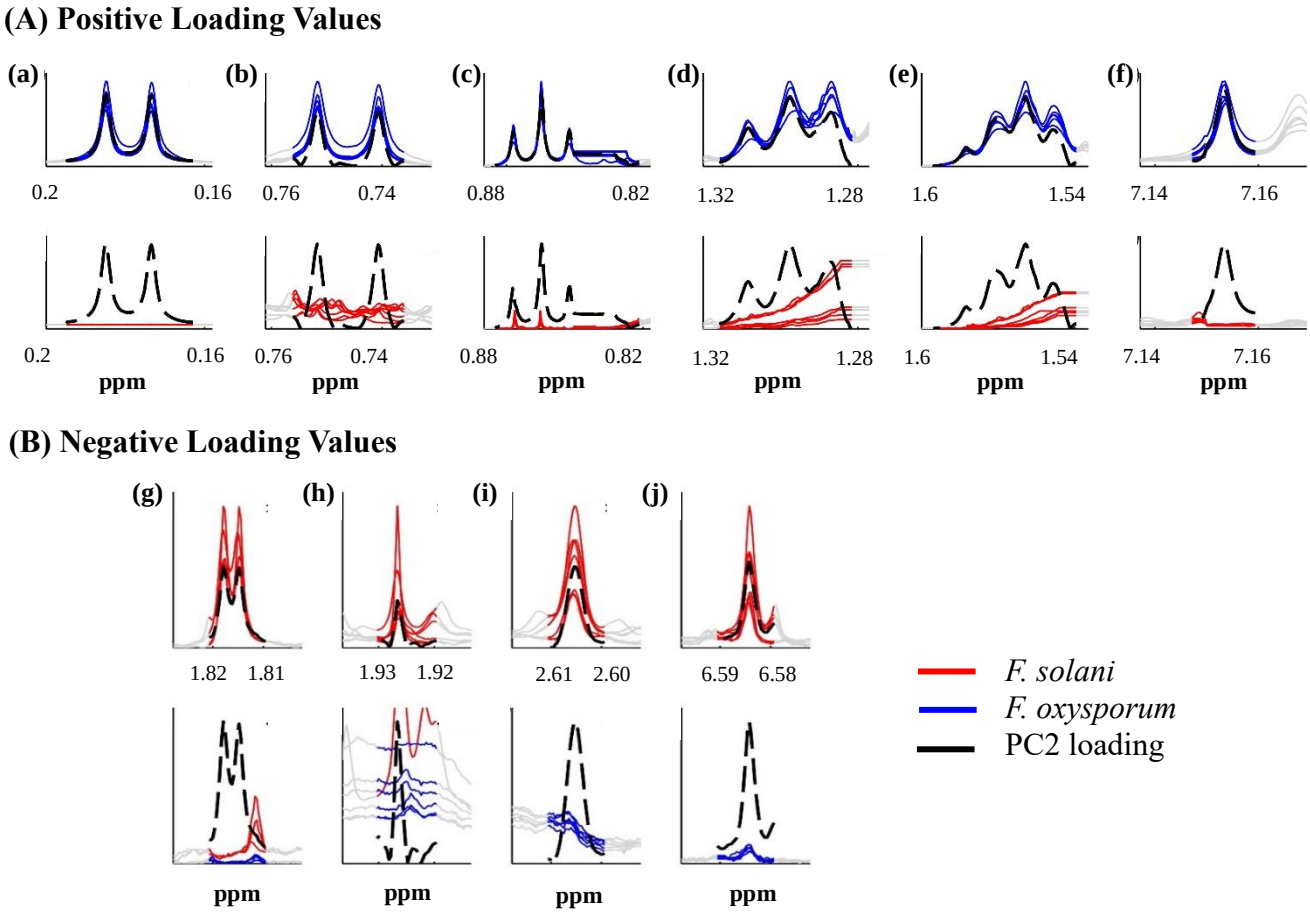

Figure 1.7. (A) Positive Loading Values: regions isolated from the positive part of the PC2 loadings overlapped with the ^{1}HNMR-spectra. The two statically relevant groups are shown in the first (peaks with high correlation >71%) and second (peaks with low correlation <71%) rows. **(B)** Negative Loading Values: region for the negative part of the PC2 loadings overlapped with the ^{1}HNMR-spectra. The two statically relevant groups are shown in the first (peaks with high correlation >75%) and second (peaks with low correlation <75%) rows.

At the end of the method, and as a direct result of PCA separation, ten important ^{1}HNMR regions were extracted from positive and negative loading values, which were submitted to molecule elucidation. An optional and sequential step for the algorithm is to set the intensity of the highly correlated ^{1}HNMR signals to the noise intensity (near zero) and then re-calculate the algorithm, enabling the dereplication of additional molecules on the sample. Figure 1.8 shows the results of the algorithm at the end of the first run. a) and d) are the isolated ^{1}HNMR peaks with high PC2 correlations; b) and c) are the matrices for both fungi species after the peak's subtractions. The peaks are selectively removed from each fungi matrix showing how the algorithm can successfully dereplicate a complex mixture. In fact, this whole procedure, from the PCA calculation to signal isolation can continue automatically until most of the signals are identified and grouped, providing a reliable and statistical dereplicate procedure.

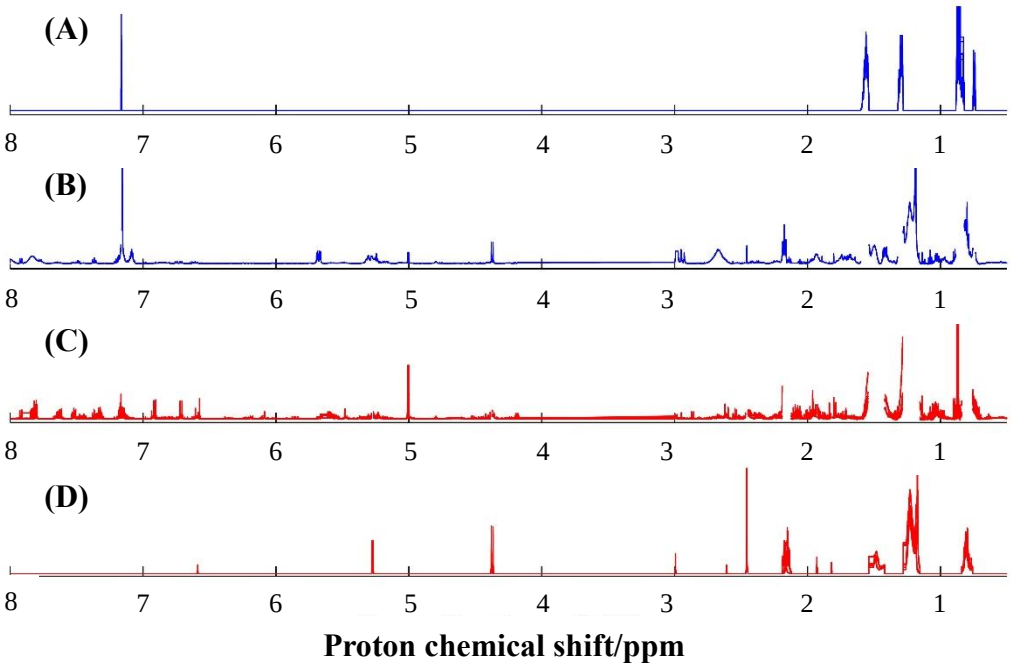

Figure 1.8. (A) ^{1}HNMR signals extracted by the correlation with the positive part of PC2 loadings and are related to the *F. oxysporum*. **(B)** Overlapped ^{1}HNMR spectra of *F. oxysporum* crude extracts after extraction of the selected peaks. **(C)** Overlapped ^{1}HNMR spectra of *F. solani* crude extracts after extraction of the selected peaks. **(D)** ^{1}HNMR signals extracted from the correlation with the positive part of PC2 loadings and are related to the *F. solani*.

3.4. Molecule elucidation

Peaks selected on the dereplication method were submitted to one-dimensional TOCSY, enabling the identification of spin systems from the corresponding molecule. Those spin system were then compared to the *in-house Fusarium* database for molecule elucidation and confirmed through 2D NMR experiments, high resolution MS and tandem MS.

3.4.1. Positive loading values

Six peaks were selected from the positive loading values (*F. oxysporum*) and submitted to 1D-TOCSY: δ 0.16 (*d*, 3H, *J* 7 Hz), δ 0.76 (*d*, 3H, *J* 6.6 Hz), δ 0.86 (*t*, 3H *J* 7.0 Hz), δ 1.29 (*m*, 2H), δ 1.56 (*m*, 2H) and δ 7.16 (*m*, 5H). 1D-TOCSY experiments revealed that all six chemical shifts belong to three spin systems, showed in Table 1.1. These spin systems were then manually compared to the in-house *Fusarium* database, suggesting the presence of two secondary metabolites commonly found in *F. oxysporum*. Spin systems I and II indicated the presence of beauvericin, a hexadepsipeptide from the enniatin family formed altering hydroxy-*iso*-valeryl (spin system II) and methylphenylalanyl (spin system I – aromatic portion), while spin system III was compatible to the saturated long chain substituent of fusaric acid, a picolinic acid derivative mycotoxin (Figure 1.9 A).

Spin system	Chemical shifts	Molecule
I	1D TOCSY: δ 7.17 – 7.05 (*d*, 5H)	Beauvericin
II	1D TOCSY: δ 0.15 (*d*, 3H, *J* 6.9 Hz); δ 0.75 (*d*, 3H, *J* 6.6 Hz); δ 1.7 (*m*, 1H), δ 4.7 (*d*, 1H, *J* 8.9 Hz)	Beauvericin
III	1D TOCSY: δ0.86 (*t*, 3H *J* 7.0 Hz), δ1.29 (*tq*, 2H), δ1.56 (*tt*, 2H), 2.66 (*t*, 2H)	Fusaric Acid

Table 1.1. 1D-TOCSY of selected peaks from dereplication method. Evaluation of the positive PC2 loading values correlated to *F. oxysporum*.

For confirmatory analysis, the presence of additional molecule signals and their spin-spin interactions were evaluated using HSQC, HMBC, 1D-TOCSY and 1D-NOESY from crude extract. Beauvericin showed additional spin systems from alanyl group, which correlates to system I on HMBC and it is formed by two diastereotopic hydrogens at δ 2.94 (*dd*, 1H, *J* 14.7, 12.8 Hz) and δ 3.29 (*dd*, 1H, *J* 14.7 and 4.6 Hz) as well as one hydrogen bonded to a tertiary carbon at δ 5.70 (*dd*, 1H, *J* 12.7 and 4.5 Hz). 1D-NOESY showed the correlation between the singlet at δ 3.05 (*s*, 3H) and spin system II. Fusaric acid also revealed an additional spin system from the pyridine ring correlated with system I on HMBC, which comprises in both aromatic signals δ 7.80 (*d*, *J* 8.2 Hz, 1H) and δ 8.01 (*d*, *J* 8.2 Hz, 1H), suggesting a *para*-substituted pyridine ring.

Confirmatory LC-DAD-ESI-HRMS/MS of *F. oxysporum* extract was performed according to the seven golden rules by Kind and Fiehn (KIND; FIEHN, 2007) and showed that fusaric acid appears at 12.3 minutes of an exploratory 50-minute gradient run, displaying two intense peaks $[M+H]^+$ *m/z* 180.0959 (error of < 1 ppm) and $[M+Na]^+$ *m/z* 202.0770 and two neutral loss fragmentation *m/z* 162.0860 and *m/z* 134.0921 related to a loss of water $[M-H_2O+H]^+$ and carboxyl group $[M-COOH+H]^+$, respectively. ESI-MS/MS analysis of fusaric acid revealed a dominant fragment of *m/z* 152.05, agreeing with data previously described in literature (BROWN et al., 2012; HU; RYCHLIK, 2012). Beauvericin appeared at 35.8 minutes with intense peaks $[M+H]^+$ *m/z* 784.3895 (error of < 3 ppm) and $[M+Na]^+$ *m/z* 806.3698. Tandem MS showed three main fragments *m/z* 541.29, *m/z* 523.27 and *m/z* 262.10, related to $[Dimer+H+H_2O]^+$, $[Dimer+H]^+$ and $[Monomer+H]^+$, respectively (BROWN et al., 2012; HU; RYCHLIK, 2012).

3.4.2. Negative loading values

Since the growth of *F. solani* in Czapek-Broth is slower than *F. oxysporum*, easily observable by the difference in mycelium size and density, it was expected that crude extracts from *F. solani* showed a higher concentration of free sugars from liquid medium and fatty acid esthers derivate from fungus primary metabolites that could interfere on the PCA analysis. In fact, out of the twelve peaks selected by the dereplication method, only four were secondary metabolites signals. Table 2 shows the molecules elucidated from the eigth excluded regions by comparison with NMR-data from Human Metabolome Database (WISHART et al., 2007), following procedure described by Bubbs (BUBB, 2003). Furthermore, detailed evaluation of the chemical data also revealed the

stereoisomers alpha-glucose by the irradiation of the anomeric proton at δ 5.01, correlating the chemical shifts δ 5.01 (*d*, 1H, *J* 3.8 Hz) δ 3.67 (*m*), δ3.57 (*m*, 1H), δ 3.25 (*dd*, 1H, *J* 3.8 Hz) and δ 3.19 (*m*, 1H) to the same spin system.

Chemical shifts	Molecule
δ 1.24 (*m*, 16H), δ 1.50 (*m*, 5H), δ 2.15 (*m*, 18H), δ 0.88 (*m*), δ 2.45 (*s*, 4H)	Fatty Acid Esther
δ 3.02 (*dd*, 4H, *J* 9.2 and 7.8Hz), δ 4.37 (*d*, 4H, *J* 7.8Hz), δ 3.75 (*dd*, *J* 11.3 Hz, 4H), δ 3.55 (*m*, 4H), δ 3.18-3.24 (*m*)	β -glucose
δ 5.29 (*d*, 1H, *J* 3.8Hz), δ 3.67 (*m*, 1H), δ 3.57 (*m*, 1H), δ 3.25 (*m*, 1H), δ 3.19 (*m*, 1H)	fructose

Table 1.2. Chemical shifts of primary metabolites found in *F. solani* AcOEt extract.

1D-TOCSY proved to be greatly challeging, due to the very small intensity of the of the four remaining peaks. HMBC suggested the presence of a 1,4-disubstituted phenyl ring system through the correlation of δ 6.59 (*d*, *J* 6.8Hz, 2H) with δ 6.93 (*d*, *J* 6.8Hz, 2H). Additionally, δ 6.93 also correlated with the diastereotopic hydrogen at δ 2.61 (*m*, 1H). Comparison with ^{1}HNMR-data from the *in house Fusarium* database suggested the depsipeptide HA 23 (Figure 1.9 B), isolated by Feng et al (FENG et al., 2002). This unusual peptide is formed by a pipecolinic acid and *O*-prenyl-substituted tyrosine residues and a polyketide chain. Confirmatory LC-DAD-ESI-HRMS of *F. solani* extract showed HA23 depsipeptide at 43.0 minutes on an exploratory 50-minute gradient, with three intense peaks $[M+H]^+$ *m/z* 601.3465 (error of < 4 ppm), $[M+Na]^+$ *m/z* 623.3262 and $[M+K]^+$ *m/z* 639.2986. No fragmentation pattern has ever been reported for this molecule, thus, for molecular confirmation, purification and isolation procedure are necessary.

(A) *F. oxysporum* **(B)** *F. solani*

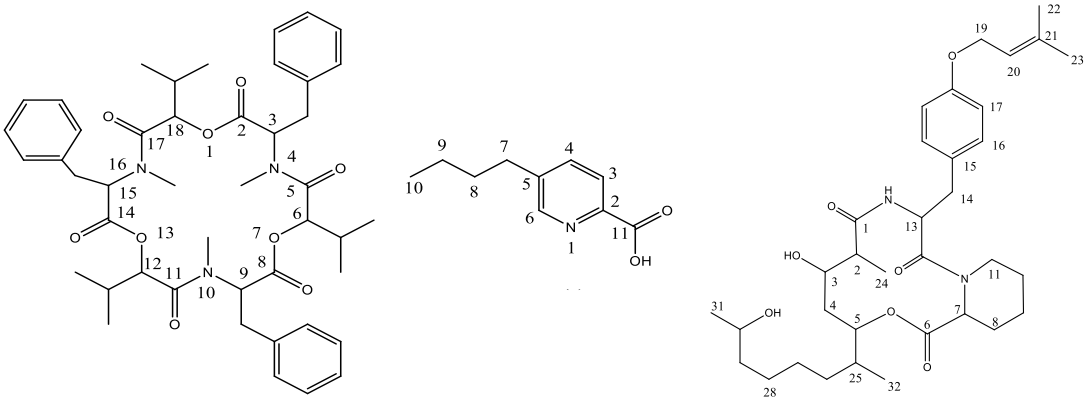

beauvericin fusaric acid HA23

Figure 1.9. (A) Chemical structure of secondary metabolites from *F. oxysporum* beauvericin and fusaric acid. **(B)** Chemical structure of secondary metabolite HA23 from *F. solani*.

4. Conclusions

PCA was sucessifully chosen for the discrimination of *Fusarium* species, allowing separation of *F. oxysporum* and *F. solani*, even in highly similar matrices. Using the loading values for the PC that best separated *F. solani* and *F. oxysporum*, the algorithm automatically identified and extracted ^{1}HNMR shifts from a complex chemical profile, enabling the identification of known secondary metabolites, including (a) hexadepsipeptide beauvericin and (b) fusaric acid, found in *F. oxysporum*, and (c) depsipeptide HA23, found in *F. solani*. Aditionally, the algorithm was also able to identify free sugars from Czapek-Broth (d) β-glucose and (e) fructose, as well as esther fatty acid from primary fungi metabolim.

The development of an *in house Fusarium* database was a crucial step for molecule elucidation, enabling the comparison of known spin system and the 1D-NMR-data obtained from a complexe matrix. Furthermore, the identification of three mycotoxin as major metabolites from fungi isolated from a healthy rizhosphere show the region competitivity and the importance of future studies regarding the discovery of new bioactive compounds.

Aditionally, as a result of PCA separation, the chemical shifts that best contributed to the *Fusarium* species chemical differences are related to compounds that are majorly found in one particular species, being an excellent methodology for chemotaxonomy and biomarkers search.

CHAPTER 2. DEREPLICATION OF MAJOR SECONDARY BY MASS SPECTROMETRY (MS)

Article title: Dereplication of Secondary metabolite from *Fusarium* species by mass-spectrometry.

Journal: Journal of the Brazilian Chemical Society (JBCS).

Status: Unpublished.

Authors: Denise M. Selegato[a] and Ian Castro-Gamboa[a*]

Affiliations:

[a] Nuclei of Bioassays, Ecophysiology and Biosynthesis of Natural Products (NuBBE), São Paulo State University (UNESP) – Araraquara, SP**,** Brazil.

Justification:

In metabolomics, some analytical issues related to the identification and quantification of metabolites in complex matrices remain a cornerstone in natural products research. Some examples of difficulties encountered in metabolic analysis include the constant re-isolation of inactive or known chemotypes, the polarity-related structural complexity and the wide metabolic dynamics, hampering chemical identification and biological correlation of these complex data.

To overcome these limitations, dereplication strategies often use more than one analytical technique, targeting to provide a comprehensive and precise response of the metabolome. Among the most common techniques in metabolomics, the integration of liquid and gas chromatography coupled with mass spectrometry (LC-MS and GC-MS) has shown to minimize the individual technical limitations and increase separation, detection, stability, sensitivity and amplitude of the detection range. Moreover, the identification of secondary metabolites in complex natural matrices by MS presents advantages to the univariate approaches of purification and isolation due to its versatility, speed and use of smaller amounts of sample, providing molecular information and composition of these metabolites.

Abstract

In metabolomic studies applied to natural products, dereplication has recently become of fundamental importance to achieve an accurate chemical response, aiming mainly to decrease complexity of crude extracts and facilitate the identification of biologically active compounds. In a dereplication study, experimental data is conventionally compared with spectroscopic and spectrometric data from known molecules, avoiding the re-isolation of known substances and ensuring rapid prioritization of promising extracts. Notwithstanding these advantages, to this date, no analytical technique has been able to dereplicate the entire chemical composition of the metabolome and, most of the times, requires the use of complementary, highly sensitive and robust analytical methods. In this chapter, the monoculture extracts of *F. oxysporum* and *F. solani* were submitted to mass spectrometry dereplication methods, aiming to identify their major chemotypes. For this, crude extracts were analyzed by liquid (LC-DAD-ESI(+)-HRMS) and LC-DAD-ESI-MS/MS) and gas chromatography (GC-EI-MS), followed by comparison of these data with those of known molecules from the literature. Results show that MS dereplication ensured a comprehensive view of metabolic production, identifying 16 different metabolites. The LC-MS dereplication identified seven major compounds for three *Fusarium* strains (*F. oxysporum* strains CSP-19b and CSP-R18 and *F. solani* strain CSP-5b), including alkaloids, picolinic acid analogues and the metabolites previously identified by NMR. Moreover, GC-MS analysis was able to identify ten different compounds, highlighting picolinic acid derivatives and primary metabolites, such as organic and secondary alcohols and acids.

Keywords: dereplication, mass spectrometry, LC-MS, GC-MS, *Fusarium*, metabolomics

1. Introduction

Metabolomics can be described as the study of quantitative and qualitative metabolic responses of an organism subject to different life routines, environmental stimuli or genetic modulations (NICHOLSON; LINDON, 2008; OLIVER et al., 1998; WAGNER; SEFKOW; KOPKA, 2003). Although recently described in the late 1990s, metabolomics conceptual basis is embedded in systems biology - an approach that treats organisms as integrated systems, measured through multifactorial quantitative responses.

In chemistry, the application of metabolomics has become a golden strategy for chemical fingerprinting and has emerged by the combination of different technological factors, including advances in high throughput analysis in both separation and detection; computational development (processors and memories capable of allocating and calculating large volumes of data) and the adequacy of statistical methods and pattern recognition, initially developed for the field of economics and later adapted for the acquisition, analysis and treatment of sets of data in biological systems (AKSENOV et al., 2017; DA SILVA et al., 2018; HONG et al., 2016; JORGE et al., 2016).

Specifically, in metabolomic applied to natural products, the development of computational tools has recently become of fundamental importance to achieve an accurate chemical response, aiming mainly to decrease complexity of crude extracts and facilitate the selection of promising samples or potential bioactive compounds (NG et al., 2009; WOLFENDER et al., 2009).

Among these strategies, dereplication has emerged as a rapid way of identifying known compounds, facilitating the detection of bioactive chemotypes and decreasing the redundant isolation of known secondary metabolites found in crude extracts. When compared to univariate approaches, dereplication can be considered a faster, greener, less expensive and less destructive alternative, decreasing the cost and the use of organic solvents to provide a better and more accurate procedure for bioactive sample selection (NG et al., 2009; WOLFENDER et al., 2009).

Conventionally, dereplication studies are based on the comparison of experimental data with robust databases, which contains spectroscopic, spectrometric and physico-chemical properties of isolated or predicted molecules. However, due to technical limitations, no analytical methods has been able to analyze the entire chemical composition of the metabolome, requiring the use of complementary, highly sensitive and robust analytical methods (ZHANG et al., 2012). For example, the integration of liquid

and gas chromatography coupled with mass spectrometry (LC-MS and GC-MS) have shown to minimize their individual technical limitations and increase separation, detection, stability, sensitivity and amplitude in the detection range. Moreover, for the identification of secondary metabolites in complex matrices, mass spectrometry (MS) coupled with separation techniques also presents advantages to the univariate approaches due to the speed and use of smaller amounts of sample, avoiding the re-isolation of known substances and ensuring rapid prioritization of extracts. Given MS is a highly sensitive technique, its use can provide molecular information through high resolution mass, fragmentation profiles and isotopic patterns.

After the selection of the fungi from the rhizosphere of *S. spectabilis* and the identification of the major compounds by NMR, the same extracts obtained in Chapter 1 from the monocultures of *F. oxysporum* (strains CSP-19b and CSP-R18) and *F. solani* (CSP-5b) were submitted to mass spectrometry dereplication, aiming to identify other major chemotypes produced by these *Fusarium* strain. For this analysis, crude extracts were submitted to liquid (LC-DAD-ESI(+)-HRMS) and LC-DAD-ESI-MS/MS) and gas chromatography (GC-EI-MS). Metabolite identification was conducted by comparison of these experimental data with those of known molecules from the literature. All the analysis of LC-MS was carried out at the Faculty of Pharmaceutical Sciences of the University of São Paulo (USP), campus of Ribeirão Preto, in collaboration with Prof. Dr. Norberto Peporine Lopes, while the CG-MS analysis was conducted at the Institute of Chemistry of Araraquara, São Paulo State University (UNESP).

2. Materials and Methods

2.1. Dereplication by LC-DAD-ESI-HRMS and LC-DAD-ESI-MS/MS

2.1.1. LC-DAD Method Optimazation

The extracts used for this chapter were prepared according to the method described in chapter 1 (topic 2.3). For the initial analysis of the chemical profile (footprinting), the extracts were submitted to chromatographic run on Shimadzo Class-LC 10 and Diodes Array Detectors (DAD) with wavelength from 190 to 800 nm. The method optimization was performed by a systematic variation of chromatographic parameters, in which exploratory runs were performed according to a complete factorial planning (Table 2.1). In this Design of Experiments (DoE), three variables were evaluated in two different levels (2^3 = 8 experiments): **(v1)** mobile phase flow rate (0.8 e 1.0 mL min^{-1}), **(v2)**

presence of acid additives (formic acid in concentrations of 0.1% and 0.05%) and **(v3)** organic solvent gradient time (40 and 50 minutes).

The best system was selected based on the highest number of detected peaks, as well as the best chromatographic resolution, evaluated by individual analysis of peak shape (efficiency), peak separation (selectivity) and column retention in every individual experiment. The changes in organic solvent gradient provides major change in retention (k) and moderate selectivity (α). The pH of the mobile phase ensures adjustment in both retention (k) and selectivity (α), as well as a moderate effect on efficiency (number of theoretical plates or N). Lastly, the flow rate of the mobile phase, while not important for retention or selectivity, promotes a moderate adjustment of efficiency.

Variables	**Description**	**Low Level (-1)**	**High Level (+1)**
V1	Mobile Phase Flow Rate	0.8 mL min^{-1}	1.0 mL min^{-1}
V2	Acid additives	0.05%	0.1%
V3	Gradient Time	40 minutes	50 minutes
Exp.	**v1**	**v2**	**v3**
1	1	1	-1
2	-1	1	1
3	1	1	1
4	-1	1	-1
5	1	-1	-1
6	-1	-1	1
7	1	-1	1
8	-1	-1	-1

Table 2.1. Description of the variables and experimental arrangement for the complete factorial planning of the fungal extracts, performed to optimize the chromatographic method.

All samples were prepared using 1.00 mg mL^{-1} of fungal extracts using the following acquisition parameters: mobile phase was ultra-pure Mili-Q (pump A, aqueous solvent) and MeOH (pump B, organic solvent); stationary phase was Kinetex C18 100R (Phenomenex), 150 x 4.60 mm and injection volume of 20 µl. For the 40-minutes exploratory gradient, the elution ramp was: 5% to 100% B in 40 minutes, 40-50 minutes in 100%, 50-55 minutes 100-5% and 55-75 minutes remaining in 5 % for the rebalancing of the column. Similarly, for the 50-minutes exploratory gradient, the organic solvent

gradient was 5% to 100% B in 50 minutes, 50-60 minutes in 100%, 60-65 minutes 100-5% and 65-75 minutes remaining in 5% for the reconditioning of the column.

For the LC data processing, all the chromatograms were exported in ASCII and preprocessed in MATLAB R2014a software. The processing steps comprised on baseline correction by airPLS algorithm (ZHANG; CHEN; LIANG, 2010), CCOW alignment (constrained correlation optimized warping) (TOMASI; VAN DEN BERG; ANDERSSON, 2004) and normalization by total area.

2.1.2. LC-DAD-ESI-HRMS and LC-DAD-ESI-MS/MS Acquisition

The high-resolution analysis (LC-DAD-ESI-HRMS) used the optimized chromatographic method in a Shimadzu LC-20 ternary analytical chromatograph. The column eluent was divided using a 5:1 splitter, with the largest flow being directed to the DAD detector and the remainder to the mass spectrometer at a flow rate of 150 μL min^{-1}. MS detection was performed in UltrOToF (Bruker) with positive ionization mode and Q-ToF analyzer at the following parameter: 3 kV capillary probe, 25 V cone; N_2 gas for nebulization, flow rate at 345 L h^{-1} and 27 L h^{-1} and temperature of 180 °C. Calibration was performed through addition of trifluoroacetic acid solution (Na-TFA, 10 mg mL^{-1}) at the beginning and end of each chromatographic analysis.

For the fragmentation analysis, LC-DAD-ESI-MS/AutoMS data were acquired in a Bruker AmaZon Speed using electrospray ionization (ESI) in the positive mode and ion trap analyzer at the following parameters: nebulizer pressure 70 psi, drying gas flow 12.0 L min^{-1}, drying gas temperature 350 °C. The MS/AutoMS mode was carried out with cycles for positive MS1 acquisition, followed by fragmentation of the two most intense ions (above > 1000 counts).

2.2. Dereplication by CG-EI-MS

2.2.1. Sample Derivatization

Derivatization was conducted by methylation and silylation reactions. Methylation was performed to form oximes targeting to block the interconversion between the cyclic and acyclic structures of reducing sugars and, hence, avoid the formation of two different chromatographic peaks related to the same metabolite. Chemically, the conversion of aldehydes and ketones to oximes using methoxamine limits interconversion of C-N

bonding and protects the molecules from decarboxylation. Similarly, silylation reaction is a process that comprises hundreds of non-spontaneous, parallel and competing reactions between molecules of various chemical classes and the derivative agent. In this, the reactive hydrogen atoms are replaced by TMS groups, reducing the polarity of specific functional groups (-COOH, -OH, $-NH_2$, -NH, CO) (FIEHN, 2017; FRIAS; GRAMACHO; PINEIRO, 2014).

For the methylation reaction, 80 μL of methoxamine hydrochloride (20 mg mL^{-1} solution in pyridine) was added in 5.00 ± 0.1 mg of crude extract solubilized in 100 μL of pyridine. The solution was left for 90 minutes in a water-bath at 30 °C. Following, silylation was conducted by adding 200 μL of MSTFA (N-methyl-N- (trimethylsilyl) - trifluoroacetamide) and heating for 30 minutes at 37 ° C. Before acquisition, the resulting solution was filtrated using 0.22 μm filter and refrigeration at 5 °C for 24 hours.

2.2.2. GC-EI-MS Data Acquisition

GC-MS analysis was performed on a QP-2010 Shimadzu gas chromatograph equipped with AOC-5000 automatic injector (Shimadzu) and coupled with a mass spectrometer. Ionization was performed by electron ionization and mass analysis and detection was conducted by a single-quadrupole. Helium was used as a carrier gas and EN5MS (30 m x 0.25 μm x 0.25 mm) was used as a column. For the analysis, 1.00 μL of the derivatized samples were injected using 1:20 slip. The method was previously optimized at a GC-FID and used the following parameters: injector and detector temperatures at 270 °C and 320 °C, respectively and flow rate of 0.7 mL min^{-1}. The gradient used was: 3 minutes at 90 °C (isothermal); increase of 3 °C min^{-1} to 280 °C and 5 minutes at 280 °C (isothermal), totaling 71.33 minutes of running. MS detector parameters were: ionization energy at 70 eV; detection range of *m/z* 40-600; acquisition of 2 spectra/s and initial acquisition time at 4.0 minutes to avoid detector saturation with by-products. For calibration and tuning, autotune FC43 (perfluorotributylamine) was used according to the equipment specifications.

3. Results and Discussion

3.1. *Dereplication by LC-DAD-ESI-HRMS and LC-ESI-MS/MS*

High Performance Liquid Chromatography (HPLC or LC) is the most used analytical

technique for the acquisition of chromatographic profiles (fingerprinting or footprinting) (ERNST et al., 2014a). In this process, metabolic separation proceeds through the different states of equilibrium between analyte, the mobile phase (organic and aqueous solvents) and the stationary phase (chromatographic column), providing a compresenhive view of the chemical composition (ERNST et al., 2014b).

The first stage for the dereplication of *Fusarium* extracts by mass spectrometry coupled to liquid chromatography was the optimization of the chromatographic method. In literature, this process is commonly performed by modifying the run parameters, such as mobile phase flow, temperature, organic solvent gradient and concentration of additives.

For a more comprehensive evaluation of this process, in this study, each fungal extract was optimized by a complete factorial planning in which three variables were tested at two levels. This systematic variation occurred by modifying the percentage of acid additives, the gradient time of the organic solvent and the mobile phase flow rate. The system response was the number of detected peaks at 254 nm, in which the best parameters gave us the highest number of peaks. Moreover, in addition to the experimental design response, for each run, the chromatograms were individually evaluated for their signal resolution (selectivity, efficiency and retention), guaranteeing the selection of a system that has high peak detection and a good dispersion of the analyte, separation between peaks and retention capacity.

The chromatograms at 254 nm of *F. oxysporum* CSP-R18, *F. oxysporum* CSP-19b and *F. solani* CSP-5b are displayed in Figure 2.1-2.3, revealing a pronounced chemical diversity of the extracts. In general, the percentage of acid additives was not relevant for the optimization of any fungal extract. However, the analysis of the other parameters revealed that each fungal extract displayed a different response during the systematic evaluation, allowing individual optimization of the methods.

In *F. oxysporum* (CSP-R18), exploratory run revealed abundant presence of polar compounds, with signals of non-polar molecules almost undetectable at 254 and 366 nm. Complete factorial planning showed that the mobile phase flow rate and gradient time are the only significant variables for optimization of the method, with detection the highest number of peaks in a 40-minute gradient and flow of 0.8 mL min^{-1} (Table 2) . Individual evaluation of the experiments showed that, regardless of the variables tested, there was a pronounced tailing of the major signal, which was only minimized with the use of basic additives (triethylamine, Supplementary Material, Figure SM3). In addition, although the

presence of additives did not influence the higher detection of peaks, the presence of 0.05% of formic acid in the mobile phase resulted in a better resolution of the signals than in 0.1%, promoting an efficient and selective elution of molecules with low, medium high polarity (Figure 2.1).

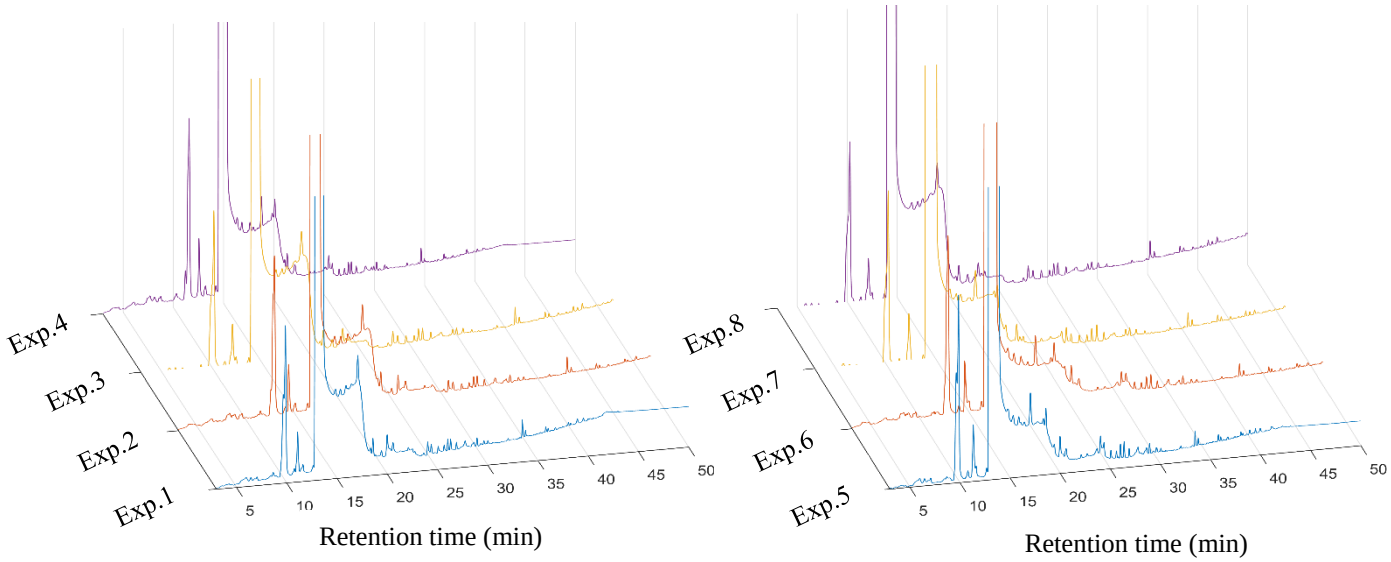

Figure 2.1. Chromatogram at 254 nm from the experiments of the Complete Factorial Planning (Exp 1-8) acquired for the method optimization of ***F. oxysporum* CSP-R18**.

For *F. oxysporum* (CSP-19b), the chromatograms also showed predominant presence of polar molecules. However, unlike *F. oxysporum* CSP-R18, the extract from CSP-19b strain also revealed other non-polar compounds as most intense signals (Figure 2.2). The experimental design revealed that the only significant variable was the mobile phase flow rate (1 mL min^{-1}). Therefore, the percentage of additives and the gradient time were non-significant parameters for the increase in the number of peaks (Table 2.2). Individual evaluation of the experiments revealed that a 40-minute gradient and 0.1% acid additives ensured the best separation of the peaks, also demonstrating better efficiency and resolution in the chromatographic run.

Finally, evaluation of *F. solani* (CSP-5b) revealed that this extract shows the highest number of peaks, with signals of high intensity throughout the entire chromatogram (Figure 2.3). For this experimental design, the gradient time and the interaction between gradient time and mobile phase flow (Table 2.2) were the most significant effects for system optimization. The best chromatographic method for this extract was obtained by a 50-minute gradient and flow at 1 mL min^{-1}. The concentration

of the acid additives did not interfere in the peak detection and neither in the improvements of the signal's resolution (Figure 2.3).

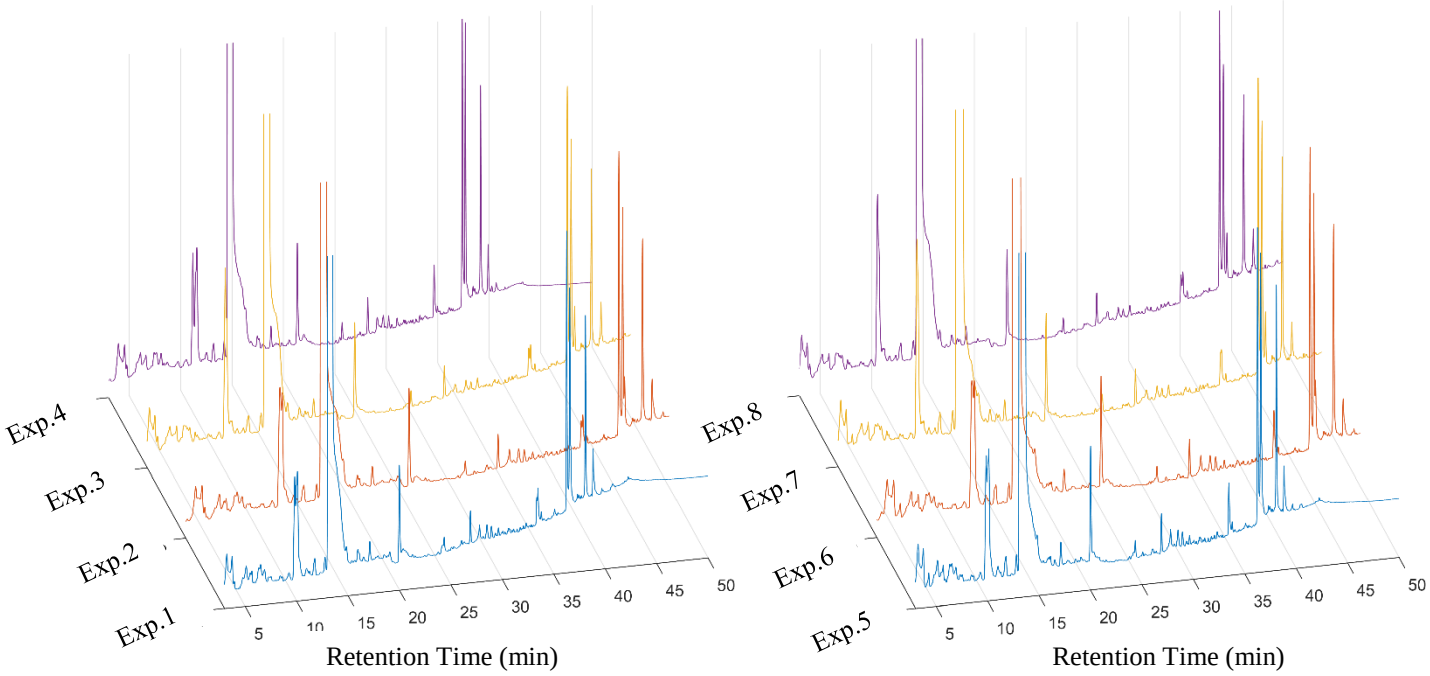

Figure 2.2. Chromatogram at 254 nm from the experiments of the Complete Factorial Planning (Exp 1-8) acquired for the method optimization of ***F. oxysporum*** **CSP-19b**.

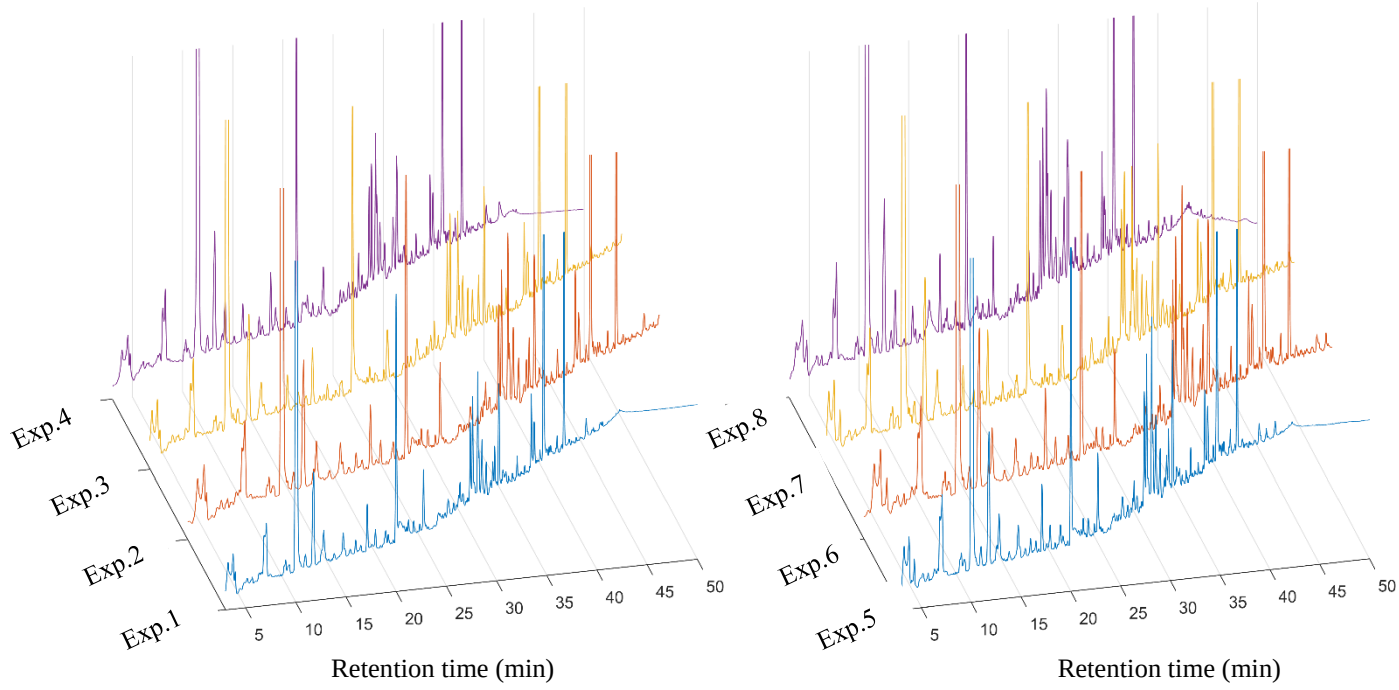

Figure 2.3. Chromatogram at 254 nm from the experiments of the Complete Factorial Planning (Exp 1-8) acquired for the method optimization of ***F. solani*** **CSP-5b**.

	CSP-R18	CSP-19b	CSP-5b
Experimental Variance	13.00	15.38	10.75
Experimental Error	3.61	3.92	3.28
Effect Variance	6.50	3.84	2.69
Effect Error	2.55	1.96	1.64
Critical *t* valueo	7.08	5.44	4.55
Significant effects	V1(-), V3(-)	V1(+)	V3(+), V1-3(+)

Table 2.2. Statistical results from the complete factorial planning for chromatographic method optimization of *Fusarium* extract. *T* value at a 95% confidence level and 4 degrees of freedom was 2.78.

The identification of secondary metabolites by LC-DAD-ESI-HRMS and LC-DAD-ESI-MS/MS was performed after the method optimization for the three fungal extracts. In metabolomics, MS detection by electrospray ionization (ESI) is the method of choice in most microbial studies, offering a greater extent of ionization and detection of polar compounds and molecules with higher molecular weight when compared to other methods (CROTTI et al., 2006; GUARATINI et al., 2005; VESSECCHI et al., 2008; ZHOU et al., 2012).

For the elucidation procedure, the UV, high resolution mass and the fragmentation patterns of experimental data were compared to spectrometric information of known metabolites. Chemical data of known compounds were obtained by consolidated libraries, such as Metlin (RAFIEI; SLENO, 2014), MassBank (HORAI et al., 2010) and MassBank of North America (MoNA), as well as an *in-house* compilation of all major *Fusarium* metabolites, totaling 41 molecules reported for the species of *F. solani* and *F. oxysporum* (taxonomic filter). The search for *Fusarium* metabolites were performed by a bibliographical survey of the main sources of research, including SciFinder, Science Direct, Pubmed and Web of Science. The database was built in .xml format and contains IUPAC, trivial name, CAS-Number, monoisotopic mass, protonated and sodiated ions and molecular formula.

The metabolic identification protocol was performed according to the seven rules proposed by Kind and Fiehn (2007) (KIND; FIEHN, 2007) and included 7 steps: (a) correction of the mass values with NaTFA calibration, (b) removal of possible impurities and contaminants, (c) proposition of the molecular formulas for relevant *m/z* using SmartFormula XR function (Data Analysis, Bruker), (d) evaluation of the error, in ppm,

between observed ions and high resolution masses described in literature, (e) evaluation of sigma values (relative to the isotope standard), (f) confirmation of the molecules by comparison of fragments present in the databases, and (g) proposition of fragmentation mechanisms. Only the detection of substances whose error between the observed and calculated high resolution mass did not exceed 10 ppm (FUNARI et al., 2013) was considered (KIND; FIEHN, 2010).

In the LC-MS dereplication, database comparison allowed the identification of seven major compounds identified for the three *Fusarium* strains, including compounds previously elucidated by NMR (Table 2.3). The depsipeptide beauvericin was the only secondary metabolite found in both species (Table 3), with major production found in *F. oxysporum* CSP-19b. Fusaric acid (5-butyl-picolinic acid) and its analogous 5-(3-butenyl)-picolinic acid were identified only for the *F. oxysporum* (CSP-R18 and 19b), both of which were already known and previously elucidated for this species (AMALFITANO et al., 2002). In addition to beauvericin and picolinic acid derivatives, LC-MS also identified the alkaloid camptothecin and one analogue 9-methoxycamptothecin, both compounds only detected for *F. solani*. The optimized chromatograms with the respective elucidated molecules are displayed in Figure 2.4. In addition, the mass spectra and the proposed fragmentation mechanisms for the molecules identified are arranged in Figures 2.5.

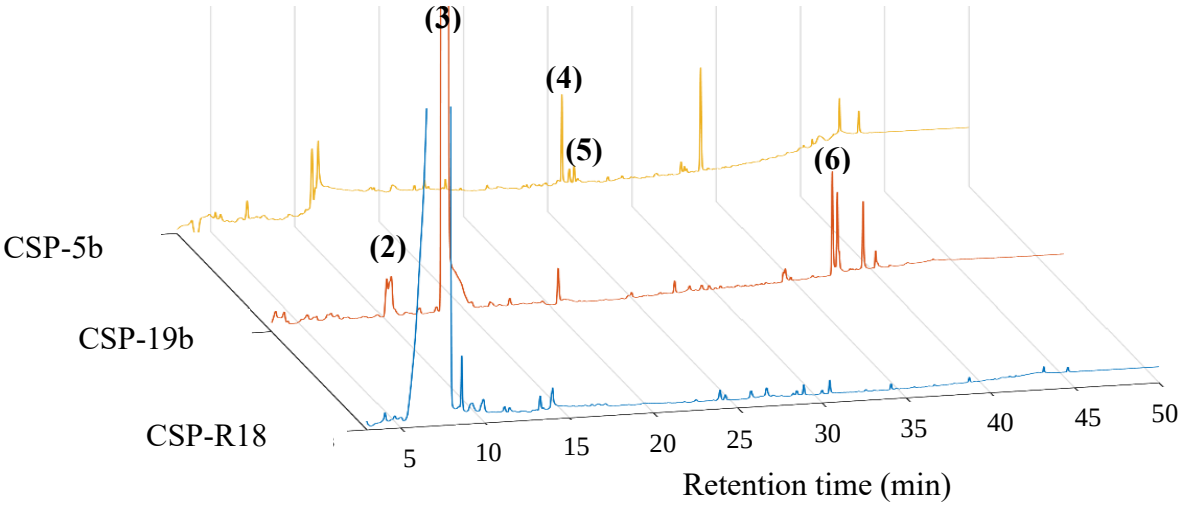

Figure 2.4. Optimized chromatograms for the three fungal extracts, *F. solani* (CSP-5b) and *F. oxysporum* (CSP-R18 and CSP-19b), and their respective molecule signals elucidated by LC-DAD-ESI-MS/MS.

	Molecule	Molecular Formula	Monoisotopic mass	Theoretical *m/z* $[M+H]^+$	Experimental *m/z* $[M+H]^+$	Error (ppm)	Fragments (*m/z*)	RT (min)	Species
1	sacarose	$C_{12}H_{22}O_{11}$	342.1162	343.1235	365.0728 $[M+Na]^+$	-3.31	203 [glucose + Na]$^+$	1.7	Czapek
2	5-(3-butenyl)-picolinic acid	$C_{10}H_{11}NO_2$	177.0789	178.0862	178.0795	-0.67	160, 132	9.3	*F. oxysporum*
3	5-butyl-picolinic acid	$C_{10}H_{13}NO_2$	179.0946	180.1019	180.0959	-0.59	162, 134	9.9	*F. oxysporum*
4	9-methoxycamptothecin	$C_{21}H_{18}N_2O_5$	378.1215	379.1288	379.2458	1.69	335	27.7	*F. solani*
5	camptothecin	$C_{20}H_{16}N_2O_4$	348.1110	349.1183	349.1963	7.80	331, 305, 287	29.6	*F. solani*
6	beauvericin	$C_{45}H_{57}N_3O_9$	783.4094	784.4168	784.3895	-2.72	806, 623, 523, 366, 266	43.4	*F. solani and F. oxysporum*

Table 2.3. Molecules identified by LC-DAD-ESI-MS/MS from the fungal extracts of *F. solani* (CSP-5b) and *F. oxysporum* (CSP-R18 and CSP-19b).

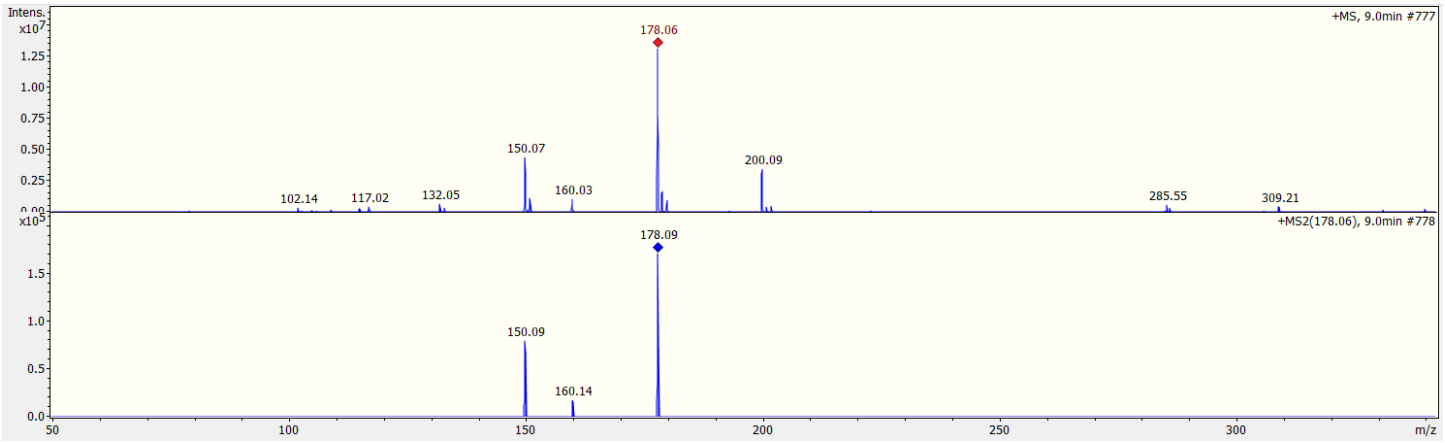

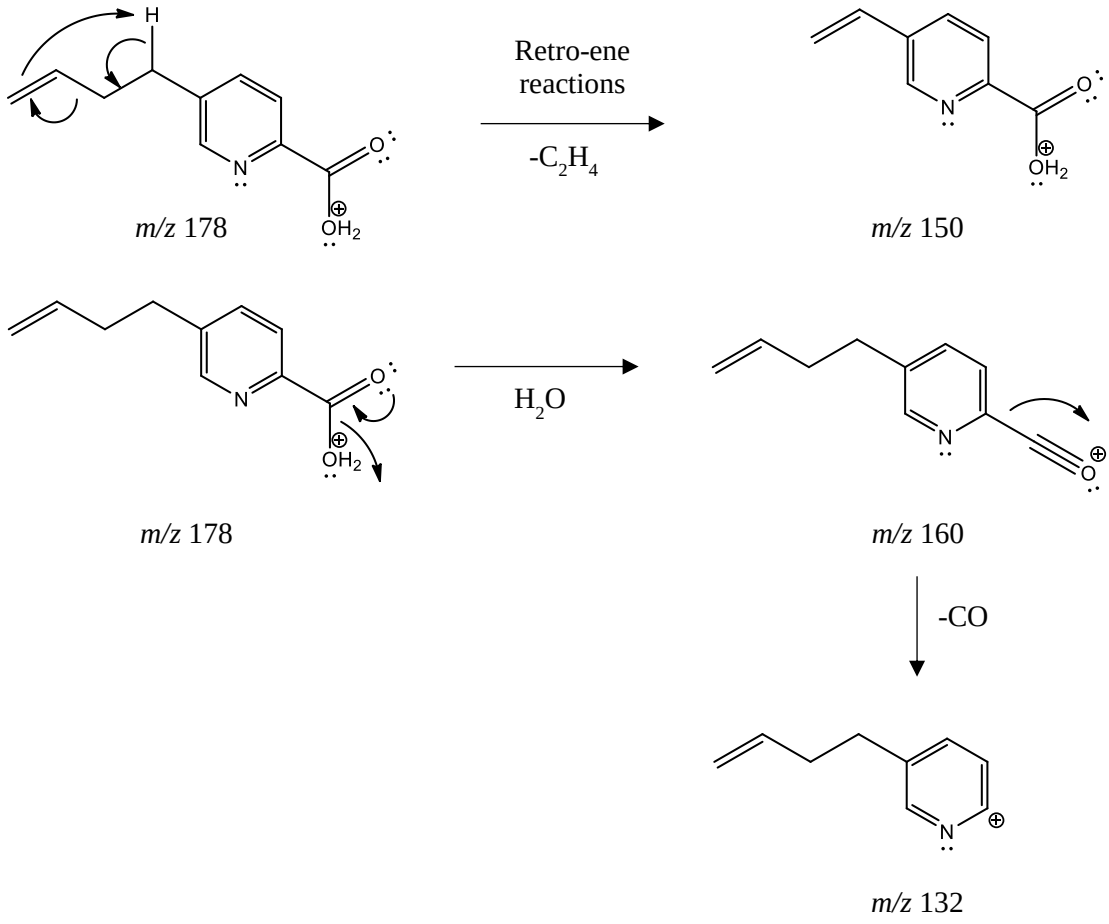

Figure 2.5. (A) Proposed fragmentation mechanism for dehydrofusaric acid. (a) MS spectrum of LC-DAD-ESI-MS run; *m/z* in red (♦) corresponds to the ion selected for fragmentation. b) MS2 spectrum for selected ion. Mechanism proposed by the author. MS Fragments in positive mode: *m/z* 150 $[M\text{-}C_2H_4+H]^+$, *m/z* 160 $[M\text{-}H_2O+H]^+$, 132 $[M\text{-}COOH+H]^+$.

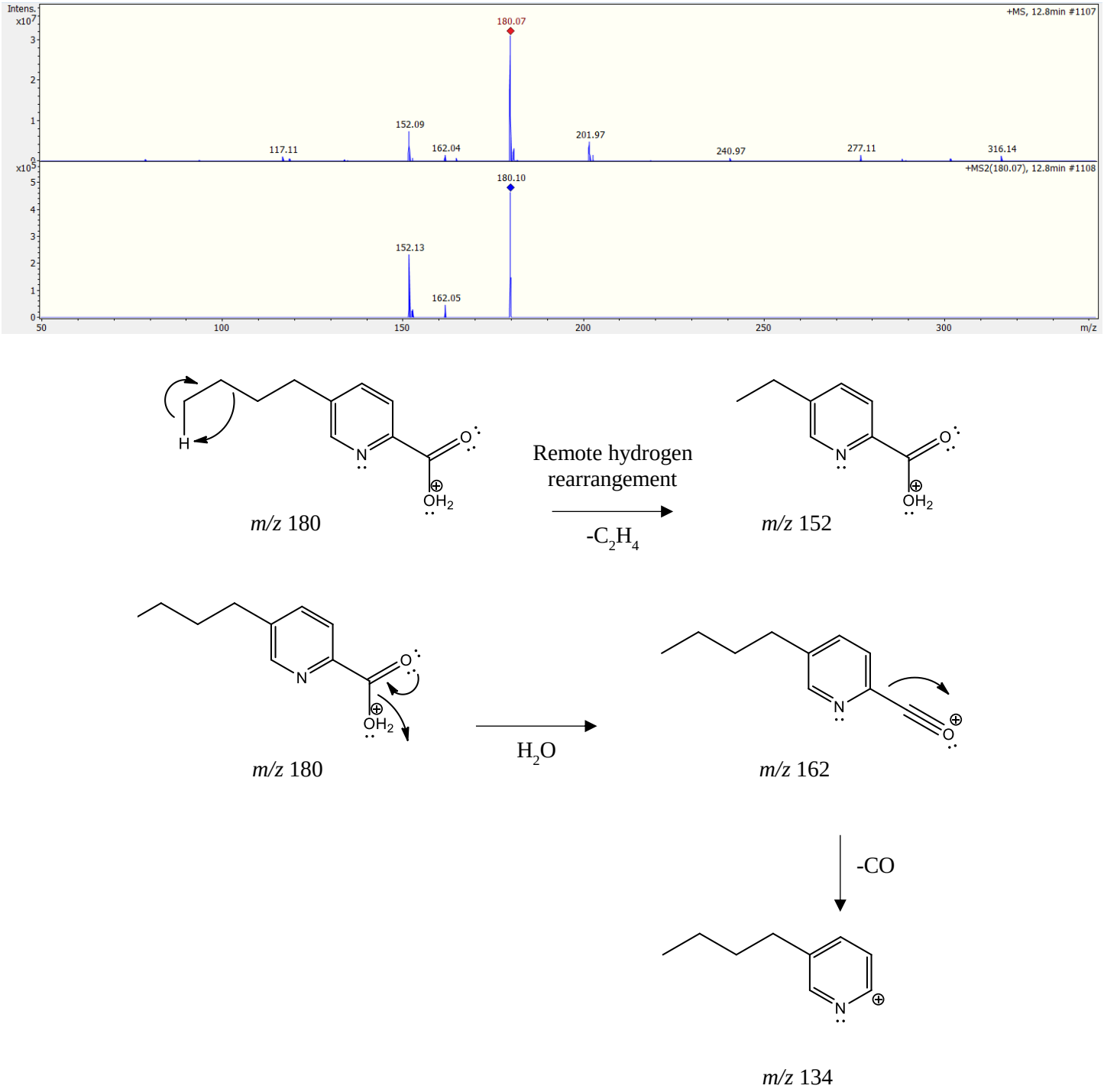

Figure 2.5. (B) Proposed fragmentation mechanism for fusaric acid. (a) MS spectrum of LC-DAD-ESI-MS run; *m/z* in red (♦) corresponds to the ion selected for fragmentation. b) MS2 spectrum for selected ion. Mechanism proposed by the author. MS Fragments in positive mode: *m/z* 152 $[M\text{-}C_2H_4+H]^+$, *m/z* 162 $[M\text{-}H_2O+H]^+$, 134 $[M\text{-}COOH+H]^+$.

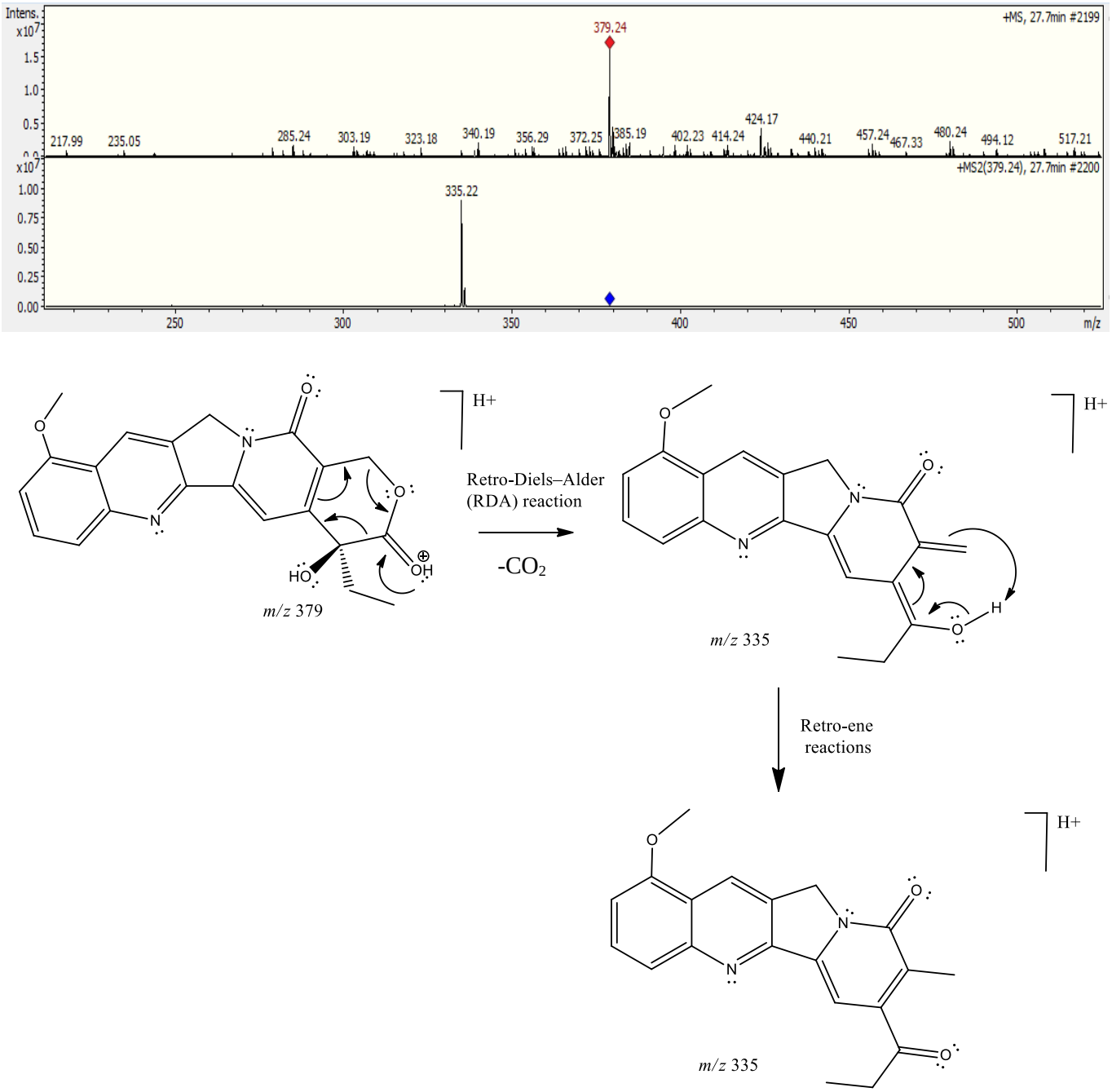

Figure 2.5. (C) Proposed fragmentation mechanism for 9-metoxycamptothecin. (a) MS spectrum of LC-DAD-ESI-MS run; *m/z* in red (♦) corresponds to the ion selected for fragmentation. b) MS2 spectrum for selected ion. Mechanism proposed by the author. MS Fragments in positive mode: *m/z* 335 $[M\text{-}CO_2+H]^+$.

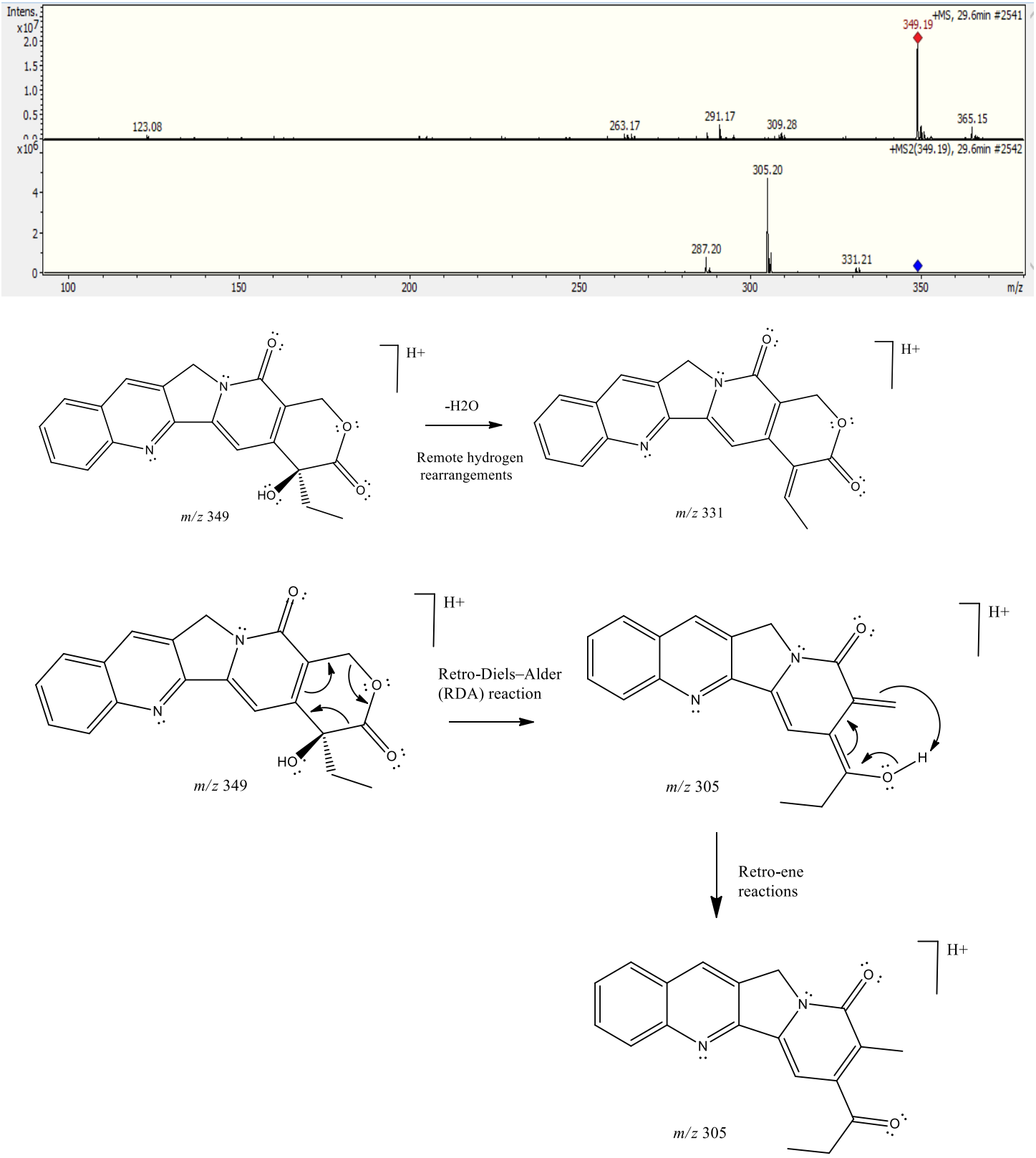

Figure 2.5. (D) Proposed fragmentation mechanism for camptothecin. (a) MS spectrum of LC-DAD-ESI-MS run; *m/z* in red (♦) corresponds to the ion selected for fragmentation. b) MS2 spectrum for selected ion. Mechanism proposed by the author. MS Fragments in positive mode: Fragments in positive mode: *m/z* 331 $[M\text{-}H_2O+H]^+$, 305 $[M\text{-}CO_2+H]^+$, 287 $[M\text{-}CO_2\text{-}H_2O+H]^+$.

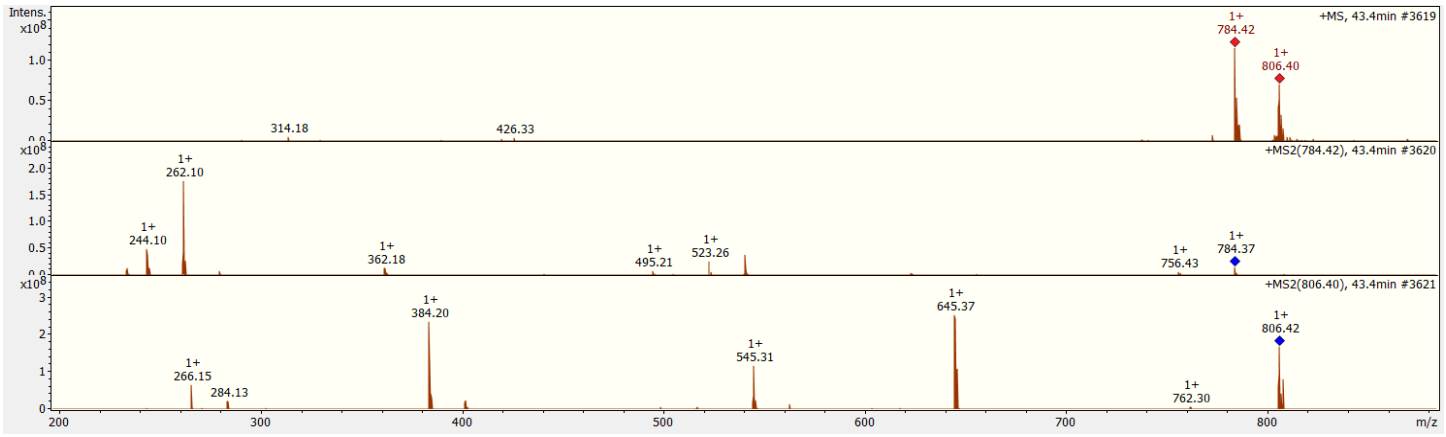

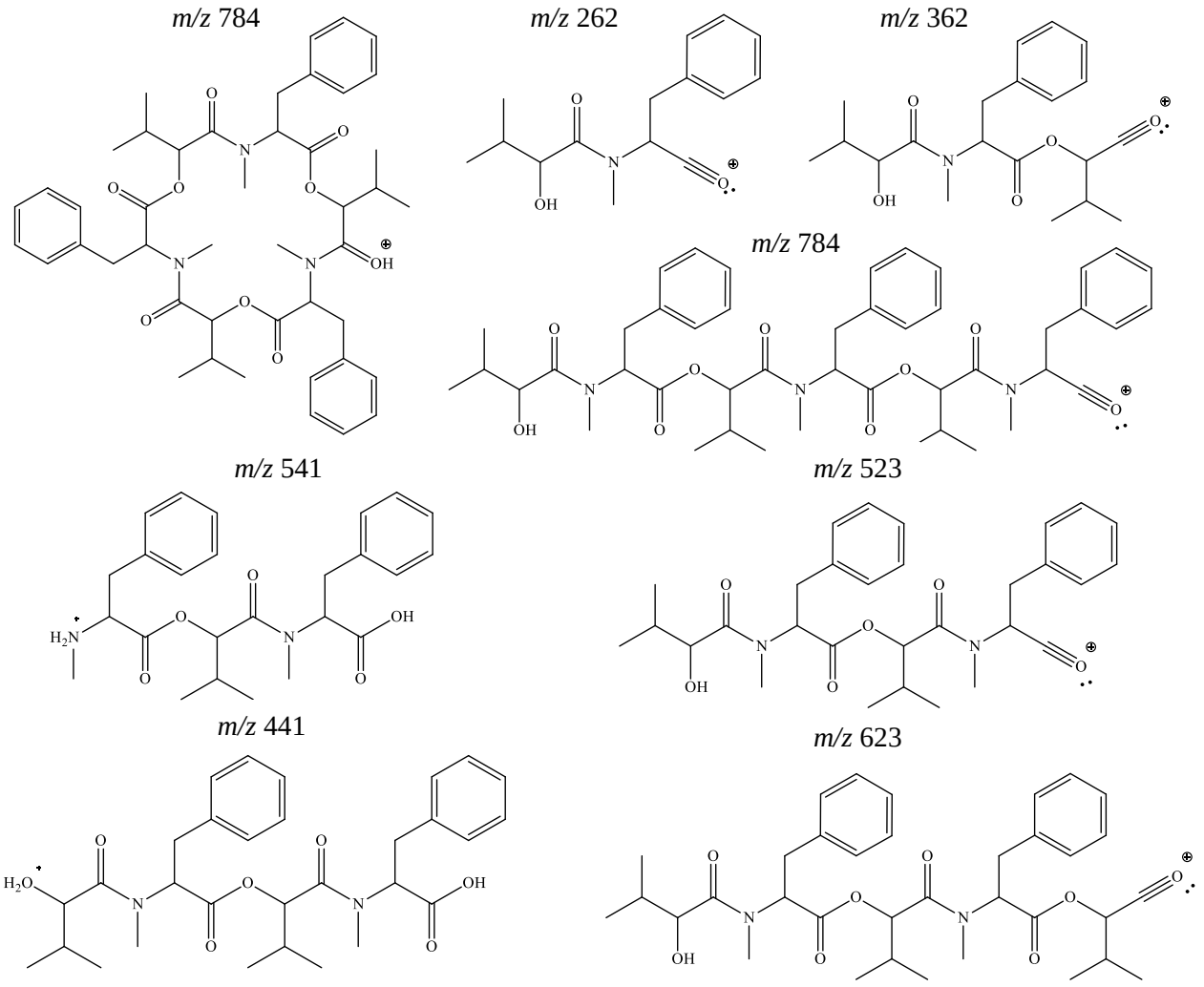

Figure 2.5. (E) Proposed fragmentation mechanism for beauvericin. (a) MS spectrum of LC-DAD-ESI-MS run; *m/z* in red (♦) corresponds to the ion selected for fragmentation. b) MS2 spectrum for selected ion. Mechanism proposed by the author. Fragments in positive mode: *m/z* 806 $[M+Na]^+$, 523 $[4\ aa + H]^+$, 623 $[5\ aa + H]^+$.

3.2. Dereplication by CG-EI-MS

Gas chromatography coupled to MS is one of the oldest analytical technique and has been established as a golden technique for the detection and quantification of volatile and semi-volatile compounds (<650 Da) (GRIFFITHS, 2008). One of the greatest advantages of CG-EM is the molecular identification process based on the combination of orthogonal information, i.e. the use of compound retention times combined with mass spectral information obtained under a standardized ionization energy (usually 70 eV) (FIEHN, 2017; KIND et al., 2009). This combination provides a highly sensitive and reproducible analysis, as well as the development of large compound libraries (patterns) for structural identification of chromatographic peaks. For example, the NIST14 (Mass Spectral Library collection of the U.S. National Institute of Standards and Technology) is composed of more than 240000 molecular structures, one third of which has retention time values and spectral information.

In this CG-EI-MS evaluation, the identification of *Fusarium* metabolite was performed through the comparison of the Linear Retention Indices (LRI) and the fragmentation profile obtained experimentally with those of metabolites present in the literature. The library used for this procedure was NIST 14 Mass Spec and we have only considered substances that displayed similarity greater than 95% similarity and an LRI error (between the observed and calculated LRI) of less 5%.

To calculate the LRI of the metabolites, we have applied a linear regression equation that uses the retention times of a hydrocarbon mixture (external reference standard C8-C40), whose LRI values are tabulated and described in literature (VAN DEN DOOL; KRATZ, 1963) (Figure SM7, Supplementary Material). The hydrocarbon mixture was composed of fatty acids (C8-C40) dissolved in chloroform in the concentrations of 0.8 mg mL^{-1} (C8-C16) and 0.4 mg mL^{-1} (C18-C40) (KIND et al., 2009).

The dereplicated compounds are displayed in Table 2.4, most of which being primary metabolites, such as organic acids and alcohols. In addition, some picolinic acid derivatives were also identified only for *F. oxysporum*, including the known fusaric acid and 2-acetyl-6-methylpiridine.

Molecule	Species	RT (min)	LRI_{calc}	LRI_{lit}	Similarity ≠	Similarity (%)
Latic acid	*F. solani*	5.8	915	922.14	0.77	96
benzeneacetic acid	*F. oxysporum*, *F. solani*	6.27	1263	1259.25	-0.29	97
Benzoic acid	*F. oxysporum*, *F. solani*	7.12	1170	1161.11	-0.76	96
n-decanoic acid	*F. solani*	15.99	1382	1366.16	-1.15	97
2-hydroxidecanoic acid	*F. solani*	23.55	1534	1586.43	3.30	99
2-acetyl-6-methylpiridine	*F. oxysporum*	6.15	1108,55	1107	-0.14	96
Fusaric acid	*F. oxysporum*	22.32	1555	1554.16	-0.05	97
1-hexanol	*F. solani*	4.45	862	858.45	-0.41	95
2,3-dihydro-3,5-dihydroxi-6-methyl-4H-piran-4-one	*F. solani*	735	1130	1138.60	0.75	95
Z-1,9-hexadecadiene	*F. solani*	27.12	1610	1673.21	3.77	94

Table 2.4. Metabolites dereplicated by CG-EM-IE data of the fungal derivatized extracts of *F. oxysporum* e *F. solani*. Molecule elucidation was performed by comparison of the experimental data with spectroscopic data from NIST 14 library. The sugars from the Czapek media were detected, however, those were not displayed in the Table.

4. Conclusion

The dereplication of mass spectrometry data was emerged as an important strategy for the structural elucidation of known compounds and allowed the identification of the main classes present in the extracts of the rhizosphere fungi *F. solani* and *F. oxysporum*. By comparison with consolidated databases, this dereplication methodology ensured a complete view of metabolic production and the discriminant analysis of chemical profiles, identifying 16 different metabolites.

The dereplication of LC-MS data allowed the elucidation of seven major compounds for the three *Fusarium* strains, including the metabolites previously identified by NMR (Chapter 1). The most abundant peak of both strains of *F. oxysporum* (CSP-19b and CSP-R18) was observed in the polar region of the chromatogram and was elucidated as fusaric

acid. Nonetheless, *F. oxysporum* CSP-19b also exhibited abundant compounds in the non-polar region, in which the depsipeptide beauvericin was the major compound. For *F. solani*, LC-MS data enabled the elucidation of camptothecin and one analogue 9-methoxycamptothecin as the most intense metabolites, both of which were found only for this species. These alkaloids are noteworthy not only for their predominant abundance in this strain, but also because of their important antineoplastic activity, which occurs due to the inhibition of the enzyme topoisomerase-I, necessary for DNA replication and transcription (SHWETA et al., 2010).

The dereplication of GC-MS data also allowed the identification of different compounds, including primary metabolites such as organic and secondary alcohols and acids. Moreover, analysis of GC-MS data also identified fusaric acid and derivatives for *F. oxysporum*, confirming once again the high abundance of picolinic acid derivatives for this specie. Figure 2.6 shows all the chemical structures described in this Chapter for both species.

The main obstacles in the dereplication of LC-MS and GC-MS data is signal coalescence, which still hinder the elucidation of minor metabolites and a holistic assessment of the chemical data. Moreover, the lack of robust and comprehensive libraries for metabolites of microbial origin still hampers the identification of the majority of metabolites. In this sense, the compilation of a database of metabolites produced by *Fusarium* was essential for the metabolic elucidation and dereplication.

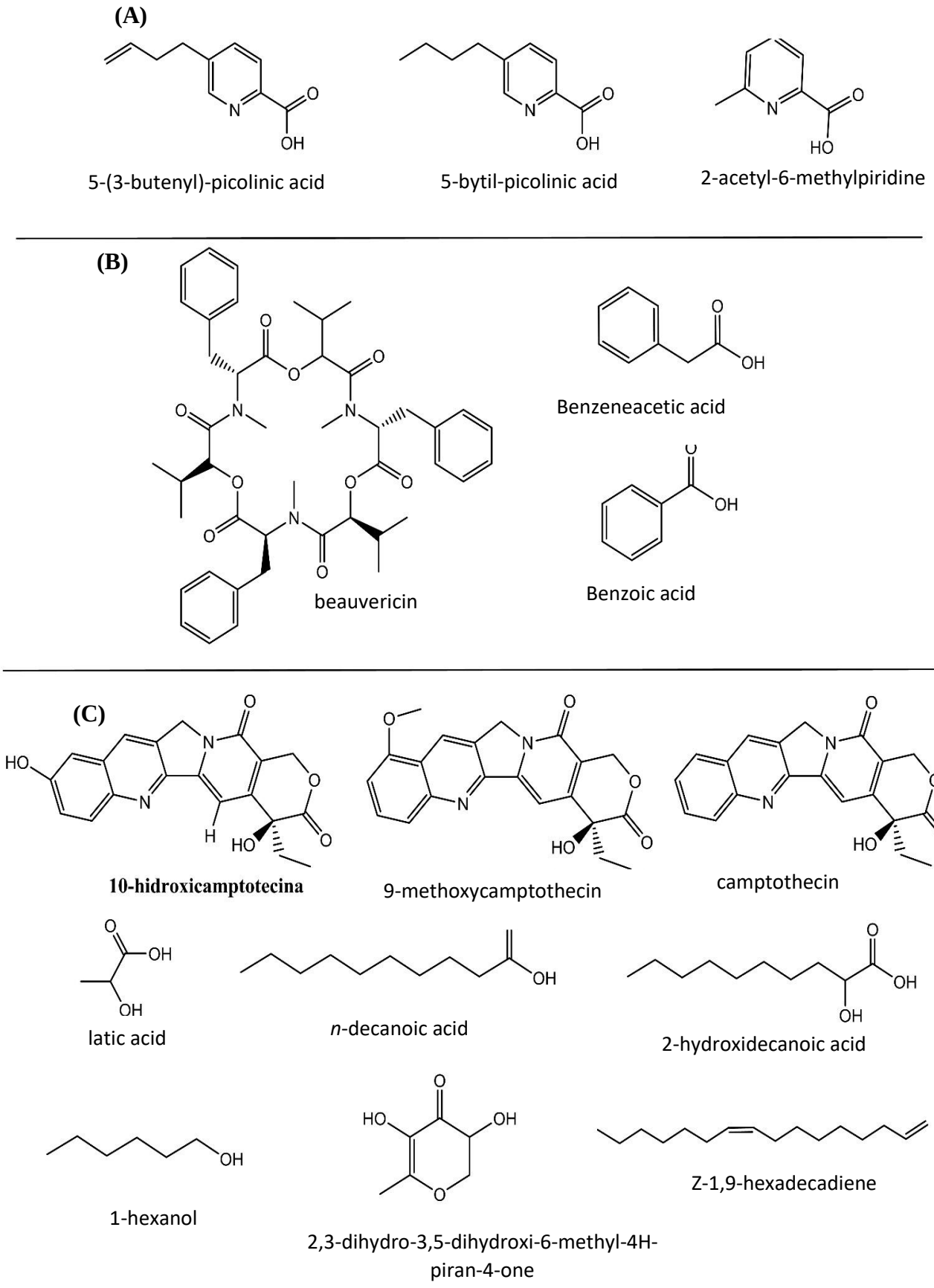

Figure 2.6. Metabolites identified by MS dereplication for (A) *F. oxysporum*, (B) Both species and (C) *F. solani*.

CHAPTER 3. DEREPLICATION BY MS/MS MOLECULAR NETWORING - SELECTION OF BIOLOGICALLY PROMISING FRACTIONS AND IDENTIFICATION OF MAJOR AND MINOR SECONDARY METABOLITES

Article title: MS/MS Molecular Networking Analysis of *Fusarium* species – evaluation of metabolic dynamics and dereplication of bioactive secondary metabolites

Authors: Denise M. Selegato[a], Ian Castro-Gamboa[a*]

Journal: Planta Medica.

Status: Unpublished.

Affiliations:

[a] Nuclei of Bioassays, Ecophysiology and Biosynthesis of Natural Products (NuBBE), São Paulo State University (UNESP) – Araraquara, SP, Brazil.

Justification:

Following the elucidation of the main secondary metabolites of both *Fusarium* strains, the fungal extracts were submitted to fractionation and biological activity in order to reduce complexity, guaranteeing a more detailed chemical response and the selection of fractions and metabolites with promising biological activity.

Fractionation was performed on a microscale using solid phase extraction (SPE), which reduces the solvent usage, analysis time and cost when compared to conventional biofractionation tests. Moreover, the selection of biologically promising fractions was evaluated by preliminary antifungal, antibacterial, antibiofilm and acetylcholinesterase inhibition assays. Fungal raw extracts were used for comparison.

Metabolite evaluation of these samples was performed by MS/MS Molecular Networking and targeted to (1) analyze the *Fusarium* metabolic dynamics (using data from both fractions and raw extracts) and identify major chemical differences between strains and (2) dereplicate major metabolites and their minor analogues in bioactive fractions.

Abstract

Microbial biosynthetic pathways elicits the production of a diversity of biologically promising secondary metabolites. Nonetheless, the large dynamic range and chemical complexity still hamper their identification and biological correlation, requiring the use of tools that provides fast and accurate evaluation of the microbial potential. Recently, MS/MS Molecular Networking has emerged as an important dereplication tool and explores the fact that chemically similar molecules have similar physical and spectroscopic properties. This approach, applied to sequential mass spectroscopy, organizes fragmentation data according to their chemical similarity, creating a network for the evaluation of the large chemical dynamics. In the current study, we generated a network of MS/MS data from *Fusarium oxysporum* and *F. solani* targeting to dereplicate biologically promising microbial secondary metabolites and analyze the metabolic dynamics in this fungi species. First, to overcome data complexity, the fungal extracts were submitted to micro-fractionation and biological activity evaluation. Following, Molecular Networking was performed for metabolite analysis and elucidation. Results show that fractionation reduced signal overlap and allowed the selection of promising bioactive fractions. Moreover, Molecular Networking contributed to the chemotaxonomical analysis of these species and revealed that for every cluster, there was at least one node from each *Fusarium* species, indicating some genetic denominator. The most bioactive samples were from *F. oxysporum*. The polar fractions displayed antifungal, antibiofilm and bacteriostatic activities and strong acetylcholinesterase inhibition, whereas the apolar were less active but exhibited strong biofilm eradication. Dereplication was performed separately according to the polarity. Analysis of the non-polar fractions led to the identification of beauvericin and 6 analogues never reported for this species: the known beauvericin A, G1 and G2 and the firstly described FOxy 01, 02 and 03. Similarly, analysis of the highly polar fractions revealed the presence of fusaric acid and dehydrofusaric acid along with 2 minor analogues never been reported for this species. In conclusion, MS/MS Molecular Networking was an efficient tool for metabolite identification and allowed the elucidation of different mycotoxins, among known and novel bioactive secondary metabolites.

Keywords: MS/MS Molecular Networking, dereplication, *Fusarium*, beauvericin analogues, picolinic acid analogues

1. Introduction

Microbial biosynthetic pathways are a result of several million years of evolutionary optimization and elicit the production of a diversity of secondary metabolites (BODE et al., 2002; HORINOUCHI, 2007). Nonetheless, the large dynamic range and chemical complexity still hamper their identification and biological correlation, requiring the development of techniques for a fast and accurate evaluation of the microbial therapeutical potential.

In the past, different purification techniques were applied as bio-guided fractionation to overcome complexity in a mixture. However, these reductionist procedures often lead to an laborious, time-consuming, non-comprehensive and expensive process of isolation and purification of the active compounds (CHEN et al., 2015; PEZZUTO, 1997). In the last decade, several methods have been developed for faster and more holist correlation between chemical and biological data, minimizing time, effort, and cost. This strategies include bioactivity fingerprinting, the use of supervised chemometric analysis and the use of liquid chromatography/mass spectrometry-guided bioassays (BITTENCOURT et al., 2015; CARDOSO et al., 2017; CHAGAS-PAULA et al., 2015; DEMBOGURSKI et al., 2018; WEGH et al., 2017).

More recently, dereplication has emerged as a multivariate strategies for the chemical and biological uncovering of microbial-matrices, being used as a fast alternative for the screening of promising species (YULIANA et al., 2011). The common denominator of these strategies is the attempt to exploit the fact that structurally similar or identical molecules share similar physical characteristics, such as UV−vis profiles, chromatographic retention times, MS, NMR chemical shifts, or biological properties. In an untargeted analysis, dereplication allows a broad range of chemical comparison between samples (QUEIROZ; WOLFENDER; HOSTETTMANN, 2009), prioritizing the identification of active molecules and, consequently, improving the process of chemotype and sample selection (ABREU et al., 2017; KUMAR et al., 2014; STERMITZ et al., 2000).

Specifically, mass spectrometry (MS)-based dereplication is critical to modern dereplication pipelines, given MS data contains a definitive characteristics of a molecule (e.g. structural architecture, chemical stability and functional groups) that can be used as proxies for chemical identification (DE OLIVEIRA et al., 2017; YANG et al., 2013). In comparison with reductionist approaches, metabolite dereplication by MS coupled with

separation techniques is more versatility, faster and uses smaller amounts of sample, avoiding the re-isolation of known substances and ensuring rapid prioritization of extracts.

Notwithstanding the analytical advantages of MS-dereplication, in practice, it is often difficult to reliably identify a given compound when solely using precursor because of the sheer number of results returned when searching databases. In the last decade, new strategies using MS patterns have been created to discriminate samples combining other spectrometric properties more than parent mass alone. Because natural product workflows typically incorporate LC-MS/MS analysis, the MS/MS data can be simultaneously acquired on most mass spectrometers, allowing data interpretation based on chemical similarity of their fragmentation data (DE OLIVEIRA et al., 2017; YANG et al., 2013).

Among the strategies to explore MS/MS data as a dereplication tool, MS/MS Molecular Networking has emerged as an important dereplication strategy and explores the fact that chemically similar molecules have similar physical and spectroscopic properties (WATROUS et al., 2012; YANG et al., 2013). This approach, applied to sequential mass spectroscopy, organizes fragmentation data according to their chemical similarity, allowing the creation of a networking for the evaluation of the large chemical dynamics, as well as the identification of known molecules and their minor analogues (WANG et al., 2016; YANG et al., 2013).

In a molecular networking analysis, close-related natural products share similar MS/MS fragmentation patterns and are grouped according to the their biosynthetic origin. The resulting clusters allow the exploration of the molecular dynamics and the identification of analogue molecules in complex data, accelerating the dereplication of metabolites. The molecular elucidation is usually performed by comparison with databases, followed by individual fragmentation studies of the proposed analogues (ALLARD et al., 2016; YANG et al., 2013).

In the current study, we generated a network of MS/MS data from *Fusarium oxysporum* (strains CSP-19b and CSP-R18) and *F. solani* (strain CSP-5b) to dereplicate biologically promising microbial secondary metabolites. As a final strategy for overcoming analytical challenges in metabolomics, the fungal extracts were first submitted to micro-fractionation, followed by biological activity. This procedure reduces signal overlap and allowed the selection of fractions with promising biological activity. Following, MS/MS Molecular Networking of these samples (MS/MS data from fractions

and raw extracts) was performed for metabolite evaluation, targeting to interpret the fungal metabolic dynamics and correlate the bioactivity to major molecules and their minor analogues in bioactive fractions. Fractionation was performed on a microscale using solid phase extraction (SPE), which reduces the solvent usage, analysis time and cost when compared to conventional biofractionation tests. Moreover, the selection of biologically promising fractions was evaluated by preliminary antifungal, antibacterial antibiofilm and acetylcholinesterase inhibition assays.

2. Materiais e Methods

2.1. Fractionation

Fungal extracts (100 mg), prepared according to protocol on Chapter 1, were fractionated by solid phase extraction (SPE) using cartridges filled with C18 silica. For activation, the columns were previously eluted with 10 volumes of Mili-Q water and 10 volumes of HPLC grade methanol, respectively. The column conditioning was carried out with 10 volumes of a 20%-MeOH.

Each column was injected with 20 mg of the extracts dissolved in the same starter-mobile phase. The elution of the mobile phases occurred with the aid of Multi Valve Manifold equipment, in which six column-volume of the mobile phases with 20, 40, 60, 80 and 100% of Methanol Grade-HPLC were respectively applied (Figure 3.1).

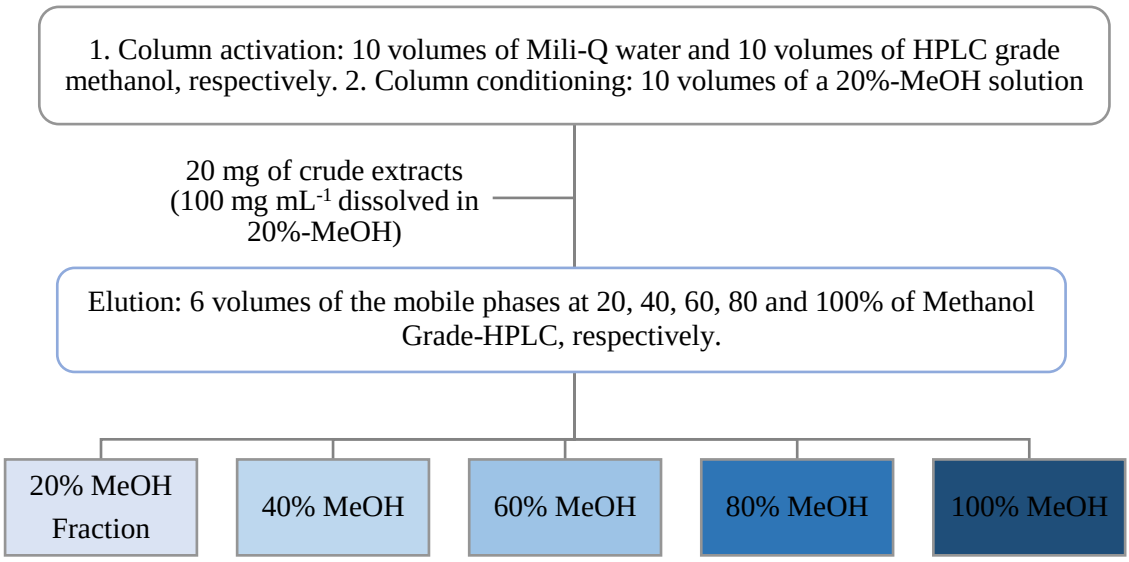

Figure 3.1. Fractioning procedure of microbial extracts by C18-Solid Phase Extraction.

Following, in order to guarantee the efficiency of the fractionation procedure, all fractions from the three *Fusarium* strains were also analysed by LC-MS (both LC-DAD-

ESI-HRMS and LC-DAD-ESI-MS/MS) using the optimized method described in Chapter 2. The chromatographic profile was obtained in a Shimadzu LC- 20, while the MS detection was acquired at a UltrOToF (Bruker) with electrospray ionization in positive mode and QToF (sequential-time and quadrupole-type analyser) type analyser for the acquisition of the high resolution mass and electrospray ionization in positive mode and ion trap type analyzer for the sequential mass data. For comparison, the LC-MS data of the raw-extracts of all *Fusarium* species were also acquired in the same method.

2.2. Biological Assays of the Fractions

2.2.1. Mobile phase optimization for the TLC Biological assay

Acetylcholinesterase inhibition and preliminary antifungal assays were performed on TLC chromatoplates. Hence, prior to the biological experiments, all fractions and extracts were tested in different mobile systems in order to verify in which proportion of solvents occurred the greatest separation of the metabolite spots.

Six types of eluent system were tested: (a) $CHCl_3$-MeOH (98:2 v/v), (b) $CHCl_3$-MeOH (97:3 v/v), (c) $CHCl_3$-MeOH (95:5 v/v), (d) Ethyl acetate-Hexane (70:30 v/v), (e) Ethyl acetate-Hexane (80:20 v/v) and (f) Ethyl acetate-Hexane (90:10 v/v). The best elution systems were selected based on the revelation of the plates in white light, short UV (254 nm) and long UV (366 nm).

2.2.2. Preliminary Antifungal Analysis - Bioautography of Cladosporium cladosporioides and C. sphaerospermum

For the evaluation of the antifungal activity, fractions (200 μg) were firstly applied in a stationary phase of silica gel (TLC plates, 20 x 10 cm, F254) from Merck. For each plate development, the chamber saturation time was 20 minutes and the solvent migration distance was 90 mm from the application point. A total of 25 μL of solution were spotted. On each plate, samples were applied with a 10 mm distance from the bottom and 20 mm from the left and right border of the plate.

After development, the plates were dried and sprinkled with spore suspension of *C. cladosporioides* (Fresen) de Vries (CCIBt 140) and *C. sphaerospermum* Penzig (CCIBt 491), according to the method of Homans and Fuch (HOMANS; FUCHS, 1970). The antifungal nystatin (5 μg) was used as a positive control. Fractions exhibiting

antifungal activity showed clear zones of fungal inhibition in the bioactive spots. For those bands, the Rf values were calculated and the results were described as (1) inactive (i), if no inhibition zone was observed, (2) weak activity (w), if the inhibition spots were smaller than the positive control, (3) moderate activity (s), if the inhibition zones were equal to the positive control or (4) strong activity (s), if the inhibition zone was superior than the nystatin control.

2.2.3. Acetylcholinesterase Inhibition Assay - Qualitative Bioautography Analysis (CCDA)

For the acetylcholinesterase inhibition assay, the fungal fractions (200 μg) were also analyzed by using silica gel 60 F254 (Merck), following the same TLC methodology described in Topic 2.2.2. (Chapter 3). Physostigmine (0.05 μg) was used as a positive control. This alkaloid displays activity in the parasympathomimetic nervous system of indirect action in the inhibition of acetylcholinesterase.

After the development of the TLC, the plates were sprinkled with an acetylcholinesterase enzyme solution and, after incubation, developed with a mixture of ethanolic acetate, 1-naphthyl and aqueous solution of Fast Blue B salt, according to Marston et al. protocol (MARSTON; KISSLING; HOSTETTMANN, 2002). The appearance of a white spot on the purple background indicates inhibition of the acetylcholinesterase activity. The Rf values of active spots were calculated and the results were described as (1) inactive (i), if no inhibition zone was observed, (2) weak activity (w), if the inhibition spots were smaller than the positive control, (3) moderate activity (s), if the inhibition zones were equal to the positive control or (4) strong activity (s), if the inhibition zone was superior than the physostigmine control.

2.2.4. Antibiofilm Assay

The fractions of all three *Fusarium* species were evaluated towards their capacity of eradicating *Staphylococcus epidermidis* biofilms. These fractions were tested against both *S. epidermidis* (strain ATCC 12228), a poor biofilm producer, and *S. epidermidis* (strain ATCC 35984), a good biofilm builder. The eradication assay was conducted at the Institute of Physics of USP of São Carlos, in collaborations with Dr. Rafaela Fernandes, Bsc. Gabriela Righetto and Profa. Dr. Ilana L. B. C. Camargo. This partnership was established by the CIBFar project (CEPID process FAPESP n. 2011/51313-3).

Initially, good and bad biofilm forming bacteria were inoculated into BHI 0.75% glucose broth, in several replicates, in a 96-well microplate, followed by incubation at 37°C for 24 hours. After the incubation period, the culture medium with planktonic bacteria was filtered and the wells washed with physiological solution 0.85%, remaining in the microplate only the newly formed biofilm. Following, the fractions were solubilized in fresh BHI medium with 0.75% glucose and added to *S. epidermidis* ATCC 34984 biofilm wells, with the eradication quantified after 24 hours.

For the eradication analysis, the wells were previously washed and stained with violet crystal, and the excess was removed with a solution of Ethanol-Acetone (8:2 v/v). The absorption was measured at 595 nm based on the comparison of the absorbances means between the good and bad biofilm builders, both without the fractions. Similarly, analysis of the fungal fractions was performed using the same comparison of the absorbance mean values between biofilm production of *S. epidermidis* ATCC 34984 and *S. epidermidis* ATCC 34984, both after the addition of the solubilized fractions. The comparison of the means was carried out by the Student T-Test, in which P value <0.05 indicates the significant difference between two means of two different samples (QIN et al., 2014). The standard deviation was used to evaluate coherence between replicates.

2.2.5. Antibacterial Assay – Determination of Minimum Inhibitory Concentration (MIC) and Minimal Bactericidal Concentration (MBC)

Antimicrobial activity was also evaluated for all fraction of the three *Fusarium* strains according to the Clinical and Laboratory Standards Institute (CLSI Guidelines 2013). These assays were conducted in collaboration with Dr. Rafaela Fernandes, Bsc. Gabriela Righetto and Profa. Dr. Ilana L. B. C. Camargo from the Institute of Physics of USP of São Carlos.

For this procedure, samples were first diluted and storage in stock solution 100x concentrated in DMSO. Previous to the tests, these stocks were diluted 1:100 in Mueller Hinton Cement Adjusted (MHCA) broth (BD Lot 3322206) and measured in duplicate at a final concentration of 512 μg mL-1 at 1% DMSO.

Negative and positive controls were prepared with Mueller Hinton Cation broth adjusted at 1% DMSO. The positive control was inoculated with the bacteria and without the presence of the samples (PANKEY; SABATH, 2004). Incubation was performed at 37 ° C for 24 hours, followed by visual reading of the results. The screening was defined

as the presence or absence of activity at the concentration tested based on the minimal inhibitory concentration (MIC). The samples that showed activity at 512 μg mL^{-1} had the minimum inhibitory concentration (MIC) and minimal bactericidal concentration (MBC) evaluated by the broth microdilution method.

2.3.MS/MS Molecular Networking

Typically, molecular networking is implemented in three fundamental steps: (1) acquisition of MS/MS spectra, (2) comparison of MS/MS data by a similarity cosine score and (3) visualization of the resulting network on Cytoscape, a tool designed to visualize correlations of large data sets which measure relatedness in MS/MS spectra.

2.3.1. LC-DAD-ESI-MS/AutoMS Data Acquisition

Automated MS/AutoMS mode is commonly prioritized in the analysis of molecular networking since it provides the simultaneous fragmentation of several ions in an extract. In practice, this process ensures that most of the metabolites in an extract are detected and fragmented in one single injection, decreasing the use of solvent and the analysis time.

LC-MS analysis was performed for all fractions (20, 40, 60, 80 and 100% MeOH) and raw extracts of all three *Fusarium* strains. LC analysis was carried out in a Shimadzu Class-LC 10 and Diodes Array Detectors (DAD) with wavelength from 190 to 800 nm using the optimized method described in Chapter 2. The column eluent was divided using a 5:1 splitter, with the largest flow being directed to the DAD detector and the remainder to the mass spectrometer. The MS/AutoMS mode was acquired in a Bruker AmaZon Speed at the following parameters: nebulizer pressure 70 psi, drying gas flow 12.0 L min^{-1}, drying gas temperature 350 °C. The automatic mode was carried out with cycles for positive MS1 acquisition, followed by fragmentation of the two most intense ions (above > 1000 counts). Calibration was performed through addition of trifluoroacetic acid solution (NaTFA, 10 mg mL^{-1}) at the beginning and end of each chromatographic analysis.

2.3.2. MS/MS Molecular Networking Analysis

Once all the data was acquired and processed using MzMine software (KATAJAMAA; OREŠIČ, 2005), the spectra were exported in a text format (mgf) and

inserted in to the Global Natural Products Social Molecular Networking (GNPS) platform to calculate the cosine similarity score. In theory, the spectra are converted into unit vectors which are paired and compared by a dot product calculation. The cosine similarity score assigned to each pair of vectors ranges from 0 to 1, where 0 represent completely different and 1 represents identical spectra.

The algorithm parameters included: mass tolerance for fragment peaks (0.3 Da), parent mass tolerance (1.0 Da), the minimum percentage of overlapping masses between two spectra (set at 45%) and the minimum percentage of matched peaks in a spectral alignment (40%). Moreover, to reduce complexity, identical MS/MS spectra were gathered in to the same consensus spectra, cosine scores below 0.5 were discarded and only relevant scores (top 10 cosine scores in K parameter) were connect.

After MS-Clustering, the text files with attributes were imported into Cytoscape 2.8.3 for visualization of nodes and edges as a network. For these analysis, the network also included selected MS/MS data of know molecules from the libraries HMDB (WISHART et al., 2007), LipidMaps (SUD et al., 2012), MassBank (HORAI et al., 2010), NIST and other.

On the Cytoscape software, the background nodes from solvent, interferers and contaminants, that were not directly connected to an ion node from the sample, were removed from the network. Moreover, the nodes were colored based on the fungal species and the edge thickness attributed to the cosine similarity scores (thickness according to cosine from 0.7 to 1). Thicker lines indicate higher similarity. Subnetworks were generated in Cytoscape from isolated portions of the larger network in order to improve the analysis of the metabolic dynamics, provide further molecule elucidation and better visibility of edge thickness and node connectivity.

3. Results and Discussion

3.1. Evaluation of the Metabolic Dynamics of F. solani and F. oxysporum by MS/MS Molecular Networking

Initial LC-MS/AutoMS experiments were carried out on individual fractions and extracts, in triplicate, resulting in a wide range of well characterized signals. MS/AutoMS mode shown to be very sensitive to detect and fragment most of the ions present in the samples, which included the ions (mostly protonated or sodiated) of all the molecules identified in the previous Chapters.

GNPS platform calculated the similarity of 1424 ions and generated a total of 378 clusters. In Cytoscape software, these networks allowed for the simultaneous exploration of known molecules and compound classes within this *Fusarium* data, contributing for the chemotaxonomical analysis of these species.

A subset with the major cluster of the molecular network generated for *Fusarium* is displayed in Figure 3.2. It shows that the clusters range in number of nodes, origin if the ion and similarity range. In almost every group, it was possible to detect at least one node that was present inf both *Fusarium* species (colored in purple), which indicated that although *F. solani* and *F. oxysporum* have different chemical profiles, these strains still share a genetic denominator for the production of the same biosynthesis pathways.

Moreover, although both strains share the same biosynthetic background, the production of secondary metabolites vary vastly (Figure 3.2). Overall, most nodes of the networking belong only to *F. oxysporum,* which indicate the bigger chemical diversity of this species.

Few clusters were grouped almost exclusively by ions from one single strain (Figure 3.2). In nature, these drastic and singular changes in the chemical behavior are most likely attributed to confer some environmental advantage to these strains under a given condition. For example, *F. oxysporum* CSP-R18 was isolated from rizotron cultures of *S. spectabilis* and produces almost all picolinic acid derivatives exclusively, while *F. oxysporum* CSP-19b was isolated from the hydroponic cultures of *S. spectabilis* and produces all major beauvericin analogues (Figure 3.3).

Lastly, because structurally similar chemical structures share similar MS/MS fragmentation patterns, molecular classes are grouped together within a network. As a result, some structurally and functionally diverse analogues were identified by comparison with MS/MS databases, which included beauvericin analogues, picolinic acid derivates and isochromenes (Figure 3.3). Furthermore, it is intriguing to note that a large number of tightly clustered nodes were not annotated, highlighting once again the lack of databases with sufficient mass fragmentation library for the unique metabolites produced by fungi and bacteria.

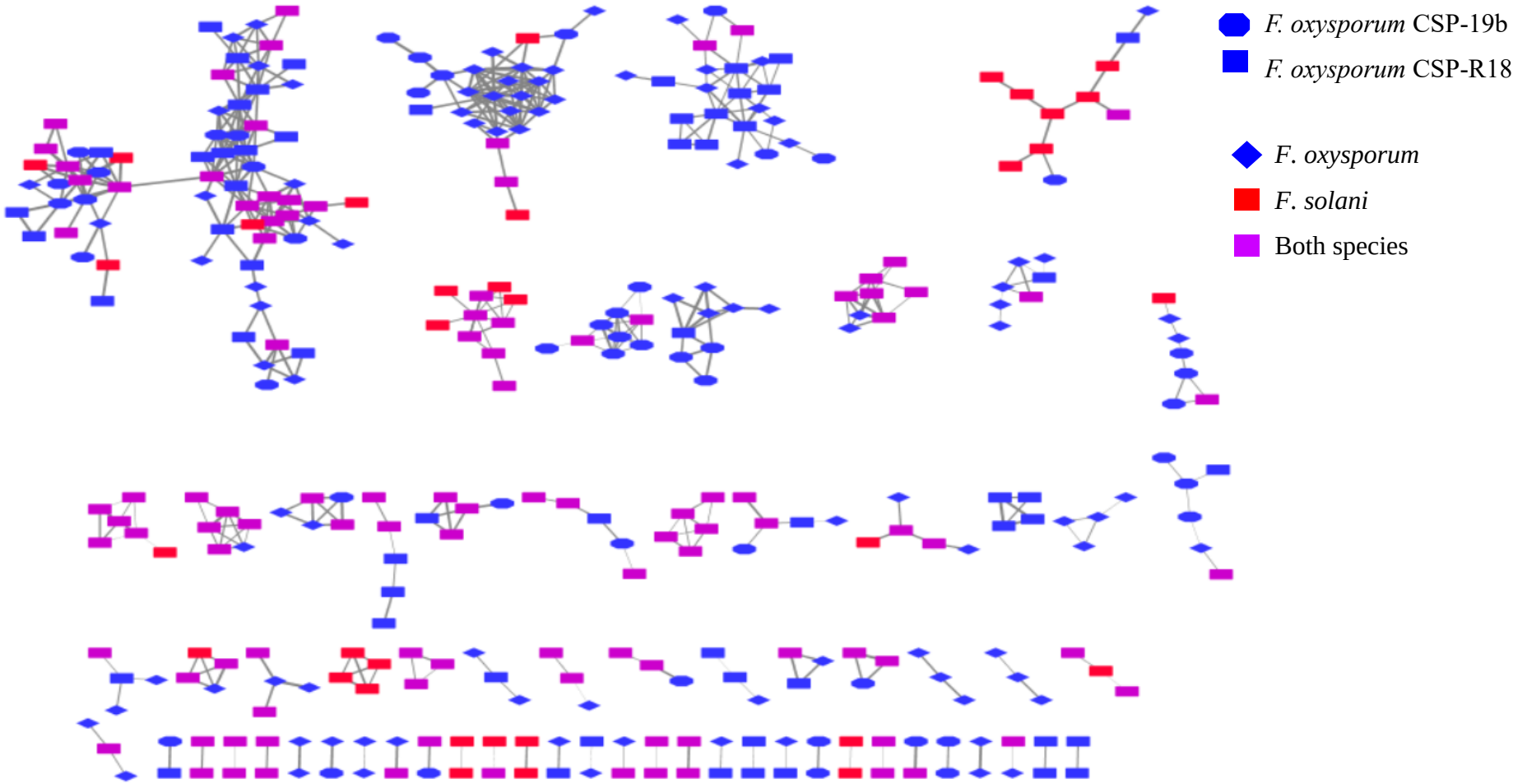

Figure 3.2. Molecular networks of MS/AutoMS data obtained from the fractions and raw extracts of *F. oxysporum* (strains CSP-19b and CSP-R18) and *F. solani* (strain CSP-5b). The nodes were colored based on the fungal species and the edge thickness were attributed to the cosine similarity scores (thickness range is based on similarity from 70 to 100%). Thicker lines indicate higher similarity.

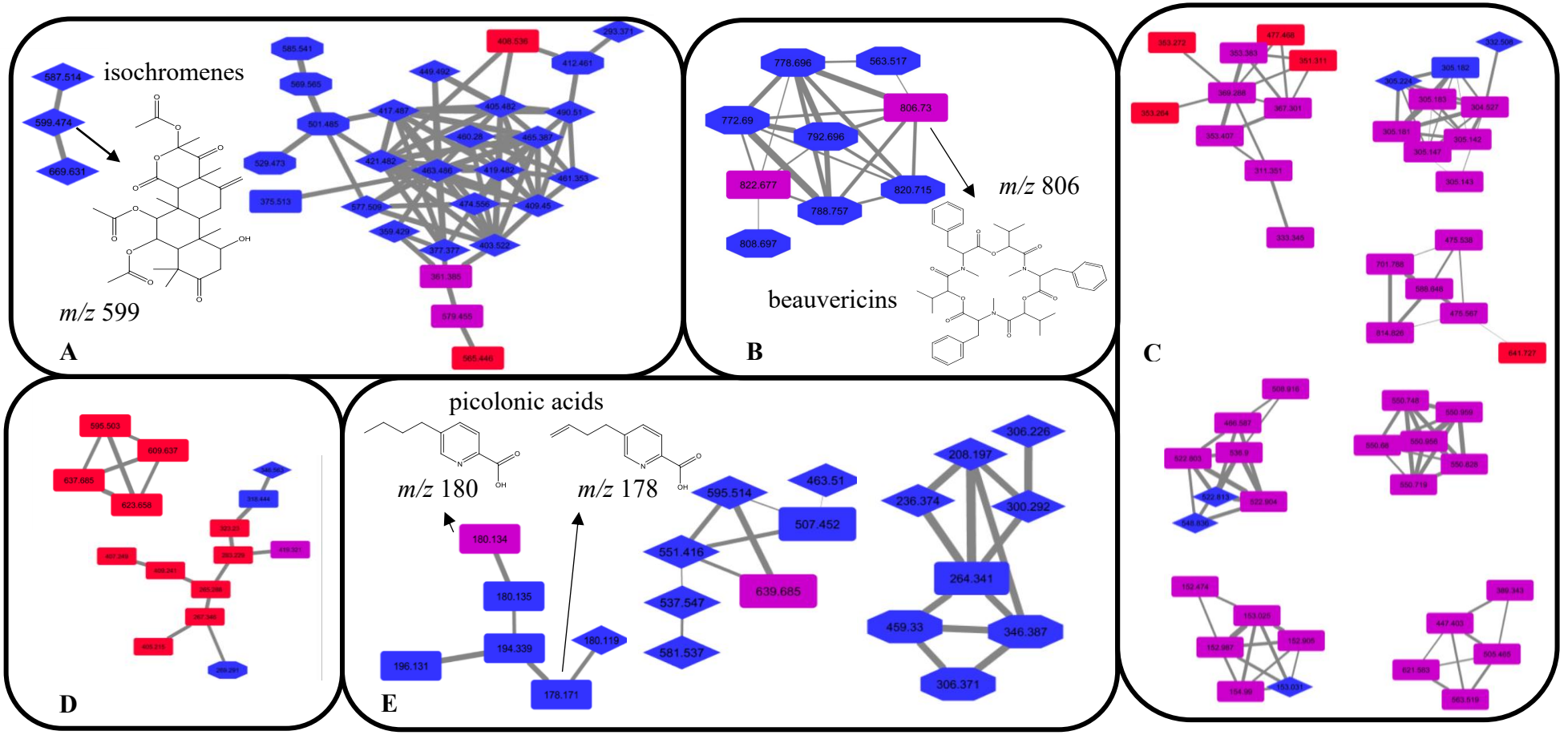

Figure 3.3. Subnetworks of MS/AutoMS data of *Fusarium* strains. Each node represents a protonated molecular ion. **(A)** Clusters found almost exclusively for *F. oxysporum* CSP-R18. **(B)** Clusters found almost exclusively for *F. oxysporum* CSP-19b. **(C)** Network of ions produced by both *Fusarium* species. **(D)** Clusters found almost exclusively for *F. solani*. **(E)** Clusters found almost exclusively for *F. oxysporum* (both CSP-19b and CSP-R18).

3.2. MS/MS Molecular Networking as a Dereplication tool – Identification of Bioactive Metabolites in Promising Fractions

3.2.1. Selection of fungal fractions with biological potential

The first step for the identification of bioactive metabolites by MS/MS Molecular Networking dereplication was the fractionation of extracts, performed in microscale for all *Fusarium* species. This procedure was carried out not only to select biologically promising fractions, but also to reduce the complexity of the data, enabling a more detailed and holistic interpretation of the metabolome.

After fractioning, all samples were dried and weighted, with their respective masses displayed in Figure 3.4. As already observed in the chromatographic analysis of Chapter 2, *F. oxysporum* CSP-R18 revealed an abundant production of polar metabolites, with 94% of the extract content present in the 20 and 40% methanolic fractions. Similarly, *F. oxysporum* CSP-19b also exhibited a high production of polar metabolites, however, for this case, there was a prominent detection of non-polar compounds, indicating the highly diverse chemical profile of this strain. Lastly, *F. solani* CSP-5b displayed significant metabolite production in fractions of all polarities. Nonetheless, fractions with medium and high polarity (60 and 80% MeOH) shows the most abundant mass, eluting 72% of the extract composition.

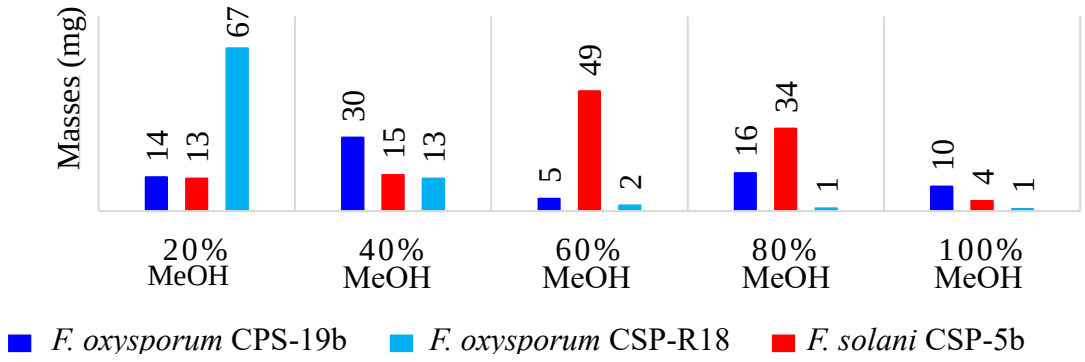

Figure 3.4. Weight of the 20, 40, 60, 80 and 100% methanolic fractions of fungi *F. solani* CSP-5b (red) e *F. oxysporum* CSP-19b (royal blue) e CSP-R18 (light blue).

LC-MS of the fractions, displayed on the Supplementary Material as Figure SM5, was conducted to ensure the efficiency of the fractioning. This analysis revealed that the fractionation procedure resulted in chromatograms of distinct micromolecular profile, as a function of its polarity, for almost every *Fusarium* species, with the exception of *F.*

oxysporum CSP-R18. For that strain, the prevalence of a very intense signal in 12.2 minutes, attributed to fusaric acid, caused column saturation and low efficiency of the process, eluting the same polar signal in high abundance at the 20, 40 and 60% MeOH fractions. Furthermore, in comparison with the chromatograms from the crude extracts, it was also possible to detect a higher number of signals, illustrating how this simples and microscale procedure could help in the prioritization of samples and the selection of biologically promising fractions.

After evaluation of the fractionation efficiency, all samples were submitted to bioactivity tests, for the selection of promising fractions. Prior to these assays, TLC mobile phase optimization was conducted for a more accurate response of the samples on the autobiography antifungal and the acetylcholinesterase inhibition assays. The results established the system Ethyl acetate-Hexane (90:10 v/v) as the best mobile mixture for *F. oxysporum* CSP-19b samples and Chloroform-Methanol (95:5 v/v) as the best elution system for samples *F. solani* CSP-5b and *F. oxysporum* CSP-R18.

Results of the bioassays, displayed on Table 3.1 and in Figures SM6 and SM7 of the Supplementary Material, show that the biological activities obtained during the screening of the fungal crude extracts (Chapter 1) belong, in fact, to specific fractions.

The most bioactive samples were from *F. oxysporum* strains. The polar fractions (20% and 40% MeOH) displayed **(1)** high antifungal action against *C. cladosporioides* and *C. sphaerospermum*, **(2)** bacteriostatic antimicrobial action against *E. faecalis* VRE80 and V583 ATCC700802 (CIM ratio of 512 and 128 μg mL^{-1} and CBM of 256 and 128 μg mL^{-1}), **(3)** strong inhibition of the enzyme acetylcholinesterase and **(4)** high percentage of biofilm eradication of *S. epidermidis* ATCC 35984 (94.4 and 94.3% inhibition for 20% and 40% CSP-R18 MeOH, respectively). In all biological results, the CSP-R18 strains was slightly more active than CSP-19b, probably due to the higher concentration of their major compound in 12.2 minutes.

Furthermore, although both *F. oxysporum* strains are very similar in the composition of polar compounds, the non-polar fractions showed significant chemical and biological differences. For example, the apolar fractions (80 and 100%) of the CSP-19b variety showed higher metabolic abundance and strong biofilm eradication (inhibition of ~ 80% and 28%, respectively), whereas for CSP-R18 this inhibition was significantly lower (41 and 22%, respectively).

The biological results of the fractions of *F. solani* were all less active than *F. oxysporum*. For this species, only samples of medium polarity (40 and 60% MeOH)

showed moderate antifungal inhibition against *C. cladosporioides* and *C. sphaerospermum*, both bioactive at the Rf 0.5 cm band from the TLC plate.

	CSP-19b 20%	**CSP-19b 40%**	**CSP-19b 60%**	**CSP-19b 80%**	**CSP-19b 100%**
Antifungal	s (Rf 0.12-0.25 cm)	m (Rf 0.12-0.25 cm)	i	i	i
Antibacterial	i	Bactericidal*	i	i	i
Acetylcholinesterase Inhibtion	s	s	s	i	i
Antibiofilm (% inhibition)	93.5	84.38	60.53	79.66	27.89
	CSP-R18 20%	**CSP-R18 40%**	**CSP-R18 60%**	**CSP-R18 80%**	**CSP-R18 100%**
Antifungal	s (Rf 0.12-0.25 cm)	s (Rf 0.12-0.25 cm)	i	i	i
Antibacterial	i	Bactericidal*	i	i	i
Acetylcholinesterase Inhibtion	s	s	w	i	i
Antibiofilm (% inhibition)	Not soluble in DMSO	94.4	94.3	40.90	22.12
	CSP-5b 20%	**CSP-5b 40%**	**CSP-5b 60%**	**CSP-5b 80%**	**CSP-5b 100%**
Antifungal	i	m (Rf 0.50 cm)	m (Rf 0.50 cm)	i	i
Antibacterial	i	i	i	i	i
Acetylcholinesterase Inhibtion	i	i	i	i	i
Antibiofilm (% inhibition)	i	i	i	i	i

Table 3.1. Biological assays of the fractions of *F. oxysporum* (strains CSP-19b and CSP-R18) and *F. solani* (CSP-5b). Legend (i) inactive, (w) weak, (m) moderate, (s) strong. *Bactericidal against *E. faecalis* VRE80 and V583 (ATCC700802).

3.2.2. Elucidation of Molecules from Promising Fractions by MS/MS Molecular Networking

The fractions that displayed the highest bioactivity were from *F. oxysporum:* 20 and 40% MeOH fractions, for both CSP-19b and CSP-R18, and 80 and 100% MeOH for CSP-19b. *F. solani*'s fractions only showed moderate activity at medium polarity fractions (40 and 60% MeOH) and was not selected for targeted dereplication.

All the selected fractions were submitted to a targeted analysis by M/MS Molecular Networking for the elucidation of promising metabolites. Network analysis was done separately for **(1)** polar fractions of *F. oxysporum* (20 and 40% MeOH) and **(2)** non-polar fractions of *F. oxysporum* CSP-19b (80 and 100% MeOH). For this process, the fragmentation of all possible analogues were individually evaluated based on the fragmentation pattern of the known metabolite for both polar and non-polar fraction and the confirmation was performed by analysis of the error, in ppm, of the high resolution mass. All the mass data obtained from the clusters on Cytoscape were also assessed by the Data Analysis software (Bruker) to confirm the protonated molecular ion and the possible adducts.

Total Ion Chromatogram (TIC) of the selected fractions are displayed at Figure 3.5. Polar fractions of *F. oxysporum* display an intense signal at 12 minutes, attributed to fusaric acid, and some other few signals of minor intensity. There was a narrow *m/z* range among the most abundant metabolites, displaying precurssor ion in between *m/z* 100-200. On the other hand, non-polar fractions were more diverse, exhibiting signals of different intensities and *m/z* range (*m/z* 300-850). The most abundant metabolite displayed precurssor ion of *m/z* 806, 788, 772, 629 and 569. The ion *m/z* 806 was elucidated as the hexadepsipeptide beauvericin, which eluted at 35.4 minutes in both CSP-19b fractions.

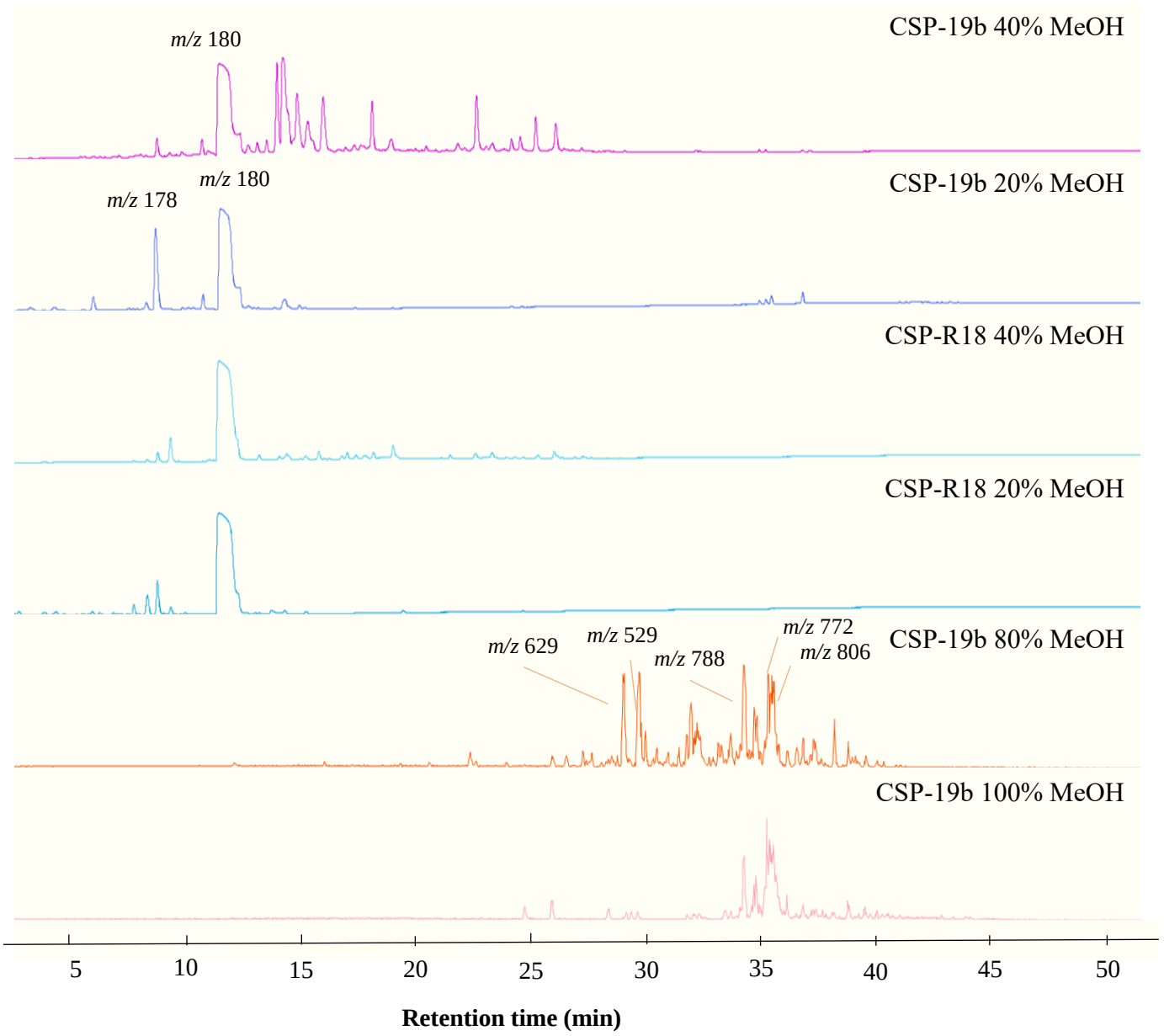

Figure 3.5. Total ion chromatogram (TIC) of the bioactive fractions selected from *F. oxysporum* (strain CSP-19b) for dereplication by MS/MS Molecular Networking.

3.2.2.1. Elucidation of metabolites from the polar fractions of F. oxysporum – Fusaric acid and analogues

The first active search was performed for the polar bioactive fractions of *F. oxysporum* and was based on the two most abundant metabolites in these samples: fusaric and dehydrofusaric acids. These mycotoxins are picolinic acid derivatives with fragmentation pattern that consisted on the loss of water at the carboxylic substituents at position 2, followed by a cleavage in the saturated aliphatic chain at position 5. Both ions

from the protonated molecules (*m/z* 180 and 178, respectively) were cluster together on Cytoscape, along with 2 other nodes, all present exclusively in *F. oxysporum* (Figure 3.6).

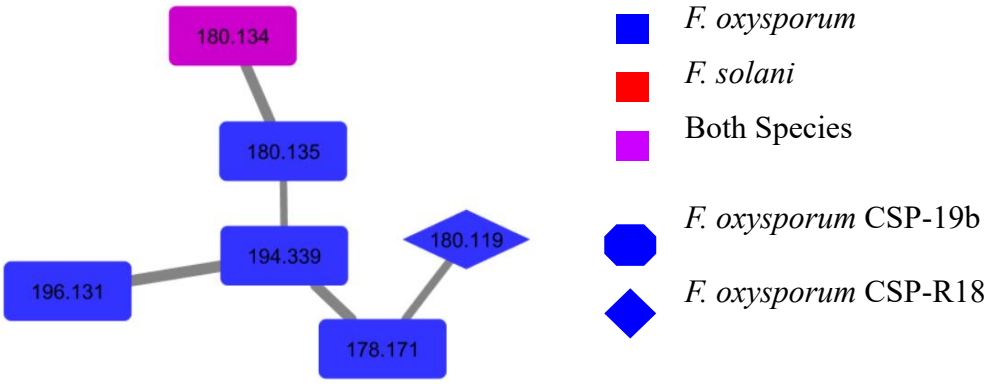

Figure 3.6. Fusaric acid cluster from MS/MS data of extracts and fractions of *F. solani* e *F. oxysporum*.

Molecule elucidation was conducted by comparative analysis with the known analogues according to Figure 3.7. The unknown nodes clustered with fusaric acid and dehydrofusaric acids were elucidated as 5-butyl-6-oxo-1,6-dihydropyridine-2-carboxylic acid (*m/z* 196) and 5-(but-9-enyl)-6-oxo-1,6-dihydropyridine-2-carboxylic acid (*m/z* 194), both metabolites never identified in any *Fusarium* species that are the formed by the oxidation of both fusaric acid and dehydrofusaric acid on the position 6 of the pyridinic ring (Table. 3.2). These compounds were also never reported as naturally occurring and have only been isolated from Chen et al (2013) by epigenetic modifier-induced biosynthesis in the endophytic *F. oxysporum* isolated from *Datura stramonium* (CHEN et al., 2013a). According to Chen and co-workers, neither compounds shows any antibacterial activity, while fusaric acid is active (MIC 25 µg mL^{-1}), indicating that the oxidation of the pyridine ring significantly diminished the antibacterial activity. The molecules were confirmed by high resolution MS and the fragmentation mechanism was proposed by the author and described in Figure 3.7.

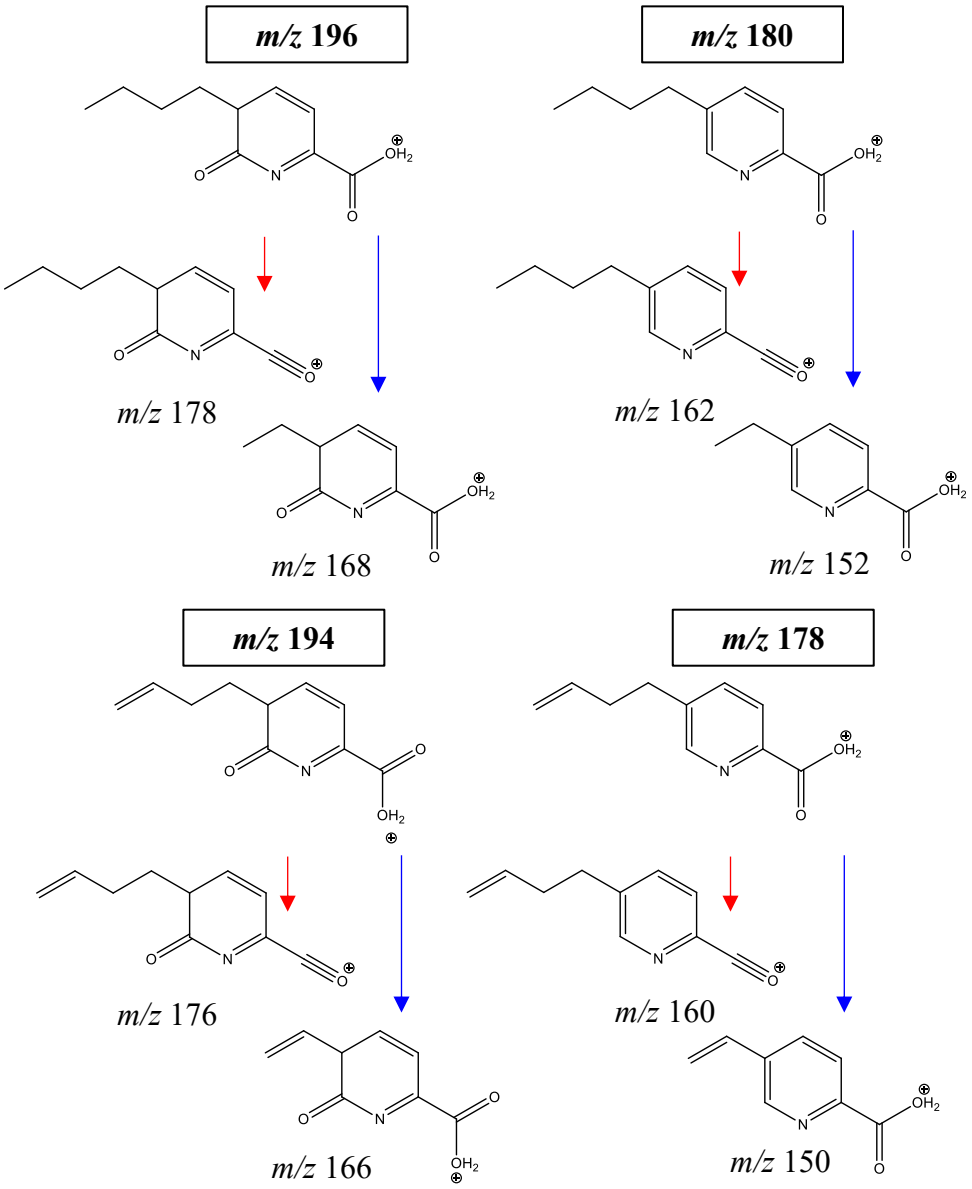

Figure 3.7. Elucidation of fusaric acid and analogues. **(→)** Loss of water $[M\text{-}C_2H_4+H]^+$ at the carboxyl substituent at position 2. **(→)** Loss of 28 $[M\text{-}C_2H_4+H]^+$. The fragmentation mechanism of fusaric acid was detailed on Chapter 2 (topic 3.1).

	Metabolite	Molecular Formula	M	Theoretical *m/z* $[M+H]^+$	Experimental *m/z* $[M+H]^+$	Error (ppm)	RT (min)	MS/MS target	Fragments (*m/z*)*	Intensity
1	5-(but-9-enyl)-6-oxo-1,6-dihydropyridine-2-carboxylic acid	$C_{10}H_{11}NO3$	193.074	194.082	194.111	-2.89	5.82	194	194, 176, 166	3.01E+08
2	5-butyl-6-oxo-1,6-dihydropyridine-2-carboxylic acid	$C_{10}H_{13}NO3$	195.089	196.097	196.09	0.75	6.29	196	196, 178, 168, 108	9.82E+08
3	dehydrofusaric acid (5-(3-butenyl)-picolinic acid)	$C_{10}H_{11}NO_2$	177.079	178.087	178.08	0.64	9.9	178	178, 160, 150, 108	1.07E+09
4	fusaric acid (5-butyl)-picolinic acid)	$C_{10}H_{13}NO_2$	179.097	180.105	180.096	0.95	11.57	180	180, 162, 152	3.09E+09

Table 3.2. Fusaric acid analogues identified by MS/MS Molecular Networking Dereplication of *F. oxysporum* (CSP-19b and CSP-R18) and *F. solani*. Fragments were obtained using the GNPS platform (Proteosafe link) and were confirmed by manual inspection.

3.2.2.2. Elucidation of metabolites from the non-polar fractions of F. oxysporum - Beauvericin and analogues

Evaluation of the non-polar fractions of *F. oxysporum* revealed the presence of beauvericin as the most abundant metabolite. This mycotoxin had already been identified for *F. oxysporum* by previous MS and NMR-dereplication analysis (Chapters 1 and 2), as well as on literature for several *Fusarium* species.

The analysis of the bioactive fractions was based on the fragmentation pattern of this cyclic hexadepsipeptide, which occurs predominantly around the peptide bonds of its monomers. The two major fragments observed are caused by the peptide bond cleavages, resulting in one carboxyl (b fragment) and one amine-terminal fragment (y fragment, Figure 3.8). Moreover, we have also evaluated unusual fragments in every monomer, such as, the breakdown of tertiary carbon that precedes or proceeds the peptide bond (a/x or c/z), cleavage of CO, NH_3 and H_2O groups or the loss of the acidic Asp and Glu residues, when present.

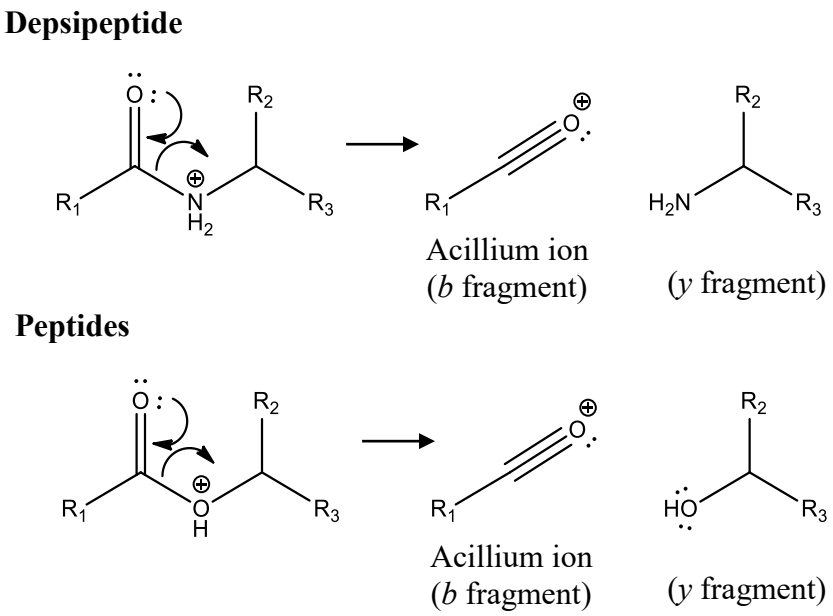

Figure 3.8. Fragmentation mechanism of peptides and depsipeptides. Alpha cleavage of the peptide bond to form b/y fragments.

The active search of beauvericin sodiated adduct at *m/z* 806.73 $[M + Na]^+$ resulted a cluster formed by this depsipeptide and 9 other minor ions, all with cosine similarity values between 73 and 91% (Figure 3.9). Most of the compounds belong exclusively to *F. oxysporum* CSP-19b, which explains the bioactivity on non-polar fractions for this

strain. With the exception of beauvericin, already elucidated for both *Fusarium* species by MS dereplication (Chapter 2), none of these nodes were detected in *F. oxysporum* CSP-R18 and only the ions of *m/z* 806.67 was detected in *F. solani*.

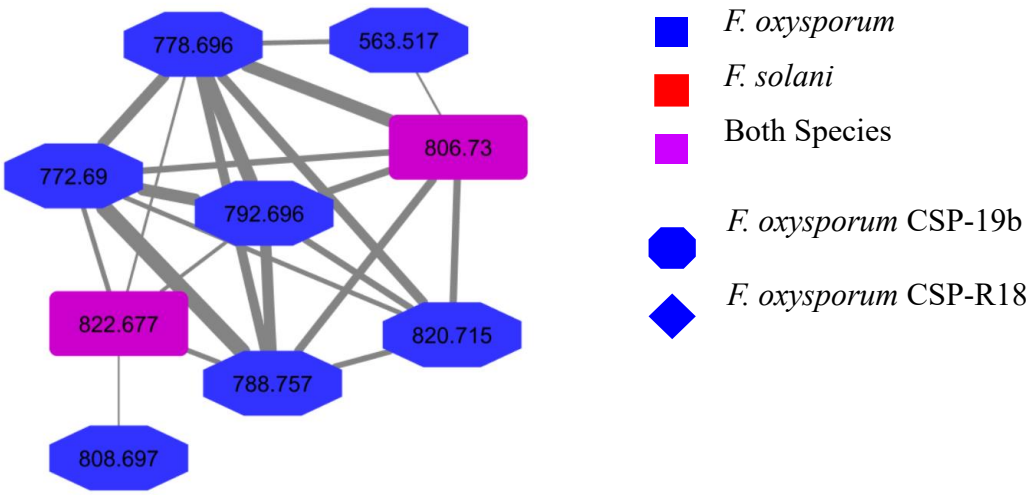

Figure 3.9. Beauvericin cluster from MS/MS data of extracts and fractions of *F. solani* e *F. oxysporum*.

Metabolite elucidation was carried out as shown in Figure 3.10. First, the depsipeptides were constructed according to the fragmentation of their six monomers found on the MS/MS spectra, allowing the proposition of chemical structures and the possible isomers (Figure 3.11). Following, metabolite confirmation was conducted by comparing the UV information and high-resolution mass data with spectrometric information of predicted metabolites. Only the detection of substances whose error between the observed and calculated high resolution mass did not exceed 5 ppm (FUNARI et al., 2013) was considered (KIND; FIEHN, 2010).

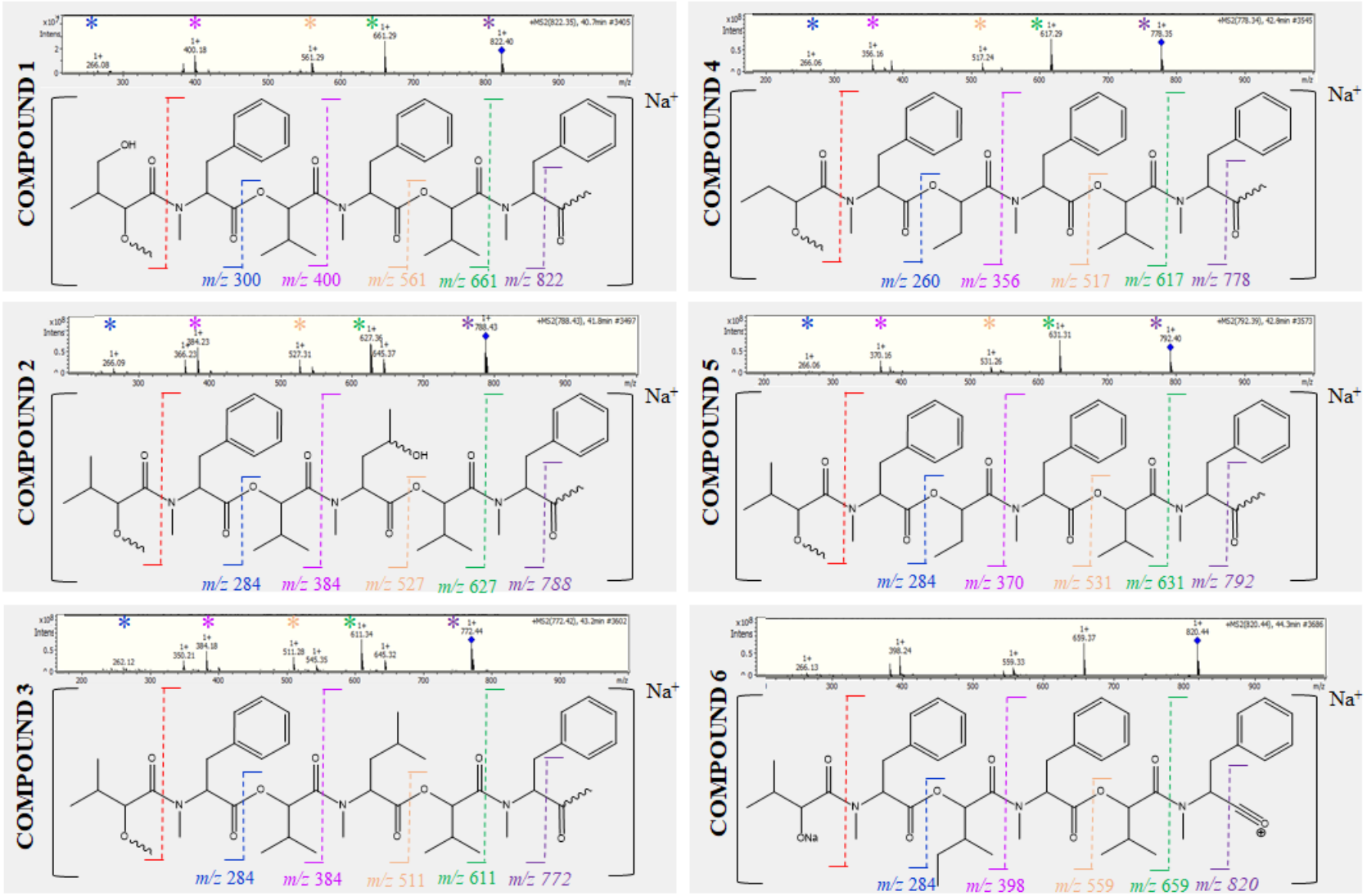

Figure 3.10. Elucidation of beauvericin analogues. Construction of depsipeptides based on the fragmentation of its monomers.

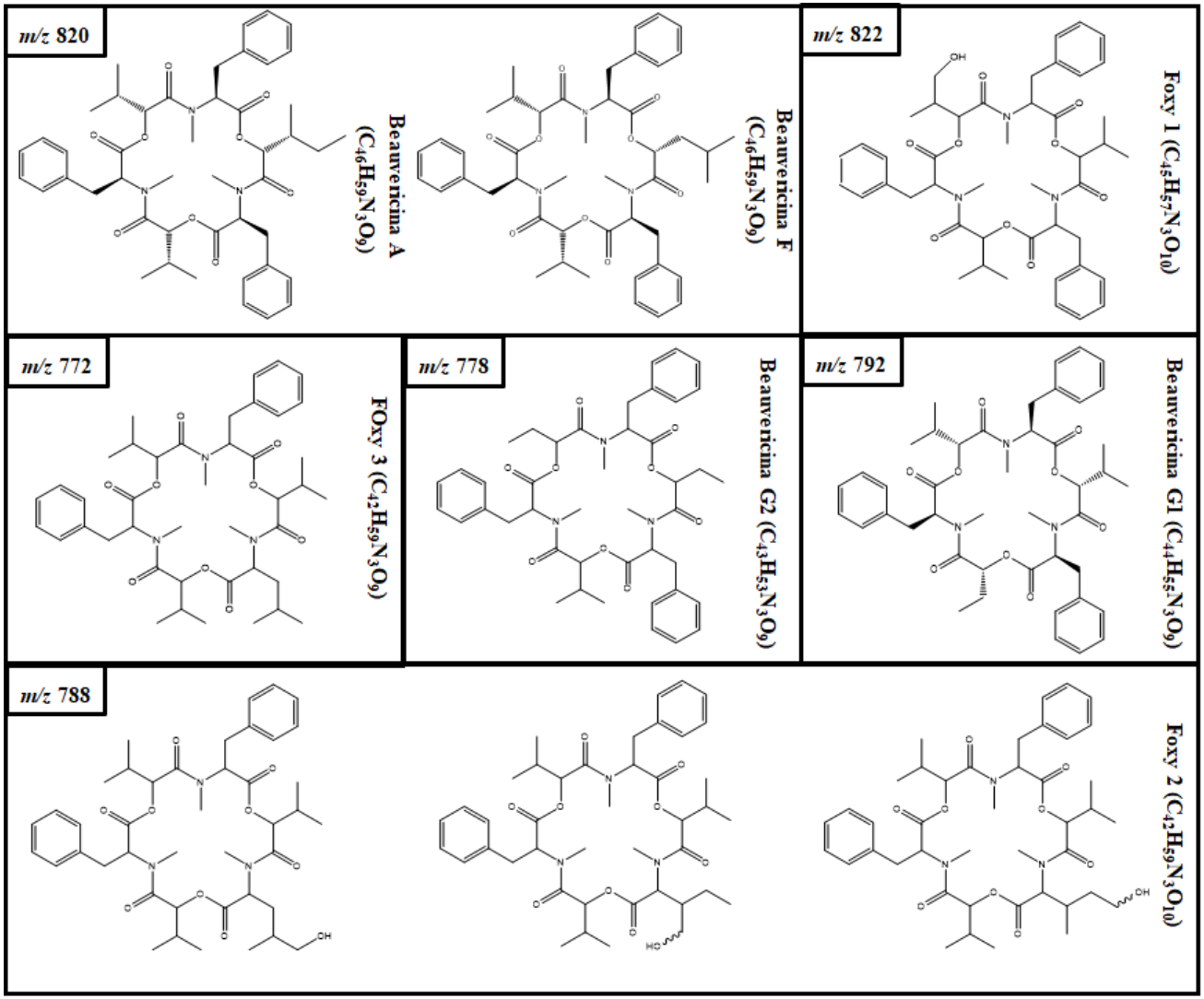

Figure 3.11. Chemical structures proposed after identification of monomers by fragmentation studies. Process for the identification of beauvericin analogues found on the same cluster at the MS/MS Molecular Networking.

For the ions that resulted in more than one possible isomers, the proposed molecules were confirmed by DOSY-NMR analysis of CPS-19b 80%. In this technique, the chemical shifts appear as a function of the diffusion coefficient, allowing the identification of similar compounds in a mixture. From the 9 minor ions, 6 were identified based on the comparative fragmentation of their monomers: the known analogues beauvericin A, beauvericin G1 and beauvericin G2 and the firstly described depsipeptides named FOxy 01, 02 and 03. Beauvericin A has already been reported in the fungal species *Beauveria bassiana* (ARBOLEDA; DELGADO; VALENCIA, 2004), however, no reports have been made regarding their biological potential. On the other hand, beauvericin G1 and G2 have only been found by a synthesis based on precursors, and thus, never natural occurring (XU et al., 2007). Beauvericin G1 and G2 have a known range of bioactivity, including anti-haptotactic and cytotoxic in human cells (XU et al., 2007). Haptotaxis is a directional cell motility that plays a critical role in cancer, acting in the formation of new blood vessels in tumors (angiogenesis), cell invasion and metastasis (CARMELIET, 2003; XU et al., 2007). The fragments and complete fragmentation mechanisms proposed for these metabolites are shown in the Supplementary Material as Figure SM8.

	Metabolite	Molecular Formula	M	Theoretical *m/z* $[M+Na]^+$	Experimental *m/z* $[M+Na]^+$	Error (ppm)	RT (min)	MS2 target	Fragments (*m/z*)*	Intensity
1	FOxy 01	$C_{45}H_{57}N_3O_{10}$	799.4043	822.3942	822.3644	2.975	40.6	822	661, 561, 400, 382, 300	2.25E+09
2	FOxy 02	$C_{42}H_{59}N_3O_{10}$	765.4200	788.4098	788.3797	3.01	41.8	788	645, 627, 527, 384, 366, 266	8.80E+08
3	beauvericin G2	$C_{43}H_{53}N_3O_9$	755.3781	778.3679	778.3395	2.844	42.4	778	778, 617, 517, 356	1.50E+09
4	beauvericin G1	$C_{44}H_{55}N_3O_9$	769.3938	792.3836	792.3541	2.949	42.7	792	631, 531, 384, 266	1.37E+09
5	FOxy03	$C_{42}H_{59}N_3O_9$	749.4251	772.4149	772.3859	2.899	43.1	772	645, 611, 545, 511, 384, 350, 262	2.16E+09
6	beauvericin	$C_{45}H_{57}N_3O_9$	783.4094	806.3992	806.3705	2.874	43.2	806	623, 523, 441, 362, 262, 244	8.47E+09
7	beauvericin A	$C_{46}H_{59}N_3O_9$	797.42513	820.4149	820.3754	3.949	44.2	820	659, 559, 398, 266	1.11E+09

Table 3.3. Beauvericin analogues identified by MS/MS Molecular Networking Dereplication of *F. oxysporum* (CSP-19b and CSP-R18) and *F. solani*. Fragments were obtained using the GNPS platform (Proteosafe link) and were confirmed by manual inspection.

4. Conclusion

MS/MS Molecular Networking allowed for the simultaneous exploration of known molecules and compound classes within this *Fusarium* data, contributing for the chemotaxonomical analysis of these species. In almost every cluster, there was at least one node present inf both *Fusarium* species, which indicated that although *F. solani* and *F. oxysporum* have different chemical profiles, these strains still share a genetic denominator for the production of the same biosynthesis pathways.

Microfraction was an excellent strategy for the separation of secondary metabolites in function of their polarity. The fractions allowed the identification of previously undetected bands on the crude extracts and increased the detection of minor compounds. Results of the bioassays after fractionation showed that the biological activities obtained during the fungal screening belong, in fact, to specific fractions.

The most bioactive samples were from *F. oxysporum* strains. The polar fractions displayed high antifungal activity against *Cladosporium*, bacteriostatic antimicrobial potential against *E. faecalis*, strong inhibition of the enzyme acetylcholinesterase and high percentage of *S. epidermidis* biofilm eradication. In all biological results, the CSP-R18 strains was slightly more active than CSP-19b. The apolar fractions only displayed activity in CSP-19b strain, which showed a high metabolic diversity and strong biofilm eradication.

Molecular Networking, combined with an individual evaluation of high resolution and fragmentation data, allowed not only the elucidation of different mycotoxins, but also the understanding of fungal biosynthetic pathways. This dereplication analysis supported the elucidation of 4 picolinic acid derivates and 7 beauvericin analogues. The benefit of such an approach was that spectra are organized based on fragmentation similarity, facilitating the identification of analogues directly in complex matrices

Detection, characterization and identification of the observed signals are still a challenge in MS-based metabolomics. In microbial studies, identification of a molecule is usually carried out by tandem mass fragmentation, in which the experimental patterns are compared with consolidated databases. However, as most molecules involved in microbial metabolic exchange are unique to these organisms, there are no comprehensive databases that has a searchable library sufficient to cover these unique molecules. In this sense, manual interpretation of fragmentation data is still required and recommended.

CHAPTER 4. REVIEW - ENHANCING CHEMICAL AND BIOLOGICAL DIVERSITY BY CO-CULTURE – WHAT WE KNOW AND WHERE DO WE GO

Article title: Enhancing Chemical And Biological Diversity By Co-Culture – What We Know And Where Do We Go

Journal: Applied Microbiology and Biotechnology.

Status: Submitted.

Authors: Denise M. Selegato[1,2], Ian Castro-Gamboa[2], Hye Kyong Kim [1], Young H. Choi[1, 3].

Affiliations:

[1] Natural Products Laboratory, Institute of Biology, Leiden University, Leiden, The Netherlands.

[2] Nucleus of Bioassays, Biosynthesis and Ecophysiology of natural products (NuBBE), Institute of Chemistry, São Paulo State University, Araraquara, Brazil.

[3] College of Pharmacy, Kyung Hee University, 02447, Seoul, Republic of Korea

Abstract

Microbial metabolites have tremendous potential to provide new therapeutic agents since extremely diverse chemical structures are found in an extensive and still little studied microbial population. Conventionally, these natural products are screened by single-strain cultures. However, owing to the absence of biotic and abiotic interactions in monocultures, the growth conditions are significantly different from those encountered in the natural environment, providing poorer profiles and the frequent re-isolation of known metabolites. In the last decade, several methods have been developed to eventually understand the physiological conditions under which microbial cryptic genes are activated, in an attempt to stimulate their biosynthesis and elicit the production of hitherto unexpressed chemical diversity. Among those, co-cultivation is considered to be one of the most efficient ways to induce silenced pathways, mimicking the competitive microbial environment for the production and comprehensive regulation of metabolites. Over the years, co-culture has become a golden genome-independent methodology for metabolome expansion and requires no prior knowledge of the signaling mechanism and fungal genome nor any special equipments for cultivation and data interpretation. Several reviews have shown the potential of co-cultivation for the production of new biological leads. However, these were mainly limited to describe relevant chemical outcomes reported in literature. Only few articles have detailed experimental, analytical and microbiological strategies for efficiently inducing bioactive molecules by co-culture. In this review paper, we have continued to shed light on the co-culture experimental workflow and contribute to the development of detailed and standardized co-cultivation methods compatible with high-throughput analytical procedures. Particularly, we have interpreted all major mixed-fermentation publications from 1978 to 2019, displaying what we know regarding different types of co-culture set-ups, metabolic inductions and interaction effects, and how these can be optimized to enhance chemical and biological diversity.

Keywords: co-culture, activation of cryptic genes, enhanced of chemical diversity.

1. Introduction

Microbial secondary metabolites, resulted from several million years of evolutionary biosynthetic optimization, have tremendous potential to provide new therapeutic agents (PETTIT, 2009). In a recent review, Newman and Cragg have shown that, even with the challenges related to unlocked genomes and unculturable strains, microbial bioactive compounds are the future for drug discovery programs (NEWMAN; CRAGG, 2016), accounting for over 42 thousand natural compounds already reported from different microbial families (LAATSCH, 2012).

The potential of these microbial secondary metabolites comes not only from an extremely diverse chemical structures but also from an extensive and still little studied microbial population. Indeed, recent whole-genome sequencing of several fungi and bacteria shows that the potential of microbial matrices to produce secondary metabolites is fairly underestimated, meaning that a much broader range of compounds could be produced if the silent genes are induced by whatever methods (BERGMANN et al., 2007; CHIANG et al., 2008; GALAGAN et al., 2005; HIBBING et al., 2010; SCHROECKH et al., 2009).

Conventionally, in the fields of microbiology, single-strain cultivation has been the standard method for the screening of secondary metabolites. However, owing to the absence of biotic and abiotic interactions, the growth conditions in monocultures are significantly different from those encountered in the natural environment (ONAKA et al., 2011; PETTIT, 2009). In nature, microbial metabolic pathways are often regulated by complex cascades, in which their chemical profiles are controlled by genes and influenced by biotic communication with external factors. For example, on competitive environments, microbial species engage in constant interactions with their neighbors, competitors and hosts, resulting in ecological effects that ensures survival and shapes the community (MOODY, 2014).

The absence of biotic and abiotic incentive is the biggest limitation of axenic cultures and limits the chemical diversity that can be obtained by one single strain. In fact, monoculture screening often provides a still increasing rate of redundancy, resulting in chemically poorer profiles and the frequent re-isolation of known secondary metabolites (HONG et al., 2009; MARMANN et al., 2014). In the last decade, several methods have been developed to eventually embody the physiological conditions under which cryptic genes are activated, in an attempt to stimulate their biosynthetic pathways and elicit the production of hitherto unexpressed chemical diversity (SCHROECKH et al., 2009; WAKEFIELD et al., 2017). Overall, these strategies have been successfully applied for the genomic activation,

simultaneously modifying different levels of the cellular machinery to regulate the production of different classes of secondary metabolites (BERTRAND et al., 2014a; HERTWECK, 2009; WAKEFIELD et al., 2017).

Among those, genetic-dependent approaches, such as mutasynthesis, heterologous expression and metabolic engineering (BERGMANN et al., 2007), have been used as one of the most effective methodologies for gene activation. However, these procedures are mostly applied for known structures and require both expensive instrumentation and a previous knowledge of the microbial genome. Contrarily, cultivation-dependent methodologies, that includes substrate feeding (DE BOER; SCHMIDT-DANNERT, 2003), small molecules modifier feeding (PETTIT, 2011b), co-culture and One Strain, Many Compounds (OSMAC) (BODE et al., 2002; RATEB et al., 2011; ROMANO et al., 2018; WEI et al., 2010), have provided a broader regulation of the metabolome, increasing chemical diversity in a more comprehensive and unsupervised manner.

Microbial co-culture involves the cultivation of two or more microorganisms in the same confined environment and has been considered to be a golden strategy to induce cryptic pathways. In mixed fermentation, microorganisms metabolize the media substrate together, mimicking the competitive microbial environment for the production and regulation of constitutively molecules (RATEB et al., 2013; WAKEFIELD et al., 2017). On these experiments, microbial communication occurs either by volatiles or *in-loco* signaling and leads to the regulation of secondary metabolites, even if the detailed inducing mechanism, in the biological and ecological context, remain largely unknown (PETTIT, 2011a; RATEB et al., 2013; SCHROECKH et al., 2009). In practical terms, co-culture is a key genome-independent method for metabolite enhancement in microbial systems given it does not require any prior knowledge of the signaling mechanism and genome, nor any special equipment for the cultivation and data interpretation (MOODY, 2014).

Based on the current research, it is accepted that mixed culture might be successfully applied to **(1)** overcome limiting steps of a desired biosynthetic pathway (ZHANG; STEPHANOPOULOS, 2016), **(2)** prevent enzymes from producing byproducts, **(3)** increase single cell protein production (TESFAW; ASSEFA, 2014)**, (4)** induce or increase bioactivity through co-culturing with challenge organisms (CHANOS; MYGIND, 2016; SUNG; GROMEK; BALUNAS, 2017), **(5)** suppress virulence of challenge microbe (MINERDI et al., 2009) and **(6)** improve the bioactive metabolite production by auxiliary microorganism (ARIANA; HAMEDI, 2017; LIU et al., 2006; SHIMIZU et al., 1999).

For the last decades, co-culture has already been established technically for the understanding of natural or synthetic interactions between cell populations of human microbiota and pathogens, as well as to improve biochemical processes in the food (ISLAM et al., 2017), solvent and oil industries (KUMARI; NARAIAN, 2016; TAO et al., 2017). Successful examples of industrially applied co-cultures can be found in wastewater treatment, soil remediation, and food and gas production (CHAUDHRY; CHAPALAMADUGU, 1991), such as dairy products (KARILUOTO et al., 2006; MARTIN et al., 2001; NARVHUS; GADAGA, 2003; SODINI; LATRILLE; CORRIEU, 2000), salami (DICKS; MELLETT; HOFFMAN, 2004) and alcoholic beverages (BEEK; PRIEST; PRIEST, 2002; CLEMENTE-JIMENEZ et al., 2005; CORT; KUMARA; VERACHTERT, 1994; FLEET, 2003; RENOUF et al., 2006).

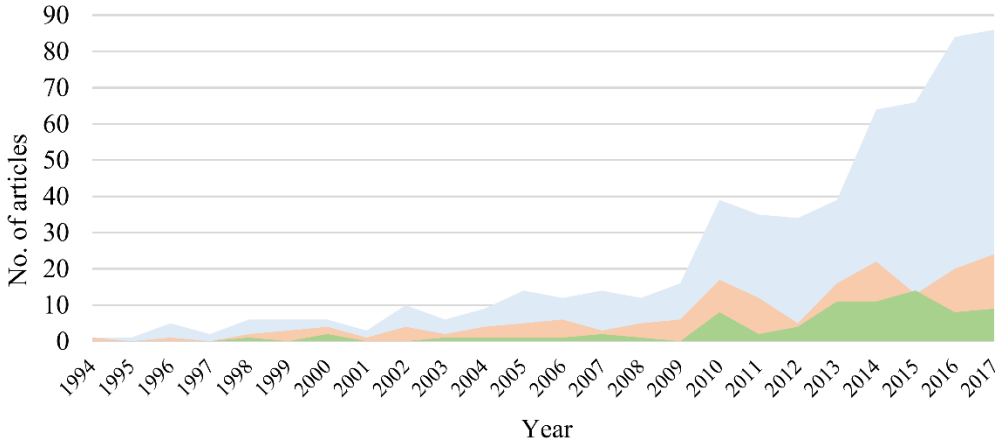

Figure 4.1. Evolution of the field of microorganism co-culture; Number of publications per year in the field of microorganism co-culture (blue), microorganism co-culture and activity (salmon) and microbial co-culture and secondary metabolites (green), as indicated by the number of publications per year from 1994 to 2019 (Web of Science/Science Direct).

Co-cultivation research that targets the enhancement of chemical diversity are still at its infancy when compared to human health and industrial processes, with even fewer reports regarding the genetic, biosynthetic and biological use of these induced compounds (Figure 4.1). In most cases, antagonistic communications, in which microbes compete for space and nutrients, are the most studied type of co-culture interaction and has been performed focusing on the induction of antinfective and anticancer metabolites as an alternative to overcome pathogen multidrug resistance (DASHTI et al., 2014; UEDA; BEPPU, 2017). Nonetheless, other types of neglected microbial interaction, other than antibiosis, has also resulted in

sporulation, biofilm formation and bioactive metabolomic variation, including amensalism, commensalism, cooperation and mutualism (UEDA; BEPPU, 2017).

Several reviews have shown the potential of co-cultivation for the production of new biological leads, however, these studies were mainly limited to describe relevant chemical outcomes reported in literature (Burgess et al. 1999; König et al. 2006; Pettit 2009; Shank and Kolter 2009; Tarkka et al. 2009; Bader et al. 2010; Pettit 2011; Goers et al. 2014; Marmann et al. 2014; Moody 2014; Netzker et al. 2015; Abdalla et al. 2017; Ueda and Beppu 2017; Onaka 2017; Stasulli and Shank 2016; Rutledge and Challis 2015). Over the last decade, only few articles have detailed experimental, analytical and microbiological strategies for efficiently inducing bioactive molecules by co-culture (AZZOLLINI et al., 2018; BERTRAND et al., 2014a, 2014b).

In this review paper, we have continued to shed light on the co-culture experimental workflow and contribute to the development of detailed and standardized co-cultivation methods compatible with high-throughput analytical procedures. Particularly, we have interpreted all major mixed-fermentation publications from 1978 to 2019, displaying what we know regarding different types of co-culture set-ups, metabolic inductions and interaction effects, and how these can be optimized to enhance chemical and biological diversity. Figure 4.2 represents a schematic workflow of the content of this review, which include **(1)** the basics for the experimental set-up, exhibiting all critical abiotic, biotic and analytical parameters for a successful metabolic induction and data interpretation, **(2)** the types of metabolic outcomes and some examples of their biosynthetic origin, **(3)** the microorganisms most used for co-cultivation and their chemical and biological potential, **(4)** the biological and ecological outcomes obtained so far on co-culture experiments, and **(5)** a brief description of the few induction trigger reported in literature. The references of all the articles reviewed from 1978 to 2019 are displayed in the Supplementary Material.

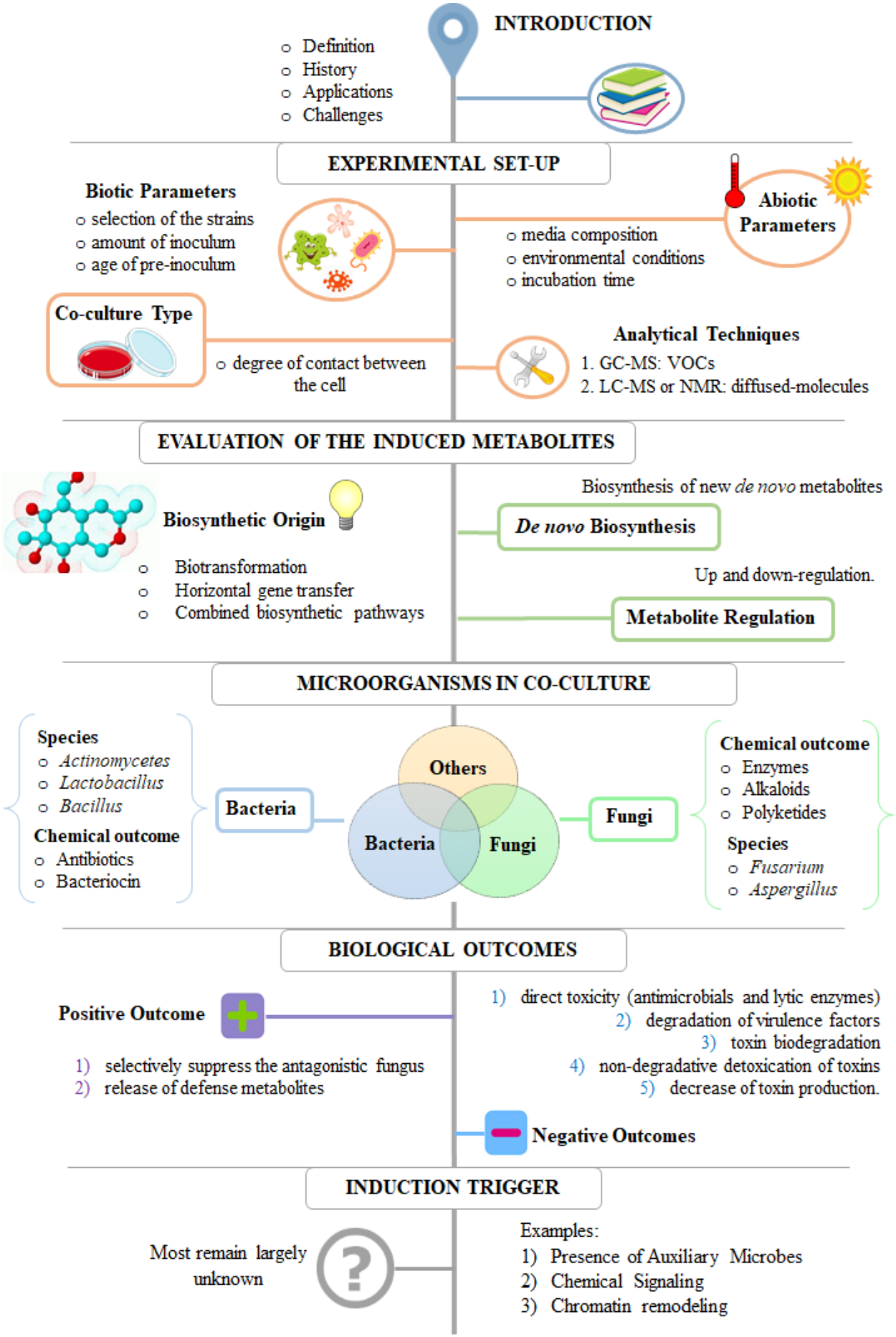

Figure 4.2. Topics for the application of co-culture for the enhancement of chemical diversity.

2. Setting up a Co-culture Experiment

2.1. Biotic and abiotic parameters

It is well known and repeatedly reported in literature that the choice of the growth conditions can immensely affect the chemical profile in axenic cultures, resulting in changes in the amount and diversity of secondary metabolite production (BODE et al., 2002; SCHERLACH; HERTWECK, 2009). In co-culture experiments, apart from these cultivation variables, the biotic parameters and the degree of cell-cell communication between strains also need careful consideration to define the best variables for the metabolic induction (Figure 4.3) (GOERS; FREEMONT; POLIZZI, 2014).

Overall, when starting an experimental design for co-culturing, several factors should be properly assessed for the optimization of the research purpose, including (1) the selection of the co-culture system, which is detailed in the section bellow; (2) the selection of the induced and challenge microbe, based on the desired type of microbe interaction (*e.g.* antibiosis, symbiosis, mutualistic and others), taxonomic criteria or biological/ecological data, (3) amount of inoculum from each strain, considering the growth rate evaluation of selected microbes, (4) age of pre-inoculum, *i.e.* the incubation period of each strain prior to co-cultivation; (5) incubation time, (6) degree of contact between the cell and (7) abiotic factors, such as temperature, pH, agitation luminosity, liquid or solid media and nutrient/water availability.

The optimization of the factors that influence a co-culture experiments can be performed by individual assessment of the variables or by systematic analysis in a Design of Experiment (DoE). Any subtle change greatly affects the production of individual metabolites, meaning that each parameter could regulate the activation of specific metabolic pathways. For example, Slattery and colleagues have demonstrated that 24-hour pre-inoculation of the inducer bacteria *Streptomyces tenjimariensis* was essential to enhance the production of the aminoglycoside antibiotics, istamycins A–B, when in co-culture with challenge marine bacterias. Simultaneous co-inoculation or pre-establishment of challenge microbes without pre-inoculation resulted in a significant decrease in the production of istamycins compared with that in S. *tenjimariensis* single culture (SLATTERY; RAJBHANDARI; WESSON, 2001). Similarly, other studies have shown that *Lactococcus lactis* increased the production of nissin, a polycyclic peptide, only in co-culture with specific bacteria that consume lactic acid as carbon source, such as *Yarrowia lipolytica* (ARIANA; HAMEDI, 2017), *Saccharomyces cerevisiae* (LIU et al., 2006) and *Kluyveromyces marxianus* (SHIMIZU et al., 1999), providing a successful increase in production in up to 85% in comparison to the control.

If the research targets to evaluate the ecological response rather than an increase in chemical diversity, it is critical to perform a detailed evaluation of all biotic and abiotic variables present in the natural biological system in order to mimic the physiological conditions that elicit the same complex reactions in nature (HOGAN, 2006). One good example is the study of mutualistic microbe *Candida albicans* and *Pseudomonas aeruginosa*, commonly encountered together in the sputum of cystic-fibrosis (CF) patient. In this CF isolates, *C. albicans* produces farnesol, a sesquiterpene that acts to inhibit both the filamentation of its producer and the swarming motility and the release of secondary metabolites in *P. aeruginosa*, demonstrating how the microbial interactions contribute to disease in polymicrobial infections (CUGINI et al., 2007; MCALESTER; O'GARA; MORRISSEY, 2008).

2.2.Types of co-cultures experiments

The selection of the type of co-culture is a critical step in the experimental workflow and should be based on purpose of study and the analytical techniques available for the evaluation of the chemical profiles. For example, if the work targets to evaluate only the chemical responses of volatiles molecules by gas chromatography and mass spectrometry, it is important to select a co-culture experimental set-up that enables volatile extraction and prevents cell-to-cell contact. Figure 4.3 shows the two most common set-ups for co-culture evaluation, considering the degree of contact between the cells and the type of induction evaluated in the study. Their applications, advantages and disadvantages are described in sections bellow.

2.2.1. Experiments without Microbial Barriers (with cell-cell contact)

In most co-culture systems, the activation of cryptic genes is achieved by the inoculation of the inducer microbe in the presence of a competing strain, without any physical barriers between them. In these systems, metabolic induction can happen either by agar-diffused signaling molecules, during direct physical contact, or by the release of volatiles in the environment, resulting in an often complex and multivariate chemical responses (BADER et al., 2010). Among these traditional cultures, the growth of both microorganisms freely in the medium elicits nature's most similar response (Figure 4.3A), providing a comprehensive evaluation and interpretation of the microbial interactions.

Notwithstanding these advantages, in nearly all studies that uses these experimental set up, the evaluation of the chemical dynamics is only carried out by agar-diffused molecules, without considering the presence and importance of volatile organic compounds (VOC) in the

microbial system (KÖNIG et al., 2006; NONAKA et al., 2011; OLA et al., 2013). So far, only very few studies report the simultaneous analysis of both chemical outcomes, increasing the concern over the proper chemical interpretation of these microbial interactions.

Generally, solid media is the standard method for the screening of bioactive metabolites since colony growth in a petri dish enables evaluation of the microbial morphological changes and individual assessment of each microbial contribution for the metabolic induction (BERTRAND et al., 2013a; YAO et al., 2016). In this experimental set-up, antagonistic interactions are readily visible in just a few days of inoculation, facilitating the target analysis of antimicrobials compounds from the confrontational zone (Moree et al. 2013; Akone et al. 2016; Serrano et al. 2017).

In 2014, Bertrand and co-workers reported that fungal co-culture in solid media could result in four major interaction types. Morphologically, the interaction between two fungi are very changeable, even within one single strain and could result in different metabolic outcomes (Figure 4.4). The first type of morphological change, named *distance-inhibition*, is usually a result of antibiosis and happens when fungal growth stops at a distance from the competing culture, possible due to release of antimicrobial secondary metabolites into the media. The second type is also a result of microbial antagonism and the release of antimicrobial metabolites, in which the fungal colonies grow until contact and form a dark precipitate in the confrontation zone, denominated *zone lines*. In the third group, both fungi grow until contact but do not produce any evidence of metabolite release or confrontation, respecting each other place in a *contact-inhibition* response. Lastly, the fourth type of interaction occurs when fungi grow until contact with partial or complete invasion of one fungus by the other, in a so-called *overgro*wth. Although there is no clear evidence of secondary metabolite production in this type, this competitive interaction is a clear result of morphological and developmental changes by microbial signaling (BERTRAND et al., 2013a, 2014a).

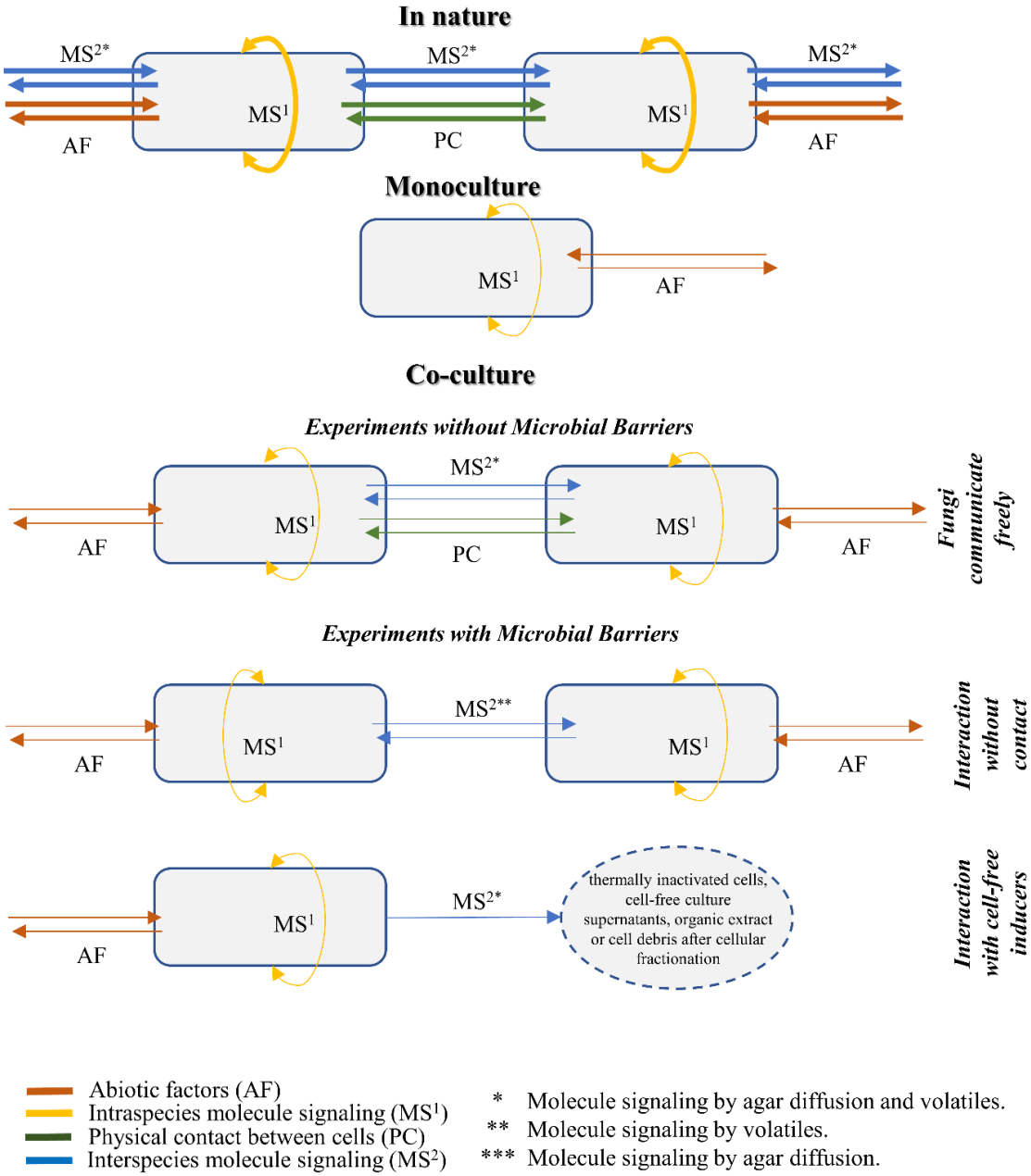

Figure 4.3. Illustration of the microbial interaction and their molecule signaling in the natural environment, monoculture and co-culture. Co-cultivation methodologies are divided in three different experimental conditions, considering the degree of contact between the cells and the type of induction evaluated on the study.

So far, only very few articles indicated the exact type of colony morphology and its corresponding biological outcome in solid media experiments. Most of co-culture reports indicate only chemical induction without any standardized description of morphological

interactions. Good examples of morphological descriptions include Glauser et al. 2009 and Bertrand et al. 2013b. Glauser and co-workers evaluated the zone line of two grapevine fungal pathogens *Eutypa lata* and *Botryosphaeria obtuse* and were able to elucidate the fungitoxic poliketides *O*-methylmellein, 4-hydroxy-8-*O*-methylmellein and 5-hydroxy-8-*O*-methylmellein only from this confrontation zone (GLAUSER et al., 2009). Similarly, Bertrand and co-workers isolated the secondary metabolite responsible for the distance-inhibition zone between *Trichophyton rubrum* and *Bionectria ochroleuca* as the polyketide 4″-hydroxysulfoxy-2,2″-dimethylthielavin, produced up-regulated in the confrontation zone between these fungi in solid culture (BERTRAND et al., 2013b).

Other than the release of interspecies secondary metabolites, the morphological changes in the presence of a challenge strain can also be a results of metabolites produced primarily to act as intraspecies signaling (BADER et al., 2010; CRESPI, 2001). In the early days, the release of these small molecules, named diffusible signal factor (DSF), was only focused on the intraspecies response of these signals in opportunistic pathogens. However, although not the focus of the review, there are increasing evidences that these molecules can promote regulation in other microbes, highlighting the important role of these molecules to disease in polymicrobial environment and infection mechanism (MCALESTER; O'GARA; MORRISSEY, 2008). Research to date shows that DSF can modulates both inducer and challenged strain by a variety of mechanism, inflecting antagonistic to mutualistic responses, morphological transitions, virulence control and release of important secondary metabolites.

For example, *Xanthomonas campestris* and *Stenotrophomonas maltophilia* produce the fatty acid *cis*-11-methyl-2-dodecenoic acid to control intraspecies biofilm formation and virulence capacities of its producers (DOW et al., 2003; HE; ZHANG, 2008; TORRES et al., 2007). However, studies have shown that, when in co-culture, this molecules can also promote hyphae inhibition in *Candida albincans* (WANG et al., 2004) as well as influence biofilm architecture, stress response and polymyxins tolerance of *Pseudomonas aeruginosa* (FOUHY et al., 2007; RYAN et al., 2008). Similarly, the α,β–unsaturated fatty acid cis-2-dodecenoic acid (BDSF), produced by *Burkholderia cenocepacia* has also been shown to produce interspecies response, being responsible for restoring biofilm and extracellular polysaccharide production in *X. campestris* and inhibiting germ tube formation of *C. albicans* (BOON et al., 2008).

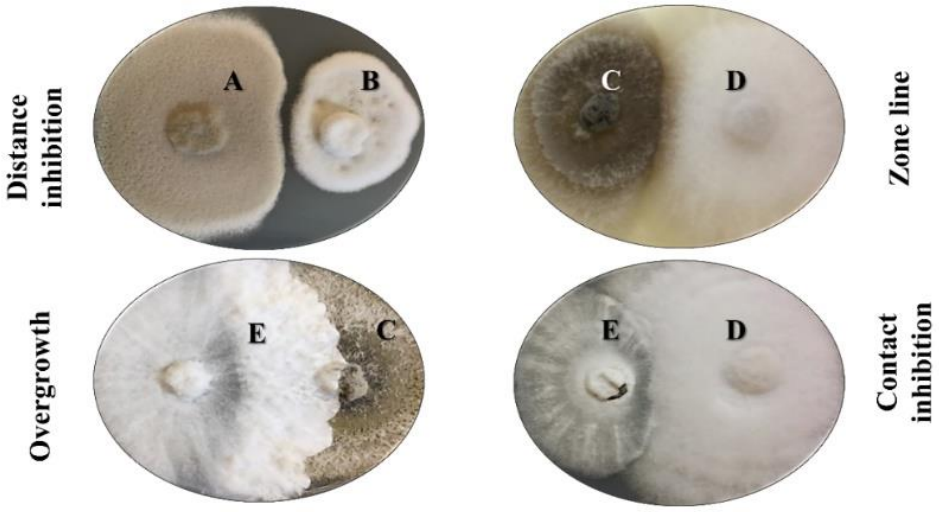

Figure 4.4. Morphological interactions in co-culture experiments with two fungi on solid media. Bertrand and colleagues reported four major morphological outcomes in these co-culture experiments in petri dish: distance inhibition, zone lines, contact inhibition and overgrowth (BERTRAND et al., 2014a).

2.2.2. Experiments with Microbial Barriers (without cell-cell contact)

While some microbial interactions in co-culture experiments depend on cell-to-cell contact, in some other circumstances, the release of induced secondary metabolites appears to be triggered even without clear evidence of contact. For this particular case, metabolic variation can be evaluated by **(i)** co-cultivation in petri dishes with some degree of isolation between the microbes or **(ii)** cultivation of inducer strains without the presence of challenge strains, using only the signaling metabolites, found as pure compounds, in extracts, cell debris or cell-free supernatants (KÖNIG et al., 2013).

In most cases, cell contact is controlled by establishing physical barriers that prevents physical contact between cells in the culture medium, which include the use of culture membranes or segregated petri dishes (BOGDANOWICZ; LU, 2013). However, if the experimental set up does not occur with two living cells, the only concern for the system is to set an adequate concentration of the metabolite(s) or mixture added to the cultures.

Benitez and co-workers have demonstrated that *Bacillus amyloliquefaciens* LBM 5006 produces higher concentration of an antibiotic peptide when in liquid co-culture with *Escherichia coli* ATCC 25922 and that this induction was not associated to the presence of living cells, enhancing bacteriocin production even with thermally inactivated cells, and *E. coli* cell debris after cellular fractionation (BENITEZ et al., 2011; CHANOS; MYGIND, 2016). On

the other hand, Cueto and co-workers have shown that the antibiotic pestalone was only induced by cell-to-cell contact between *Pestalotia* sp and an antibiotic-resistant marine α-proteobacterium and that in neither organic extracts or cell-free culture supernatants the chlorinated benzophenones were detected (CUETO et al., 2001).

2.3.Analytical Techniques

Regardless of the biotic and abiotic conditions, the chemical evaluation of the co-culture experiment needs to assess both diffused metabolites and VOCs for a comprehensive analysis of the microbial interaction. Only recently, efforts have been made to develop methodologies that provide this holistic analysis of molecular dynamics. For instance, in 2018, Azzollini and co-workers have shown a strategy for the concomitant analysis of volatile and non-volatile metabolomes in co-culture systems, in which the fungi are directly grown in vials. In this methodology, each vial is first submitted to head space solid phase microextraction gas chromatography mass spectrometry (HS-SPME-GC-MS) for the analysis of VOCs. Following, the corresponding solid culture is extracted with organic solvents and analyzed by liquid chromatography and high-resolution mass spectrometry (LC-HRMS) for the evaluation of diffused molecules (AZZOLLINI et al., 2018).

Generally, molecules released in the culture medium are extracted by routines extraction protocols (ROSS et al., 2014; SERRANO et al., 2017). Nonetheless, these processes are not specific for microbial analysis and still need improvement for a more rapid perspective of the chemical profile. One example of successful methodological developments was proposed by Bertrand and co-workers. In their approach, fast and simultaneous assessment of the metabolites were performed by down-scaled co-culture using multi-well plates, strongly stimulating fungal growth. Moreover, the use of a 12 well-plate ensured rapid and efficient generation of a large number of replicates and had a reliably up-scale using a large-scale 15 cm for metabolite purification and isolation. These results partially overcome the difficulties of 9 cm plates regarding growth rate of different fungi, metabolic changes based on the duration of growth and lack of sufficient material for isolation, providing a rational way to highlight the metabolic induction (BERTRAND et al., 2014b).

The chemical interpretation of diffused molecules in co-cultures is usually carried out by mass spectrometry and successful results were achieved using both LC-MS (BERTRAND et al., 2014b; HOSHINO et al., 2015a) and MS-imaging methodologies (MOREE et al., 2012, 2013). Moreover, due to the complexity of the isolated compounds, identification of the

induced metabolites often requires the use of complementary analytical tools, such as 1D and 2D Nuclear Magnetic Resonance (ANGELL et al., 2006; WANG et al., 2013).

Opposingly, VOC profiles are obtained by headspace trapping using static and dynamic techniques and chemical analysis is always conducted by gas chromatography–mass spectrometry analysis. Recently, Brasch and co-workers have demonstrated the isolation of stereochemically pure in co-culture experiments using enantioselective GC-MS. In this study, these induced metabolites were trapped using solid-phase-micro-extraction (SPME) fibres that were inserted into the dishes through a small hole and left in place for 2 hours to allow VOC adsorption. Some practical approaches to volatile analysis using solid phase microextraction (SPME)-GC-MS can be found at Tholl and co-workers (THOLL et al., 2006).

3. Metabolite induction in mixed cultures

The activation of cryptic genes coded for unexplored secondary metabolites makes co-cultivation a golden genome-independent method for chemical enhancement in microbial system. The presence of a biotic trigger usually leads to an increase in metabolite detection either by regulation of previously known compounds (SUNG; GROMEK; BALUNAS, 2017) or by the synthesis of new *de novo* metabolites (KUROSAWA et al., 2008; PETTIT, 2009) (Figure 4.5).

Recent data has suggested that metabolic induction can happens either by the activation of pathways from only one strain or by a combined effort between the competing species. However, so far, only few studies have reported the detailed biosynthetic pathway of induced compounds in co-cultures and were mainly limited to describe the chemical and biological properties of these secondary metabolites. Single culture gene activation is genetically simpler and usually leads to regulation (up or down-regulated) of major bioactive secondary metabolites and the production of analogues from these known chemotypes (ZHU; LIN, 2006). Multispecies activation, on the other hand, is much more complex and provides metabolite enhancement by multistep strategies, such as biotransformation (HOEFLER et al., 2012; MOREE et al., 2012), horizontal gene transfer (KUROSAWA et al., 2008) and the production of metabolites from combined pathways.

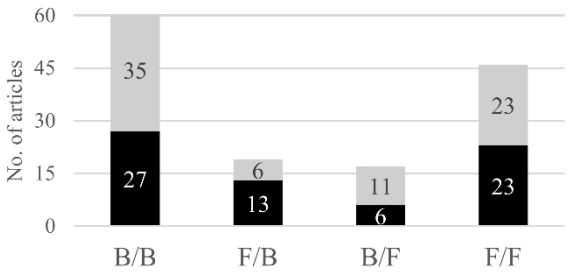

Figure 4.5. Co-culture metabolite induction reported for the 141 articles reviewed between the years of 1978 and 2019. Induction mechanisms is presented according to the microbial pair used in the study. "Up-regulation" (gray) is reported when the compound is also found in the axenic cultures, but in lower concentration. "*De novo* biosynthesis metabolites" (black) are metabolites that are not detected on axenic cultures. "Other" includes co-cultures that used other micro-organisms, such as oomycetes and algae.

One excellent example of biotransformation was provided by Moree and co-workers, which studied the production and regulation of phenazines in the bacteria *P. aeruginosa*. Phenazines play an important role on bacteria defense, acting on electron shuttling, biofilm development and the production of toxic superoxides. When in co-culture with the fungus *A. fumigatus, P. aeruginosa* produced higher amounts of these secondary metabolites. Using MALDI-TOF and imaging mass spectrometry (MALDI-IMS), combined with MS/MS networking, Moree have shown that, even though there was an up-regulation of phenazine compounds on the confrontation zone, *A. fumigatus* is able to rapidly converts these compounds into other chemical derivatives with lower antifungal activity, enhanced bacterial toxicity and the ability to induce fungal siderophores. This is particularly interesting for an ecological perspective because, although phenazines have been studied for decades, few detailed the bioconversion or sequestering of these metabolites in multispecies environment (MOREE et al., 2012).

Kurosawa and co-workers have also revealed an unusual co-culture induction, in which actinomycin genes from a highly stable antibiotic producer *Streptomyces padanus* were transferred to a multi-antibiotic resistant mutant of *Rhodococcus fascians* that does not produce antibiotics. In a liquid co-culture experiment, they have confirmed that a horizontal gene transfer from *S. padanus* to *R. fascians* led to the production of two aminoglycosides antibiotics by *Rhodococcus*, named rhodostreptomycin A and B. These compounds strongly act against *S. padanus* until complete bacteria elimination. Moreover, genomic analysis revealed that, in mixed cultures, *Rhodococcus* harbors a large DNA segment of *Streptomyces* strain, illustrating

the underreported microbial capability to produce newly described and potent antibiotics (KUROSAWA et al., 2008).

The absolute majority of experiments that reports up-regulated metabolites are focused on the evaluation of known antibiotics (*e.g.* bacteriocins, aminoglycosides, quinolines and other) and enzymes involved in ecological and industrial processes to improve their understanding for biotechnological and pharmaceutical purposes (Figure 4.6). For *de novo* biosynthesis, the most common metabolite classes reported are alkaloids (PARK et al., 2009; ZHU et al., 2013; ZHU; LIN, 2006; ZUCK; SHIPLEY; NEWMAN, 2011) and polyketides (CHAGAS; DIAS; PUPO, 2013; ONAKA et al., 2011; ROSS et al., 2014; SCHROECKH et al., 2009; WATANABE; IZAKI; TAKAHASHI, 1982), indicating that fungi and bacteria could produce both classes as a defense strategy in antibiosis interaction (Figure 4.6). For example, Chagas, Dias and Pupo have shown that the interactions between the endophytic fungi *Alternaria tenuissima* and *Nigrospora sphaerica* have significantly increased the production of polyketides alterperylenol and stemphyperylenol, the latter displaying antifungal and cytotoxic effects against *N. sphaerica*. Moreover, these induced compounds were shown to act only against endophytic fungi, with no reported phytotoxicity to the host plant *Smallanthus sonchifolius*, even at high concentrations, indicating a selective antifungal activity and an important ecological outcome between endophyte-endophyte and endophytes-host plants (CHAGAS; DIAS; PUPO, 2013). Similarly, Zhu and co-workers have shown the production of the new alkaloid aspergicin, together with neoaspergillic acid and ergosterol, during co-culture of two marine-derived mangrove epiphytic *Aspergillus* sp, in which both aspergicin and neoaspergillic acid show significant antibacterial activity against gram-positive bacteria *S. aureus*, *Staphylococcus epidermidis* and *B. subtilis*, as well as three gram-negative bacteria *Bacillus dysenteriae*, *Bacillus proteus*, and *E. coli* (ZHU et al., 2011).

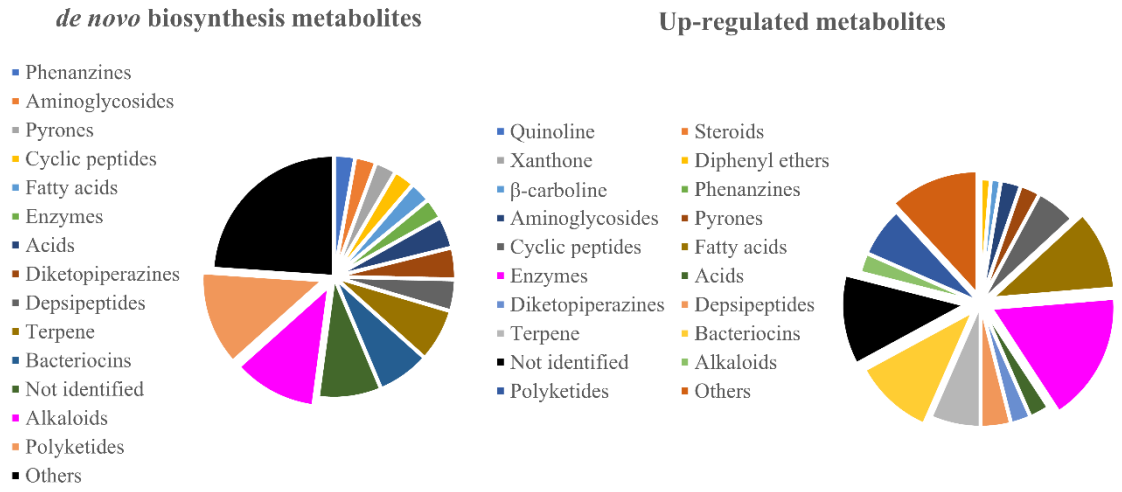

Figure 4.6. Metabolite classes produced on *de novo* biosynthesis and up-regulated co-culture experiments.

It is important to state that one of the major difficulties of metabolite screening in microbial co-culture is to find each micro-organism is responsible for the production of the induced metabolite. Although most reports indicate the inducer microorganisms only based on comparison with the axenic cultures or by evaluation of confrontation zone and isolated mycelial parts, confirmation can only be achieved by a detailed genetic study combined with a deep knowledge of the microbial biosynthetic pathway (BOGDANOWICZ; LU, 2013).

4. Microorganisms in mixed cultures

The great diversity of microbial species encountered in nature makes co-culture experiments a standard choice for the evaluation of unexplored secondary metabolites. In fact, scaling law predicts that Earth is home to upward of 1 trillion (10^{12}) microbial species (LOCEY; LENNON, 2016), offering unlimited opportunities for combining an nearly infinite number of interactions.

On early days, most co-cultures were performed using two fungi or two bacterias (Figure 4.7), majorly due to the difficulties over growth rate and reproducibility among eukaryotes and prokaryotes experiments. However, owing to the fact that microorganisms co-exist in close associations to each other, alongside to the recent development in media culture and microbiology techniques, the interactions of microbes from different phylogenetic orders have been increasingly evaluated, including the study of fungi/bacteria, bacteria/fungi, oomycete/oomycete (OJIKA et al., 2011) or the incubation of a fungus and a bacterium or more than two microbes in the same system (PETTIT et al., 2010).

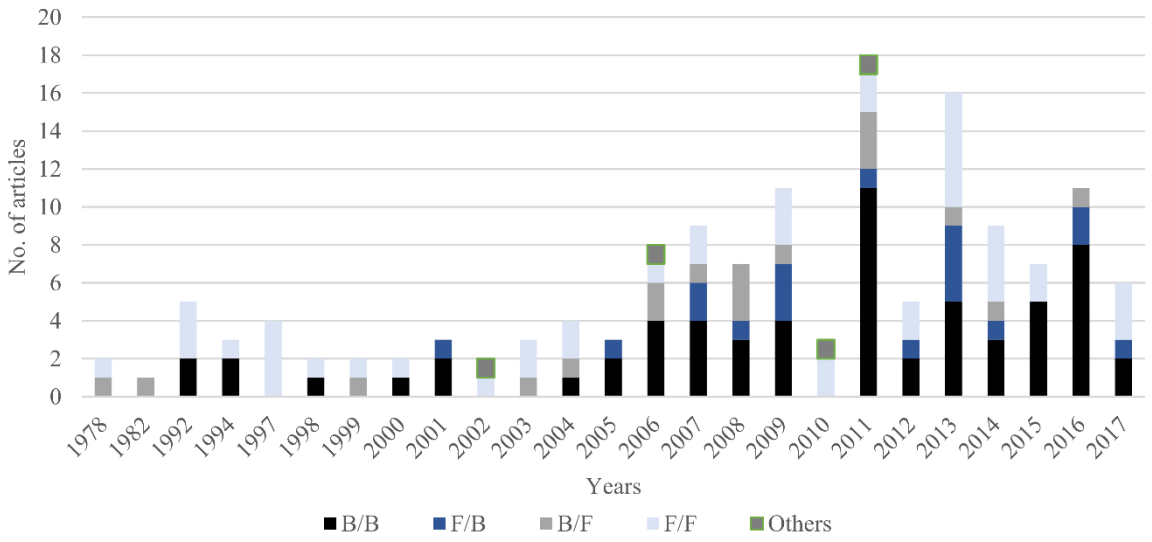

Figure 4.7. Microorganisms pair-wise used in co-culture experiments since 1978.

Among the untraditional co-cultures, bacterial/fungi, in which the bacterium is the inducer strain, or fungi/bacteria, in which the fungus produces the induced metabolites, have been the most used for the discovery of new leads. For instance, in 2011, Dusane and co-workers have demonstrated that the co-culture of four marine epibiotic bacteria (*Bacillus* sp. S3, *Bacillus pumilus* S8, *Bacillus licheniformis* D1 and *Serratia marcescens* V1) with pathogenic or biofouling fungi (*C. albicans* and *Yarrowia lipolytica*) and bacteria (*P. aeruginosa* and *B. pumilus*) led to the enhancement of antifungal activity against *Y. lipolytica*, antibacterial activity against *P. aeruginosa* and *B. pumilus* and biosurfactant activity, emphasizing the ecological and biotechnological implications of interspecies interactions for the microbial environment (DUSANE et al., 2011).

Furthermore, recent studies of microbial co-culture have also appraised the use of more than two microorganism in one petri dish. Pettit and co-workers have simultaneously co-cultured five fungi (*Ovadendron sulphureoochraceum*, *Ascochyta pisi*, *Emericellopsis minima*, *Cylindrocarpon destructans* and *Fusarium oxysporum*) for the biosynthesis of potential antineoplastic substances, resulting in a *de novo* production of lateritin, a *N*-methylated depsipeptide that inhibits the growth of a mini-panel of human cancer cell lines, has antibacterial activity against gram-positive bacteria *Micrococcus luteus*, *S. aureus*, *E. faecalis* and *S. pneumoniae*) and antifungal potential against *C. albicans* (PETTIT et al., 2010).

4.1. Bacterial Co-culture

Evaluation of the reported bacterial co-culture experiments from 1978 to 2019 revealed that the majority of inducer strains were gram-positive from the genus *Streptomyces*, which is the largest genus in the Actinomycetes order (NETZKER et al., 2015), *Bacillus* and *Lactobacillus* (Figure 4.8).

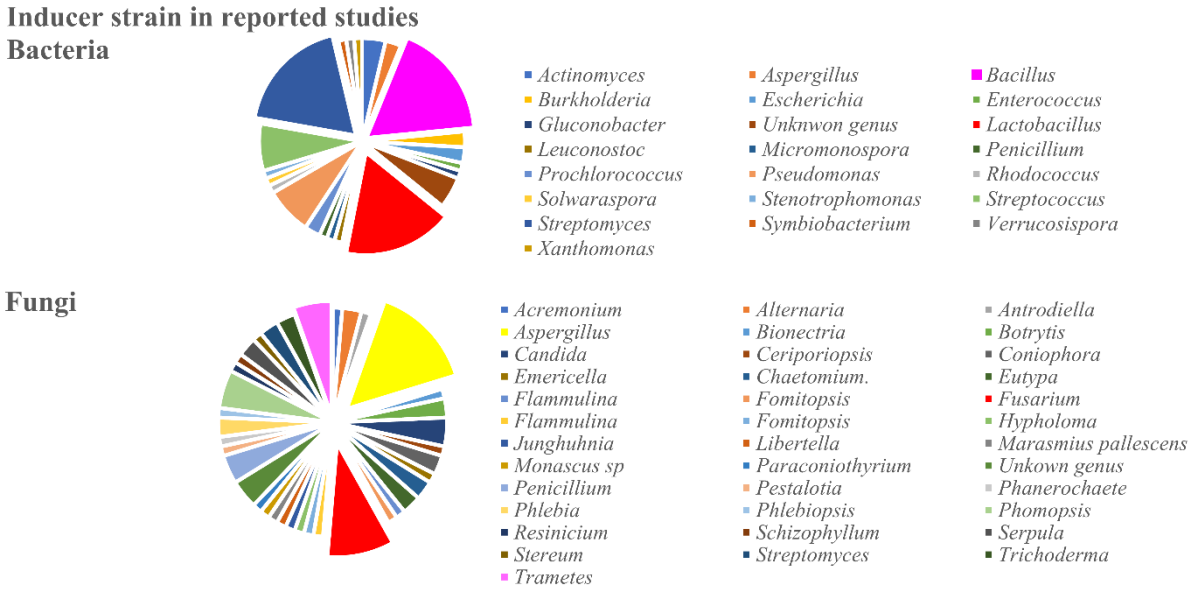

Figure 4.8. Bacteria and fungi inducer strains in reported co-culture studies from 1978 to 2019.

Actinomycetes are the richest reported microbial source of bioactive secondary metabolites, producing polyketides, phenazines, peptides, isoprenoids, indolocarbazoles and sterols (NETT; IKEDA; MOORE, 2009). Because the genome of this family is much larger than necessary for basic functioning (GALAGAN et al., 2005), most species dedicate a substantial fraction of their genes for the production of natural products (KNIGHT et al., 2003), eliciting metabolites with antibiotics, antifungals, anthelminthics and antitumor potential (SUNG; GROMEK; BALUNAS, 2017; TRAXLER et al., 2013; VALLIAPPAN; SUN; LI, 2014). Over the years, several drug leads were produced by this family, featuring the importance of co-culture for the biotechnological improvement in these targeted metabolites (OMURA et al., 2001). The commercially available compounds include the antituberculosis/antibiotic streptomycin, produced by *Streptomyces griseus*, the immune suppressant used for reducing transplant rejection tacrolimus, produced by *S. Tsukubaensis*, and the pesticide and antifungal avermectin, a macrocyclic lactone derivative produced by *S. avermitilis* (MOODY, 2014) .

Among all Actinomycetes, *Streptomyces* is the most important genus, being extensively studied in single and co-culture for the production of antibiotics. Mixed cultivation studies of this species is often performed with pathogen or mycolic-acid containing bacteria for the production of both new and up-regulated aminoglycosides (CARLSON et al., 2015; SLATTERY; RAJBHANDARI; WESSON, 2001; TURPIN et al., 1992), diterpene (CHO; KIM, 2012), indolocarbazole alkaloids (HOSHINO et al., 2015b; SHAH et al., 2008), hydroxamic acid (TRAXLER et al., 2013), polycyclic polyketide (ONAKA et al., 2011), pigments (ONAKA et al., 2011), polyenes (YAKOVLEVA; BULGAKOVA, 1978), butanolide chojalactones (HOSHINO et al., 2015a), macrolactams (HOSHINO et al., 2015c), enzymes (HOEFLER et al., 2012) and naphthoquinone (SUNG; GROMEK; BALUNAS, 2017), demonstration how little-explored the biosynthetic pathways of these gram-positive bacterias are.

Lactobacillus are lactic acid gram-positive bacteria and are also known to produce important antimicrobial compounds. This antibiotics, generally called bacteriocins, are biologically active proteins commonly used as preservative in the food industry (TODOROV, 2009), acting in a broad-inhibition spectrum against several bacterial contaminants. For the last decades, multi-species antibiotic resistance has led to the urgent development of protocols to improve the amount and diversity of bacteriocin production in *Lactobacillus* species, and, in this sense, co-culture is, by far, the most used strategy (ARIANA; HAMEDI, 2017; BAREFOOT et al., 1994; CHANOS; MYGIND, 2016; CHEIRSILP; SHIMIZU; SHIOYA, 2003; DI CAGNO et al., 2009; GE et al., 2014; KOS et al., 2011; LIU et al., 2006; MALDONADO; RUIZ-BARBA; JIMÉNEZ-DÍAZ, 2004; MAN; MENG; ZHAO, 2012; ROJO-BEZARES et al., 2007; SHIMIZU et al., 1999; TABASCO et al., 2009). The most general co-culture mechanism to up-regulate the biosynthesis of these compounds is the presence of an auxiliary species, given bacteriocin production is higher in less acid environment. In the same environment, the auxiliary microbes, that can be fungi (*Saccharomyces cerevisiae*, *Yarrowia lipolytica*, *Kluyveromyces marxianus*) or bacteria (*Lactococcus*, *Bacillus*, *Streptomyces*), consume lactic and acetic acids instead of the carbon source from the culture media, which is used by the main microorganism, increasing yielding and diversity of bacteriocin derivatives (ARIANA; HAMEDI, 2017; CHEIRSILP; SHIMIZU; SHIOYA, 2003; LIU et al., 2006; SHIMIZU et al., 1999; TADA et al., 2007). More recently, apart from metabolite consumption by auxiliary microbes, other factors have also been reported to influence bacteriocin yielding in co-culture and include the presence of quorum sensing messenger (BAREFOOT et al., 1994; CHANOS; MYGIND, 2016; TABASCO et al., 2009)

and the selection of resistant strains as challenge microbes (MALDONADO; RUIZ-BARBA; JIMÉNEZ-DÍAZ, 2004; ROJO-BEZARES et al., 2007).

Bacillus species, in particular *B. subtilis*, *B. amyloliquefaciens*, *B. pumilus* and *B. cereus*, have been broadly studied over the last decade as an inducer strain in co-culture experiments, eliciting metabolites that act as antimicrobials (AGHCHEH; KUBICEK, 2015; BENITEZ et al., 2011; MOREE et al., 2013; PETERSON et al., 2006; SCHNEIDER et al., 2012; STRAIGHT; WILLEY; KOLTER, 2006; TRISCHMAN et al., 2004), biosurfactants (DUSANE et al., 2011) and quorum-sensing inhibitors against fungi and bacteria (DUSANE et al., 2011). *Bacillus* species are known spore-forming soil bacteria, and, hence, rely on antagonistic responses towards challenge strains as a competitive advantage during colonization in this environment. In fact, antibiosis in soil microbiome ensures development and resource availability of this species when in competition with other soil microbes, including Cytophaga-Flavobacterium (PETERSON et al., 2006), *Streptomyces griseus* (SCHNEIDER et al., 2012) and *Streptomyces coelicolor* (STRAIGHT; WILLEY; KOLTER, 2006). Berleman and co-workers have shown that the proteobacterium *Myxococcus xanthus* responds to *B. subtilis*, *E. coli* and *Saccharomyces cerevisiae* by altering chemical and developmental patterns. Specifically, the presence of bacteria induces *M. xanthus* rippling, which is a undulatory movement utilized as a mechanism to efficiently consume nondiffusing growth substrates, maximizing predation and the scavenge for nutrient (BERLEMAN et al., 2006).

4.2. *Fungal Co-culture*

In co-culture in which fungi act as inducer microbes, there is a higher species diversity reported in literature, displaying, by consequence, broader chemical and biological outcomes (Figure 4.8). Among the most studied fungi species, pathogenic *Fusarium* and *Aspergillus* represent the major genus, being cultivated with both fungi and bacteria to chemically and ecologically evaluate the virulence factors responsible for these species' pathogenicity.

Aspergillus has a well-known chemical diversity. During the ongoing search for novel bioactive metabolites from microbes, co-culture of this specie with bacteria and fungi isolated from different environment has led to the discovery of several newly described compounds, as well as up-regulated compounds, being the most studied inducer fungus reported in mixed fermentation. Research to date has shown that co-cultivation of *Aspergillus* species, mainly *A. fumigatus*, has led to an increased production of alkaloids (RATEB et al., 2013; ZUCK;

SHIPLEY; NEWMAN, 2011), meroterpenes (KÖNIG et al., 2013) and archetypal polyketides (SCHROECKH et al., 2009), which display strong cytotoxic (PARK et al., 2009; ZUCK; SHIPLEY; NEWMAN, 2011), antimicrobial (EBRAHIM et al., 2016; KÖNIG et al., 2013; MEYER; STAHL, 2003; MOREE et al., 2012; PARK et al., 2009; SCHROECKH et al., 2009), antiprotozoal (RATEB et al., 2013) and antiosteoporosis activities (SCHROECKH et al., 2009). For example, Konig and co-workers have evaluated *t*he airborne-pathogenic fungus *A. fumigatus*, which is the major cause of life-threatening invasive mycoses in immunocompromised patients. When in co-culture with *Streptomyces rapamycinicus* isolated from the same environment, there was an activation of previously silent polyketide synthase, resulting in the production of fumicyclines A-B. These meroterpenes were not produced in axenic cultures and display moderate activity against *S. rapamycinicus*, contributing to the understanding of the pathobiology of this human pathogen (KÖNIG et al., 2013).

Fusarium is a filamentous fungus commonly found in the soil, being a normal constituent of the rhizosphere communities of plants (GORDON; MARTYN, 1997). In nature, some *Fusarium* strains are pathogenic to different plant species and are responsible for the destruction of crops worldwide. Others, however, live symbiotically in the roots, being feed out of the plant's exudate without invading the vascular system or causing disease (ALABOUVETTE et al., 2009). *Fusarium* infection in plants is a highly complex phenomenon, requiring a cascade of regulated processes (BOHNI et al., 2016; NOTZ; MAURHOFER; DUBACH, 2002; SCHOUTEN et al., 2004; VAN RIJ et al., 2005) and hence, a broad strategy for the understanding of the disease and the development of control protocols. One of the primary mechanisms of these wilt-inducing strains are the release of toxic secondary metabolites, which are often regulated by biotic and environmental factors (ALABOUVETTE et al., 2009). The existence of soils that naturally limit the incidence of *Fusarium* wilts has emerged the use of co-culture for the evaluation of the physiological conditions that promotes this inhibition, as well as the microbial communities that controls the expression of toxic secondary metabolites (BAO; LAZAROVITS, 2001). Minerdi and co-workers have evaluated the relationship between the non-pathogenic and wild *Fusarium* strains and a consortium of bacteria found in a *Fusarium*-wilt suppressive soil from *Serratia*, *Achromobacter*, *Bacillus* and *Stenotrophomonas* genus. In this study, they have demonstrated that sesquiterpenes volatiles, mainly caryophyllenes, emitted from the non-pathogenic strain in mixed culture, are capable of negatively influence mycelial growth and gene expression of virulence genes of pathogenic strains. However, typing experiments have shown that these wild *Fusarium* strain, when isolated from the soil bacteria, becomes pathogenic, causing the same wilt symptoms as the

pathogenic strain (MINERDI et al., 2009). Other than the ecological role of *Fusarium* in soil, co-cultures with this species with other microorganism revealed that the chemical and biological outcome of are highly dependent on the challenged species. Co-cultivation with *Alternaria tenuissima*, *Sarocladium strictum*, *Saccharopolyspora erythraea* and *Bacillus subtilis* have led to an increased production of, respectively, trichothecenes (MÜLLER et al., 2012), polyketides (BOHNI et al., 2016), decalin-type tetramic acid analogues (WHITT et al., 2014), ennantins and coumarins (OLA et al., 2013), emphasizing the multifactorial capacity of this genus.

5. Biological outcomes in mixed cultures

Microbial interactions are the result of a co-evolution process and leads to the adaptation and specialization of the community (BRAGA; DOURADO; ARAÚJO, 2016). In nature, the specificity of these interactions according to the challenge microbe regulates the microbial genome and enables the activation of different biosynthetic routes and the induction of different chemical responses in one single strain. Vinale and co-workers have shown that co-culturing the biocontrol agent *Trichoderma harzianum* M10 and the endophyte *Talaromyces pinophilus* F36CF led to an increased accumulation of siderophores for both fungi and a decrease in the production of 3-*O*-methylfunicone and herquline B by *T. pinophilus* F36CF. Moreover, although there was not a significant change in the production of harzianic and iso-harzianic acids by *T. harzianum* M10, co-culture with F36CF induced the production of the harziaphilic acid, a novel siderophore that displays antifungal activity, promotes plant growth and selectively reduces cancer cell proliferation without affecting viability of colorectal cancer and healthy colonic epithelial cells (VINALE et al., 2009, 2017).

In co-cultures experiments, just like in nature, the microbial interactions (and the overall chemical and biological outcomes) can be generally divided in positive, neutral or negative effects (ALABOUVETTE et al., 2009; TARKKA; SARNIGUET; FREY-KLETT, 2009). For example, the balance between pathogenic and non-pathogenic microorganisms governs the dispersion of some plant diseases in soil (ALABOUVETTE et al., 2009), in which nonpathogenic strains suppress the virulence of pathogenic ones in a antagonist manner. As a result, the pathogenic strains had a negative effect in co-culture, while the plant and the nonpathogenic strains displayed a positive outcome.

The biological outcome is also a direct result of microbial interactions and the activation of cryptic genes. As different metabolites are induce depending on the challenge microbe, the

biological response can also deeply vary. In 2013, Traxler and collaborators have demonstrated the antibiotics, antifungals, and anticancer properties of *Streptomyces coelicor* are deeply related to the microbials that inhabit their surroundings. When interacting with different species of actinomycetes, *S. coelicor* creates an *idiosyncratic* social networking that is based on the secretion of different desferrioxamines with acyl side chains of various lengths (TRAXLER et al., 2013).

In terms of bioactivity in co-culture experiments, most reports target to enhance the production and diversity of antimicrobial compounds by antibiosis interactions, biologically evaluating the induced metabolites only for this purpose. Hence, it comes as no surprise that the three major outcomes of the publications from 1978 to 2019 were antibacterial (~45%), antifungal (~18%) and anticancer (~11%) (Figure 4.9). Furthermore, several reviews have evaluated the antibiotic potential of co-cultures (ABDALLA; SULIEMAN; MCGAW, 2017; BURGESS et al., 1999; UEDA; BEPPU, 2017) and a brief overview of the major antimicrobial developments is described below.

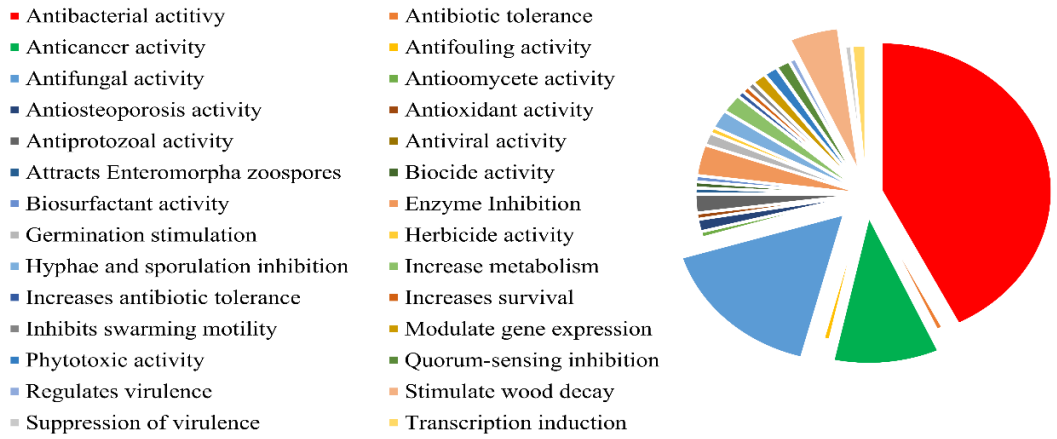

Figure 4.9. Main biological outcomes reported for co-culture experiments.

5.1.Antimicrobial compounds

The most well-known natural products from microbial sources are, undoubtedly, the antibiotics (DEMAIN, 1999). The golden age of those secondary metabolites, that occurred from the early 1940s to the late 1970s, was flared by the penicillin discovery, in 1928, by Alexander Fleming, revolutionizing the treatment of bacterial infections and the control of endemic diseases, such as gonorrhea, pneumonia, infected wounds and scarlet fever (BADER et al., 2010; DEMAIN; ELANDER, 1999; KNIGHT et al., 2003).

In the early years, although little understood, co-culture was already applied as a successful strategy to increase microbial metabolite production, with enhanced yields of known antibiotics penicillin, antimycin, tetracyclines, griseofulvin, bacitracin and levorine, mycoheptin, as well as novel compounds from antimicrobial-inducer strains, such as *Streptomyces*, *Penicillium* and *Lactobacillus* (YAKOVLEVA; BULGAKOVA, 1978). The continuous armamentarium of new antibiotics was so overwhelming, that it was believed that infectious diseases would be conquered and eradicated by the end of the 20th century (CONLY; JOHNSTON, 2005).

In reality, between 1970s and nowadays, the discovery of antimicrobial compound has been dramatically reduced, with a decrease of 56% in the past 20 years. The reason for this decline is multifactorial and can be mainly attributed to the lack of reproducibility of microbial matrices, the identification and constant re-isolation of the main chemotypes, the introduction of combinatorial chemistry, the need for high investments during clinical trials and the increasing bureaucracy of Regulatory Barriers and the lack of interest of pharmaceutical companies (CONLY; JOHNSTON, 2005).

Along with the decrease in the discovery rate, the constant inappropriate use and prescribing, as well as the extensive agricultural application of these substances has driven to a multidrug resistance and a global health emergency, urging the need to produce and discovery new therapeutic agents (APPELBAUM, 2006). Strategies to induce antibiotic discovery often apply genetic and metabolic engineering and are based on bioinformatic analysis, overexpression of biosynthetic genes, cellular biochemistry and the expression and regulation of targeted genes (DEMAIN; SANCHEZ, 2009; GAISSER et al., 2002; HAHN et al., 2006). Moreover, post genomic approaches, such as One Strain Many Compounds (OSMAC) and co-culture, have also been complementary implemented, increasing both metabolite diversity and yielding (MOODY, 2014).

For co-culture, most experiments to enhance antibiosis cultures pathogenic communities with known antibiotic inducer strains (MOODY, 2014). However, recent studies have demonstrated that the induction of antibiotic metabolites could be as prevalent as when the challenged strain comes from the same environment. Mearns-Spragg have shown that twelve out of the 16 marine strains showed increased antimicrobial activity towards human pathogens *S. aureus*, *E. coli* and *P. aeruginosa* following exposure (MEARNS-SPRAGG et al., 1998). However, similarly, Oh and co-workers have demonstrated that co-culture of marine-derived fungus *Emericella* sp and marine actinomycete *Salinispora arenicola* resulted on the enhanced production of antimicrobials emericellamides A and B, which are fungi cyclic depsipeptide

with moderate antimicrobial activity against MRSA and weak cytotoxicity against the HCT-116 human colon carcinoma cell lines (OH et al., 2007).

The concentration of induced metabolite needed to culminate in antibiotic activity has also generated some controversy, since there is growing evidence suggesting that antibiotic molecules, found in smaller concentration in their own natural environment, can also act as signaling molecules, mediating responses other than death (DAVIES, 2006; FAJARDO; MARTÍNEZ, 2008; MOODY, 2014). In fact, it has been shown that subinhibitory levels of various antibiotic metabolites can upregulate expression of SOS-response and methyl-mismatch repair genes (MESAK; MIAO; DAVIES, 2008), alter virulence factor expression in different bacteria (LINARES et al., 2006; SKINDERSOE et al., 2008), decrease biofilm mass (STARNER et al., 2008), control colony morphology (DIETRICH et al., 2008) and alter multiple gene promoters in clinically relevant species, such as *S. aureus* (GOH et al., 2002; MESAK; MIAO; DAVIES, 2008; MOODY, 2014; SHANK; KOLTER, 2009). One excellent example of antimicrobial signaling is provided by Amano and co-workers, which showed that promomycin, a diffusible siderophore acts as an antibiotic, while at subinhibitory concentrations, stimulates production of other antibiotics in *S. griseorubiginosus* and other *Streptomyces* strains (AMANO et al., 2010).

The ever expanding volume of genomic sequencing data continues to facilitate identification of new antibiotic biosynthetic pathways, allowing access to a vast and unexplored reservoir of metabolic diversity (DEMAIN; SANCHEZ, 2009). However, scientists do not yet know how to fully take advantage of the microbial abilities. For instance, Ohnishi and co-workers have determined the complete genome sequence of streptomycin-producer *Streptomyces griseus* IFO 13350, in which 34 gene clusters or genes were attributed for the biosynthesis of secondary metabolites. Nonetheless, they have also observed that secondary metabolism and morphogenesis was only partially activated by *S. griseus* A-factor regulatory cascade, remaining unknow other possible mechanism for activation of these cryptic genes (OHNISHI et al., 2008).

5.2.Negative outcomes

Microbes interact antagonistically by a multitude of mechanisms. These include **(1)** direct toxicity against the competitive strain by the release of antimicrobials and lytic enzymes, **(2)** degradation of virulence factors, **(3)** toxin biodegradation, **(4)** non-degradative detoxication of toxins and **(5)** decrease of toxin production. Undoubtedly, during antibiosis, microbes tend

to induce not one, but a plethora of metabolites, produced by different pathways to prevent the development of pathogen resistance (TARKKA; SARNIGUET; FREY-KLETT, 2009).

The production and release of antimicrobial compounds by antagonistic relations in mixed fermentation has been extensively reported in literature. Recently, Stierle and co-workers have demonstrated that co-culture fermentation of *Penicillium fuscum* and *P. camembertii/clavigerum* isolated from acidic and metal-rich waters of Berkeley Pit Lake yielded eight new 16-membered-ring macrolides, as well as three known antibiotic, each of them displaying a varied antimicrobial activity against MRSA, *Bacillus anthracis*, *Streptococcus pyogenes*, *C. albicans* and *Candida glabrata* (STIERLE et al., 2017). In the same sense, Sung, Groomek and Balunas have shown that *Streptomyces* sp. strain PTY087I2, when cultures with human pathogens *Bacillus subtilis*, methicillin-sensitive and methicillin-resistant *S. aureus* (MSSA and MRSA, respectively) and *P. aeruginosa* enhanced the production of naphthoquinone antibiotics granaticin, granatomycin D, and dihydrogranaticin B, which strongly enhanced biological activity against the gram-positive human pathogens used in these experiments (SUNG; GROMEK; BALUNAS, 2017).

Other than direct toxicity, antagonistic metabolites released in mixed culture could also act as virulence suppressor, regulating morphological transition and antibiotic resistance. For instance, *P. aeruginosa* and *C. albicans* co-colonize numerous human body niches. In a normal healthy host, *P. aeruginosa* and *C. albicans* inhabits the gut without any significant pathogenesis. However, in immunocompromised hosts, both strains can cause fatal sepsis. In an attempt to determine the pathophysiological impact of these interactions, Lopez-Medina and co-workers have cultured both pathogens in a murine model, and have demonstrated that the fungus *C. albicans* inhibits the virulence of *P. aeruginosa* by inhibiting bacterium pyochelin and pyoverdine gene expression, which plays a critical role in iron acquisition and virulence (LOPEZ-MEDINA et al., 2015).

Although most of the metabolites released during antagonistic interspecific interactions are non-enzymatic, some enzymes are also secreted as an antibiosis response to the presence of another microorganism (SCORE; PALFREYMAN; WHITE, 1997). In these mixed cultivation, enzymes are often used as a resistance mechanism, providing toxin degradation into less toxic compounds or conversion of metabolites to more bioactive molecules (Freitag and Morrell 1992; Score et al. 1997; Savoie and Mata 1999; Iakovlev and Stenlid 2000; Baldrian 2004; Ferreira Gregorio et al. 2006; Bergmann et al. 2007; Chi et al. 2007; Schouten et al. 2008; Hiscox et al. 2010; Hoefler et al. 2012; Moree et al. 2012; Schneider et al. 2012; Schouten et al. 2004; Schouten et al. 2008; White and Boddy 1992).

Among the studies that focused on enzymatic variation, the basidiomycetes rot fungi are of great interest due to their ability to degrade lignin and other xenobiotic, such as pesticides, polyaromatic hydrocarbons, polychlorinated biphenyls nitro explosives, and other toxic chemicals, being of biotechnological importance for treatment of industrial dye effluents, biodegradation of organic pollutants and waste (GAO et al., 2010). In the comprehensive investigation of rot fungi, co-culture have been repetitively used to enhance those abilities (Freitag and Morrell 1992; Score et al. 1997; Savoie and Mata 1999; Iakovlev and Stenlid 2000; Baldrian 2004; Ferreira Gregorio et al. 2006; Chi et al. 2007; Hiscox et al. 2010; White and Boddy 1992). For example, Hiscox and co-workers showed that *Trametes versicolor*, a wood decay fungi, when culture with *Stereum gausapatum*, *Daldinia concentrica*, *Bjerkandera adusta*, *Fomes fomentarius* and *Hypholoma fasciculare*, resulted in increased production of oxidizing enzymes, in which laccase and Mn-activities appeared up-regulated in all confrontation zones (HISCOX et al., 2010). Overall, *T. versicolor* have also shown enhanced enzyme activity against fungi, including *Pleurotus ostreatus* (BALDRIAN, 2004), *Trichoderma harzianum* (FREITAG; MORRELL, 1992), *Acremonium sphaerospermum*, *Fusarium reticulatum*, *Humicola grisea*, *Penicillium rugulosum*, *Bacillus subtilis*, *Escherichia coli*, *Endomyces magnusii* and soil fungi (BALDRIAN, 2004), demonstrating how this species can be of biotechnological use for enzymatic production.

Enzymatic production in antagonistic cultures usually happens only in the confrontation zone as a defense mechanism. For example, in the search for metabolites exchanged between *Bacillus subtilis* and *Streptomyces* sp. Mg1, Hoefler and co-workers have established that, during early stages of interaction, *B. subtilis* produces surfactin, a cyclic lipopeptide that inhibits the fungus aerial growth and spore development. However, imaging mass spectrometry (IMS) showed that in the confrontation zone, there was an enhanced production of the enzyme surfactin hydrolase, acting on this lipopeptide to produce a hydrolyzed molecule that was not active to inhibits the fungus aerial growth (HOEFLER et al., 2012).

Alternative strategies can be concomitantly applied to fight antagonistic fungi. In 2008, Schouten and collaborators have demonstrated that the resilient pathogenic fungi *Botrytis cinerea* employs, other than phytotoxic metabolites, two different strategies against other pathogenic fungi (SCHOUTEN et al., 2008). When in co-culture, *B. cinerea* resists the broad-spectrum phenolic antibiotic 2,4-diacetylphloroglucinol (2,4- DAPG) by both degradative and non-degradative defense mechanisms. Results showed that while the efflux pump BcAtrB prevents antibiotic accumulation in the cell, up-regulation of extracellular laccase degrades the

remaining antibiotic, creating a double resistance mechanisms against this exogenous toxic compounds (SCHOUTEN et al., 2008; TARKKA; SARNIGUET; FREY-KLETT, 2009).

Fusarium species has also shown a multifactorial response against antagonist microbes. The human and phytopathogenic *F. oxysporum* has been shown to interrupt 2,4-DAPG antibiotic activity by deacetylation of this compound into the less toxic derivatives monoacetyl-phloroglucinol and phloroglucinol (SCHOUTEN et al., 2004). However, non-degradative mechanisms also act on their cross-domain signaling, forcing the antagonist microbe to attenuate toxin production. For instance, fusaric acid is a polyketide produced by different species of *Fusarium*. In mixed cultures, up-regulation of this compound acts to increase antimicrobial activity (BOHNI et al., 2016), while also repressing the production of toxins (DUFFY; SCHOUTEN; RAAIJMAKERS, 2003; NOTZ; MAURHOFER; DUBACH, 2002; VAN RIJ et al., 2005). Indeed, studies that focused on the toxin suppression of picolinic acid derivatives showed that, when in co-culture with biocontrol strains of *Pseudomonas*, *Fusarium* increased fusaric acid production, enhancing the suppression of key virulence factor of the biocontrol strains, such as phenazine-1-carboxamide, auto-inducer N-hexanoyl-L-homoserine lactone (C6-HSL) (VAN RIJ et al., 2005) and 2,4-diacetylphloroglucinol (DAPG) (NOTZ; MAURHOFER; DUBACH, 2002).

5.3. Positive outcomes

In general, positive interactions are overlooked during co-culture experiments for drug discovery and only few reports have been made about the biological response in this communication system. Nonetheless, Ueda and Beppu have studied the interaction between different *Streptomyces* strain targeting to identify intra and interspecific signaling and revealed that interspecific stimulation of antibiotic production occurs at a higher frequency in mutualistic interaction rather than antagonistic (UEDA; BEPPU, 2017), demonstration the potential of positive interaction for chemical induction.

In nature, interactions between microbes are often complex and multispecies. In fact, the use of mechanisms to preserve beneficial microbes is a common component of host-microbe mutualisms and shows how the natural microbiota synergistically confers benefits to hosts. For example, Scott and co-workers have demonstrated how a bacterium could help protect the symbiosis between a southern pine beetle *Dendeoctonus frontalis* and *Entomocorticium* sp., a fungus that inhabits the beetle storage compartment and helps nourish the beetles' larvae. Using a co-cultivation approach, Scott and co-workers demonstrated that, in presence of antagonistic

fungi *Ophiostoma minus*, actinomycete bacteria from the same storage compartment produce a linear polyene peroxide that selectively suppress the antagonistic fungus, but only slightly affects the beneficial fungus *Entomocorticium sp* (SCOTT et al., 2008; SHANK; KOLTER, 2009).

In plants, polymicrobial environments are also a common source of secondary metabolites that have positive effects. For example, the plant rizhosphere contains a large microbiome, fed by root exudates, that promotes plant growth and defense by a multitude of unknown mechanism. Peterson have shown than the presence of *Bacillus cereus* UW85 in soybean root exudate with *Cytophaga-Flavobacterium* group could enhance bacteria populations as a result of the secretion of peptidoglycan from *B. cereus*. Indeed, these peptidoglycan fragments stimulate the growth of bacteria, suggesting a commensal relationship among both microbes (PETERSON et al., 2006). Similarly, Maier has also reported mutualistic relation between gram-positive bacteria from the Actinomyces family and *Amanita muscaria*, both isolated from the rhizosphere of a spruce stand. While all Actinomyces promoted growth of fungal hyphae, others also acted inhibit growth of pathogenic fungi such as *Heterobasidion annosum* and *Armillaria obscura,* demonstrating how microbes protect their host and environment against unwanted pathogens (MAIER et al., 2004).

In the plant's aerial parts, mutualistic relations between endophytic microbes has also provided selective antibiosis against pathogens. Meyer and Stahl have shown that *Aspergillus giganteus* produced an antifungal polyketide only in the presence of pathogenic strains of filamentous fungi. In the presence of pathogenic *F. oxysporum*, there was an increase expression of the polyketide encoding gene, whereas incubation with bacteria and yeast resulted in gene suppression, indicating the selective and multifactorial way bacterias interacts for defense mechanism (MEYER; STAHL, 2003).

In human health, opportunistic infections are also polymicrobial and the interactions these microorganisms have been shown to shape the pathogenicity and prognostic of the diseases. For instance, *P. aeruginosa* and *S. aureus* are two human opportunistic pathogens commonly co-isolated from medical equipment, skin, eyes and respiratory tract of people with cystic fibrosis (CF). Analysis of sputum of CF patients, conducted by Hoffman and collaborators, has led to the identification of 4-hydroxy-2-heptylquinoline-*N*-oxide, a quinoline produced by *P. aeruginosa* that suppress *S. aureus* respiration, protecting *S. aureus* from death by commonly used aminoglycoside antibiotics. Furthermore, prolonged growth of both pathogenic bacteria have also selected specific *S. aureus* strains, which are known for aminoglycoside resistance and persistence in chronic infections (HOFFMAN et al., 2006).

The beneficial interactions in nature is not limited to pathogen suppression, and, most of the times, the exact mechanism of cooperation is not always fully understood. *Bacillus thuringiensis* is a biological insecticide used since the 1950s to control insects that affect natural landscapes, agriculture or transmit pathogens (HÖFTE; WHITELEY, 1989). The insecticidal mechanism of this opportunistic insect pathogen is based on the accumulation of endotoxins crystalized inclusions during sporulation, which are inserted into the membranes of the moth midgut cells, leading to cell lysis. Most reports of commercial *B. thuringiensis* sprays attributes insect death to starvation or direct septicemia. However, Broderick and co-workers have demonstrated that *B. thuringiensis* insecticidal activity is also dependent on the presence of *Enterobacter* sp., a bacterium commonly found on the gypsy moth midgut. Co-culture of both microorganisms shows that the midgut bacteria enhances *B. thuringiensis* septicemia, increasing, by consequence, the insecticidal activity. Furthermore, elimination of these bacteria from the moth's midgut abolishes *B. thuringiensis* insecticidal activity, evidencing how closely the bacteria contributes to *B. Thuringiensis* mortality (BRODERICK; RAFFA; HANDELSMAN, 2006; SHANK; KOLTER, 2009).

6. Induction triggers

So far, we have discussed the basic parameters of a co-culture experiment, the mechanisms of metabolite induction, the microorganisms most used in these experiments and the outcomes reported in literature. However, no evaluation has been made of the precise trigger factors responsible for gene activation. The induction triggers, just like the biological outcome, are multifactorial and directly related to the inducer and challenge microbes. In co-culture experiments, the most important trigger factors is cell-to-cell contact, in which *in loco* communication, molecule signaling and physical contact are mandatory for the chemical outcome (BENITEZ et al., 2011; BERLEMAN et al., 2006). However, other mechanism for induction have also been reported in literature, and include signaling chemicals, the presence of auxiliary microorganisms and chromatin remodeling (GACEK; STRAUSS, 2012)

We have repeatedly stated that the presence of signaling molecules shape the microbial interactions, playing an important regulatory role in the onset of cryptic metabolite production. Indeed, small molecules provide inter and intraspecies gene expression and increase the knowledge and biotechnological application of promising co-cultivation. Research to date has reported that the presence of γ-butyrolactone autoregulators (HORINOUCHI, 2007), goadsporin (ONAKA et al., 2001), siderophores (TRAXLER et al., 2013; YAMANAKA et al.,

2005), ionophores (AMANO et al., 2011), promomycin (AMANO et al., 2010), ATP synthesis inhibitors (FUJIMOTO et al., 2016) and mycolic acid (ADNANI et al., 2015; HOSHINO et al., 2015b, 2015c, 2015a; ONAKA et al., 2011) are key factors for the chemical induction in different co-culture experiments. For instance, Sonnenbichler and co-workers have demonstrated that the stimulation of the metabolite synthesis is not induced by cell-to-cell contact nor by the presence of cell-wall constituents, such as polypeptides and polysaccharides, and that signaling molecules were exclusively related to compounds enhancement (SONNENBICHLER; DIETRICH; PEIPP, 1994). On this study, they have shown that mixed culture of the Basidiomycetes *Heterobasidion annosum* and *Gloeophyllum abietinum* resulted in an enhanced production of the antimicrobial metabolites oosponol and oospoglycol by *G. abietinum* and that, in *H. Annosum*, this latter polyketide acted as a signaling for the induced synthesis of fomajorin S (H35a) and fomannosin, two unspecific defense sesquiterpenes (SONNENBICHLER; DIETRICH; PEIPP, 1994; UEDA; BEPPU, 2017).

Mycolic-acid containing bacteria have also been shown to induce chemical diversity. However, in this case, the trigger factors have been attributed not only to the molecule signaling, but also by a simultaneous cell-to-cell contact. In previous studies, mycolic acid-containing bacteria have been reported to enhance the chemical diversity of several species (HOSHINO et al., 2015b, 2015c, 2015a) (ADNANI et al., 2015) and provide novel secondary metabolites from different biosynthetic pathways, including newly antibiotic polyketide (ONAKA et al., 2011) and cytotoxic indolocarbazole alkaloid, butanolide chojalactones and tricyclic macrolactams (HOSHINO et al., 2015b, 2015c, 2015a). However, only in 2011, Onaka and co-workers have demonstrated that neither the mycolic acid nor the living cells alone were capable of stimulating metabolite enhancement, requiring the direct interaction between the mycolic acid-present in the cell-wall of the living bacteria and strains of *Streptomyces*. Further, they also reported that the induction mechanism during mixed cultivation is completely independent from substance-mediated induction, the latter being described as a completely separate event (ONAKA et al., 2011).

The presence of auxiliary microorganism is commonly applied in co-culture when one microbe can improve the bioactive metabolite production of other by consuming inhibiting-metabolites in the media. As discussed previously, examples of auxiliary microbes include the enhancement of nisin and kefiran production in *Lactobacillus* species by mixed cultivation with lactic acid consuming strains (ARIANA; HAMEDI, 2017; CHEIRSILP; SHIMIZU; SHIOYA, 2003; LIU et al., 2006; SHIMIZU et al., 1999; TADA et al., 2007). In nature, this auxiliary interaction is even more complex, as reported by Cheirsilp and co-workers

(CHEIRSILP; SHIMIZU; SHIOYA, 2003). In this study, they have demonstrated that kefiran production in kefir grains happens by a complex microflora consisting of homo and heterofermentative lactic acid bacteria, lactose-assimilating yeast, and non-lactose-assimilating yeast. While bacteriocin production is increased by lactic acid consuming bacteria, the non-lactose-assimilating yeast survive by consuming galactose, which is a product of the lactose-assimilating microorganisms, ensuring balance in the environment (CHEIRSILP; SHIMIZU; SHIOYA, 2003).

Genetic approaches have provided more insight into the precise induction trigger during interspecies interaction. In this sense, the impact of chromatin remodeling by specific modifiers during microbial communication has gained increased attention in the last years (NETZKER et al., 2015). Particularly, a variety of chromatin modifiers have been stated to regulate secondary metabolite biosynthesis in filamentous fungi (Roze et al. 2007; Soukup et al. 2012; Netzker et al. 2015), being fairly detailed in previous reviews (GACEK; STRAUSS, 2012; NETZKER et al., 2015). For instance, Roze and co-workers have shown that acetylation of histone H4 by chromatin modifier acetyltransferases (HATs) in *Aspergillus parasiticus* led to the stimulation of the aflatoxin biosynthetic gene cluster (ROZE et al., 2007), which encode several bioactive mycotoxins synthesized by a small number of Aspergilli on susceptible food and crops (ROZE et al., 2007).

7. Conclusion and Perspectives

Microbes play a pivotal role in drug discovery program and exploitation of the metabolic potential via mixed fermentation is proven to be an effective way to enhance natural product diversity. However, to satisfy the constant need for new biological lead, and to overcome the continuous multidrug resistance in pathogenic strains, it is fundamental to understand the physiological and genetic circumstances for the induction of these promising compounds. So far, these regulatory mechanisms of silenced genes remain poorly reported and understood.

The unlimited microbial combinations and the vast biological and chemical responses, combined with increasingly sophisticated analytical techniques for chemical detection and quantification, illustrate the potential of mixed fermentation in activating genes cluster that encode promising and unexplored secondary metabolites. Accumulating evidence indicates that co-cultivation is dependent on both biotic and abiotic parameters, including growth variables (media, temperature, pH, agitation, luminosity, incubation period), the selection of the co-culture system, the selection of the inducer and challenge microbes, amount and age of

inoculum from each strain and degree of contact between the cells. Therefore, for each experimental culture, it is highly recommended a detailed optimization of all parameters. Furthermore, a greater understanding of the underlying molecular mechanisms is also critical for deriving general mechanisms. For example, if the research targets to evaluate ecological or pathogenic response within a system, secondary metabolism should be studied in the context of its native ecosystem, properly mimicking the natural physiological conditions to elicit the same (or similar) complex pathways as seen in nature.

On most reported experiments, antagonistic interactions are the driving force that promotes biosynthesis of biologically active compounds. However, the evaluation of mutualistic and the multifactorial relations in nature has also resulted in a significant variation of the metabolic profile, remaining a neglected approach on most reported studies. Changing our view of microbial intercellular signaling can enable the use of the right conditions for cells to communicate and, hence, generate new bioactive molecules.

There is an urgent need to standardize the detailed experimental procedures regarding the type of interaction, the selection of challenge microbes and the possible trigger factors during communication, since this information could shed a light on the intimate process involving the metabolite production. Unravelling the production conditions and signal transduction include understanding not only of abiotic factors interferences, but also global regulators and modifiers, providing a systematic investigation of the microbial metabolome profiles. Specifically, to induce silent secondary metabolite biosynthesis, the growing assessment of microbial genomics has provided valuable insights into the biosynthesis pathways, offering a cheaper alternative for the discovery and engineering of these untapped bioactive structures. Only by a deeper knowledge of species identification and gene regulation, aligned with robust analytical development, these combined metabolic pathways can be optimized, offering a biotechnological potential and, hence, several opportunities for industry and science.

The methodological advancements made in analytical protocols for microbial sources and the development of methods for the simultaneous analysis of metabolite variations represent the greatest advances in the field. To overcome some of the challenges overmentioned on this review, multidisciplinary collaborations are fundamental for a careful analysis and validation of the collected data, assuring a holistic understanding of the ecological, biological, chemical and genetic information, helping the scientific community in the constant race between the new drug discovery and the continuous emergence of resistance mechanisms.

CHAPTER 5. EXPANSION OF THE MICROBIAL METABOLOME - INDUCING CRYPTIC ANTIMICROBIAL SECONDARY METABOLITES BY CO-CULTURE

Article title: Enhancement of microbial chemical diversity – Inducing cryptic antimicrobial secondary metabolites by co-culture.

Journal: RSC Advances.

Status: Unpublished.

Authors: Denise Medeiros Selegato[1,2], Özlem Erol[1], Rafael Teixeira Freire[3], Ian Castro-Gamboa[2], Young Hae Choi[1]

Affiliations:

[1] Natural Products Laboratory, Institute of Biology, Leiden University, Leiden, The Netherlands.

[2] Nucleus of Bioassays, Biosynthesis and Ecophysiology of natural products (NuBBE), Institute of Chemistry, São Paulo State University, Araraquara, Brazil.

[3] Medway Metabonomics Research Group, University of Greenwich, Chatham Maritime, Kent, UK.

Abstract

Microbial metabolites have great potential to provide new pharmaceutical leads given a high diversity of chemical structures are found in an unexplored and extensive microbial population. Conventionally, metabolite screening in microorganisms is performed in monocultures, in the absence of biotic and abiotic interaction found in nature, seriously limiting the chemical diversity that can be obtained by one single strain. Over the last decade, several methods have been developed aiming to understand the conditions under which biosynthetic cryptic genes are activated. Among those, co-culture have revealed widespread potential for the production of bioactive metabolites and are mainly focused on the induction of unexplored antimicrobial compounds, as an alternative to drug resistance. In co-cultivation, the microbial selection still remains a challenge due to the extreme outcomes of one single species in a high-throughput system. Here, we show the development of a strategy to enhance chemical diversity using co-culture in solid media. Specifically, we have cultured *Diaporthe eres*, *Fusarium oxysporum*, *Alternaria alternata*, *Colletotrichum acutatum* and *Xylaria cubensis* in pairs to select co-cultures that show antagonistic interactions and promising metabolic induction. The selected co-cultures were evaluated by different biotic aspects of the chemical induction by fast analysis by High-performance thin-layer chromatography (HPTLC), including the identification of the inducer strain and best incubation period. Moreover, HPTLC and NMR-based metabolomics were used for the identification of the induced compounds and correlation of those to antibacterial and antifungal activities. Results show that each fungi species displayed different responses in the presence of challenge strains, in both morphological patterns and chemical responses. Furthermore, evaluation of the selected co-culture in their optimum biotic environment showed an increase not only in chemical diversity, but also in the antimicrobial activity. Multivariate data analysis revealed that this antimicrobial potential was correlated to secondary metabolites from *F. oxysporum* and *D. eres*. On one hand, when in co-culture with *C. acutatum*, *F. oxysporum* increased the production of the beauvericin in up to 3-fold, a depsipeptide that displayed strong antifungal and antibacterial activity. On the other, co-culture of *Diaporthe* revealed the induction of a *de novo* metabolite from the bisanthraquinone class, a secondary metabolite not produced in axenic cultures that exhibits a moderate antibacterial and antifungal activities.

Keywords: co-culture, enhancing chemical diversity, activation of cryptic secondary metabolites, antimicrobial induction

1. Introduction

Natural products continue to play a pivotal role in modern drug-based therapy of various diseases. Among those, microbial secondary metabolites have shown great potential to provide new pharmaceutical leads (NEWMAN; CRAGG, 2016; PETTIT, 2009) given a high diversity of chemical structures are found in a little studied and extensive microbial population (BERGMANN et al., 2007; CHIANG et al., 2008; GALAGAN et al., 2005; HIBBING et al., 2010; SCHROECKH et al., 2009). Indeed, recent whole-genome sequencing of several fungi and bacteria has shown that the potential of microbial matrices to produce bioactive compounds is fairly underestimated, meaning that a much broader range of metabolites could be produced if the silent genes are induced by whatever methods (BERGMANN et al., 2007; CHIANG et al., 2008; GALAGAN et al., 2005; HIBBING et al., 2010; SCHROECKH et al., 2009).

Conventionally, metabolite screening in microbial bioprospection is performed in monocultures, in the absence of biotic and abiotic interaction common placed in nature. However, the lack of these interaction seriously limits the chemical diversity that can be obtained by one single strain and results in the a decrease in the frequency of isolation of new compounds and redundant re-isolation of known secondary metabolites (MARMANN et al., 2014; PETTIT, 2009).

Over the last decade, several methods have been developed aiming to understand and optimize the conditions under which biosynthetic cryptic genes are activated, targeting to maximize the chemical diversity obtained from microbial species (SCHROECKH et al., 2009; WAKEFIELD et al., 2017). Amid those, genetic-dependent approaches are extensively applied for gene activation in monoculture studies have been shown to regulate the production of known important metabolites (AGHCHEH; KUBICEK, 2015; BERGMANN et al., 2007).

More recently, the increasing resistant of pathogenic microbe has propelled the urgent search for faster methodologies for the screening of antimicrobial compounds in microbial matrices. In this sense, post-genomic strategies have emerged as an inexpensive alternative for the enhancement of chemical diversity, regulating known secondary metabolites as well as stimulating the production of previously unexpressed chemical diversity (BERTRAND et al., 2014a; HERTWECK, 2009; WAKEFIELD et al., 2017). These methodologies include One Strain, Many Compounds (OSMAC) (BODE et al., 2002; WEI et al., 2010), substrate feeding (DE BOER; SCHMIDT-DANNERT, 2003), co-culture (BERTRAND et al., 2014a; PETTIT, 2009) and biotransformation (HEGAZY et al., 2015; VENISETTY; CIDDI, 2003) and

successfully modify different levels of the cellular machinery for the modulation of fungi biosynthesis.

The production and regulation of induced secondary metabolites highly depends on both biotic interactions and overall growth conditions. Particularly, in co-cultures experiments, microorganisms metabolize the media substrate together, mimicking the natural and competitive microbial environment for the encryption of silenced genes coded for novel compounds. Research to date indicates that co-culture could overcome limiting steps of a desired biosynthetic pathway, prevent enzymes activity, increase bioactivity or suppress the virulence of pathogens, ensuring survival and shaping the community. In practice, the capacity to react to biotic interactions is unique, meaning that one single microbial strain could activate different biosynthetic pathways and, hence, produce completely different chemical profile, depending on the biotic stimuli, resulting in unlimited possibilities for pairwise experiments (NETZKER et al., 2015; PETTIT, 2009).

Antagonistic communications, in which microbes compete for space and nutrients, are the most studied type of co-cultures (DAVIES, 2006; FAJARDO; MARTÍNEZ, 2008; MOODY, 2014) and are mainly focused on the induction of unexplored antinfective and anticancer metabolites, as an alternative to overcome resistance (UEDA; BEPPU, 2017). In solid media, four fungi morphology changes have been reported based on the microbial interaction, in which two show clear sign of antagonistic outcome. The first, named *distance-inhibition* **(1)**, happens when fungal growth stops at a distance from the competing culture due to release of antimicrobial secondary metabolites into the media. The second type, *zone lines* **(2)**, fungal colonies antagonistically stops at a distance, producing a dark precipitate in the confrontation zone. Furthermore, in *contact-inhibition* **(3)** and *overgrowth* **(4)**, both morphological outcomes are a result of signaling triggered by microbial interaction and, although there is no clear evidence of antimicrobial metabolite production, these outcomes can also lead to enhanced chemical diversity. In *contact-inhibition* **(3)**, both fungi grow until contact and respect each other place. In *overgrowth* **(4)**, however, the fungi grow until contact, followed by partial or complete invasion of one fungus by the other (BERTRAND et al., 2013b, 2014a).

In microbial metabolomics, the large dynamic range and diversity of metabolites in the microbial matrices still hamper the selection of samples with biological potential. In addition, the huge metabolic variation of one single strain based on the environmental conditions (both biotic and abiotic) creates reproducibility issues during antimicrobial screening, requiring highly sensitive and robust analytical methods. Thin-layer chromatography (TLC) is a golden technique for the analysis of natural products and has several advantages for fingerprinting

analysis such as low cost, short measuring time, samples parallel analysis, low use of solvent, no interference from previous analysis and fast extraction of bands for further assessment or bioactivity tests (AUDOIN et al., 2014; MILOJKOVIĆ-OPSENICA et al., 2013; MORLOCK; RISTIVOJEVIC; CHERNETSOVA, 2014). Prior to the application of TLC as a metabolomics tool, the low resolution and signal reproducibility were limiting drawbacks of this technique. However, in the last decade, high-performance thin-layer chromatography (HPTLC) has provided increased resolution and high signal robustness for this chromatographic system, allowing detection of many metabolites groups and robust multivariate data analysis of different natural matrices (AUDOIN et al., 2014; LIU et al., 2018). For chemical fingerprinting, HPTLC has been increasingly used as an informative analytical technique in chemotaxonomy and routine study of complex matrices, emerging as a fast alternative to gas chromatography (GC) or high performance liquid chromatography (HPLC) for both targeted and untargeted analysis (AUDOIN et al., 2014).

The development of a new methodologies in microbial metabolomics can facilitate the identification of new antimicrobial natural products. In this sense, this works aimed to develop a strategy to enhance the chemical and biological diversity using co-culture in solid media. Specifically, we have culture *Diaporthe eres*, *Fusarium oxysporum*, *Alternaria alternata*, *Colletotrichum acutatum* and *Xylaria cubensis* in pairs to select co-cultures that show antagonistic interactions and promising metabolic induction. The selected co-cultures were evaluated by different biotic aspects of the chemical induction by fast analysis by High-performance thin-layer chromatography (HPTLC), including the identification of the inducer strain and best incubation period. Moreover, HPTLC and NMR-based metabolomics were used for the identification of the induced compounds and correlation of those to antibacterial and antifungal activities.

2. Materials And Methods

2.1. Fungi strains

The selection of the fungi strains was based on three main criteria: (i) the genus should be found in nature as both plant-associated and pathogenic microbes (CHEN et al., 2013b; FAN et al., 2014; GOMES et al., 2013; IMAZAKI; KADOTA, 2015; LIMA et al., 2012; MANICI; CAPUTO; SACCÀ, 2017; WANG et al., 2014); (ii) the species should have been isolated in highly competitive environments and (iii) the microbes should have at least one bioactive secondary metabolite reported in the literature.

Based on these criteria, we have targeted five species of filamentous fungi from five different fungi families named *Fusarium oxysporum* (Nectriaceae), *Diaporthe eres* (Diaporthaceae), *Colletotrichum acutatum* (Glomerellaceae), *Xylaria cubensis* (Xylariaceae) and *Alternaria alternata* (Pleosporaceae).*Fusarium oxysporum* was isolated from the rhizosphere of *Senna spectabilis,* in July of 2012, in the Southeast region of Brazil, one of the most comprehensively studied sites in Latin America, with a microbial community dominated by *Fusarium*. The genetic identification was done by analysis of the Internal Transcribed Spacer (ITS) sequence and deposited at GenBank under access number LC055797.1. *Diaporthe eres*, *Colletotrichum acutatum*, *Xylaria cubensis* and *Alternaria alternata* were purchased from Westerdijk Fungal Biodiversity Institute and deposited in the reference collection of the CBS-KNAW Westerdijk Fungal Biodiversity Institute, Utrecht, Netherlands under access number CBS 110.85, CBS 112760, CBS 116.85 and CBS 102.47, respectively.

2.2. Incubation parameters and metabolite extraction in solid media

Plugs of the selected fungi were grown in petri dishes containing 20.0 mL of Czapek-Agar (Sigma Aldrich) ($NaNO_3$, 1.5 g L^{-1}; KH_2PO_4, 0.5 g L^{-1}; $MgSO_4$, 0.25 g L^{-1}; $FeSO_4$. $7H_2O$, 0.025 g L^{-1}; KCl, 2.5 g L^{-1}; D-glucose, 30.0 g L^{-1} and agar 20.0 g L^{-1}). For the evaluation of co-culture experiments, same-sized 10 mm plugs of each fungus were placed 3 cm from the border. For the monoculture control, a 10 mm agar plug of a fungal pre-culture was inoculated in the centre of a 9 cm petri dish. Czapek was selected as the solid media given there is growing evidence that shows that the use of media with reduction of nutriments increases the competition between two microorganisms and leads to an increased number of *de novo* induced metabolites (BERTRAND et al., 2014b; RIGALI et al., 2008). All inoculated plates were incubated at 25 °C for 12 days in the dark in a microbiological incubator with temperature control.

For the metabolite extraction, the fungal cultures were excised from the petri dish with a razor blade in 3 cm × 1 cm pieces, transferred to a mortar, frozen with liquid nitrogen and grinded. The grained material was then resuspended in 200 mL of water, sonicated in an ultrasonic bath for 45 minutes (temperature of 25°C and 35,000 oscillations per second) and vacuum filtered to remove agar and mycelium. Following, the aqueous supernatant was extracted with three portions of ethyl acetate (3x of 100 mL) and the resulting organic solutions were dehydrated with anhydrous sodium sulfate (20 g of ≥ 99% $NaSO_4$, Sigma Aldrich), vacuum filtrated and evaporated to dryness.

2.3. High-performance thin-layer chromatography (HPTLC) - Data Acquisition and Processing

The first step of the HPTL analysis was the optimazation of the mobile phase, in which two mobile phases with different polarities were tested, polar mobile phase ethyl acetate-formic acid-acetic acid-water (100:11:11:27, w/w/w/w) and a non-polar mobile phase toluene-ethyl acetate (Tol-EtOAc 8:2, v/v). The selection of the best mobile phase was based on the number of detected spots under UV light (254 and 366 nm) before and after anisaldehyde derivatization in sulfuric acid and heating.

For the HPTLC analysis, samples were applied at a final concentration of 3.0 mg mL^{-1} in a stationary phase of silica gel (HPTLC plates, 20 x 10 cm, F254) from Merck. The procedure was conducted at a CAMAG HPTLC operational system equipped with an automatic TLC sampler (version 4), derivatizer device (version 1.0 AT), TLC plate heater (version III), and TLC visualizer (CAMAG, Switzerland).

For each plate development, the chamber saturation time was 20 minutes and the solvent migration distance was 90 mm from the application point. After development, HPTLC plates were sprayed with 2 mL of anisaldehyde-H_2SO_4 solution (Sigma Aldrich) using an automatic derivatizer, followed by heating on a TLC plate heater at 100°C for 3 minutes. Plates images at white light, 254 nm and 366 nm, before and after derivatization, were acquired using a TLC visualizer.

A total of 25 μL of solution were spotted in 8 mm bands. On each plate, samples were applied with a 10 mm distance from the bottom and 20 mm from the left and right border of the plate. The distance amongst the bands was 10.5 mm. A pool of all of the samples was applied in each plate as the Quality Control (QC).

Chemical data was extracted from the HPTLC plate images by rTLC software (version 2.0, available at http://shinyapps.ernaehrung.uni-giessen.de/rtlc/) according to the method developed by Fichou *et al.* (2016). Dimensions used for image extraction were the same as those used for the sample application onto the plates. For data integration, 128 units were used as the pixel width (FICHOU; RISTIVOJEVIĆ; MORLOCK, 2016). The rTLC software produces integrated data from red (R), green (G) and blue (B) channels and creates individual converted chromatograms for each corresponding color (RGB channels). Moreover, rTLC also provides the gray channel (mean value of the RGB channels), which was used for the chemical analysis after normalization with QC, UV Scaling, warping and baseline correction (FICHOU; RISTIVOJEVIĆ; MORLOCK, 2016).

2.4. [1]HNMR Analysis - Data Acquisition and Processing

^{1}H NMR spectra of the blank and fungal cultures were acquired on a Bruker 600 MHz Advance II spectrometer (Bruker, Germany) equipped with a 5 mm triple resonance inverse cryoprobe and a z-gradient system. Prior to data acquisition, automatic tuning and matching of the probe was performed, as well as manual shimming and automatic proton pulse calibration (*pulsecal*, Bruker). ^{1}H NMR analysis was performed in 3mm tubes and acquired by water 1D-water presaturation pulse sequence with composite pulses at the following parameters time domain (TD) 32 k; number of scans (NS) 64; spectral width (SW) 20 ppm; water signal irradiation point (o1) 4.84 ppm; temperature 298 K and relaxation delay (d1) 1.5 s.

After acquisition, the ^{1}H NMR spectra were automatically reduced to ASCII files. Spectral intensities were scaled to internal standard, aligned using ICOSHIFT algorithm. The regions of δ 1.2–1.4 were excluded from the analysis because of the residual signals. The final processed data was exported in Comma-separated values (.csv) and imported to MATLAB for multivariate analysis.

2.5. Multivariate Data Analysis

MVDA was performed using Matlab (v. r2017a, Matworks, Natick, Massachusetts, EUA). Principal component analysis (PCA) was carried out by NIPALS algorithm (ANDRECUT, 2008) using HPTLC-Data. Partial Least Squares Discriminant Analysis (PLS-DA) was applied for the processed ^{1}HNMR data according to the antibacterial response, in which 1: moderate antibacterial activity and 2: high antibacterial activity.

2.6. Molecule Elucidation

For metabolite elucidation, STOCSY was applied to all targeted bioactive chemical shifts selected from the PLS-DA loadings (CLOAREC et al., 2005). Chemical connectivity of the targeted bucket (driver peak) was analyzed by STOCSY correlation and covariance algorithm using MATLAB R2017a software (Mathworks, Natick, MA, USA). For confirmation and individual compound assessment, 2D NMR experiments were acquired and interpreted using MestreNova 12.0.3 software17 (MestreLab Research SL, Santiago de Compostela, Spain).

For two dimensional-NMR acquisition, (1) gradient-selected heteronuclear single quantum coherence (HSQC) was performed by phase-sensitive ge-2D multiplicity edited HSQC using PEP and adiabatic pulses with gradients in back-inept, (2) gradient-selected heteronuclear

multiple bond correlation (HMBC) was acquired by phase-sensitive ge-2D HMBC using a two-fold low-pass J-filter; and (3) *J*-resolved measurement was performed using a standard pulse sequence with 25 Hz CW-based water signal suppression. For HMBC and HSQC acquisition, each parameter of 1H (f2) and 13C (f1) were as follows: frequency 600.13 and 150.92 MHz, time domain (TD) 2 k and 512 increments, spectral width (SW) 10 and 230 ppm, number of scans (NS) 64, relaxation delay (d1) 1.00 s and measuring temperature 298 K. The long-range coupling constant used for HMBC was 8.0 Hz.

2.7. Biological assays

2.7.1. Antifungal assay – Disc diffusion assay

Disc diffusion assay was used to determine which fungus was the inducer strain, by application of the extract from the confrontation zone on both strains from the pairwise culture. For the fungi sporulation, spore solution of *F. oxysporum* and *A. alternata* were obtained by growing 10 mm agar plug of the selected fungi in 20.0 ml of Potato Dextrose Agar (Sigma Aldrich), while *C. acutatum* and *D. eres* were obtained by inoculation on 20.0 ml Oatmeal-Agar (Difco - Oatmeal 60 g L^{-1}; Bacto Agar 12.5 g L^{-1}).

All fungal pre-culture were inoculated in the centre of a 9 cm petri dish and plates were incubated at 25 °C for 10 days in the dark. After incubation, 10.0 ml of sterile distilled water was added to the fungal cultures, scraped with a plastic smear loop and transferred to another petri dish. This procedure was repeated a total of 3 times and the final solution was vortexed for one minute and left to rest for 15 minutes to allow the particles to settle down. To determine the number of cells in the resulting spore solution, an automatic cell counter was used according to the manufacturer's instructions. 10 µl of the upper supernatant of the spore solution was loaded onto the TC20 system (Bio-Rad, Hercules, CA, USA) counting slides and the number of cells was determined with a TC20 automated cell counter (Bio-Rad, Hercules, CA, USA). All solutions were diluted with sterile water until final concentration of 1.10 ^{6}cell mL^{-1} and the remaining were stored at -80 °C.

Preparation of the solid media for the disc diffusion assay was conducted by the addition of 20 mL of Czapek-Agar (Sigma Aldrich, Netherlands) and 500 µL the fungus spore solution at a cell concentration of 1.10^{6} cells mL^{-1}. After solidification of the solid media with the spores, 4 wells of 7 mm were pierced in each plate and tested solution was added in triplicates with concentrations of 500, 200, and100 µg mL^{-1}. All the solutions were prepared in

ethyl acetate and the fourth well of each plate was used as a negative blank (only containing ethyl acetate).

2.7.2. Antibacterial assay

Anti-microbial activity was examined against two Gram positive strains (*Bacillus cereus* and *Staphylococcus aureus*) and two gram negative strains (*Pseudomonas fluorescens* and *Escherichia coli)* purchased from The Netherlands Culture Collection of Bacteria. Antimicrobial assay was performed according to Clinical and Laboratory Standards Institute (CLSI) guidelines. Spectinomycin was used as a positive control at a concentration of 100 mg mL^{-1}.

Bacteria were incubated at 37 °C in growth medium Mueller-Hinton Broth medium (MHB) (Sigma-Aldrich) until an optical density (OD) of 0.1. Following, the cells were diluted to 10^6 CFU mL^{-1} before inoculation in 96-well plate. Stock solutions of the extracts and isolated compounds were prepared in 100% dimethyl sulfoxide (DMSO), in a concentration of approximately 25 mg mL^{-1}, and stored at -20 °C until use. Each stock solution was diluted with broth medium in serial dilutions of factor 2 in the range of 512 to 64 μg mL^{-1} before use. A volume of 100 μL of the broth containing the test bacteria was aliquoted to each well of the 96-well microtiter plate and the minimum inhibitory concentration (MIC) was determined after incubation at 30 °C overnight. The MIC was recorded as the highest dilution concentration of the plant extract resulting in growth inhibition (absence of turbidity) of the bacteria.

3. Results and Discussion

3.1. Selection of promising pairwise strains – Evaluation of Chemical Induction from Antagonistic Interactions

The first step of the strategy for the enhancement of the chemical profile was the selection of promising pairwise strains, which was based on the antagonistic morphological response of the colonies in solid media co-culture and the *de novo* metabolite induction. Analysis of solid agar was preferred as opposed to liquid culture-based growth given some microbial behavior, including many developmental processes and production of certain secreted factors, have only been observed when the microbes were grown on agar (WATROUS et al., 2012). Furthermore, soft-agar culturing is very common in microbiology laboratories. For this procedure, plugs of the five selected fungi *F. oxysporum, D. eres, A. alternata, X. cubensis* and *C. acutatum* were inoculated in solid media both as single and co-cultures and their morphological behavior was

monitored daily. Co-culture plates were inoculated on opposite sides of a single 9 cm petri dish, while monocultures of individual filamentous fungi were inoculated in the center of the petri dishes. All plates were incubated for 12 days, at 25 °C, in the dark. Pairwise strains that display antagonistic interactions (*i.e.* distance-inhibition and zone line) had their metabolites extracted and the chemical data was assessed by HPTLC.

Bertrand and co-workers reported, in 2014, that fungi co-culture in solid media resulted in four major morphological outcomes *distance-inhibition* (1), *zone lines* (2), *contact-inhibition* (3) and *overgrowth* (4). Indeed, our fungal screening revealed that all four interactions have also been observed for the co-culture of the five selected fungi, with unique morphological response observed against each specific challenge microbe (Table 5.1). Overall, *X. cubensis* displayed majorly overgrowth responses, regardless of the challenge strains, with the exception of *X. cubensis*/*F. oxysporum*, that grew to a contact-inhibition (Fig. 5.1 A). Similarly, *C. acutatum* exhibited a significant distance-inhibition zone with all other challenge microbes, with the exception of *X. cubensis*, that overgrew *C. acutatum* colony. The morphological responses of *F. oxysporum, D. eres and A. alternata* were broader and showed completely different outcomes for each single species. For example, *F. oxysporum* displayed distance-inhibition, zone line, contact inhibition and *Fusarium* overgrowth with *C. acutatum, D. eres, X. cubensis* and *A. alternata*, respectively. Moreover, in *F. oxysporum* co-culture experiments with *D. eres* and *A. alternata*, the initial morphological response were zone line and distance-inhibition, respectively. However, after 12 days of inoculation, we observed that *F. oxysporum* overcame the inhibition barrier, growing over the challenge fungi in an overgrowth interaction (Supplementary Material, Fig. SM9).

Co-culture	Type of interaction	Metabolite detection (Rf on HPTLC)
F. oxysporum and *X. cubensis*	Contact inhibition	N/A
F. oxysporum and *D. eres*	Zone line/*Fusarium* overgrowth	0.08 and 0.57
F. oxysporum and *A. alternata*	Distance-inhibition/*Fusarium* overgrowth	N/D
F. oxysporum and *C. acutatum*	Distance-inhibition	0.08 and 0.35
X. cubensis and *D. eres*	*Xylaria* Overgrowth	N/A
A. alternata and *X. cubensis*	*Xylaria* Overgrowth	N/A
A. alternata and *D. eres*	Distance-inhibition	018, 0.42 and 0.57
C. acutatum and *A. alternata*	Distance-inhibition	N/D
C. acutatum and *D. eres*	Distance-inhibition	0.57
C. acutatum and *X. cubensis*	*Xylaria* Overgrowth	N/A

Table 5.1. Morphological outcomes between co-culture of the selected fungi in solid media. N/A – co-cultures that did not display clear sign of antibiosis and, hence, were not selected for chemical analysis. N/D – co-cultures that did not display any differences in comparison with single-culture of their respective fungi.

Out of the ten co-cultures performed with the five selected strain, we have observed that six of them showed clear antagonistic responses, *i.e.* pairwise strains with distance-inhibition and zone line interactions (*F. oxysporum*/*D. eres*; *F. oxysporum*/*A. alternata*; *F. oxysporum*/*C. acutatum*; *A. alternate*/*D. eres*; *C. acutatum*/*A. alternata*; and *C. acutatum*/*D. eres*). The chemical profiles of these co-cultures were systematically evaluated for each set of samples based on the HPTLC data (Fig. 5.1 B) and compared to those obtained from monocultures. The mobile phase used for these HPTLC analysis was the non-polar mixture of Toluene-Ethyl acetate (8:2).

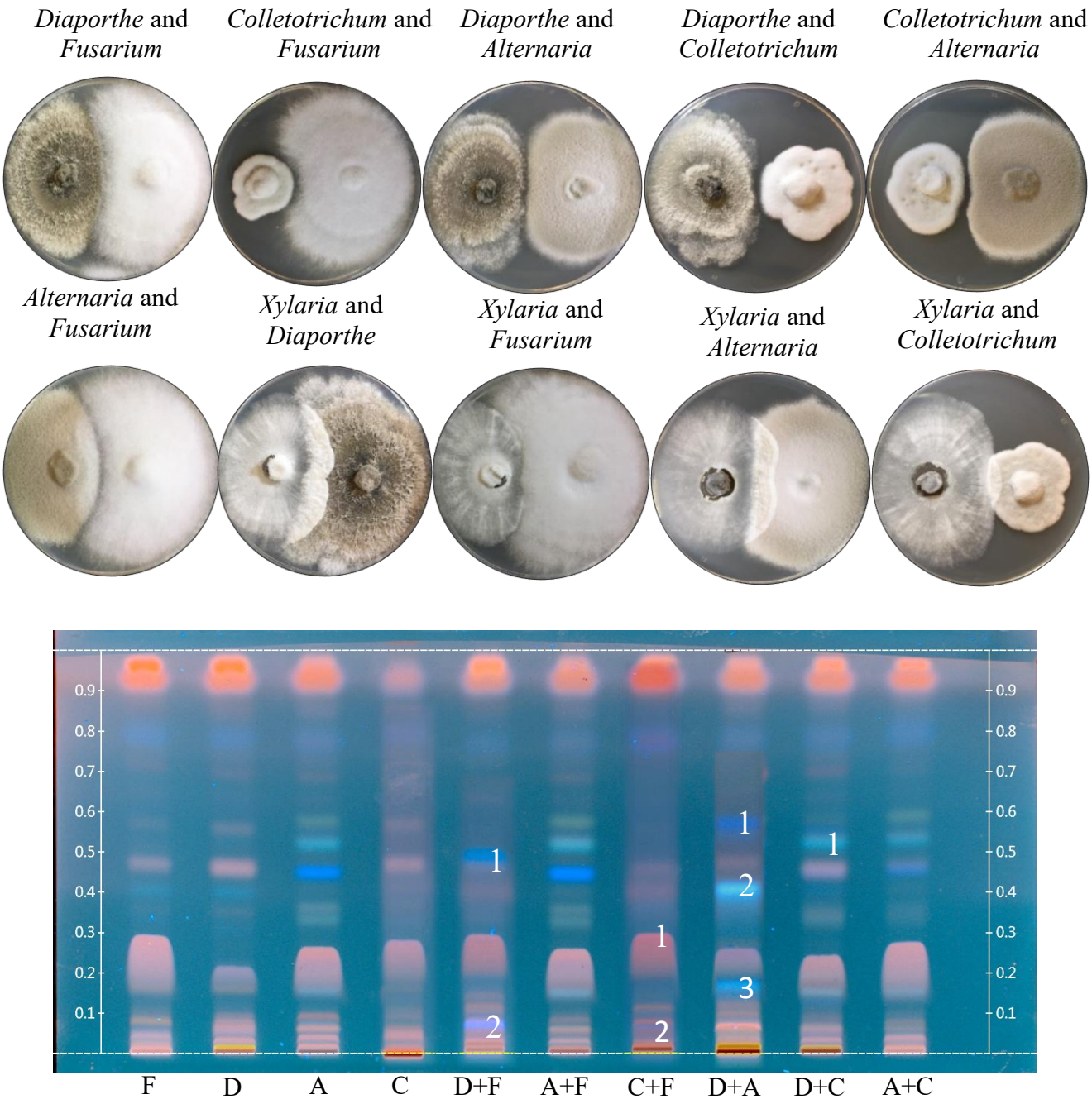

Figure 5.1. (A) Co-cultures of selected fungus strains. Selection of promising co-culture that display antagonistic communication on the confrontation zone. **(B)** HPTLC data of single culture and co-culture from antagonistic interactions. The induced metabolites in co-cultures are numbered. Labels: *F. oxysporum*/*D. eres* (F+D*); F. oxysporum*/*C. acutatum* (F+C); *D. eres*/*A. alternata* (D+A); *D. eres*/*C. acutatum* (D+C), *A. alternata* (A), *C. acutatum* (C); *D. eres* (D); *F. oxysporum* (F).

HPTLC plates were interpreted using both UV light (254 and 366 nm) and anisaldehyde in sulfuric acid and heating, providing a universal perspective of the samples. Evaluation of the chemical data revealed that only four co-cultures *F. oxysporum*/*D. eres* (D+F), *F. oxysporum*/*C. acutatum* (C+F), *A. alternata/D. eres* (D+A) and *C. acutatum*/*D. eres* (D+C) exhibited a strong metabolite induction and displayed induced spots on the co-culture experiments that were not detected on monoculture of the respective fungi (Fig. 5.1 B). In addition, both *F oxysporum/A. alternata* and *C. acutatum*/*A. alternata* have not demonstrated any significant differences from the single-culture, most likely due to the weak induction of metabolites, that were not detected by HPTLC and, therefore, were not selected for further biological and chemical assessment.

3.2. Optimization of biotic parameters - Evaluation of inducer strain and incubation period for the induction of secondary metabolites in selected co-culture

It is well known and repeatedly reported in literature that the choice of the biotic and abiotic parameters immensely affects the chemical profile in co-cultures, resulting in changes in the amount and diversity of secondary metabolite production (BODE et al., 2002; SCHERLACH; HERTWECK, 2009). In co-culture experiments, these variables are often neglected, resulting in issues related to sampling and reproducibility. In this study, to optimize the antimicrobial induction of the selected co-cultures, as well as address the analytical issues of microbial data, two strategies were applied to determine each strain is inducing the chemical enhancement and the best incubation period for the production of these induced metabolites. The first consisted on the evaluation of the metabolic induction in different extraction points, targeting to select the best incubation period for metabolite induction. The second was performed to determine which strain was responsible for the chemical outcome and was evaluated by (1) metabolite extraction of the confrontation zone and adjacent mycelial part and (2) disc diffusion assay of the extract from the confrontation zone against both isolated strains. Moreover, to guarantee reproducibility, all abiotic parameters (temperature, luminosity, type and volume of solid media) were carefully monitored, with incubation at 25 °C, in the dark, in plates containing 20.0 mL of Czapek-agar.

3.2.1. Determination of inducer strain in co-culture experiments

In drug discovery program, one of the major difficulties of microbial co-culture is to find which microorganism is producing the metabolic outcome (*i.e.* inducer strain). The knowledge

of the biosynthetic pathway of the inducer strain can help the optimization of biotechnological processes and the molecule elucidation of the often-complex induced compounds. Most reports only suggest the inducer microorganisms based on bias comparison with the axenic cultures and some knowledge of the microbial biosynthetic pathway, however, very few reports perform chemical and/or genetical analysis for confirmation.

To evaluate the individual contribution of each strain for the induction of *de novo* metabolites and, by consequence, determine the strain that induces the metabolic production, two different strategies were applied. The first targeted to evaluate the confrontation zone and adjacent mycelial parts by separately extracting their metabolites for comparison by HPTLC. For that, all three agar regions were separately excised with a razor blade as 1 cm ×1 cm piece and compared with single cultures of *F. oxysporum*, *D. eres*, *A. alternata* and *C. acutatum*. The second strategy was only applied when HPTLC comparison was not conclusive and consisted in an antifungal assay of the extract from the confrontation zone (CZ) on both strains from the pairwise strains. This procedure was conducted by individual inoculation of the spore solution of the selected fungi in solid media, followed by assessment of the CZ extract by disc diffusion assay at concentration of 500 μg mL^{-1}.

Evaluation of HPTLC data from the confrontation zone and adjacent mycelial parts showed that all three parts extracted from the plate were significantly different from the single-culture control, evidencing the potential of co-culture to diversify the chemical profile. Chemical data of co-cultures *D. eres*/*A. alternata* and *D. eres*/*C. acutatum* showed that their induced secondary metabolites were produce in both the confrontation zone and the isolated fungus region (Fig. 5.2 A), indicating that the induction signaling happens by both agar-diffused metabolites and volatiles organic compounds (VOC). Moreover, other than the previously reported induced metabolite, individual analysis of the three isolated regions allowed the detection of other low abundance induced compounds at Rf 0.21 and 0.08, produced by *D. eres* in co-cultures with both *A. alternata* and *C. acutatum*, illustrating the excellent combination of solid media individual extraction with simultaneous comparative analysis by HPTLC. The co-culture of *D. eres*/*A. alternata* initially displayed three induced compounds, two of which were produced by *D. eres* (Rf 0.18 and 0.57), one that is produced by *A. alternata* (Rf 0.42). Similarly, *D. eres*/*C. acutatum* induced metabolite was also produced by *D. eres* at Rf 0.57, indicating that this metabolite could be produced as a general defense response.

Separately analysis of co-cultures *F. oxysporum*/*D. eres* and *F. oxysporum*/*C. acutatum* were more challenging, given most induced metabolites were only detected in the confrontation

zone. For these particular cases, disc diffusion assay was an excellent alternative, determining not only which fungus was the inducer strain, but also the antifungal potential of the *de novo* secondary metabolites. For example, HPTLC data of *F. oxysporum*/*C. acutatum* was inconclusive to determine the induced strain of both induced metabolites at Rf 0.08 and 0.35, however, disc diffusion assay of the extract from the confrontation zone showed a strong antifungal activity against *C. acutatum* and an absence of activity in *F. oxysporum*, suggesting that the latter is the one responsible for the induction (Fig. 5.2 B). On the other hand, HPTLC data of *F. oxysporum*/*D. eres* showed that the induced metabolite at Rf 0.08 is produced in both the confrontation zone and *F. oxysporum* isolated region, while the spot at Rf 0.51 was only produced by in the confrontation zone as a major metabolite. Disc diffusion assay of the confrontation zone extract in both isolated spore solutions revealed a small antifungal potential against *F. oxysporum* and an absence of antifungal activity against *D. eres*, indicating that, for this pairwise, the induced metabolite at Rf 0.57 is, in fact, produced by *D. eres* (Fig. 5.2 C).

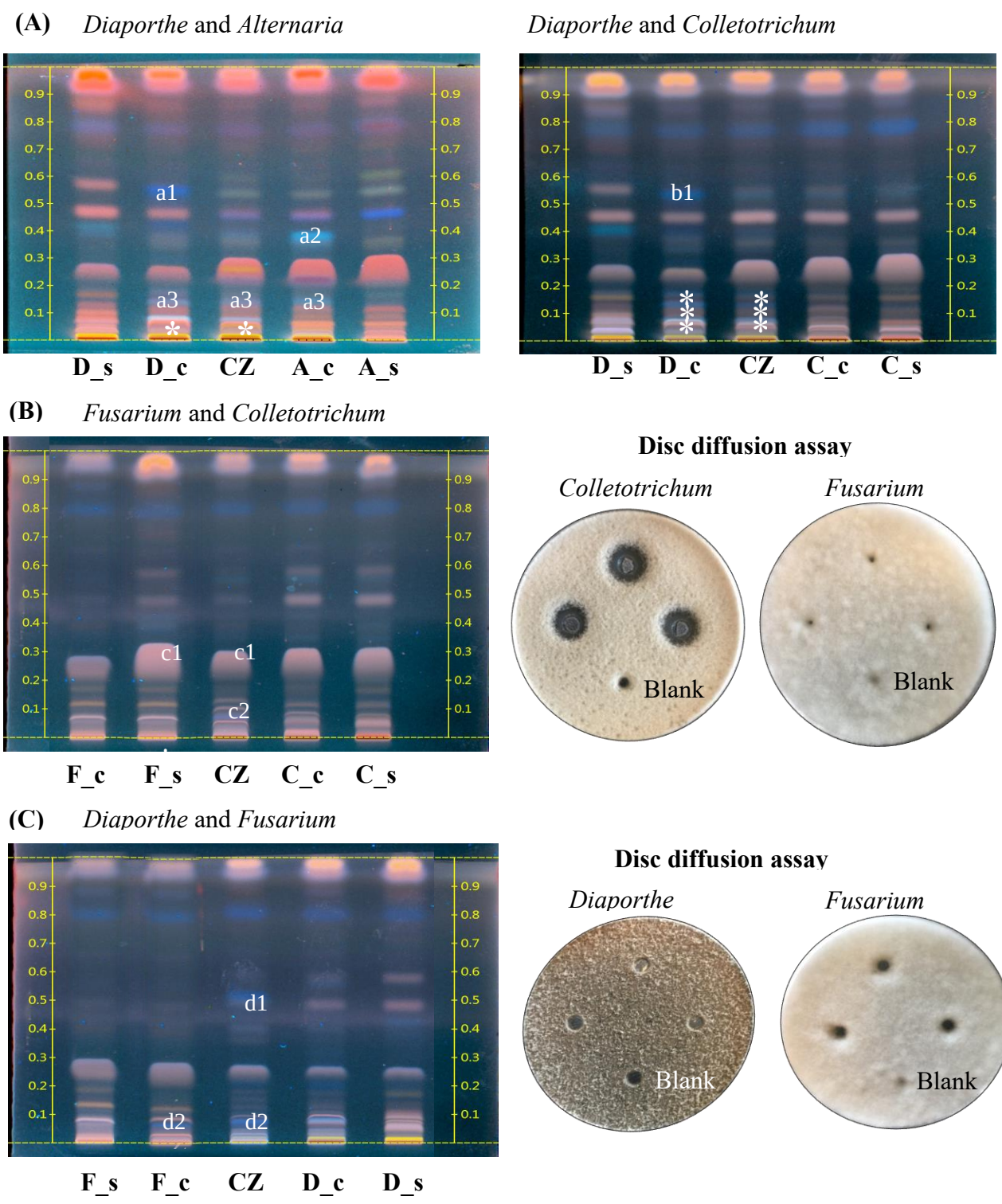

Figure 5.2. Evaluation of biotic parameters for the induction of secondary metabolites in selected co-culture. The induced metabolites are numbered. **(A)** HPTLC data of confrontation zone and adjacent mycelial parts of selected co-cultures *D. eres*/*A. alternata* and *D. eres*/*C. acutatum*. HPTLC data of confrontation zone and adjacent mycelial parts of selected co-cultures and disc diffusion assay with 500 µg mL^{-1} of the confrontation zone extract of **(B)** *D. eres*/*F. oxysporum* and **(C)** *C. acutatum*/ *F. oxysporum*.

3.2.2. Evaluation of induced metabolites in different extraction points

The best incubation period of the selected co-cultures was evaluated to determine at each day of the fungal growth there was the highest metabolite induction. For that purpose, all inoculated plates were incubated at 25 °C, in the dark, and their metabolites were extracted in four different days (4, 6, 9 and 12 days), which comprises one point of the exponential phase (day 4) and three different points of the stationary phase of the fungi growth (days 6, 9 and 12).

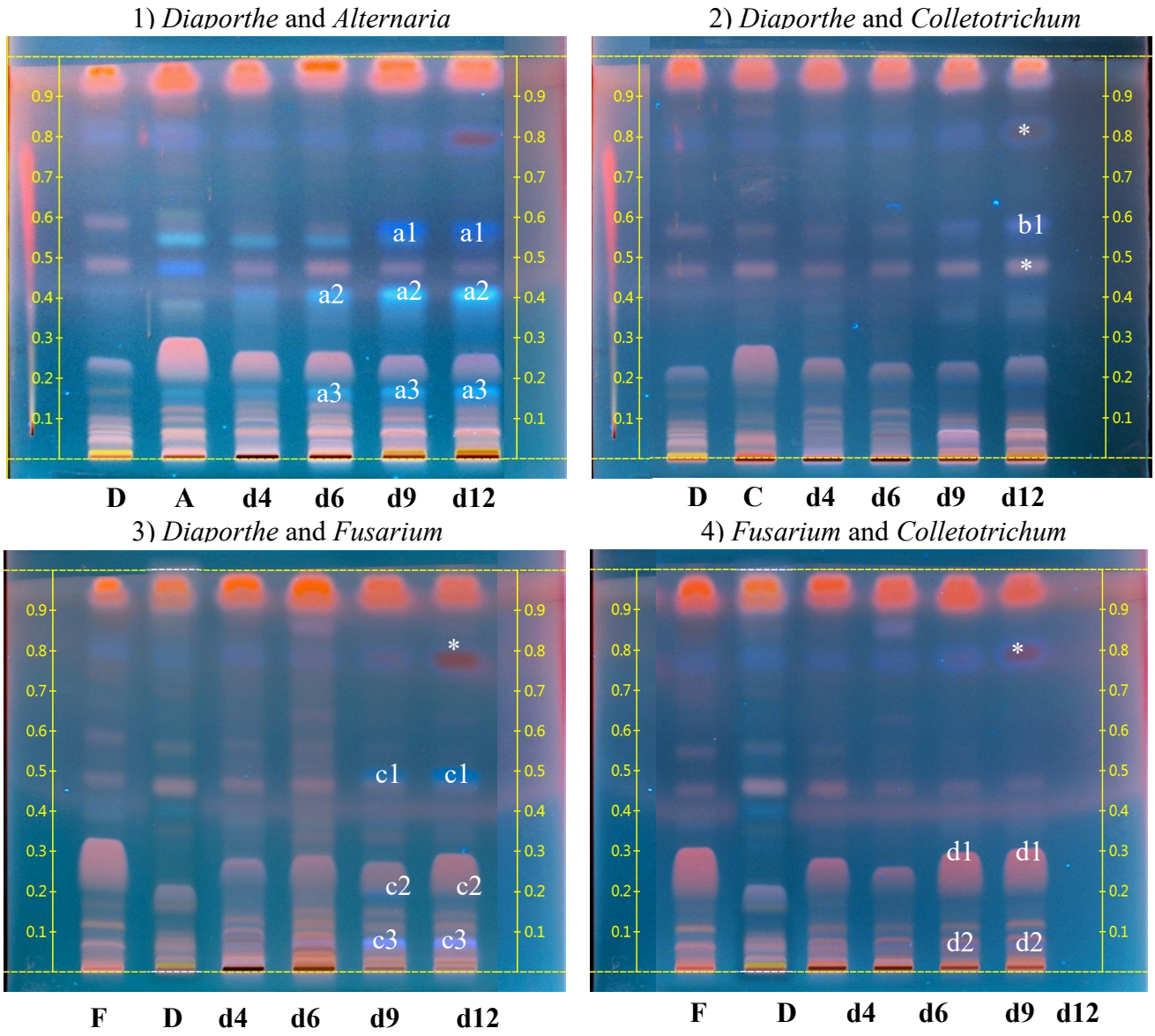

Figure 5.3. Evaluation of biotic parameters for the induction of secondary metabolites in selected co-culture. The induced metabolites in co-culture are numbered. Evaluation of induced metabolite variation in different extraction points (4, 6, 9 and 12 days).

To evaluate the *de novo* induction of metabolites during fungal growth, the chemical profile of the selected co-cultures were analyzed by HPTLC and single cultures of *F. oxysporum*, *D. eres*, *A. alternata* and *C. acutatum* were used as control. Co-culture extracts revealed that the chemical enhancement of the induced metabolites occurs majorly in the stationary phase, after the fungi start to compete for space and nutrients, with higher production of induced compounds at day 12. Moreover, each induced compound was produced in different time points of the stationary phase, with spots of all targeted induced metabolites only completely detectable at day 12 (Fig. 5.3).

3.3. Metabolic profiling of selected co-cultures by HPTLC

Metabolomics analysis of the fungal co-cultures were performed by culturing all of the four selected pairs in triplicates (10 petri dishes per replicate). Incubation was performed at 25 °C, in the absence of light and in plates containing 20.0 mL of Czapek-agar. To highlight the metabolite modifications that are caused by fungal interactions, an HPTLC-fingerprinting method was adapted to the analysis of metabolites extracted in the agar solid media after 12 days of growth. The development of this method included the optimization of the mobile phase, revelation solution and injection volume to detect the largest possible number of metabolites over a specific range of polarities. The repeatability of the fingerprinting method, as well as the metabolite profiles of replicates was evaluated to ensure that satisfactory statistical results were obtained even when screening a large number of samples.

HPTLC metabolic fingerprinting was applied to detect the induced metabolites of the selected co-culture experiments. Figure 5.4 A illustrates the HPTLC data of all triplicates in a non-polar mobile phase. Overall, single cultures produces much less non-polar metabolites than co-culture and the major metabolic differences of co-culture experiments consisted in the presence of blue induced bands (at 366 nm, after anisaldehyde derivatization and heating at 100°C), detected at a broad range of polarity (Rf from 0.08 to 0.57) after elution with Toluene-Ethyl Acetate. Moreover, in the region of Rf 0.35 in the co-culture of *F. oxysporum*/*C. acutatum*, there was an abundant production of a red-like band, which was, by far, the most prominent induction.

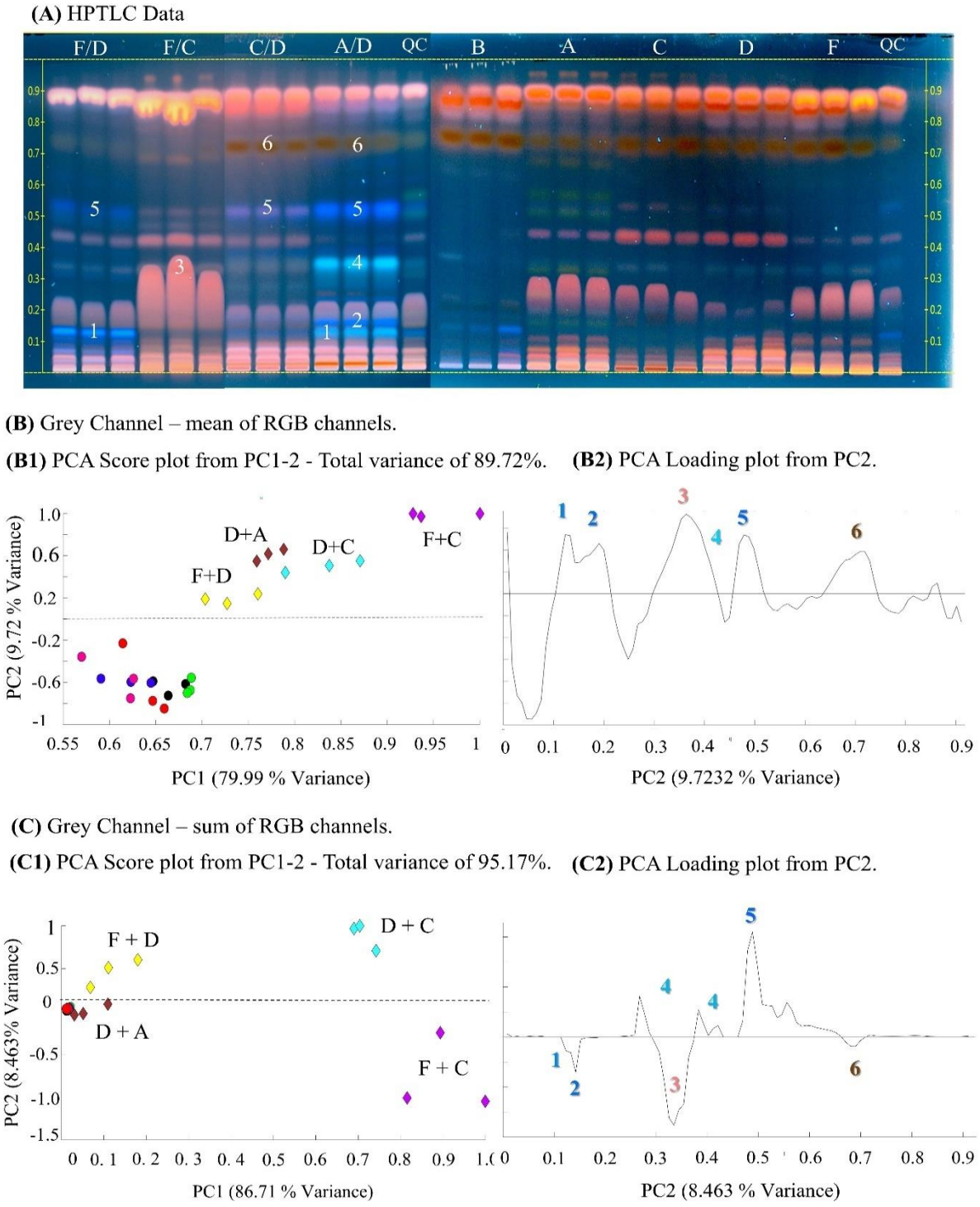

Figure 5.4. (A) HPTLC data of all triplicates in a non-polar mobile phase (Toluene-Ethyl acetate 8:2 v/v). **(B)** PCA analysis using the mean of all RGB channels. PCA score plot from PC1-2 displays a total variance of 89.72%. **(C)** PCA analysis of the sum of all RGB channels. PCA score plot from PC1-2 displays a total variance of 95.17%. Labels: *F. oxysporum*/*D. eres* (F/D)*; F. oxysporum*/*C. acutatum* (F/C); *D. eres*/*A. alternata* (A/D); *D. eres*/*C. acutatum* (C/D), *A. alternata* (A), *C. acutatum* (C); *D. eres* (D); *F. oxysporum* (F); Czapek blank (B) and Quality control (mixture of all samples) (QC).

To overview the metabolites of both co-culture and single-culture control, a unsupervised Principal Component Analysis (PCA) was applied to the processed HPTLC data. For a better evaluation of the chemical data, two different datasets were tested using the HPTLC data after conversion by the rTLC software (FICHOU; RISTIVOJEVIĆ; MORLOCK, 2016): (1) the grey channel that consists on the mean value of all the other RGB channels and a (2) grey channel that represents the sum of all other RGB colors. These datasets were selected based on the distinct chemical information each one best brings to the multivariate data analysis and both matrices were preprocessed using the same experimental protocol.

Score plots revealed that PCA using the mean RGB values separated the samples into single and co-culture over PC2, while PCA using the sum RGB values grouped all the single culture in null-variance and only discriminated the co-cultures over PC2 (Figure 5.4 B and C). Although both display a PC2 explained variances of ~ 9%, analysis of the loading values revealed that the mean RGB values contains the differences between all co-culture and mono-cultivation and correlated co-cultures to the bands at RFs 0.08, 0.18, 0.35, 0.42, 0.57 and 0.72. On the other hand, the sum RGB values gave us a more detailed information about these induced metabolites and correlated *Diaporthe*/*Colletotrichum* and *Diaporthe*/*Fusarium* with the RFs at 0.42, 0.57 and the *Fusarium*/*Colletotrichum* and *Diaporthe*/*Alternaria* with the RFs at 0.08, 0.18, 0.35 and 0.72. Moreover, only by using the sum RGB values, it was possible to discrimination the bands at 0.35 (from the co-culture *F. oxysporum* and *C. acutatum*) and Rf 0.42 (from the co-culture of *D. eres* and *A. alternata*), which were convoluted and undistinguished in the other unsupervised analysis.

3.4. Antimicrobial bioactivity of co-culture samples and correlation with metabolomics data by PLS-DA

Although the metabolic influence of single and co-culture was successfully detected in PCA from the HPTLC data, the unsupervised analysis alone did not provide any information about the biological response of these induced compounds. Therefore, to investigate in detail the antimicrobial effect of these co-cultural matrices, antibacterial assays against two Gram-positive strains (*B. cereus* and *S. aureus*) and two Gram-negative strains (*P. fluorescens* and *E. coli*) were performed according to CLSI guidelines.

All single cultures of *F. oxysporum*, *D. eres*, *A. alternata* and *C. acutatum* displayed an absence of antibacterial activity, while the selected co-cultures displayed an increased antimicrobial response and a broad range of MIC values against the tested bacterial strains

(Table 5.2). Co-cultures of *F. oxysporum*/*D. eres* (I) and *F. oxysporum*/*C.* a*cutatum* (II) showed high antibacterial against *P. fluorescens*, *S. aureus* and *E. coli* and an absence of activity against *B. cereus*. On the other hand, the co-cultures *A. alternata*/*D. eres* (III) and *C. acutatum*/*D. eres* (IV) showed moderate activity against *S. aureus* and a high activity against *B cereus*, being inactive against all tested gram-negative strains.

	MIC values on Gram-positive		**MIC values on Gram-negative**	
	B. cereus	***S. aureus***	***P. fluorescens***	***E. coli***
F + C	I	256	256	256
F + D	I	256	256	256
D + A	256	512	I	I
D + C	256	512	I	I
A	I	I	I	I
C	I	I	I	I
D	I	I	I	I
F	I	I	I	I

Table 5.2. Antibacterial activity of selected co-culture and their respective isolated fungi against two Gram-positive strains (*B. cereus* and *S. aureus*) and two gram-negative strains (*P. fluorescens* and *E. coli*). Antibacterial was evaluated by the MIC values and spectinomycin was used as a positive control at a concentration of 100 mg mL^{-1}. Labels: *F. oxysporum*/*D. eres* (F+D*); F. oxysporum*/*C. acutatum* (F+C); *D. eres*/*A. alternata* (D+A); *D. eres*/*C. acutatum* (D+C), *A. alternata* (A), *C. acutatum* (C); *D. eres* (D); *F. oxysporum* (F). Activity: inactive (I), moderate antibacterial activity (512 μg mL^{-1}) and high antibacterial activity (256 μg mL^{-1}).

The induced secondary metabolites of the selected co-culture were accurately determined by unsupervised HPTLC-metabolomics. However, for the correlation of their production with the antimicrobial activity, we used ^{1}HNMR data, given this technique has more information about the chemical structure of the induced metabolites and was the only analytical matrix validated for the supervised chemometric analysis. For this correlation, a supervised PLS-DA

was applied using the antibacterial response (1: moderate antibacterial activity and 2: high antibacterial activity), with a well-validated model obtained by permutation test using 100 permutations (Q2 value of 0.78 and R2 value of 0.94).

Score plot of PLS-DA showed a very clear discrimination between samples with moderate and high antibacterial activities (Fig. 5.5 A). Both *Diaporthe*/*Alternaria* and *Diaporthe*/*Colletotrichum* co-cultures show moderate antimicrobial activity and appeared close on the negative portion of PC1, indicating that both systems induces the bioactive metabolites in similar amounts. For *Fusarium*/*Colletotrichum* and *Fusarium*/*Diaporthe*, however, the production of the bioactive induced compound varies abundantly, displaying an significant up-regulation in the co-culture *Fusarium*/*Colletotrichum*.

The distribution of the samples on the PLS-DA score plot also suggests the origin of the bioactive metabolites. The co-cultures that shows moderate bioactivity have *Diaporthe* as the common strain, while the ones with high antibacterial results have *Fusarium*. Moreover, although *Fusarium*/*Diaporthe* displayed strong antibacterial results, the replicates appeared close to null on the *x*-axis, which suggests a tendency towards the co-cultures with moderate bioactivity, explained by the presence of *Diaporthe* as the challenged strain.

PLS-DA loading plot revealed the major chemical shifts correlated to the antibacterial activity (Table 5.3). The selection of these signals was based on a threshold cut, displayed on Figure 5.5B, which was optimized separately for the positive and negative loading values to select only the most intense and important signals.

Chemical shifts	**Loading Correlation**
δ7.25 (*s*), δ7.24 (*d*, *J* 1.7 Hz), δ5.37 (*m*), δ3.14 (*s*), δ2.27 (*t*, *J* 7.4 Hz), δ1.52 (*d*), δ0.93 (*d*, *J* 6.5 Hz), δ0.85 (*d*, *J* 6.9 Hz), δ0.24 (*d*, *J* 6.9 Hz)	(+) High Antibacterial Activity
δ7.45 (*dd*, *J* 5.2 and 3.1 Hz, 1H), δ7.21 (*dd*, *J* 9.6 and 3.7 Hz, 1H), δ6.95 (*s*), δ5.80 (*ddt*, *J* 17, 10.2 and 6.7 Hz), δ4.02 (*t*, *J* 6.6 Hz), δ3.93 (*s*, 3H), δ2.81 (*t*, *J* 7.4 Hz), δ2.56 (*t*, *J* 7.4 Hz), δ2.04 (*m*)	(-) Moderate Antibacterial Activity

Table 5.3. Chemical shifts correlated to the high and moderate antimicrobial activity by the PLS-DA loading plot.

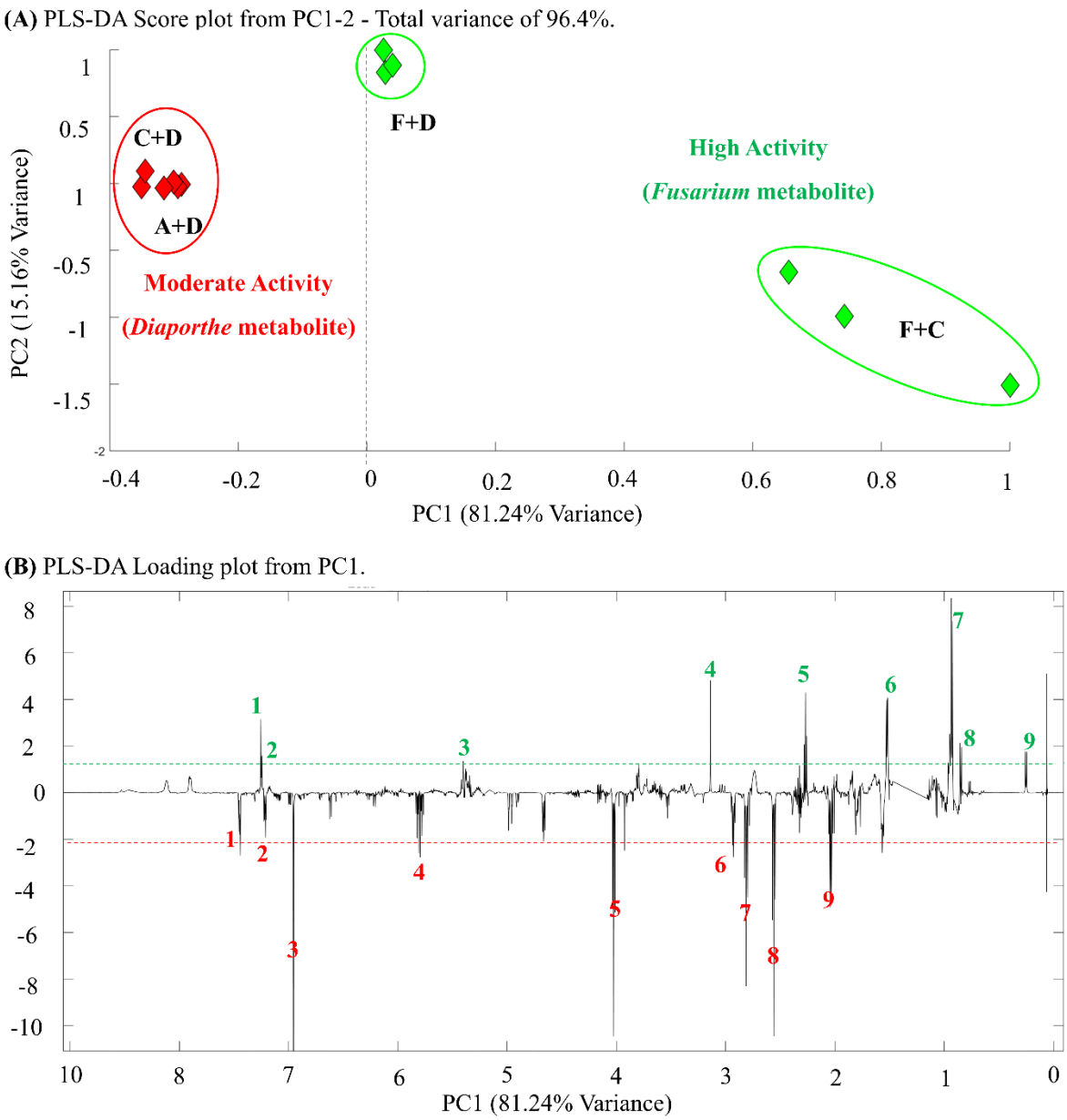

Figure 5.5. (A) PLS-DA score plot from PC1-2 (total variance of 96.4%) of the processed ^{1}HNMR data of co-culture experiments based on antibacterial activity (1: moderate antibacterial activity and 2: high antibacterial activity). **(B)** PLS-DA loading plot from PC1 (total variance of 81.24%).

3.5. Elucidation of Bioactive Induced Secondary Metabolite – Chemical Identification and biological activity

For molecule assessment, first, all the chemical shifts correlated to the moderate and high antimicrobial activity by PLS-DA were submitted to Statistical Total Correlation Spectroscopy (STOCSY). STOCSY analysis enables digital separation of these signals, it is

not limited to the usual connectivities of two-dimensional NMR methods and takes advantage of the multicollinearity of the signals intensity in a ^{1}HNMR spectra (CLOAREC et al., 2005).

Following, for molecule confirmation, these connectivities found on the STOCSY were evaluated by 1D and 2D NMR (HSQC, HMBC, 1D-TOCSY and 1D-NOESY). Lastly, for definitive metabolite correlation, the only induced band from the co-culture *Fusarium*/*Colletotrichum* (at RF 0.35) and both induced bands from *Diaporthe*/*Colletotrichum* (at RFs 0.57 and 0.72), found by the PCA analysis of HPTLC data, were scrapped of the plate and submitted to ^{1}HNMR, targeting to compare the chemical information and confirm both the induction and biological activity.

3.5.1. Fusarium metabolites

STOCSY experiments were performed for all signals extracted from the PC1 positive loading plot of the PLS-DA analysis and revealed two sets of chemical data, displayed in Table 5.4. Comparison of these data with spectroscopic information from an in-house *Fusarium* database suggested the presence of one secondary metabolites from *F. oxysporum* (Figure 5.6A) and one fatty acid derived from the Czapek medium (Figure 5.7A), present in all the co-culture and monoculture samples.

The induced secondary metabolite from *F. oxysporum* was beauvericin, a hexadepsipeptide from the enniatin family that has been already extensively discussed in this thesis (SELEGATO et al., 2016a). This cyclic peptide was produced on both *Fusarium* co-cultures, exhibiting significant up-regulation in *Fusarium*/*Colletotrichum.* Evaluation of the ^{1}HNMR from the scrapped HPTLC band and the PLS-DA results showed the same chemical shifts found on the PC1 loading plot correlated to high antibacterial activity were also detected at the Rf 0.35 from the co-culture of *F. oxysporum*/*C. acutatum*, confirming that these compound was indeed the most induced metabolite in co-culture. Although the resolution between the bands was insufficient to be separated in a pure state, the semi-purified bands were successfully analyzed and confirmed based on comparison of reference metabolites from available databases.

Comparison with the monoculture of *F. oxysporum* showed that this fungus produces the cyclic peptide in axenic cultures, however, in co-culture with *C. acutatum*, this metabolite appeared up-regulated in more than 3-fold, indicating that this increase was a direct result of the presence of this challenge microbes. In co-culture with *Diaporthe*, we have also detected the presence of beauvericin, however, for this system, the production of the mycotoxin fusaric

acid appeared to be more significant, illustrating the specific regulation of the metabolome according to the environmental biotic conditions (Supplementary Materials, Figure SM10A).

Beauvericin have already revealed strong antimicrobial potential against several gram-positive bacteria, gram-negative bacteria and fungi, which explains the increase in the antimicrobial activity of the mixed culture (CASTLEBURY et al., 1999; DZOYEM et al., 2017; MECA et al., 2010; SONDERGAARD et al., 2016; ZHANG et al., 2016). For instance, studies have demonstrated that this compound is active against *Candida albicans*, *E. coli*, *S. aureus*. *B. pumilus*, *B. cereus*, *B. mycoides*, *B. sphaericus*, *Paenibacillus alvei*, *P. azotofixans*, *P. macquariensis*, *P. pulvifaciens* , *P. validus*, *Eubacterium biforme*, *Peptostreptococcus anaerobius*, *P. productus*, *Bifidobacterium adolescentis* and *Clostridium perfringens* (CASTLEBURY et al., 1999; DZOYEM et al., 2017; MECA et al., 2010; SONDERGAARD et al., 2016; ZHANG et al., 2016). Although reports have shown sensitivity against *B. cereus*, beauvericin did not show any activity against the *B. cereus* strain tested in our study, which could suggest resistance of this bacteria to the cyclic compound.

Driver peak	Correlated chemical shifts	Antimicrobial activity	Metabolite
δ7.25 (*s*)	δ7.24 (*d*, *J* 1.7 Hz), 5.80 (*m*), δ3.80 (*dd*, 1H, *J* 11.5, 3.0 Hz), δ3.39 (*dd*, 1H, *J* 14.7, 4.6 Hz), δ3.14 (*s*), δ3.03 (*dd*, 1H, *J* 14.7, 12.8 Hz), δ1.52 (*d*, *J* 6.5 Hz), δ0.93 (*d*, *J* 6.9 Hz), δ0.85 (*d*, *J* 6.5 Hz), δ0.24 (*d*, *J* 6.9 Hz)	High	Beauvericin
δ2.27 (*t*, *J* 7.4 Hz)	δ5.37 (*m*), δ2.02 (*d*, *J* 5.8 Hz), δ1.60 (*dt*, *J* 14.5 and 7.2 Hz)	None: present in all samples	From the Czapek medium

Table 5.4. STOCY correlation of the chemical shifts found on the PLS-DA loading values for high antimicrobial activity. Molecules were elucidated in *F. oxysporum* samples.

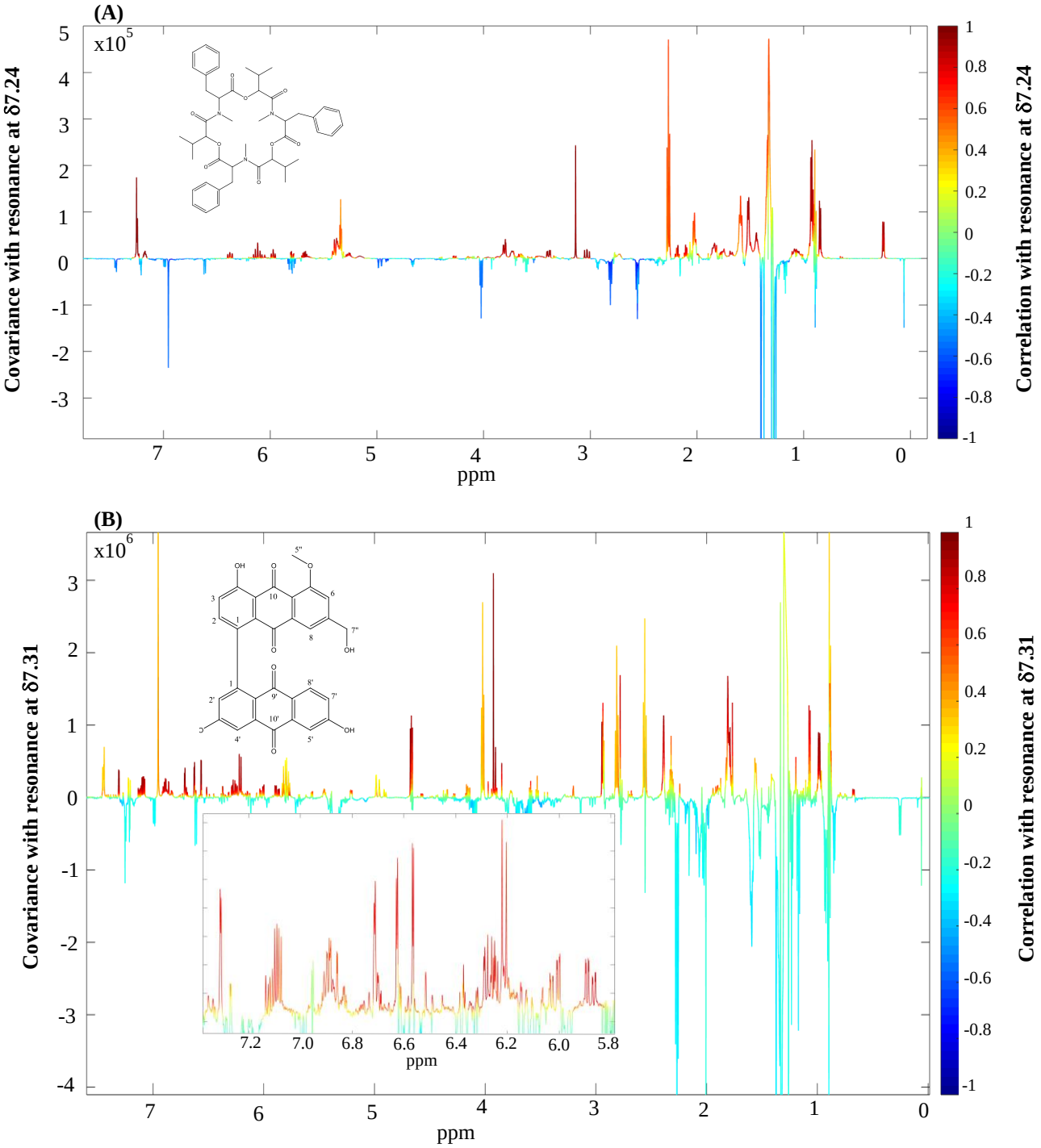

Figure 5.6. STOCY correlation and covariance of the signals from the induced metabolites found on the PLS-DA loading values. **(A)** Signals correlated to δ7.25 (*s*) were elucidated as beauvericin, identified in *F. oxysporum* samples; these chemical shifts were found on the PLS-DA loading values attributed to high antimicrobial activity. **(B)** Signals correlated to δ7.31 (*d*, *J* 2.1 Hz, 1H) were elucidated as the bisanthraquinone, identified in *D. eres* samples; these chemical shifts were found on the PLS-DA loading values attributed to moderate antimicrobial activity.

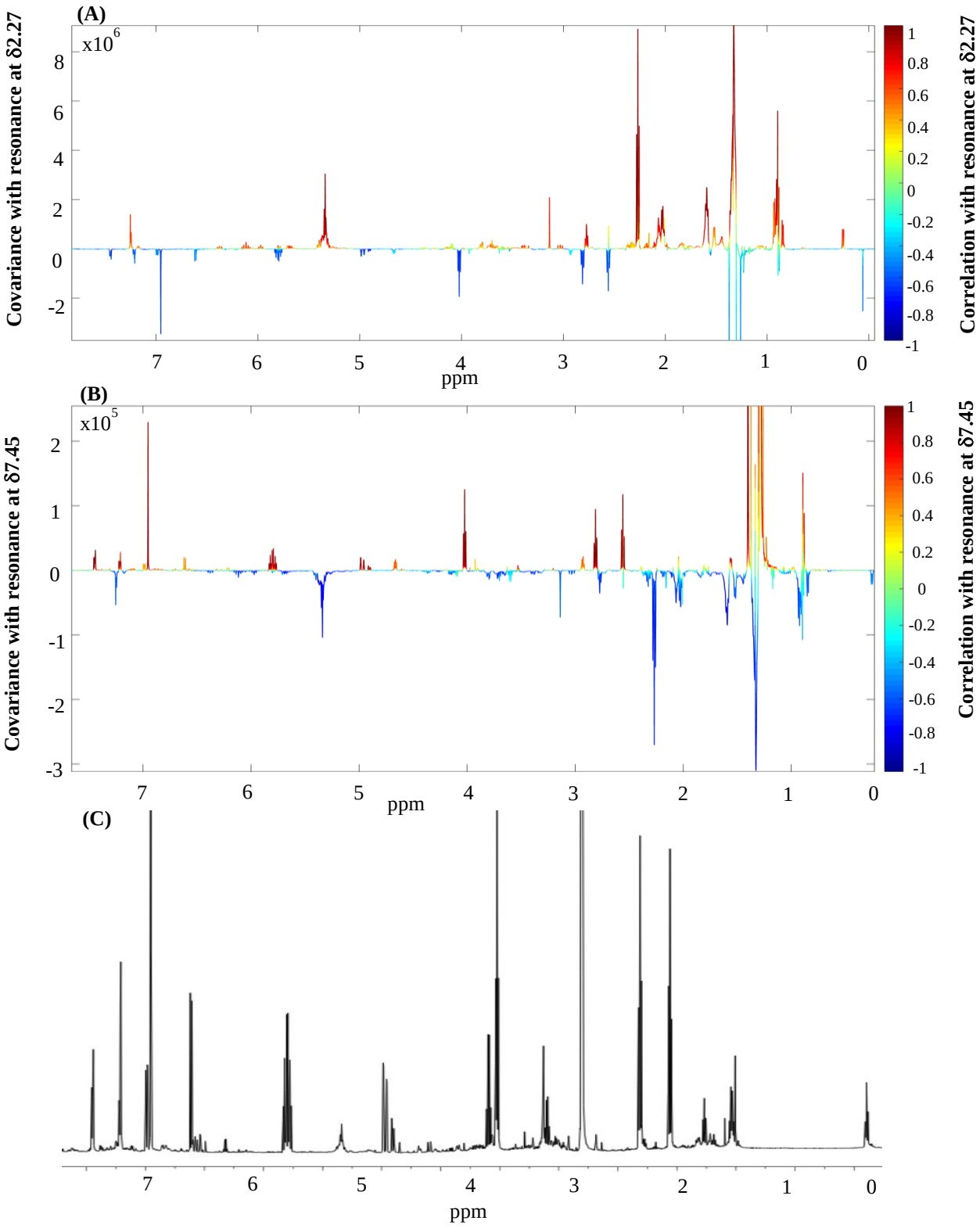

Figure 5.7. STOCY correlation and covariance of the signals from the Czapek metabolites found on the PLS-DA loading values. Signals correlated to **(A)** δ2.27 (*t*, *J* 7.4 Hz) and **(B)** δ7.45 (*dd*, *J* 8.2 and 2.2 Hz) were attributed to metabolites from the Czapek Broth. **(C)** ^{1}HNMR spectra of Czapek medium. Comparison between ^{1}HNMR spectra of Czapek and fungal cultures are displayed at the Supplementary Material as Figure SM11.

3.5.2. Diaporthe Metabolites

STOCSY experiments were performed for all signals extracted from the PC1 negative loading plot of the PLS-DA analysis and revealed two sets of chemical data, displayed in Table 5.5. The first chemical dataset was attributed to a metabolite derived from the Czapek medium (Figure 5.7B), present in all the co-culture and monoculture samples. For the second dataset, on the other hand, comparison between the STOCSY data and spectroscopic information from consolidated literature on *Diaporthe* metabolites did not suggested the presence of a known secondary metabolites, which indicate that this metabolite could be attributed to a compounds that is not produced under standard conditions.

Driver peak	**Correlated chemical shifts**	**Antimicrobial activity**	**Metabolite**
δ7.45 (*dd*, *J* 8.2 and 2.2 Hz)	δ7.21 (*d*, *J* 2.4 Hz, 1H), δ6.95 (*s*) δ5.80 (*ddt, J* 17.0, and 3.3 Hz) δ4.99 (*dd, J* 3.7 and 1.8 Hz) δ4.96 (*dd, J* 3.7 and 1.8 Hz) δ4.02 (*t*, *J* 6.6 Hz), δ2.81 (*t*, *J* 7.4 Hz), δ2.56 (*t*, *J* 7.4 Hz), δ2.04 (*d*, *J* 7.4 Hz), δ0.89 (*t, J* 6.9 Hz)	None: present in all samples	From the Czapek medium
δ7.31 (*d*, *J* 2.1 Hz, 1H)	δ7.09 (*dd*, *J* 9.7 and 5.5 Hz, 1H) δ6.89 (*m*) δ6.72 (*d*, *J* 2.7 Hz, 1H) δ6.63 (*d*, *J* 2.7 Hz, 1H) δ6.57 (*d*, *J* 2.2 Hz, 1H) δ6.22 (*d*, *J* 9.7 Hz, 2H) δ3.93 (*s*, 3H)	Moderate	Bisanthraquinone 1

Table 5.5. STOCY correlation of the chemical shifts found on the PLS-DA loading values for moderate antimicrobial activity. Molecules were elucidated in *D. eres* samples.

Evaluation of the ^{1}HNMR from the scrapped HPTLC band and the PLS-DA results showed the same chemical shifts found on the PC1 loading plot, correlated to moderate antibacterial activity, were also detected at the Rf 0.57 from the co-culture of *D. eres*/*C. acutatum* and *D. eres*/*A. alternata*, confirming that this compound was indeed only induced in co-cultures (Supplementary Material, Figure SM10B). Although the resolution between the bands was insufficient to be separated in a pure state, the semi-purified bands were successful elucidated by evaluation of 1D and 2D NMR data.

Uni and bidimensional NMR attributed the induced signals to a metabolite from the bisanthraquinone family. The chemical shits, their respective multiplicity and connectivities are shown in Table 5.6 and the proposed molecule is displayed in Figure 5.6B. Moreover, LC-MS analysis indicated an intense ion on *Diaporthe* co-cultures with experimental *m/z* 523.3232 $[M+H]^+$, which corroborated further with the proposed molecule.

N.	^{1}H (ppm)	^{13}C (ppm)	^{13}C-HMBC
1	–	-	-
2	δ6.89 (*m*, 2H)	141	-
3	δ6.28 (*m*, 1H)	-	-
4	-	117	
5''(OCH_3)	δ3.93 (*s*, 3H)	-	166
6	δ6.57 (*d*, *J* 2.2 Hz, 1H)	-	
7''(CH_2OH)	δ1.80 (*s*, 3H)	-	-
8	δ7.31 (*d*, *J* 2.1 Hz, 1H)	123	22, 98
9	-	54	-
10	-	-	-
1'	-	-	-
2'	δ6.63 (*d*, *J* 2.7 Hz, 1H)	-	-
3'	–	-	-
4'	δ6.72 (*d*, *J* 2.7 Hz, 1H)	-	81
5'	δ6.89 (m, 1H)	-	-
6'	–	-	-
7'	δ7.09 (*dd*, *J* 9.7 and 5.5 Hz, 1H)	-	132, 146, 156
8'	δ6.22 (*d*, *J* 9.7 Hz, 2H)	-	151, 91
9'	–	-	-
10'	–	-	-

Table 5.6. Molecule elucidation of newly induced secondary metabolite from *D. eres*.

Bisanthraquinones are produced in several species of *Diaporthe* and represent one of the major metabolic classes in this species (AGUSTA; OHASHI; SHIBUYA, 2006; BRADY et al., 2000; TIAN et al., 2018). Metabolites such as cytoskyrin A have been reported as anticancer

agents (BRADY et al., 2000), however, this induced compound has never been reported in nature nor has been biologically assessed. Evaluation of the antifungal and antimicrobial activity of this newly induced metabolite showed an moderate antibacterial activity against *S. aureus*, a strong antibacterial activity against *B. cereus* and a moderate antifungal activity against *F. oxysporum*, illustrating their selective bioactivity according to challenged microbe.

4. Conclusion

Solid cultivation was selected over liquid media for the screening of metabolite induction in fungal co-cultures for the following reasons: (i) provides a faster fungi growth and cheaper analysis than liquid media, (ii) allows visualization of the fungi morphological response (iii) facilitates excision of a part of the agar media for further chemical and biological analysis, (iv) enables selective analysis of the confrontation zone and adjacent mycelial parts (v) provides visual analysis of the fungus growth rate.

The first part of the co-culture strategy aimed to select promising pairwise culture by the metabolite extraction of antagonistic interactions. For that, the five selected fungi species were culture in pairs and the chemical profiles of the ones that displayed distance-inhibition and zone line interactions were evaluate by HPTLC. After the selection of promising co-cultures, the second step of the co-culture strategy was to evaluate the biotic parameters that affect the metabolite induction. In the last decade, it has been extensively reported that these biotic factors immensely affect the chemical profile in co-cultures and results in changes in the amount and diversity of secondary metabolite. In co-culture experiments, these variables are often neglected, resulting in issues related to sampling and reproducibility. In this study, to optimize the antimicrobial induction of the selected co-cultures, as well as address the analytical issues of microbial data, two strategies were applied to determine each strain is inducing the chemical enhancement and the best incubation period for the production of these induced metabolites.

Limitations in the analytical techniques encourages integration of methodologies. In this sense, HPTLC and NMR-metabolomics were an excellent alternative for the multivariate analysis of the microbial chemical profile. For instance, HPTLC presents several advantages, such as short measuring time, relatively low cost for equipment, high signal robustness and fast isolation directly from the plate. Supervised chemometric analysis of the co-cultures by PLS-DA led to the identification of **(1)** the up-regulated depsipeptide beauvericin in *Fusarium* co-cultures, a mycotoxin that displays high antibacterial activity against *S. aureus*, *P. fluorescens*, *E. coli* and strong antifunal activity agasint *C. acutatum*; and **(2)** the newly described

bisanthranquinone 1, produced by *D. eres* as a *de novo* bioshynthetized compound that displays high antibacterial against *B. cereus*, a moderate antibacterial activity against *S. aureus* and a moderate antifungal activity agasint *F. oxysporum*.

Although some features of our experimental system limit extrapolation of our results to the experience of wild fungi, our study has revealed some properties of these microbial interaction that likely have ecological relevance. First, each fungi species display fundamentally different responses in the presence of challenge strains, both in morphological patterns and specific chemical responses. These differences could influence the connectivity of these two strains within the microbial network in the wild. Second, the co-culture methodology provided an increase in the chemical diversity, as well as a selective increase in the antimicrobial activity. While co-culture with *F. oxysporum* increased the production of beauvericin in up to 3-fold, co-culture with *D. eres* induced the production of the bisanthraquinone 1, a induced metabolite not produced in monoculture.

CHAPTER 6. EXPANSION OF THE MICROBIAL METABOLOME - A SYSTEMS APPROACH TO IMPROVE BIOACTIVE METABOLITE PRODUCTION BY OSMAC AND ^{1}HqNMR

Article title: Improvement of Bioactive Metabolite Production in Microbial Cultures - A systems approach by OSMAC and ^{1}HqNMR.

Journal: Magnetic Resonance in Chemistry.

Status: Accepted.

Authors: Denise Medeiros Selegato[a], Rafael Teixeira Freire[b], Alan César Pilon[c], Carolina Rabal Biasetto[a], Haroldo Cesar de Oliveira[d], Lucas Magalhães de Abreu[e], Angela Regina Araujo[a], Vanderlan da Silva Bolzani[a], Ian Castro-Gamboa[a*]

Affiliations:

[a] *Nucleus of Bioassays, Biosynthesis and Ecophysiology of natural products (NuBBE), Organic Chemistry Depart., Institute of Chemistry, São Paulo State University (UNESP), St. Prof. Francisco Degni, 55, Quitandinha, Post code 14800-060, Araraquara, SP, Brazil.*

[b] *Medway Metabonomics Research Group, University of Greenwich, Post Code ME4 4TB, Chatham Maritime, Kent, UK.*

c Núcleo de Pesquisa em Produtos Naturais e Sintéticos (NPPNS), Faculdade de Ciências Farmacêuticas, São Paulo University (USP), Avenida do Café s/n, Monte Alegre, Post Code 14040-903, Ribeirão Preto, SP, Brazil.

[d] *Laboratório de Micologia Clínica, Núcleo de Proteômica, Faculdade de Ciências Farmacêuticas de Araraquara, São Paulo State University (UNESP), Rodovia Araraquara Jaú, Km 01 - s/n, Campos Ville, Post Code 14800-903, Araraquara, SP, Brazil.*

[e] *Departamento de Fisiopatologia, Universidade de Viçosa (UFV), Campus Universitário, s/n, Post Code 36570 000, Viçosa, MG, Brazil.*

Abstract

Traditionally, the screening of metabolites in microbial matrices is performed by monocultures. Nonetheless, the absence of biotic and abiotic interactions, generally observed in nature, may limit the chemical diversity produced by a strain, leading to "poorer" chemical profiles. During the last decade, several methods have been developed to understand the physiological conditions under which cryptic genes are activated in an attempt to induce the production of previously unexpressed metabolites. Among those, the One Strain Many Compounds (OSMAC) strategy has been successfully applied to increase metabolic production through a systematic variation of growth parameters. The complexity of the chemical profiles resulted from OSMAC application has required increasingly robust and accurate techniques for the quali- and quantitative evaluation of microbial matrices. In this sense, deconvolution-based ^{1}HNMR quantification strategies have emerged as a promising approach to decrease metabolic complexity, providing a comprehensive perspective for metabolomics studies. Our present work shows an integrated strategy for the rapid production and quantification of compounds from microbial sources. Specifically, the OSMAC-Design of Experiments (DoE) approach was used to optimize the production of bioactive compounds fusaric acid, cytochalasin D and 3-nitropropionic acid in microbial matrices and a deconvolution-based ^{1}HNMR quantification tool for their quantifications. The results showed that OSMAC-DoE increased the production of the target metabolites by up to 33% and that Global Spectral Deconvolution (GSD, MestreNova) was able to automatically extract accurate NMR integrals, even when the targeted chemical shifts were heavily coalescence with other resonances. Moreover, the GSD-based ^{1}HNMR quantification was not only reproducible for all species, but also exhibited validated results that were often more selective and accurate than comparative methods, allowing robust quantification directly in complex matrices, In general, this strategy proved to be useful for the up-regulation of metabolites using a reduced number of experiments and fast quantification of compounds directly in complex matrices.

Keywords: NMR, ^{1}H, ^{1}HNMR quantification, Global Spectral Deconvolution, post-genomic strategy, One Strain Many Compounds, secondary metabolite enhancement.

1. Introduction

Micro-organisms have shown a great potential to provide pharmaceutical leads (NEWMAN; CRAGG, 2016; PETTIT, 2009) given a high diversity of chemical structures are found in a little studied and extensive microbial population (BERGMANN et al., 2007; CHIANG et al., 2008; GALAGAN et al., 2005; HIBBING et al., 2010; SCHROECKH et al., 2009). In their most recent review, Newman and Cragg have shown that, even with the challenges related to unlocked genomes and unculturable strains, microbial bioactive compounds are the future for drug discovery programs (NEWMAN; CRAGG, 2016), accounting for over 42 thousand natural compounds already reported from different microbial families (LAATSCH, 2012).

Conventionally, the screening of these microbial metabolites has been performed in monocultures, in the absence of biotic and abiotic interactions commonly observed in nature. However, the lack of these interactions seriously limits the chemical diversity that can be obtained by one single strain, consequently decreasing the rate of discovery of new compounds (MARMANN et al., 2014; PETTIT, 2009). In fact, recent whole-genome sequencing of various fungi and bacteria have shown that the potential of microorganisms to produce bioactive compounds in monocultures is fairly underestimated, meaning that a much larger range of metabolites could be produced if the silent genes - not expressed in standard laboratory conditions - were induced (BERGMANN et al., 2007; CHIANG et al., 2008; GALAGAN et al., 2005; HIBBING et al., 2010; SCHROECKH et al., 2009).

Specifically, the interactions between the strains and the environment determine individual viability and community plasticity and are directly associated with the activation of a myriad of biosynthetic pathways, including those related to the expression of cryptic genes [6–9]. In the studies that evaluate these interactions, changes in the abiotic factors are mainly based in mimicking the environmental conditions in the succession of events that determine gene expression and, ultimately, affect the phenotypic response of organisms.

Among those, One Strain, Many Compounds (OSMAC) is one of the most used post-genomic strategies and involves the manipulation of culture parameters, such as media composition, temperature, agitation and luminosity, in an attempt to stimulate, in quantity and diversity, the production of secondary metabolites from a single microbial source (BODE et al., 2002; HUSSAIN et al., 2017; ROMANO et al., 2018; WEI et al., 2010). Usually, OSMAC uses Design of Experiments (DoE) to systematically evaluate

the effect of different growth parameters, estimating the optimized conditions for the production of new metabolites, as well as the regulation of known compounds (BRACARENSE; TAKAHASHI, 2014; OOIJKAAS et al., 1999; PIMENTA et al., 2010).

Although post-genomic strategies represent successful methodological advances in the expansion of the microbial metabolome, analytical issues related to the identification and quantification of metabolites in complex matrices remain a cornerstone in microbial natural products research. Some examples of difficulties encountered in microbial metabolic analysis include the constant re-isolation of inactive or known chemotypes, the polarity-related structural complexity and the wide metabolic dynamics, requiring highly sensitive and robust analytical methods (ITO; MASUBUCHI, 2014).

In microbial metabolomics, proton nuclear magnetic resonance (^{1}HNMR) is one of the most used analytical techniques for metabolic fingerprinting, providing a comprehensive and near-universal solution for metabolite detection and highly reproducible chemical data with minimal sample preparation (MARKLEY et al., 2017; PAULI et al., 2012). Quantitatively, NMR experiments also offer an unbiased view of the chemical composition, allowing rapid and non-destructive compound quantification and purity assessment (DAGNINO; SCHRIPSEMA, 2005; HOLZGRABE et al., 2005; LARIVE; JAYAWICKRAMA; ORFI, 1997).

Traditionally, the analysis and quantification of metabolites by ^{1}HNMR experiments are performed by direct comparison of the signal integrals values and the corresponding number of protons (for a given known chemical shift) between the samples and a standard reference. Over the past decade, challenges regarding the integration, area selection, baseline distortion and lack of appropriate shimming were successfully overcome by the development of technological advances, such as increased frequency and homogeneity of magnetic fields (up to 1 GHz), selective and robust pulse sequences for solvent suppression and sensitive cryoprobes, allowing metabolic quantification in standard solutions or simple mixtures, even without the presence of reference compounds (HOLZGRABE et al., 2005; RIZZO; PINCIROLI, 2005).

Currently, the problems related to chemical shift coalescence commonly found in microbial samples have further hindered the direct application of this technique in the metabolomics field (AKOKA; BARANTIN; TRIERWEILER, 1999; DAGNINO; SCHRIPSEMA, 2005; LARIVE; JAYAWICKRAMA; ORFI, 1997; SIMMLER et al., 2014; WATANABE; SUZUKI; OSHIMA, 2010; WIDER; DREIER, 2006). In this sense,

the incorporation of deconvolution algorithms have assisted with the detection and quantification of metabolites in complex mixtures, without the need for chromatographic separation and even in the presence of highly overlapping signals (PHANSALKAR et al., 2017; SIMMLER et al., 2014). Examples of efficient automatic spectra deconvolution tools are the Bayesian Automated Metabolite Analyzer for NMR (BATMAN) and Global Spectrum Deconvolution (GSD), although BATMAN requires some knowledge in the R package language (HAO et al., 2014), while GSD was conceptually not developed for quantification (COBAS; SEOANE; SÝKORA, 2008; COBAS; SYKORA, 2009).

Our present work shows an integrated strategy for the rapid optimization and monitoring of bioactive compounds in microbial sources. Specifically, we have selected important secondary metabolites from three fungal families (Nectriaceae, Xylariaceae and Diaporthaceae) aiming to up-regulate and quantify their production in these complex matrices. For the regulation of the microbial metabolome, we have systematically varied temperature, agitation and luminosity by a OSMAC-Design of experiment. Following, metabolite monitor was conducted by a deconvolution-based ^{1}HNMR quantification methodology using Global Spectral Deconvolution (GSD) algorithm. The OSMAC-DoE response was carried out using two different chemical responses. The first used the mean value of the raw extract and contained information relative to the untargeted metabolic production. The second used the content of each targeted bioactive metabolites (purity, %), aiming to show in each abiotic condition occurs the highest up-regulation of these bioactive compounds, regardless of the fungal growth rate.

2. Material and Methods

2.1. Fungi Isolation and Identification

Fungi from the Nectriaceae, Xylariaceae and Diaporthaceae families were cultured in Czapek-Broth ($NaNO_3$, 1.5 g L^{-1}; KH_2PO_4, 0.5 g L^{-1}; $MgSO_4$, 0.25 g L^{-1}; $FeSO_4.7H_2O$, 0.025 g L^{-1}; KCl, 2.5 g L^{-1}; and D-glucose, 30.0 g L^{-1}) and their mycelia were filtered and freeze-dried with liquid nitrogen for genetic identification. *Fusarium oxysporum* was isolated from the rhizosphere of *Senna spectabilis* cultured on sand hydroponics (CARDOSO, 2015), while *Xylaria cubensis* and *Diaporthe anacardii* were isolated from the leaves of *Eugenia brasiliensis* according to previously reported isolation methods (BIASETTO, 2016).

Molecular identification was done by analysis of the Internal Transcribed Spacer (ITS) sequence. After isolation, the DNA was amplified by polymerase chain reaction (PCR) using the primers ITS1 (5'-CTTGGTCATTTAGAGGAAGTAA-3') and ITS4 (5'-TCCTCCGCTTATTGATATGC-3'). Following, the PCR products were sequenced using fluorescent dideoxynucleotides based on the a modified Sanger method (SANGER; NICKLEN; COULSON, 1977) in an automated sequencer ABI Prism 3130 (Applied Biosystems, USA) and BigDye® Terminator v3.1 Cycle sequencing kit (Applied Biosystems, USA). The sequences were compared with others available in GenBank using the Basic Local Alignment Search Tool (BLASTn) algorithm (ALTSCHUL et al., 1997). The identification results available at the Supplementary Material as Table SM3.

2.2. Fungal growth – One Strain, Many Compounds (OSMAC)-based Design of Experiment (DoE)

Strains of the selected fungi were inoculated separately following a complete factorial design, in which temperature, agitation and luminosity were evaluated in two different levels, totaling 8 experiments (3 variables tested in 2 levels, $2^3 = 8$ experiments). The systematic variation of the growth parameters is described in Table 6.1 and all the variables were controlled by a microbiological incubator with an orbital shaker (Solab, Brazil). The OSMAC-DoE experiments were performed in biological triplicate to ensure experimental reproducibly, in which the same fungal pre-culture was used to inoculate all erlenmeyer sets.

Microbial species	**Variable n.**	**Variable description**	**Levels**	
			Low (-1)	**High (1)**
F. oxysporum	1	Luminosity	Absent	24hrs
	2	Agitation	Absent	110 rpm
	3	Temperature	14°C	25°C
X. cubensis	1	Agitation	Absent	110 rpm
	2	Luminosity	Absent	24hrs
	3	Temperature	25°C	35°C
D. anacardii	1	Agitation	Absent	110 rpm
	2	Luminosity	Absent	24hrs
	3	Temperature	25°C	35°C

Experiments	V1	V2	V3
1	-1	-1	1
2	-1	1	1
3	1	-1	1
4	1	1	1
5	1	-1	-1
6	-1	1	-1
7	1	1	-1
8	-1	-1	-1

Table 6.1. Variables and experimental display of OSMAC complete factorial planning for each selected fungi *F. oxysporum*, *X. cubensis* and *D. anacardii*. Each OSMAC-experiment was performed in triplicate.

First, the fungal pre-cultures for *F. oxysporum* and *D. anacardii* were plated using a high cell number (1.10^6 cells ml^{-1}) in 20 mL of Czapek-agar (Sigma Aldrich, Brazil). For *X. cubensis*, the same account of pre-inoculum was added in 20 mL of Potato Dextrose Agar (PDA, Sigma Aldrich, Brazil).

	Liquid Media	Incubation Period (days)	Description	Ref.
F. oxysporum	Czapek	28	- carbon-rich and free amino acid media. - glucose, as source of carbon, yeast extract nitrogen and a neutral pH.	(BACON et al., 1996; BURMEISTER et al., 1985; SELEGATO et al., 2016b)
X. cubensis	PDB	28		(AMARAL et al., 2014; CAFÊU et al., 2005; CHEN et al., 2011; KLAIKLAY et al., 2012; WEI et al., 2015)
D. anacardii	PDB at neutral pH or Czapek	8		(CHOMCHEON et al., 2005; FLORES et al., 2013; LU et al., 2015; POLONIO et al., 2016; PRINCE et al., 2012)

Table 6.2. Determination of best abiotic conditions for growth of each selected fungus. Selection was based on previous optimization studies in liquid media. Description contains the b**es**t media conditions found on literature for the production of the targeted metabolites.

Following, for each DoE replicate, a 7 mm agar plug of this selected fungus was inoculated in three erlenmeyer flasks containing 300 mL of culture medium each (Sigma Aldrich, Brazil). In this procedure, *F. oxysporum* and *D. anacardi* were inoculated in Czapek-broth (Sigma Aldrich, Brazil), whereas *X. cubensis* was added to Potato Dextrose Broth (PDB, Sigma Aldrich, Brazil). Prior to inoculation, the medium was autoclaved at 121°C for 20 minutes. Incubation time was also specfic for each strain and was determined based on previous optimization studies, displayed in Table 6.2. For the metabolite extraction, we used the same protocol describied in Chapter 1 (topic 2.3).

2.3. Bioactive Metabolite Quantification

2.3.1 ^{1}HNMR Parameters Optimization and Acquisition

All OSMAC-DoE organic extracts (after extraction and clean-up treatment) were submitted to ^{1}HNMR acquisition for the quantification of the selected bioactive compounds. The spectra were acquired on a Bruker Ascend III HD of 14.09 Tesla spectrometer (Bruker, Germany) using a triple resonance cryoprobe (^{1}H, ^{13}C and ^{15}N) and gradient generator coils at the Z coordinate. *F. oxysporum* samples were prepared by dissolving 3.00 ± 0.1 mg of each extract and 4.50 mM of benzyl benzoate in 750 µL of dimethyl sulfoxide-d_6 (DMSO 99.9% D, Sigma-Aldrich, USA). Similarly, *D. anacardii* and *X. cubensis* samples were prepared solubilizing 3.00 ± 0.1mg from each OSMAC experiment and 3.00 mM of benzyl benzoate in 700 µL of deuterated methanol-d_4 (MeOD 99.9% D, Sigma-Aldrich, USA).

The optimization of ^{1}HNMR parameters was performed according to the reported methods (HONG et al., 2013; PAULI; JAKI; LANKIN, 2005; SIMMLER et al., 2014). Before acquisition, the probe tuning, matching and shimming were manually setup. Then, the pulse was calibrated using the *pulsecal* sequence (Bruker). A 90^{o} pulse sequence (zg, Bruker) was applied to determine the spectral width (SW, Bruker) and chemical shift value for the suppression of the remaining water signal (O1, Bruker). The amount of internal standard (IS) included was evaluated using a range of concentrations (1, 2, 4, 6, 8 and 10 mM) for each individual sample. Longitudinal relaxation (T1) was estimated by inversion-recovery pulse sequences at incremented delay times (D7, Bruker) and final selective pulse (zg, zgesgp, or zgcppr) was applied for quantification acquisition after receiver gain (RG, Bruker) and number of scans optimization (NS, Bruker).

The inversion-recovery method was performed with a calibrated pulse and initiated with a single acquisition using a null time between the 180° and 90° pulses (d7 0s and NS 1). Simultaneous spectra were acquired with incremented values of d7 up to intensity reach values close to zero for all signals of interest. Depending on signal of the analytes and IS (negative or positive), d7 was increased or decreased. For every spectrum, we considered at least (7.2s d7) between acquisitions. T1 was estimated according to Equation 1, in which τnull represents the minimum time required for the longitudinal magnetization to reach thermal equilibrium (pass in the x-y planes during its recovery).

$$\mathrm{T1} = \frac{\tau_{null}}{\ln 2} = 1.44\tau_{null}$$

Equation 1. T1 Estimation.

Relaxation delay (d1) was set based on the T1 estimated value and the acquisition time (AQ), according to Equation 2. The FID repetitions (number of scans) was optimized manually until all the targeted chemical shifts exhibited a suitable signal-to-noise ratio (S/N > 250), assuring with 99% certain that the measured integral falls within + 1% of the true values (at least 5T1).

$$\mathrm{d1} = 5\mathrm{T1} - \mathrm{AQ}$$

Equation 2. Estimation of relaxation delay (d1).

For *F. oxysporum* samples, water suppression was performed by gradient-based 1D excitation sculpting using a 180° water-selective pulse (zgesgp, Bruker) at the following parameters τnull 1.0 s; T1 1.443 s; pulse duration (P1) 6.88 μs; time domain (TD) 64 k; NS 16; SW 13 ppm; o1 δ 4.88; temperature 296.2 K; relaxation delay (d1) 2 s, inter-pulse delay (d2) 24 μs; and dummy scans (DS) 4. Excitation sculpting water suppression used a double pulse-field gradient spin echo methodology, producing excellent suppression (square of the single method) during ^{1}HNMR acquisition.

For *X. cubensis* samples, water suppression was performed by 1D-water pre-saturation using composite pulses (zgcppr, Bruker) at the following parameters τnull 4 s; T1 5.772; P1 6.59 μs; TD 64 k; NS 32; SW 10 ppm; temperature 296.2 K; d1 2 s; inter-pulse delay (d2) 24 μs; o1 δ 4.88 (s), DS 4. In this case, water presaturation was performed by a composite pulse instead of excitation sculpting pulse to prevent the broader notch

bandwidth near the water peak caused by the latter, hampering proper quantification of cytochalasin D chemical shifts at δ 5.18 (*d*, *J* 2.5 Hz, 1H, H-19), δ5.12 (*s*, 1H, H-12β) and δ 5.23 (*m*).

For the quantification of nitropropionic acid on *D. anacardii* samples, zg pulse sequence (Bruker) was performed at the following parameters τnull 2 s; T1 2.882; P1 6.46 μs; TD 64 k; NS 32; SW 10 ppm; temperature 296.2 K; o1 δ 4.88 (*s*); d1 2 s; d2 24 μs; DS 4. A simple 30° pulse was used for *D. anacardii* ^{1}HNMR acquisition because the 3-NPA chemical shift at δ 4.67 (*t*, *J* 6.0 Hz, 2H, H-3) could not be quantified after water suppression, given the closeness to the water signal at δ 4.88 (*s*).

2.3.2. ^{1}HNMR Deconvolution – Global Spectral Deconvolution (GSD)

Initially all ^{1}HNMR data are referenced by the solvent signal and phase corrected manually. Then, proton NMR deconvolution was performed by Global Spectral Deconvolution (GSD) algorithm, available at MestreNova software (MestreLab, Spain) (COBAS; SEOANE; SÝKORA, 2008; COBAS; SYKORA, 2009). GSD is a fully automatic peak picking tool that filters relevant information and deconvolutes metabolite signals while discarding undesirable interferences of the ^{1}HNMR spectrum. This algorithm automatically reduces the frequency domain spectrum to shape Lorentzian lines without any baseline drift and noise interference.

In this procedure, GSD first recognizes, by a peak picking recognition algorithm, the set of signals, eliminating baseline distortions, spikes, environmental radiofrequency (RF) and receiver noise. Then, the recognized signals are corrected in relation to inhomogeneity of magnetic field, molecular dynamics, theoretical transitions, peaks overlapping and artifacts (rotational sidebands).

The output of GSD is a final numerical peak table that contains spectral parameters for Lorentzian lines, including frequency, line width, amplitude, area and, phase, which are plotted as a ‘‘peak list’’ created by a synthetic deconvoluted spectrum (BERNSTEIN et al., 2013; COBAS; SEOANE; SÝKORA, 2008; COBAS; SYKORA, 2009). In this study the GSD algorithm was optimized using 10 fitting cycles (refinement level 3) and high resolution. These parameters were individually optimized based on noise, baseline and resolution of each spectrum.

2.3.3. ^{1}HNMR Quantification

The quantification was performed by comparing the integrals of the bioactive secondary metabolite with the internal reference added to the samples. For this procedure, an optimized amount of internal standard benzyl benzoate TraceCERT > 99% (Fluka Analytical, Sigma-Aldrich) was used in all OSMAC-DoE experiments. The selection of this IS was based on requirements, such as (i) stability in the deuterated solvent, (ii) not to be reactive, hygroscopic, volatile, toxic, carcinogenic or mutagenic (iii) not to have any residual water marks and (iv) appear in a region of the spectrum deconvoluted from other signals.

Quantification was measured using the GSD-deconvoluted area values of all the targeted secondary metabolites according to Equation 3, where mg_{target}, PA_{target} and ME_{target} represent the analyte's mass, peak area and equivalent mass (molecular mass divided by the number of nuclei associated with the quantified signal), respectively, while $mg_{internal\ std.}$, $PA_{internal\ std.}$ and $ME_{internal\ std.}$ represent the internal standard's mass, peak area and equivalent mass (PAULI et al., 2014).

$$mg_{target} = \frac{PA_{target}\ x\ ME_{target}\ x\ mg_{internal\ std.}}{ME_{internal\ std.}\ x\ PA_{internal\ std.}}$$

Equation 3. ^{1}HNMR quantification using known concentration of internal standard.

2.3.4. Validation of GSD-based ^{1}HNMR Quantification Methodology

The ^{1}HNMR quantification protocol was validated by evaluation of selectivity, metabolite stability, precision, accuracy and linearity response, according to previously described ^{1}HNMR validation protocols (MALZ; JANCKE, 2005).

The selectivity was evaluated for all quantified signals on a ^{13}CHSQC spectrum. The pulse sequence used for two dimensional NMR analysis was phase-sensitive ge-2D multiplicity edited ^{13}CHSQC using PEP and adiabatic pulses with gradients in back-inept (hsqcedetgpsisp2.4, Bruker) at the following parameters for ^{1}H (f2) and ^{13}C (f1), respectively: spectrometer frequency 600.13 and 150.91 MHz; TD 512 and 512; SW 14 and 230 ppm; NS 32; d1 1.50 s and temperature 295.2 K.

Metabolite short term stability was evaluated over a 48-hour period by multiple ^{1}HNMR acquisition of the lowest concentration sample, every 2 hours, to determine loss

by degradation. Similarly, precision was determined by six measurements of ^{1}HNMR in a short period of time, systematically changing specific parameters such as operator, automation and time.

Accuracy was evaluated by the measurement of the internal standard concentration by GSD-based ^{1}HNMR quantification, as well as three other validated methodologies **(1)** gravimetric, **(2)** classical approach of internal standard-based quantification using area values from manual integration (IS-^{1}HqNMR) (RUNDLOF et al., 2010) and **(3)** Electronic Reference To access *In vivo* Concentrations 2 (ERETIC2) tool from Bruker (ERETIC2-^{1}HqNMR). ERETIC2 is a commercial PULCON (Pulse Length–based Concentration determination) methodology that digitally adds reference signals by an electronic device, enabling determination of absolute concentrations (AKOKA; BARANTIN; TRIERWEILER, 1999; HONG et al., 2013; WATANABE et al., 2016). In this study, the ERETIC2 reference signal was based on sucrose standard from Bruker (2 mM) prepared in 10% D_2O and 90% H_2O solvent are was digitally added in the spectra using TopSpin software (Bruker).

The linearity of the calibration curve was assessed using a calibration curve of different concentrations of IS benzyl benzoate. This metabolite was selected after careful consideration on reactivity, miscibility and peak convolution and the calculation was based on the singlet area at δ5.32 (*s*, 2H, CH_2, H-8). Calibration standard solutions of five concentration levels were prepared in deuterated organic solvent at concentrations of 1, 2, 4, 10 and 20 mM.

2.4. OSMAC-DoE response

All the extracts from the OSMAC-experiments were weighted and submitted to ^{1}HNMR quantification analysis. The OSMAC-DoE response was carried out using two different datasets. The first used the mean value (in mg) of the raw extract obtained from each DoE experiment, which contains information relative to the fungal growth and overall metabolic production. The second used the purity of each targeted bioactive metabolites in the OSMAC-crude extract, calculated according to Equation 4, aiming to demonstrate the effect of the abiotic conditions (variables) on the up-regulation of the targeted compounds, regardless of the fungal growth rate. Statistically compelling effects were calculated at 95% confidence level, and only effects above the critical *t* values were considered significant for the system response.

$$\text{P (\%)} = \frac{Targeted\ metabolite\ concentration}{\text{Raw} - \text{extract mass}}\ x\ 100$$

Equation 4. Determination of the purity (P, in %) of the targeted analytes.

3. Results and Discussion

In order to facilitate the visualization of the proposed strategy for the optimization and quantification of microbial bioactive compounds, we have delineated a graphical scheme, shown in Figure 6.1. In the following sections, we describe in detail the workflow of this methodology, which includes the selection of the microbial strains and the bioactive compounds (step 1), fungal growth and production of target compounds by a OSMAC-DoE strategy, and metabolite quantification by GSD-based ^{1}HNMR quantification (step 2) and the selection of optimized parameters for the metabolic production by OSMAC-DoE (step 3).

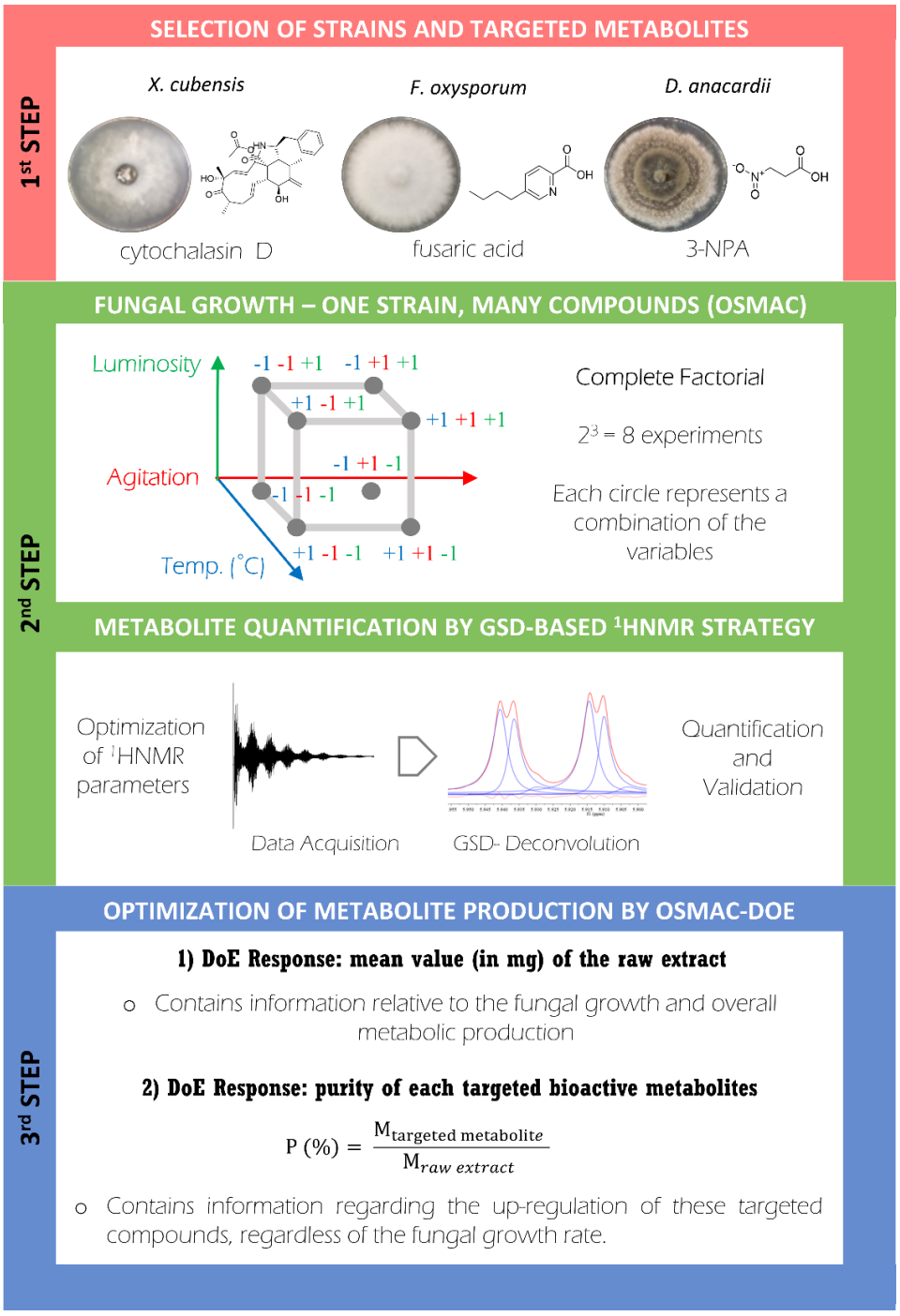

Figure 6.1. Graphical visualization of the integrated OSMAC-DoE with GSD-based ^{1}HNMR quantification strategy. In the first step were selected strains based on the most relevant bioactive compounds previously described in literature (*X. cubensis* - cytochalasin D, *F. oxysporum* - fusaric acid and *D. anacardii* - 3-NPA). The second step consisted on the fungal growth by a OSMAC-DoE strategy, followed by metabolite extraction and quantification by deconvolution-based ^{1}HNMR quantification. The third step was the selection of optimized parameters for the metabolic production using different datasets as OSMAC response.

1st Step - Selection of Fungal Strains and Bioactive Compounds

The first step of this strategy was the selection of bioactive compounds from microbial sources. The selection was based on the most common plant-associated fungi that produced biologically important bioactive metabolites. In this study, we have selected fusaric acid, cytochalasin D and 3-nitropropionic acid (NPA), produced by *F. oxysporum*, *X. cubensis* and *D. anacardii*, respectively. These metabolite are abundantly produced by these strain and display and different chemical properties and biosynthetic pathways.

F. oxysporum is a filamentous fungus that produces several pathogenic mycotoxins including trichothecenes, enniantins and fumosinin. Among these, fusaric acid (5-butylpyridine-2-carboxylic acid) is a polyketide and picolinic acid derivative abundantly produced under different growth conditions, displaying a variety of bioactivity, including antifungal, antioomycete, antimicrobial and herbicidal activities (HAN et al., 2014; SON et al., 2008; SONG; YEE, 2001). Economically, this metabolite has been directly associated with *Fusarium* wilt, a trans-boundary disease which affects different crops world-wide, such as sugarcane, potatoes, bananas and tomatoes, causing cracks in the tree stalk, leaf breakage, leaf yellowing, necrosis and death, summing hundreds of millions of dollars in production losses (MICHIELSE; REP, 2009).

Likewise, *X. cubensis* has been reported to produce a variety of bioactive compounds, such as cytochalasins, xanthones, cyclopeptides, α-pyrones and terpenes, in which cytochalasin D, also known as zygosporin A and lygosporin A, is a bactericidal, antitumoral, antifungal and phytotoxic agent that has been extensively studied with regard to its ecological and biological significance (CAFÊU et al., 2005; CHAPLA; BIASETTO; ARAUJO, 2013; WAGENAAR et al., 2000; WEI et al., 2015).

Lastly, the endophytic *D. anacardii*, also known as *Phomopsis anacardii* in its asexual form, is a filamentous fungus that produces 3-nitropropionic acid as major metabolite. This compound, although a small molecule, displays a large range of biological activities including nematicidal action, antibacterial activity against *Mycobacterium tuberculosis* and neurotoxicity (BROWNELL et al., 2004; CHOMCHEON et al., 2005; SCHWARZ et al., 2004).

2nd Step - Quantification of Bioactive Compounds by GSD-based 1HNMR quantification

Following the selection of the fungal strains and the bioactive compounds, an OSMAC-DoE approach was applied for each fungus to systematically vary their growth parameters and induce changes in the chemical outcome. The experimental design was based on a complete factorial design, in which temperature, agitation and luminosity were systematically varied in two different levels. After the incubation period, the same-sized mycelia were vacuum filtered and the aqueous supernatant extracted with organic solvent (ethyl acetate). The resulting organic extracts for all DoE experiments were evaporated to dryness, weighted and submitted to ^{1}HNMR analysis according to the optimized acquisition parameters.

The ^{1}HqNMR spectra for all three fungi revealed the high complexity of the chemical data, as well as significant changes in the chemical profile according to the OSMAC experimental conditions. Overall, *F. oxysporum* showed most characteristic signals in the aliphatic (δ 1-3) and highly deshielded aromatic (δ 7-9) regions, while *X. cubensis* and *D. anacardii* displayed high signal abundance on both the aromatic (δ 6-7) and olefinic spectral (δ 4-6) regions.

After fingerprinting analysis, the targeted metabolites were evaluated in each OSMAC-DoE experiment by an active search of their chemical shifts, signal multiplicity and coupling constants. Moreover, for every experiment in which the chemical data indicated the presence of the targeted metabolites, confirmation was performed by 2DNMR experiments, including connectivity studies by ^{13}CHSQC, ^{13}CHMBC, COSY and TOCSY. For fusaric acid and cytochalasin D, found in *F. oxysporum* and *X. cubensis*, respectively, the targeted chemical shifts were majorly isolated from the other signals, whereas 3-NPA triplets from *D. anacardii* appeared completely convoluted. All ^{1}HNMR spectra for the three fungi strains, assigned chemical shift tables of the bioactive compounds and their connectivities are available at the Supplementary Materials as Table SM4-SM6 and Figure SM12-SM15.

Following ^{1}HNMR acquisition, GSD deconvolution algorithm were applied providing the area of the signals related to the target metabolites. Manual integration was also performed as a method comparison. For fusaric acid and cytochalasin D, the integrals values between manual integration and GSD revealed no significant differences, given that most of the chemical shifts were isolated or slightly convoluted (Figure 6.2).

However, for 3-nitropropionic acid, the signals were completely convoluted and only with GSD algorithm was possible to estimate the integral values (Figure 6.2). In this case, the deconvolution was fundamental not only for the adjustment of areas values, but for confirmation of metabolite, i.e., the assignment of multiplicity and coupling constants. Figure 6.2 shows the results of both GSD algorithm (blue) and manual integration (red) for all three strains. It is possible to observe that values obtained of GSD were similar with manual integration data, in cases where the chemical shifts were isolated or partly, and different in situation where presence of overlapped signals was prominent. All individual GSD-deconvoluted peaks superimposed with the experimental spectrum are available at the Supplementary Materials as Figures SM16-SM18.

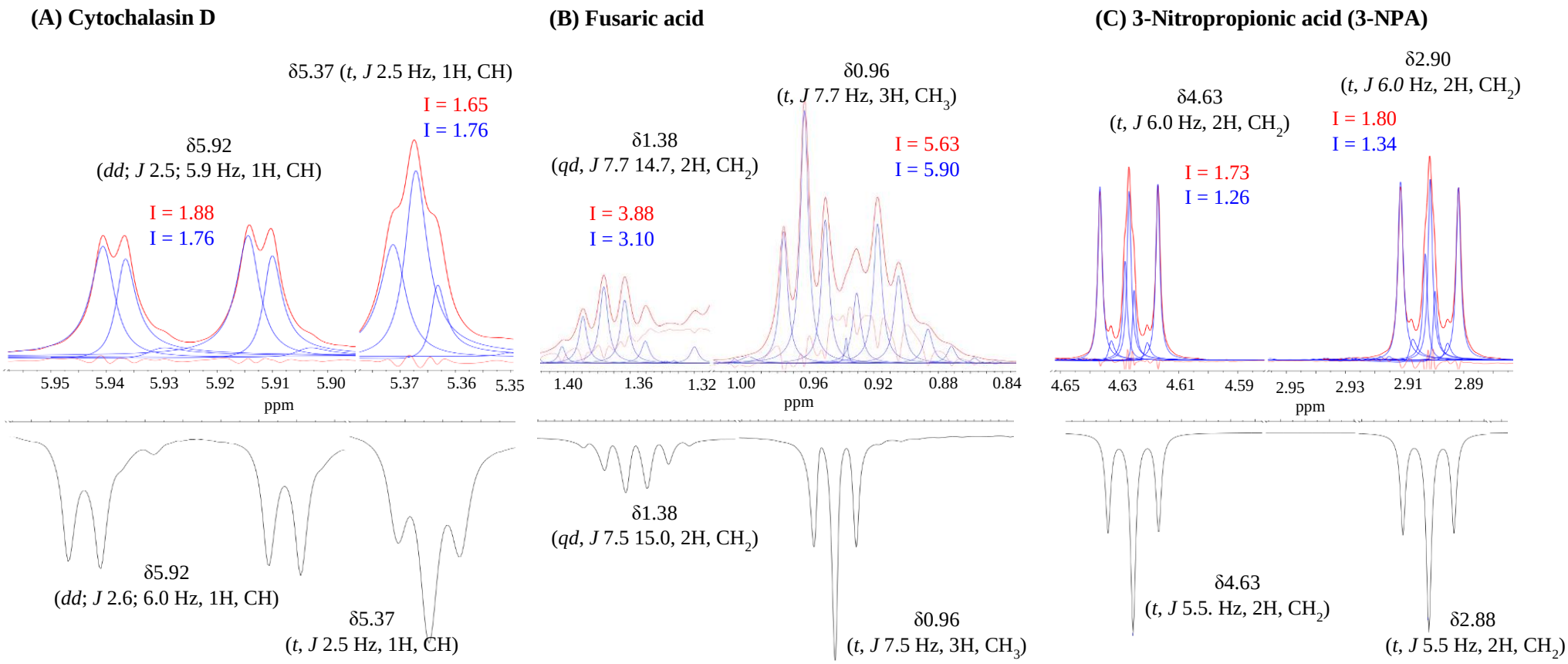

Figure 6.2. Illustration of the deconvolution protocol for the target chemical shifts of **(A)** cytochalasin D, **(B)** fusaric acid, **(C)** 3-nitropropionic acid. The chemical shifts of the bioactive metabolites from the fungal ^{1}HNMR spectra are displayed in red. The deconvoluted GSD spectra are shown in blue. The standard spectra for the targeted metabolites are demonstrated in black.

Quantification of the targeted metabolites was performed using the area values provided by the GSD algorithm and was based on the comparison between the chemical shifts from the analytes and the internal standard. We have also compared the GSD method with two others consolidated ^{1}HNMR quantitative methodologies in order to evaluate the improvements of the use of deconvolution-area values in the method's accuracy, selectivity and precision. The methodologies used for comparison were applied for the three selected metabolites in every OSMAC-experiments and consisted on the classical approach (1) using internal standard-based quantification and area values from manual integration (IS-^{1}HqNMR) (RUNDLOF et al., 2010) and (2) the Electronic Reference To access *In vivo* Concentrations 2 (ERETIC2) tool available in Topspin Bruker (ERETIC2-^{1}HqNMR) (AKOKA; BARANTIN; TRIERWEILER, 1999; HONG et al., 2013; WATANABE et al., 2016).

The quantification results using all ^{1}HNMR strategies have shown low standard deviation between the replicates, which ensures the reproducibility between the sample triplicates (Figure 6.3). However, for GSD-based ^{1}HNMR quantification, this high reproducibility is particularly important given that all chemical shifts from the targeted metabolites were deconvoluted and considered for quantification in every sample replicate. Owing to the need for isolated signals for the manual integration quantification method, the GSD deconvolution offers a greater benefit since that provides a larger number of signals that can be used for quantification, which also increases the selectivity of this strategy.

Chemical analysis of *F. oxysporum* and *X. cubensis* have shown that most chemical shifts from the targeted analytes were isolated in the spectra, resulting in similar area values by GSD and manual integration. Therefore, the results obtained by GSD-based ^{1}HNMR quantification were similar to those obtained by IS-^{1}HqNMR and ERETIC2-^{1}HqNMR (Figure 6.3), often exhibiting the results that are the mean values of both comparative methods. For *D. anacardii*, on the other hand, high signal coalescence hampered accurate metabolite quantification by manual integration and ERETIC approaches and only after GSD-deconvolution, the area values of 3-NPA were well-adjusted for quantification (Figure 6.3). In this case, GSD-based ^{1}HNMR quantification outperformed the others methods both in selectivity, due to the higher number of quantified chemical shifts, accuracy and precision by the use of adjusted-area values, allowing quantification of signals even in complex crude extracts.

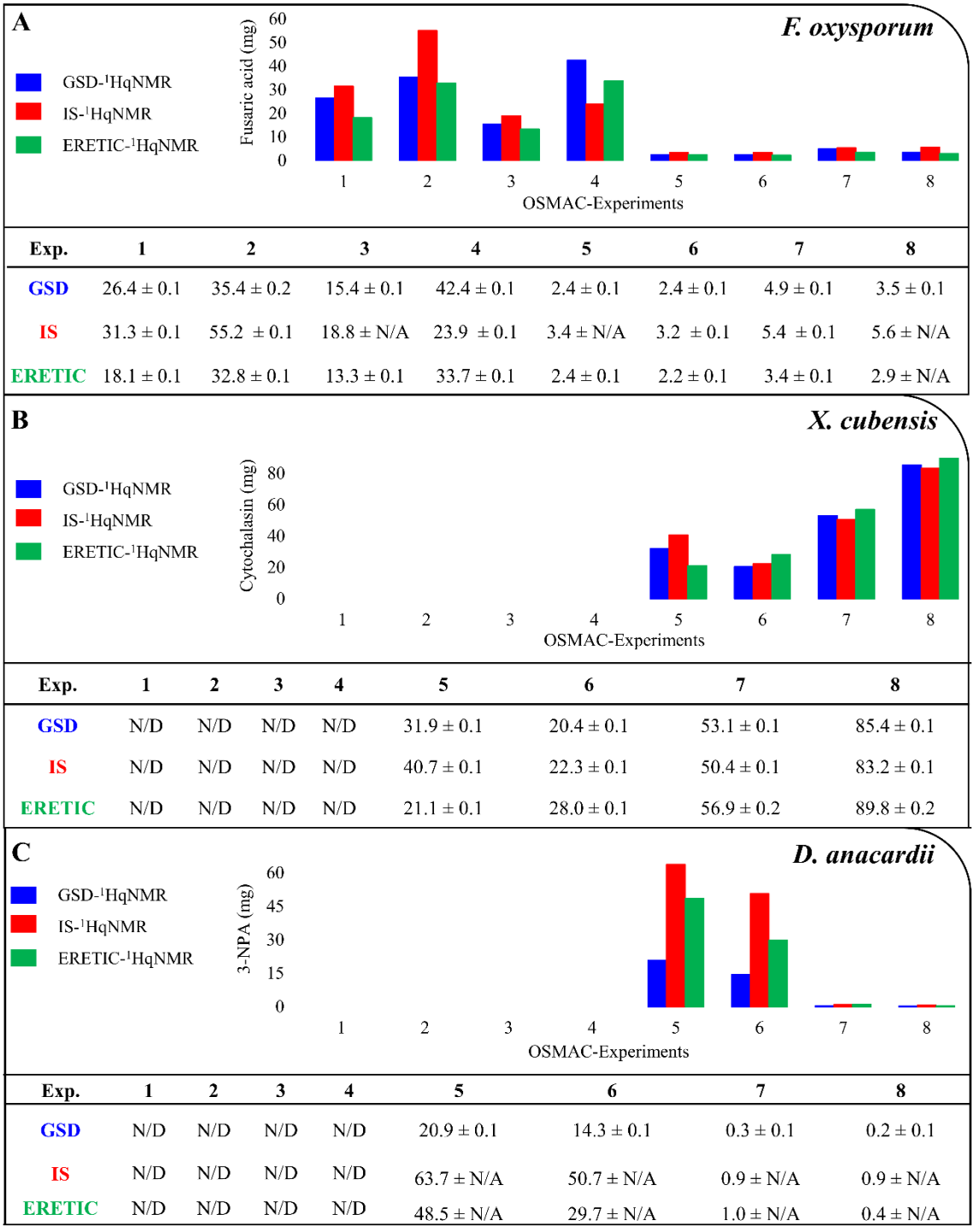

Exp.	1	2	3	4	5	6	7	8
GSD	26.4 ± 0.1	35.4 ± 0.2	15.4 ± 0.1	42.4 ± 0.1	2.4 ± 0.1	2.4 ± 0.1	4.9 ± 0.1	3.5 ± 0.1
IS	31.3 ± 0.1	55.2 ± 0.1	18.8 ± N/A	23.9 ± 0.1	3.4 ± N/A	3.2 ± 0.1	5.4 ± 0.1	5.6 ± N/A
ERETIC	18.1 ± 0.1	32.8 ± 0.1	13.3 ± 0.1	33.7 ± 0.1	2.4 ± 0.1	2.2 ± 0.1	3.4 ± 0.1	2.9 ± N/A

Exp.	1	2	3	4	5	6	7	8
GSD	N/D	N/D	N/D	N/D	31.9 ± 0.1	20.4 ± 0.1	53.1 ± 0.1	85.4 ± 0.1
IS	N/D	N/D	N/D	N/D	40.7 ± 0.1	22.3 ± 0.1	50.4 ± 0.1	83.2 ± 0.1
ERETIC	N/D	N/D	N/D	N/D	21.1 ± 0.1	28.0 ± 0.1	56.9 ± 0.2	89.8 ± 0.2

Exp.	1	2	3	4	5	6	7	8
GSD	N/D	N/D	N/D	N/D	20.9 ± 0.1	14.3 ± 0.1	0.3 ± 0.1	0.2 ± 0.1
IS	N/D	N/D	N/D	N/D	63.7 ± N/A	50.7 ± N/A	0.9 ± N/A	0.9 ± N/A
ERETIC	N/D	N/D	N/D	N/D	48.5 ± N/A	29.7 ± N/A	1.0 ± N/A	0.4 ± N/A

Figure 6.3. Quantified values of (a) fusaric acid in *F. oxysporum*, (b) cytochalasin D in *X. cubensis* and (c) 3-nitropropionic acid in *D. anacardii* through the OSMAC-DoE strategy. The results were divided according to the ^{1}HNMR quantification methods: GSD-based ^{1}HNMR quantification, IS-^{1}HqNMR and ERETIC2-^{1}HqNMR. The amount of target metabolites was calculate as the mean value of the replicates (mg) ± their standard deviation. N/D (not detected) and N/A (not applied).

The OSMAC-experiments of *X. cubensis* and *D. anacardii* have not displayed any detected chemical shifts for the targeted metabolites in experiments conducted in high temperature, indicating an absence of their production under this condition (Figure 6.3). However, for *D. anacardii*, OSMAC-experiments carried out at 35°C displayed a small production of cytochalasin D, which indicates the immense potential of these microbial matrices to expand their metabolome according to the environmental conditions. The GSD-based ^{1}HNMR quantification protocol was validated and the results of selectivity, metabolite stability, precision, accuracy and linearity are showed in the Supplementary Material, Figures SM19-SM21 and Table SM16. Moreover, quantification results of the bioactive metabolites in all OSMAC experiments using different NMR methodologies are detailed in the Supplementary Materials as Tables SM7-SM15.

3rd Step - Optimization of Bioactive Compounds Production by OSMAC-DoE

After the application of the GSD-based ^{1}HNMR quantification, the last step of the strategy was to use these results as a response in the OSMAC-DoE, aiming to evaluate in which growth conditions occurs the highest up-regulation of the bioactive compounds. For this procedure, a complete 2^3 factorial design were carried out using two different responses (Table 6.3). The first used the mean value (in mg) of the crude extracts obtained from each OSMAC-DoE experiment and contains information on the fungal growth, i.e., the overall up-regulation of "all compounds" in the same time. The second uses the purity percentage value (metabolite content) of each target bioactive metabolites revealing in each abiotic conditions their productions is optimized, regardless of the fungal growth rate.

Statistical analysis of DoE strategies using both datasets revealed that the variables contributed in different ways for the metabolic production and fungal growth, displaying unique interactions to increase targeted and untargeted chemical production. For *X. cubensis*, complete factorial planning revealed that only temperature was significant to increase both fungal growth and cytochalasin D up-regulation (Table 6.4) and that neither luminosity and agitation influenced the chemical response. The optimized condition for the cytochalasin D production was set at 25°C, reaching 26% of total amount of the crude extract.

DoE Exp	*F. oxysporum*		*X. cubensis*		*D. anacardii*		
	Extract (mg)	F. A. purity (%)	Extract (mg)	C. D purity (%)	Extract (mg)	3-NPA purity (%)	C. D purity (%)
1	65.3	40.56	76.8	0	67.2	0	2.23
2	130.5	27.09	50.1	0	53	0	5.92
3	98.43	15.69	111.8	0	16.3	0	0.77
4	159.3	26.64	44.8	0	24.9	0	0.88
5	32.2	7.43	159.2	20.05	62.7	33.29	0
6	17.6	13.78	247.6	8.25	72	19.92	0
7	15.8	26.47	307.2	17.28	17.2	1.66	0
8	45.4	7.67	328.4	26.01	6.7	3.10	0

Table 6.3. The results of the OSMAC-DoE experiments for *F. oxysporum, X. cubensis and D. anacardii*. Each fungus presents a data set with mean value (in mg) of the crude extracts and a percentage purity value (%) of the target bioactive metabolites obtained from the crude extracts. F.A.: Fusaric acid; C. D: cytochalasin D;

For *D. anacardii*, DoE analysis revealed that only the presence of agitation was significant to vary the comprehensive metabolite production and that temperature and luminosity only slightly influenced the chemical outcome. Nonetheless, for the targeted up-regulation of 3-NPA, the presence of agitation was not the only effect that increased its induction and that temperature was also important for the metabolite enhancement. The optimized condition for the production of this compound was 110 rpm and 25 °C, increasing the bioactive metabolite production by up to 33% of amount of extract (critical *t* values of 9.33 at 95% confidence level, Table 6.4).

For *F. oxysporum*, the OSMAC-DoE results were antagonistic between total metabolic production and fusaric acid up-regulation because some effects that positively influence untargeted metabolic production negatively influence fusaric acid up-regulation. On one hand, the presence of agitation and higher levels of temperature increased the overall metabolite production (Table 6.4). On the other, although higher levels of temperature also contributes to fusaric acid production, the absence of agitation and luminosity were important abiotic conditions for this compound regulation,

increasing fusaric acid production in more than 30% at a dark and room temperature static growth.

OSMAC-DoE	*F. oxysporum*		*X. cubensis*		*D. anacardii*	
	Extracts (mg)	**F. A. purity (%)**	**Extracts (mg)**	**C. D purity (%)**	**Extracts (mg)**	**3-NPA purity (%)**
Exp. variance	263.06	87.58	1683.23	14.64	59.04	22.60
Exp. error	16.21	9.35	41.02	3.82	7.68	4.75
Effect variance	131.53	43.79	841.61	7.32	29.52	11.30
Effect error	11.46	6.17	29.01	2.70	5.43	3.36
Critical *t* value	31.84	18.3	80.54	7.51	15.08	9.33
Significant effects	T(+), A-T(+)	T(+), L-T(-), A-L (+)	T(-)	T(-)	A(+)	T(-), T-A(-), A(+)

Table 6.4. Statistical results of OSMAC-DoE. Critical values of Student's *t* distribution at a 95% confidence level and 4 degrees of freedom is 2.776. Significant effects and their respective level of low (-) or high (+) are displayed as temperature (T), agitation (A) and luminosity (L). F.A.: Fusaric Acid; C. D: cytochalasin D.

The Figure 6.4 summarizes the influence of abiotic factors on global chemical behavior of three strains. For OSMAC-DoE performed using the raw-extract, temperature was the most important variable for the enhancement of global metabolic production for *X. cubensis* and *F. oxysporum*, reaching an increase in 3 and 4-fold at 25°C, respectively (Figure 6.4A). Similarly, agitation was particularly important for *D. anacardii*, playing only a minor role in fungal growth for both *X. cubensis* and *F. oxysporum*. At 110 rpm, *Diaporthe* increased its metabolite production in up to 3-fold. Overall, luminosity was not a significant variable in none of the selected species, exhibiting similar chemical outcomes in low and high levels.

Contrarily, the evaluation of DoE results using the percentage purity value of the targeted metabolites as response (Figure 6.4B) showed that all abiotic parameters played an significant role in all fungi. Temperature was still the most important abiotic parameter in all species, inducing the highest metabolic production at room temperature. At 25 °C, we observed a significant increase in production of all bioactive metabolites, in which cytochalasin D, fusaric acid and 3-NPA exhibited 17, 27 and 14% of purity, respectively. Agitation was also found to statistically increase bioactive metabolite production in *F.*

oxysporum and *D. anacardii*, displaying particularly important results for 3-NPA production, increased by 13-fold at 110 rpm. Although cytochalasin D was not statistically influenced by agitation, there was a tendency towards up-regulation of this compound at static growth. Lastly, despite not statistically significant, luminosity also revealed a tendency towards a higher metabolic induction in the lower level of luminosity for all selected metabolites, displaying up-regulated purity of these compounds in the absence of light.

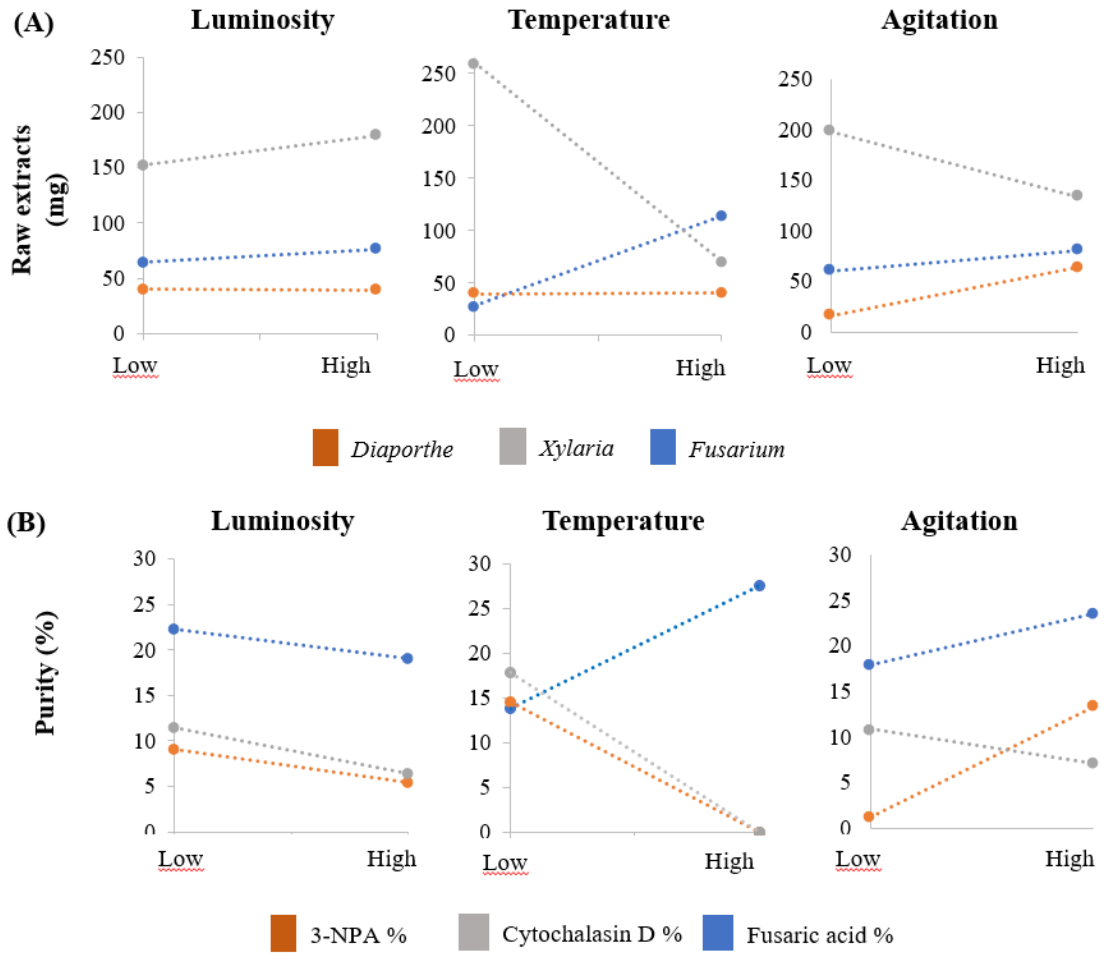

Figure 6.4. Effects analysis for the OSMAC-DoE 2^3 complete factorial design. **(A)** effect of luminosity, temperature and agitation on amount of global metabolites (extracts in mg)**; (B)** effect of luminosity, temperature and agitation on production of target metabolites, regardless of the fungal growth rate. The graphs show the variation in the chemical response between the mean values of all the variable at low and high levels. Steepness of the lines indicates the strength of the relationship.

4. Conclusion

The combination of OSMAC and DoE increased the production of the targeted metabolites in only 8 experiments, regulating both overall metabolic production and the percentage of these bioactive compounds in raw extracts. The use of different datasets for the DoE response was a key step to obtain a comprehensive enhancement of these compounds and revealed that the abiotic parameters contributed in different ways for the metabolic production, sometimes displaying different interactions to increase the fungal growth and to up-regulate the targeted metabolites.

The OSMAC-Doe results show that the abiotic factors played a specific and essential role on metabolite regulation. For the evaluation of the overall fungal metabolic production (fungal growth), temperature was determinant for *X. cubensis* and *F. oxysporum*, while for *D. anacardii*, agitation influenced the higher growth. On the other hand, to increase the content of the targeted metabolites, all the variables influenced equally in all three fungi, displaying unique interactions according to the biosynthetic pathway of the bioactive compounds.

The use of Global Spectral Deconvolution (GSD) was fundamental as it allowed for the selective suppression of undesirable signals and allowed the precise extraction of the NMR integrals even in regions where the signals of the target compounds were overlapped with other resonances. In addition, the GSD-based ^{1}HNMR quantification was not only reproducible for all species, but also exhibited validated results that were often more selective and accuracy than comparative methods. For highly coalesced chemical shifts, GSD-based ^{1}HNMR quantification proved to be unique, allowing the robust and rapid measurement of convoluted signals directly in complex natural matrices.

Although often used to increase fungal growth, to these date, only few reports have indicated the use of OSMAC as a tool to optimize a particular biosynthetic pathway (HEWAGE et al., 2014; LIU et al., 2016). Furthermore, this is the first time the integration of OSMAC and deconvolution-based ^{1}HqNMR has been described and has proved to be an excellent strategy to improve and monitor bioactive metabolic production in microbial cultures and can be applied to any fungal and bacterial, as long as careful considerations are given for the experimental procedure. For example, the selection of the microbial species and target compounds, the growth variables for the OSMAC experimental design and the ^{1}HNMR quantification parameters (deuterated solvent, internal standard and acquisition method) are critical for a successful response.

FINAL CONSIDERATIONS – DISCUSSION AND CONCLUSION

Microbial secondary metabolite can be described as the future for the drug discovery programs. Even with the problems related to unlocked genomes and unculturable strains, these plant-associated fungi were capable of producing extremely diverse chemical structures found on extensive and still little explores microbial populations, being an unlimited source of complex and biologically active structures.

However advantageous, some difficulties in both the analytical and microbiological fronts still hampers chemical and biological interpretation. While the metabolite screening in monocultures tend to produce chemically poorer profiles and the identification of the same known metabolites, the analytical issues includes matrix complexity and the difficulties in identifying minor metabolites directly in these complex matrices.

To overcome the analytical difficulties in the identification and detection of metabolites in microbial matrices, dereplication has shown to be a rapid strategy to identify known secondary metabolites, minimizing time, effort, and cost. In these methodology, the best way to obtain a comprehensive analysis of the metabolome is by the combination of analytical platforms, such as mass spectrometry (LC- and GC-MS), capillary electrophoresis (CE), infrared (IR), UV spectroscopy, and NMR spectroscopy.

Among the analytical techniques, HPTLC was a powerful tool for chemical fingerprinting analysis and presents several advantages, such as short measuring time, relatively low cost, high signal robustness, the use of different derivatization methods and fast isolation directly from the plate. Although presenting some major limitations, such as low sensibility and the absence of information over the chemical structures, the use of high performance plates, automatic processes for application and development, and the possibility of plate conversion by new software has increased the use of this technique, providing reproducible results for exploratory and untargeted analysis.

Considering metabolites coverage, sensitivity and resolution, NMR and MS methodologies are currently the most popular methods for both targeted and untargeted metabolomics and are complementarily used to obtain detailed chemical information on the biological system.

On one hand, NMR provides a highly reproducible and non-destructive analysis with minimal sample preparation, enabling the detailed elucidation of wide range of metabolic groups, including unknown compounds, isomers and compounds difficult to ionize or

derivatize for MS. However, the difficulty of NMR to be hyphenated with chromatographic introductory systems and relative low-sensitivity has made this technique most used to the analysis of only most abundant secondary metabolites, which can be confirmed by the application of bidimensional techniques and deconvolution tools.

On the other hand, mass spectrometry offers high sensitivity and resolution with structure information deduced from accurate mass, fragmentation patterns or isotope distribution. If combined to different separation techniques, such as liquid or gas chromatography, this technique provides information over major and minor compounds in complex matrices, enabling a comprehensive analysis of the metabolome.

Regardless of the methods, one common difficulty is the evaluation of microbial profiles is the lack of robust databases that contains spectroscopic and spectrometric information of the secondary metabolites produced by microorganism. In this sense, the development of an in-house database was a crucial step for molecular elucidation by comparison of experimental data with predicted or reference chemical data.

Other than the combination of analytical techniques for the screening of secondary metabolites, other strategies could also be used to reduce complexity before and after the chemical analysis. For instance, prior to the analytical evaluation, micro-fractionation could be performed in microscale, in function of their polarity, allowing the identification of minor compounds and metabolites previously undetected in raw extract. Moreover, the evaluation of the fractions by preliminary biological activity can help the selection of fractions that shows promising results.

After the application of the analytical techniques for the screening of compounds, computational tools could also help the chemical interpretation. This strategies include the use of deconvolution tools, such as Statistical Total Correlation Spectroscopy (STOCSY) and Global Spectral Deconvolution (GSD), the application of statistical and pattern recognition algorithms, such as design of experiments and MS/MS Molecular Networking, and the use of both supervised and unsupervised chemometric analysis, presenting an unbiased evaluation of the metabolome, as well as statistical correlation of the chemical and biological data.

Although the application of analytical techniques and computational tools represent successful methodologies to increase the detection and identification of secondary metabolites, the issues related to cryptic genome can only be overcome by the use of genomic and post-genomic strategies to increase the chemical diversity obtained by one single microbial source. Over the last decade, these post-genomic strategies has been used

to increase the production of known metabolites and induction of novel chemical structures.

In co-culture experiments, studies have shown an increase in the production of bioactive known structures, as well as the induction of novel compounds not produced in axenic cultures. For each fungus species, different chemical and biological responses can be obtained according to the competitive species, providing unlimited biosynthetic possibilities. If the study targets the identification of antimicrobial compounds, the use of solid media can help the selection of pairs that display antagonistic behavior, given solid media allows rapid fungal growth, rapid visualization of morphological changes and the separate extraction of important regions.

Contrarily to co-culture, One Strain, Many Compounds (OSMAC) strategy is more extensively applied to increase the production of known compounds. In this strategy, the combination with design of experiments can enhance the production of these targeted compounds in few experiments statistically revealing the abiotic parameters that contributed for the metabolic production.

Overall, it is necessary the combination of post-genomic strategies, state-of-the-art analytical techniques and the use of computational and statistical tools for the comprehensive analysis of the microbial metabolome. The selection of the best methodologies needs to be based on a careful evaluation of the chemical profile, a literature search over the available chemical, genomic and biological information of the selected species, as well as the purpose of study and the expected outcomes. Often, only by the combination of organic chemistry, analytical analysis, microbiology and statistics, we can obtain the best and most comprehensive results, being fundamental that these fields work without distinction in an integrative and unique manner.

REFERENCES

ABDALLA, M. A.; SULIEMAN, S.; MCGAW, L. J. Microbial communication: A significant approach for new leads. **South African Journal of Botany**, v. 113, n. October, p. 461–470, 2017.

ABREU, A. C. et al. Looking to nature for a new concept in antimicrobial treatments: Isoflavonoids from Cytisus striatus as antibiotic adjuvants against MRSA. **Scientific Reports**, v. 7, n. 1, p. 3777, 2017.

ADNANI, N. et al. Investigation of interspecies interactions within marine micromonosporaceae using an improved co-culture approach. **Marine Drugs**, v. 13, n. 10, p. 6082–6098, 2015.

AGHCHEH, R. K.; KUBICEK, C. P. Epigenetics as an emerging tool for improvement of fungal strains

used in biotechnology. **Applied Microbiology and Biotechnology**, v. 99, n. 15, p. 6167–6181, 2015.

AGUSTA, A.; OHASHI, K.; SHIBUYA, H. Bisanthraquinone Metabolites Produced by the Endophytic Fungus Diaporthe sp. **Chemical & Pharmaceutical Bulletin**, v. 54, n. 4, p. 579–582, 2006.

AHMAD, S. et al. Microbial biotransformation of beclomethasone dipropionate by Aspergillus niger. **Brazilian Journal of Pharmaceutical Sciences**, v. 50, n. 4, p. 903–910, 2014.

AKOKA, S.; BARANTIN, L.; TRIERWEILER, M. Concentration measurement by proton NMR using the ERETIC method. **Analytical Chemistry**, v. 71, n. 13, p. 2554–2557, 1999.

AKONE, S. H. et al. Inducing secondary metabolite production by the endophytic fungus Chaetomium sp . through fungal e bacterial co-culture and epigenetic modi fi cation. **Tetrahedron**, v. 72, p. 6340–6347, 2016.

AKSENOV, A. A. et al. Global chemical analysis of biology by mass spectrometry. **Nature Reviews Chemistry**, v. 1, p. 54, 5 jul. 2017.

ALABOUVETTE, C. et al. Microbiological control of soil-borne phytopathogenic fungi with special emphasis on wilt-inducing Fusarium oxysporum. **New Phytologist**, v. 184, n. 3, p. 529–544, 2009.

ALLARD, P. M. et al. Integration of Molecular Networking and In-Silico MS/MS Fragmentation for Natural Products Dereplication. **Analytical Chemistry**, v. 88, n. 6, p. 3317–3323, 2016.

ALTSCHUL, S. F. et al. Gapped BLAST and PSI-BLAST:a new generation of protein database search programs. **Nucleic Acids Research**, v. 25, n. 17, p. 3389–3402, 1997.

ALY, A. H. et al. Fungal endophytes from higher plants: A prolific source of phytochemicals and other bioactive natural products. **Fungal Diversity**, v. 41, p. 1–16, 2010.

ALY, A. H.; DEBBAB, A.; PROKSCH, P. Fungal endophytes: Unique plant inhabitants with great promises. **Applied Microbiology and Biotechnology**, v. 90, n. 6, p. 1829–1845, 2011.

AMALFITANO, C. et al. HPLC analysis of fusaric acid, 9,10-dehydrofusaric acid and their methyl esters, toxic metabolites from weed pathogenic Fusarium species. **Phytochemical Analysis**, v. 13, n. 5, p. 277–282, 2002.

AMANO, S. et al. Promomycin, a polyether promoting antibiotic production in Streptomyces spp. **Journal of Antibiotics**, v. 63, n. 8, p. 486–491, 2010.

AMANO, S. et al. A cryptic antibiotic triggered by monensin. **Journal of Antibiotics**, v. 64, n. 10, p. 703, 2011.

AMARAL, L. DA S. et al. An HPLC evaluation of cytochalasin D biosynthesis by Xylaria arbuscula cultivated in different media. **Nat Prod Commun**, v. 9, n. 9, p. 1279–82, 2014.

ANDRECUT, M. Parallel GPU Implementation of Iterative PCA Algorithms. **Journal of Compoutational Biology**, v. 16, n. 11, p. 1593–1599, 2008.

ANGELL, S. et al. Pyocyanin Isolated from a Marine Microbial Population: Synergistic Production between Two Distinct Bacterial Species and Mode of Action. **Chemistry and Biology**, v. 13, n. 12, p. 1349–1359, 2006.

APPELBAUM, P. C. The emergence of vancomycin-intermediate and vancomycin-resistant Staphylococcus aureus. **Clinical Microbiology and Infection**, v. 12, n. SUPPL. 1, p. 16–23, 2006.

ARBOLEDA, J. W.; DELGADO, F. D.; VALENCIA, A. J. **Deteccion de beuavericina en el hongo entomopatógeno Beauveria bassiana mediante el uso de anticuerpos monoclonalesRevista Colombiana de Entomología**, 2004.

ARIANA, M.; HAMEDI, J. Enhanced production of nisin by co-culture of Lactococcus lactis sub sp. lactis and Yarrowia lipolytica in molasses based medium. **Journal of Biotechnology**, v. 256, n. July, p. 21–26, 2017.

AUDOIN, C. et al. Development of a work-flow for high-performance thin-layer chromatography data processing for untargeted metabolomics. **Journal of Planar Chromatography**, v. 27, n. 5, p. 328–332, 2014.

AZZOLLINI, A. et al. Dynamics of metabolite induction in fungal co-cultures by metabolomics at both volatile and non-volatile levels. **Frontiers in Microbiology**, v. 9, n. FEB, p. 1–12, 2018.

BACON, C. W. et al. Production of fusaric acid by Fusarium species. **Applied and Environmental Microbiology**, v. 62, n. 11, p. 4039–4043, 1996.

BADER, J. et al. Relevance of microbial coculture fermentations in biotechnology. **Journal of Applied Microbiology**, v. 109, n. 2, p. 371–387, 2010.

BALDRIAN, P. Increase of laccase activity during interspecific interactions of white-rot fungi. **FEMS Microbiology Ecology**, v. 50, n. 3, p. 245–253, 2004.

BAO, J. R.; LAZAROVITS, G. Differential Colonization of Tomato Roots by Nonpathogenic and Pathogenic Fusarium oxysporum Strains May Influence Fusarium Wilt Control. **Phytopathology**, v. 91, n. 5, p. 449–456, 2001.

BAREFOOT, S. F. et al. Identification and Purification of a Protein That Induces Production of the Lactobacillus acidophilus Bacteriocin Lactacin Bt. **Applied and Environmental Microbiology**, v. 60, n. 10, p. 3522–3528, 1994.

BAYDOUN, E. et al. Microbial transformation of anti-cancer steroid exemestane and cytotoxicity of its metabolites against cancer cell lines. **Chemistry Central Journal**, v. 7, n. 1, p. 1–7, 2013.

BEEK, S. V; PRIEST, F. G.; PRIEST, F. G. Evolution of the Lactic Acid Bacterial Community during Malt Whisky Fermentation : a Polyphasic Study. **Applied and Environmental Microbiology**, v. 68, n. 1, p. 297–305, 2002.

BENITEZ, L. et al. Antimicrobial activity of Bacillus amyloliquefaciens LBM 5006 is enhanced in the

presence of Escherichia coli. **Current Microbiology**, v. 62, n. 3, p. 1017–1022, 2011.

BERGMANN, S. et al. Genomics-driven discovery of PKS-NRPS hybrid metabolites from Aspergillus nidulans. **Nature Chemical Biology**, v. 3, n. 4, p. 213–217, 2007.

BERLEMAN, J. E. et al. Rippling is a predatory behavior in Myxococcus xanthus. **Journal of Bacteriology**, v. 188, n. 16, p. 5888–5895, 2006.

BERNSTEIN, M. A. et al. Optimization and automation of quantitative NMR data extraction. **Analytical Chemistry**, v. 85, n. 12, p. 5778–5786, 2013.

BERTRAND, S. et al. Detection of metabolite induction in fungal co-cultures on solid media by high-throughput differential ultra-high pressure liquid chromatography-time-of-flight mass spectrometry fingerprinting. **Journal of Chromatography A**, v. 1292, p. 219–228, 2013a.

BERTRAND, S. et al. De novo production of metabolites by fungal co-culture of Trichophyton rubrum and Bionectria ochroleuca. **Journal of Natural Products**, v. 76, n. 6, p. 1157–1165, 2013b.

BERTRAND, S. et al. Metabolite induction via microorganism co-culture-A potential way to enhance chemical diversity for drug discovery. **Biotechnology Advances Journal**, v. 32, p. 1180–1204, 2014a.

BERTRAND, S. et al. Multi-well fungal co-culture for de novo metabolite-induction in time-series studies based on untargeted metabolomics. **Mol. BioSyst.**, v. 10, n. 9, p. 2289–2298, 2014b.

BIASETTO, C. R. **Fungos endofíticos em Eugenia brasiliensis: prospecção química, biológica, enzimática e avaliação do co-cultivo e epigenética em Xylaria cubensis, Diaporthe sp. e Colletotrichum sp**. [s.l.] Sáo Paulo State University, 2016.

BITTENCOURT, M. L. F. et al. Metabolite profiling, antioxidant and antibacterial activities of Brazilian propolis: Use of correlation and multivariate analyses to identify potential bioactive compounds. **Food Research International**, v. 76, p. 449–457, 2015.

BLAISE, B. J. et al. Two-dimensional statistical recoupling for the identification of perturbed metabolic networks from NMR spectroscopy. **Journal of Proteome Research**, v. 9, n. 9, p. 4513–4520, 2010.

BODE, H. B. et al. Big effects from small changes: possible ways to explore nature's chemical diversity. **Chembiochem**, v. 3, n. 7, p. 619–627, 2002.

BOGDANOWICZ, D. R.; LU, H. H. Studying cell-cell communication in co-culture. **Biotechnology Journal**, v. 8, n. 4, p. 395–396, 2013.

BOHNI, N. et al. Production of fusaric acid by Fusarium spp. in pure culture and in solid medium co-cultures. **Molecules**, v. 21, n. 3, p. 370–386, 2016.

BOON, C. et al. A novel DSF-like signal from Burkholderia cenocepacia interferes with Candida albicans morphological transition. **ISME Journal**, v. 2, n. 1, p. 27–36, 2008.

BRACARENSE, A. A. P.; TAKAHASHI, J. A. Modulation of antimicrobial metabolites production by

the fungus Aspergillus parasiticus. **Brazilian Journal of Microbiology**, v. 45, n. 1, p. 313–321, 2014.

BRADY, S. F. et al. Cytoskyrins A and B, new BIA active bisanthraquinones isolated from an endophytic fungus. **Organic Letters**, v. 2, n. 25, p. 4047–4049, 2000.

BRAGA, R. M.; DOURADO, M. N.; ARAÚJO, W. L. Microbial interactions: ecology in a molecular perspective. **Brazilian Journal of Microbiology**, v. 47, p. 86–98, 2016.

BRO, R.; SMILDE, A. K. Principal component analysis. **Analytical Methods**, v. 6, p. 2812–2831, 2014.

BRODERICK, N. A.; RAFFA, K. F.; HANDELSMAN, J. Midgut bacteria required for Bacillus thuringiensis insecticidal activity. **Proceedings of the National Academy of Sciences**, v. 103, n. 41, p. 15196–15199, 2006.

BROWN, D. W. et al. Identification of gene clusters associated with fusaric acid, fusarin, and perithecial pigment production in Fusarium verticillioides. **Fungal Genetics and Biology**, v. 49, n. 7, p. 521–532, 2012.

BROWNELL, A.-L. et al. 3-Nitropropionic acid-induced neurotoxicity - Assessed by ultra high resolution positron emission tomography with comparison to magnetic resonance spectroscopy. **Journal of neurochemistry**, v. 89, p. 1206–1214, 2004.

BUBB, W. A. NMR spectroscopy in the study of carbohydrates: Characterizing the structural complexity. **Concepts in Magnetic Resonance Part A**, v. 19A, n. 1, p. 1–19, 2003.

BURGESS, J. G. et al. Microbial antagonism: a neglected avenue of natural products research. Journal of Biotechnology 70(1-3):27-32. [Archidoris pseudoargus p. 30. **Journal of Biotechnology 70**, v. 70, p. 27–32, 1999.

BURMEISTER, H. R. et al. Isolation and characterization of two new fusaric acid analogs from Fusarium moniliforme NRRL 13,163. **Applied and Environmental Microbiology**, v. 50, n. 2, p. 311–314, 1985.

CAFÊU, M. C. et al. Substâncias antifúngicas de Xylaria sp., um fungo endofítico isolado de palicourea marcgravii (Rubiaceae). **Quimica Nova**, v. 28, n. 6, p. 991–995, 2005.

CANDES, E. J. et al. Robust Principal Component Analysis? **J. ACM**, v. 58, n. 3, p. 1–37, 2011.

CARDOSO, P. **Metabolomic evaluation of interactions in rhizosphere between Senna spectabilis and associated microorganisms**. [s.l.] São Paulo State University, 2015.

CARDOSO, S. et al. A Chemometrics Approach for Nuclear Magnetic Resonance Data to Characterize the Partial Metabolome Banana Peels from Southern Brazil. **Journal of Integrative Bioinformatics**, v. 14, n. 4, p. 1–10, 2017.

CARLSON, S. et al. Phylum-specific regulation of resistomycin production in a streptomyces sp. via microbial coculture. **Journal of Natural Products**, v. 78, n. 3, p. 381–387, 2015.

CARMELIET, P. Blood vessels and nerves: common signals, pathways and diseases. **Nature Reviews**

Genetics, v. 4, p. 710, 1 set. 2003.

CASTLEBURY, L. A. et al. Use of a bioassay to evaluate the toxicity of beauvericin to bacteria. **World Journal of Microbiology and Biotechnology**, v. 15, n. 1, p. 131–133, 1999.

CHAGAS-PAULA, D. A. et al. Prediction of anti-inflammatory plants and discovery of their biomarkers by machine learning algorithms and metabolomic studies. **Planta Medica**, v. 81, n. 6, p. 450–458, 2015.

CHAGAS, F. O.; DIAS, L. G.; PUPO, M. T. A Mixed Culture of Endophytic Fungi Increases Production of Antifungal Polyketides. **Journal of Chemical Ecology**, v. 39, n. 10, p. 1335–1342, 2013.

CHANOS, P.; MYGIND, T. Co-culture-inducible bacteriocin production in lactic acid bacteria. **Applied Microbiology and Biotechnology**, v. 100, n. 10, p. 4297–4308, 2016.

CHAPLA, V. M.; BIASETTO, C. R.; ARAUJO, A. R. Endophytic Fungi: An Unexplored and Sustainable Source of New and Bioactive Natural Products. **Revista Virtual de Química**, v. 5, n. 3, p. 421–437, 2013.

CHAUDHRY, G. R.; CHAPALAMADUGU, S. Biodegradation of halogenated organic compounds. **Microbiological Review**, v. 55, n. 1, p. 59–79, 1991.

CHEIRSILP, B.; SHIMIZU, H.; SHIOYA, S. Enhanced kefiran production by mixed culture of and. **Journal of Biotechnology**, v. 100, n. 1, p. 43–53, 2003.

CHEN, H.-J. et al. Epigenetic modifier-induced biosynthesis of novel fusaric acid derivatives in endophytic fungi from Datura stramonium L. **Natural Products and Bioprospecting**, v. 3, n. 1, p. 20–23, 2013a.

CHEN, J. et al. Diversity and Taxonomy of Endophytic Xylariaceous Fungi from Medicinal Plants of Dendrobium (Orchidaceae). **PLoS ONE**, v. 8, n. 3, p. e58268, 2013b.

CHEN, L. et al. Bioactivity-guided fractionation of an antidiarrheal Chinese herb Rhodiola kirilowii (Regel) Maxim reveals (-)-epicatechin-3-gallate and (-)-epigallocatechin-3-gallate as inhibitors of cystic fibrosis transmembrane conductance regulator. **PLoS ONE**, v. 10, n. 3, 2015.

CHEN, Z. et al. New cytochalasins from the marine-derived fungus xylaria sp. SCSIO 156. **Helvetica Chimica Acta**, v. 94, n. 9, p. 1671–1676, 2011.

CHI, Y.; HATAKKA, A.; MAIJALA, P. Can co-culturing of two white-rot fungi increase lignin degradation and the production of lignin-degrading enzymes? **International Biodeterioration and Biodegradation**, v. 59, n. 1, p. 32–39, 2007.

CHIANG, Y. M. et al. Molecular Genetic Mining of the Aspergillus Secondary Metabolome: Discovery of the Emericellamide Biosynthetic Pathway. **Chemistry and Biology**, v. 15, n. 6, p. 527–532, 2008.

CHO, J. Y.; KIM, M. S. Induction of Antifouling Diterpene Production by Streptomyces cinnabarinus PK209 in Co-Culture with Marine-Derived Alteromonas sp. KNS-16. **Bioscience, Biotechnology, and Biochemistry**, v. 76, n. 10, p. 1849–1854, 2012.

CHOMCHEON, P. et al. 3-Nitropropionic acid (3-NPA), a potent antimycobacterial agent from endophytic fungi: Is 3-NPA in some plants produced by endophytes? **Journal of Natural Products**, v. 68, n. 7, p. 1103–1105, 2005.

CLEMENTE-JIMENEZ, J. M. et al. Influence of sequential yeast mixtures on wine fermentation. **International Journal of Food Microbiology**, v. 98, n. 3, p. 301–308, 2005.

CLOAREC, O. et al. Statistical Total Correlation Spectroscopy: An Exploratory Approach for Latent Biomarker Identification from Metabolic 1 H NMR Data Sets. **Analytical Chemistry**, v. 77, n. 5, p. 1282–1289, 2005.

COBAS, C.; SEOANE, F.; SÝKORA, S. **Global Spectral Deconvolution (GSD) of 1D-NMR spectra**. SMASH Conference. **Anais**...Santa Fe: 2008

COBAS, C.; SYKORA, S. **The Bumpy Road towards Automatic Global Spectral Deconvolution**. 50th ENC Conference. **Anais**...Asilomar: 2009

CONLY, J. M.; JOHNSTON, B. L. Where are all the new antibiotics? The new antibiotic paradox. **Canadian Journal of Infectious Diseases and Medical Microbiology**, v. 16, n. 3, p. 159–160, 2005.

CORT, S.; KUMARA, H. M. C. S.; VERACHTERT, H. Localization and Characterization of ox-Glucosidase Activity in Lactobacillus brevis. **Applied and Environmental Microbiology**, v. 60, n. 9, p. 3074–3078, 1994.

COUTINHO, I. D. et al. Metabolite profiling of sugarcane genotypes and identification of flavonoid glycosides and phenolic acids. **Journal of Agricultural and Food Chemistry**, v. 64, n. 21, p. 4198–4206, 2016.

CRESPI, B. J. The evolution of social behavior in microorganisms. **Trends in Ecology & Evolution**, v. 16, n. 4, p. 178–183, 2001.

CROTTI, A. E. M. et al. Espectrometria de massas com ionização por "Electrospray": Processus químicos envolvidos na formação de íons de substâncias orgânicas de baixo peso molecular. **Quimica Nova**, v. 29, n. 2, p. 287–292, 2006.

CUETO, M. et al. Pestalone, a New Antibiotic Produced by a Marine Fungus in Response to Bacterial Challenge. **Journal of Natural Products**, v. 64, p. 1444–1446, 2001.

CUGINI, C. et al. Farnesol, a common sesquiterpene, inhibits PQS production in Pseudomonas aeruginosa. **Molecular Microbiology**, v. 65, n. 4, p. 896–906, 2007.

DA SILVA, R. R. et al. Propagating annotations of molecular networks using in silico fragmentation. **PLoS Comput Biol**, v. 14, n. 4, p. e1006089, 2018.

DAGNINO, D.; SCHRIPSEMA, J. 1H NMR quantification in very dilute toxin solutions: Application to anatoxin-a analysis. **Toxicon**, v. 46, n. 2, p. 236–240, 2005.

DASHTI, Y. et al. Production of induced secondary metabolites by a co-culture of sponge-associated

actinomycetes, Actinokineospora sp. EG49 and Nocardiopsis sp. RV163. **Marine Drugs**, v. 12, n. 5, p. 3046–3059, 2014.

DAVIES, J. Are antibiotics naturally antibiotics? **Journal of Industrial Microbiology and Biotechnology**, v. 33, n. 7, p. 496–499, 2006.

DE BOER, A. L.; SCHMIDT-DANNERT, C. Recent efforts in engineering microbial cells to produce new chemical compounds. **Current Opinion in Chemical Biology**, v. 7, n. 2, p. 273–278, 2003.

DE OLIVEIRA, G. G. et al. Dereplication of Flavonoid Glycoconjugates from Adenocalymma imperatoris-maximilianii by Untargeted Tandem Mass Spectrometry-Based Molecular Networking. **Planta Medica**, v. 83, n. 7, p. 636–646, 2017.

DEMAIN, A. L. MINI-REVIEW Pharmaceutically active secondary metabolites of microorganisms. **Applied Microbiology and Biotechnology**, v. 52, p. 455–463, 1999.

DEMAIN, A. L.; ELANDER, R. P. The β-lactam antibiotics: past, present, and future. **Antonie van Leeuwenhoek**, v. 75, p. 5–19, 1999.

DEMAIN, A. L.; SANCHEZ, S. Microbial drug discovery: 80 Years of progress. **Journal of Antibiotics**, v. 62, n. 1, p. 5–16, 2009.

DEMBOGURSKI, D. S. O. et al. Brown propolis-metabolomic innovative approach to determine compounds capable of killing Staphylococcus aureus biofilm and Trichomonas vaginalis. **Food Research International**, v. 111, n. February, p. 661–673, 2018.

DI CAGNO, R. et al. Molecular adaptation of sourdough Lactobacillus plantarum DC400 under co-cultivation with other lactobacilli. **Research in Microbiology**, v. 160, n. 5, p. 358–366, 2009.

DICKS, L. M. T.; MELLETT, F. D.; HOFFMAN, L. C. Use of bacteriocin-producing starter cultures of Lactobacillus plantarum and Lactobacillus curvatus in production of ostrich meat salami. **Meat Science**, v. 66, n. 3, p. 703–708, 2004.

DIETRICH, L. E. P. et al. Redox-active antibiotics control gene expression and community behavior in divergent bacteria. **Science**, v. 321, n. 5893, p. 1203–1206, 2008.

DOS SANTOS, V. S. et al. Metabolomics as a tool for understanding the evolution of Tabebuia sensu lato. **Metabolomics**, v. 13, n. 6, p. 1–11, 2017.

DOW, J. M. et al. Biofilm dispersal in Xanthomonas campestris is controlled by cell-cell signaling and is required for full virulence to plants. **Proceedings of the National Academy of Sciences**, v. 100, n. 19, p. 10995–11000, 2003.

DUFFY, B.; SCHOUTEN, A.; RAAIJMAKERS, J. M. Pathogen Self-defense: Mechanisms to Counteract Microbial Antagonism. **Annual Review of Phytopathology**, v. 41, n. 1, p. 501–538, 2003.

DUSANE, D. H. et al. Cross-species induction of antimicrobial compounds, biosurfactants and quorum-sensing inhibitors in tropical marine epibiotic bacteria by pathogens and biofouling microorganisms.

Current Microbiology, v. 62, n. 3, p. 974–980, 2011.

DZOYEM, J. P. et al. Cytotoxicity, antioxidant and antibacterial activity of four compounds produced by an endophytic fungus Epicoccum nigrum associated with entada abyssinica. **Brazilian Journal of Pharmacognosy**, v. 27, n. 2, p. 251–253, 2017.

EBRAHIM, W. et al. Metabolites from the Fungal Endophyte Aspergillus austroafricanus in Axenic Culture and in Fungal-Bacterial Mixed Cultures. **Journal of Natural Products**, v. 79, n. 4, p. 914–922, 2016.

ERNST, M. et al. A new metabolomic protocol for Brazilian "Cerrado" plants. **Planta Medica**, v. 80, n. 16, p. SL2, 2014a.

ERNST, M. et al. Mass spectrometry in plant metabolomics strategies: From analytical platforms to data acquisition and processing. **Natural Product Reports**, v. 31, n. 6, p. 784–806, 2014b.

FAJARDO, A.; MARTÍNEZ, J. L. Antibiotics as signals that trigger specific bacterial responses. **Current Opinion in Microbiology**, v. 11, n. 2, p. 161–167, 2008.

FAN, N.-W. et al. Secondary metabolites from the endophytic fungus Xylaria cubensis. **Helvetica Chimica Acta**, v. 97, n. 4, p. 1689, 2014.

FENG, Y. et al. A Novel Cyclodepsipeptide, HA23, from a Fusarium sp. **Organic Letters**, v. 4, n. 12, p. 2095–2096, 1 jun. 2002.

FERREIRA GREGORIO, A. P. et al. Changes in production of lignin degrading enzymes during interactions between mycelia of the tropical decomposer basidiomycetes Marasmiellus troyanus and Marasmius pallescens. **Mycological Research**, v. 110, n. 2, p. 161–168, 2006.

FICHOU, D.; RISTIVOJEVIĆ, P.; MORLOCK, G. E. Proof-of-Principle of rTLC, an Open-Source Software Developed for Image Evaluation and Multivariate Analysis of Planar Chromatograms. **Analytical Chemistry**, v. 88, n. 24, p. 12494–12501, 2016.

FIEHN, O. **Metabolomics by Gas Chromatography-Mass Spectrometry: the combination of targeted and untargeted profiling**. [s.l: s.n.]. v. 114

FLEET, G. H. Yeast interactions and wine flavour. **International Journal of Food Microbiology**, v. 86, n. 1–2, p. 11–22, 2003.

FLORES, A. C. et al. Production of 3-nitropropionic acid by endophytic fungus Phomopsis longicolla isolated from Trichilia elegans A. JUSS ssp. elegans and evaluation of biological activity. **World Journal of Microbiology and Biotechnology**, v. 29, n. 5, p. 923–932, 2013.

FOUHY, Y. et al. Diffusible signal factor-dependent cell-cell signaling and virulence in the nosocomial pathogen Stenotrophomonas maltophilia. **Journal of Bacteriology**, v. 189, n. 13, p. 4964–4968, 2007.

FRAIGE, K. et al. Metabolite and proteome changes during the ripening of Syrah and Cabernet Sauvignon grape varieties cultured in a nontraditional wine region in Brazil. **Journal of Proteomics**, v.

113, p. 206–225, 2015.

FREITAG, M.; MORRELL, J. J. Changes in selected enzyme activities during growth of pure and mixed cultures of the white-rot decay fungus Trametes versicolor and the potential biocontrol fungus Trichoderma harzianum. **Canadian Journal of Microbiology**, v. 38, n. 4, p. 317–23, 1992.

FRIAS, C. F.; GRAMACHO, S. A.; PINEIRO, M. Cromatografia gasosa-espectrometria de massas e derivatização assistida por microondas na identificação de isômeros de glicose: Uma prática para o ensino avançado em análise e caracterização de compostos orgânicos. **Quimica Nova**, v. 37, n. 1, p. 176–180, 2014.

FUJIMOTO, M. et al. Developmental defect of cytochrome oxidase mutants of streptomyces coelicolor A3(2). **Microbiology (United Kingdom)**, v. 162, n. 8, p. 1446–1455, 2016.

FUNARI, C. S. et al. High resolution ultra high pressure liquid chromatography-time-of-flight mass spectrometry dereplication strategy for the metabolite profiling of Brazilian Lippia species. **Journal of Chromatography A**, v. 1259, p. 167–178, 2012.

FUNARI, C. S. et al. Metabolômica, uma abordagem otimizada para exploração da biodiversidade brasileira: Estado da arte, perspectivas e desafios. **Quimica Nova**, v. 36, n. 10, p. 1605–1609, 2013.

GACEK, A.; STRAUSS, J. The chromatin code of fungal secondary metabolite gene clusters. **Applied Microbiology and Biotechnology**, v. 95, n. 6, p. 1389–1404, 2012.

GAISSER, S. et al. Engineered biosynthesis of novel spinosyns bearing altered deoxyhexose substituents. **ChemComm**, v. 4, n. 6, p. 618–9, 2002.

GALAGAN, J. E. et al. Sequencing of Aspergillus nidulans and comparative analysis with A. fumigatus and A. oryzae. **Nature**, v. 438, n. 7071, p. 1105–1115, 2005.

GAO, D. et al. A critical review of the application of white rot fungus to environmental pollution control. **Critical Reviews in Biotechnology**, v. 30, n. 1, p. 70–77, 2010.

GAUDÊNCIO, S. P.; PEREIRA, F. Dereplication: Racing to speed up the natural products discovery process. **Natural Product Reports**, v. 32, n. 6, p. 779–810, 2015.

GE, J. et al. Bacillus subtilis enhances production of Paracin1.7, a bacteriocin produced by Lactobacillus paracasei HD1-7, isolated from Chinese fermented cabbage. **Annals of Microbiology**, v. 64, n. 4, p. 1735–1743, 2014.

GLAUSER, G. et al. Differential Analysis of Mycoalexins in Confrontation Zones of Grapevine Fungal Pathogens by Ultrahigh Pressure Liquid Chromatography / Time-of-Flight Mass Spectrometry and Capillary Nuclear Magnetic Resonance. **Journal of Agricultural and Food Chemistry**, v. 57, n. 4, p. 1127–1134, 2009.

GOERS, L.; FREEMONT, P.; POLIZZI, K. M. Co-culture systems and technologies: taking synthetic biology to the next level. **Journal of The Royal Society Interface**, v. 11, n. 96, p. 20140065–20140065,

2014.

GOH, E.-B. et al. Transcriptional modulation of bacterial gene expression by subinhibitory concentrations of antibiotics. **Proceedings of the National Academy of Sciences**, v. 99, n. 26, p. 17025–17030, 2002.

GOMES, R. R. et al. Diaporthe: A genus of endophytic, saprobic and plant pathogenic fungi. **Persoonia: Molecular Phylogeny and Evolution of Fungi**, v. 31, p. 1–41, 2013.

GORDON, T. R.; MARTYN, R. D. The Evolutionary Biology of Fusarium Oxysporum. **Annu. Rev. Phytopathol**, v. 35, p. 111–28, 1997.

GRIFFITHS, J. A Brief History of Mass Spectrometry. **Anal Chem**, v. 80, p. 5678–5683, 2008.

GUARATINI, T. et al. Balance of xanthophylls molecular and protonated molecular ions in electrospray ionization. **J Mass Spectrom**, v. 40, n. 7, p. 963–8., 2005.

GUIZELLINI, F. C. et al. PARAFAC HPLC-DAD metabolomic fingerprint investigation of reference and crossed coffees. **Food Research International**, v. 113, n. January, p. 9–17, 2018.

HAHN, D. R. et al. Butenyl-spinosyns, a natural example of genetic engineering of antibiotic biosynthetic genes. **Journal of Industrial Microbiology and Biotechnology**, v. 33, n. 2, p. 94–104, 2006.

HAN, Z. et al. A quick, easy, cheap, effective, rugged, and safe sample pretreatment and liquid chromatography with tandem mass spectrometry method for the simultaneous quantification of 33 mycotoxins in Lentinula edodes. **Journal of Separation Science**, v. 37, n. 15, p. 1957–66, 2014.

HAO, J. et al. Bayesian deconvolution and quantification of metabolites in complex 1D NMR spectra using BATMAN. **Nature Protocols**, v. 9, n. 6, p. 1416–1427, 2014.

HE, Y. W.; ZHANG, L. H. Quorum sensing and virulence regulation in Xanthomonas campestris. **FEMS Microbiology Reviews**, v. 32, n. 5, p. 842–857, 2008.

HEGAZY, M.-E. F. E. F. et al. Microbial biotransformation as a tool for drug development based on natural products from mevalonic acid pathway: A review. **Journal of Advanced Research**, v. 6, n. 1, p. 17–33, 2015.

HERTWECK, C. Hidden biosynthetictreasures brought to light. **Nature Chemical Biology**, v. 5, n. 7, p. 450–452, 2009.

HEWAGE, R. T. et al. One strain-many compounds (OSMAC) method for production of polyketides, azaphilones, and an isochromanone using the endophytic fungus Dothideomycete sp. **Phytochemistry**, v. 108, p. 87–94, 2014.

HIBBING, M. E. et al. Bacterial competition: surviving and thriving in the microbial jungle. **Nature Reviews Microbiology**, v. 8, n. 1, p. 15–25, 2010.

HISCOX, J. et al. Changes in oxidative enzyme activity during interspecific mycelial interactions involving the white-rot fungus Trametes versicolor. **Fungal Genetics and Biology**, v. 47, n. 6, p. 562–

571, 2010.

HOEFLER, B. C. et al. Enzymatic resistance to the lipopeptide surfactin as identified through imaging mass spectrometry of bacterial competition. **Proceedings of the National Academy of Sciences**, v. 109, n. 32, p. 13082–13087, 2012.

HOFFMAN, L. R. et al. Selection for Staphylococcus aureus small-colony variants due to growth in the presence of Pseudomonas aeruginosa. **Proceedings of the National Academy of Sciences**, v. 103, n. 52, p. 19890–19895, 2006.

HÖFTE, H.; WHITELEY, H. R. Insecticidal crystal proteins of Bacillus thuringiensis. **Microbiological reviews**, v. 53, n. 2, p. 242–255, 1989.

HOGAN, D. A. Talking to Themselves : Autoregulation and Quorum Sensing in Fungi. **Eukaryotic Cell**, v. 5, n. 4, p. 613–19, 2006.

HOLZGRABE, U. et al. Quantitative NMR spectroscopy - Applications in drug analysis. **Journal of Pharmaceutical and Biomedical Analysis**, v. 38, n. 5 SPEC. ISS., p. 806–812, 2005.

HOMANS, A. L.; FUCHS, A. Direct bioautography on thin-layer chromatograms as a method for detecting fungitoxic substances. **Journal of Chromatography A**, v. 51, n. C, p. 327–329, 1970.

HONG, J. et al. Plant metabolomics: An indispensable system biology tool for plant science. **International Journal of Molecular Sciences**, v. 17, n. 6, 2016.

HONG, K. et al. Actinomycetes for marine drug discovery isolated from mangrove soils and plants in China. **Marine Drugs**, v. 7, n. 1, p. 24–44, 2009.

HONG, R. S. et al. Survey of ERETIC2 NMR for quantification. **Journal of the Korean Magnetic Resonance Society**, v. 17, n. 2, p. 98–104, 2013.

HORAI, H. et al. MassBank: A public repository for sharing mass spectral data for life sciences. **Journal of Mass Spectrometry**, v. 45, n. 7, p. 703–714, 2010.

HORINOUCHI, S. Mining and Polishing of the Treasure Trove in the Bacterial Genus Streptomyces. **Bioscience, Biotechnology, and Biochemistry**, v. 71, n. 2, p. 283–299, 2007.

HOSHINO, S. et al. Chojalactones A-C, cytotoxic butanolides isolated from streptomyces sp. cultivated with mycolic acid containing bacterium. **Organic Letters**, v. 17, n. 6, p. 1501–1504, 2015a.

HOSHINO, S. et al. Arcyriaflavin E, a new cytotoxic indolocarbazole alkaloid isolated by combined-culture of mycolic acid-containing bacteria and Streptomyces cinnamoneus NBRC 13823. **Journal of Antibiotics**, v. 68, p. 342–344, 2015b.

HOSHINO, S. et al. Niizalactams A-C, Multicyclic Macrolactams Isolated from Combined Culture of Streptomyces with Mycolic Acid-Containing Bacterium. **Journal of Natural Products**, v. 78, n. 12, p. 3011–3017, 2015c.

HU, L.; RYCHLIK, M. Biosynthesis of 15N3-labeled enniatins and beauvericin and their application to stable isotope dilution assays. **Journal of Agricultural and Food Chemistry**, v. 60, n. 29, p. 7129–7136, 2012.

HUSSAIN, A. et al. Novel bioactive molecules from Lentzea violacea strain AS 08 using one strain-many compounds (OSMAC) approach. **Bioorganic and Medicinal Chemistry Letters**, v. 27, n. 11, p. 2579–2582, 2017.

IAKOVLEV, A.; STENLID, J. Spatiotemporal Patterns of Laccase Activity in Interacting Mycelia of Wood-Decaying Basidiomycete Fungi. **Microbial Ecology**, v. 39, n. 3, p. 236–245, 2000.

IMAZAKI, I.; KADOTA, I. Molecular phylogeny and diversity of Fusarium endophytes isolated from tomato stems. **FEMS Microbiology Ecology**, v. 91, n. 9, p. 1–16, 2015.

ISLAM, S. et al. Coproduction of hydrogen and volatile fatty acid via thermophilic fermentation of sweet sorghum stalk from co-culture of Clostridium thermocellum and Clostridium thermosaccharolyticum. **International Journal of Hydrogen Energy**, v. 42, n. 2, p. 830–837, 2017.

ITO, T.; MASUBUCHI, M. Dereplication of microbial extracts and related analytical technologies. **The Journal of antibiotics**, v. 67, p. 353–369, 2014.

JARUSSOPHON, S. et al. Automated molecular formula determination by tandem mass spectrometry (MS / MS). **Analyst**, v. 134, p. 690–700, 2009.

JOLLIFFE, I. T. **Principal Component Analysis**. Springer S ed. [s.l.] Springer-Verlag New York, 2002.

JORGE, T. F. et al. MASS SPECTROMETRY-BASED PLANT METABOLOMICS: METABOLITE RESPONSES TO ABIOTIC STRESS. **Mass Spectrometry Reviews**, v. 35, p. 620–649, 2016.

KARILUOTO, S. et al. Effects of yeasts and bacteria on the levels of folates in rye sourdoughs. **International Journal of Food Microbiology**, v. 106, n. 2, p. 137–143, 2006.

KATAJAMAA, M.; OREŠIČ, M. Processing methods for differential analysis of LC/MS profile data. **BMC Bioinformatics**, v. 6, 2005.

KELL, D. B. Metabolomics and systems biology: Making sense of the soup. **Current Opinion in Microbiology**, v. 7, n. 3, p. 296–307, 2004.

KIND, T. et al. FiehnLib: Mass spectral and retention index libraries for metabolomics based on quadrupole and time-of-flight gas chromatography/mass spectrometry. **Analytical Chemistry**, v. 81, n. 24, p. 10038–10048, 2009.

KIND, T.; FIEHN, O. Seven Golden Rules for heuristic filtering of molecular formulas obtained by accurate mass spectrometry. **BMC Bioinformatics**, v. 8, p. 1–20, 2007.

KIND, T.; FIEHN, O. Advances in structure elucidation of small molecules using mass spectrometry. **Bioanalytical Reviews**, v. 2, n. 1, p. 23–60, 2010.

KLAIKLAY, S. et al. Metabolites from the mangrove-derived fungus xylaria cubensis PSU-MA34. **Archives of Pharmacal Research**, v. 35, n. 7, p. 1127–1131, 2012.

KNIGHT, V. et al. Diversifying microbial natural products for drug discovery. **Applied Microbiology and Biotechnology**, v. 62, n. 5–6, p. 446–458, 2003.

KÖNIG, C. C. et al. Bacterium Induces Cryptic Meroterpenoid Pathway in the Pathogenic Fungus Aspergillus fumigatus. **ChemBioChem**, v. 14, n. 8, p. 938–942, 2013.

KÖNIG, G. M. et al. Natural products from marine organisms and their associated microbes. **ChemBioChem**, v. 7, n. 2, p. 229–238, 2006.

KOS, B. et al. Coculture-inducible bacteriocin biosynthesis of different probiotic strains by dairy starter culture Lactococcus lactis. **Mljekarstvo**, v. 61, n. 4, p. 273–282, 2011.

KUMAR, B. et al. **Potential of metabolomics in preclinical and clinical drug developmentPharmacological Reports**, 2014.

KUMARI, S.; NARAIAN, R. Decolorization of synthetic brilliant green carpet industry dye through fungal co-culture technology. **Journal of Environmental Management**, v. 180, p. 172–179, 2016.

KUROSAWA, K. et al. Rhodostreptomycins, antibiotics biosynthesized following horizontal gene transfer from Streptomyces padanus to Rhodococcus fascians. **Journal of the American Chemical Society**, v. 130, p. 1126–1127, 2008.

LAATSCH, H. **Antibase Version 4.0 - The Natural Compound IdentifierAntibase Version 4.0 - The Natural Compound Identifier**Wiley-VCH Verlag GmbH & Co. KGaA, , 2012.

LARIVE, C. K.; JAYAWICKRAMA, D.; ORFI, L. Quantitative Analysis of Peptides with NMR Spectroscopy. **Applied Spectroscopy**, v. 51, n. 10, p. 1531–1536, 1997.

LIMA, J. S. et al. Genetic Diversity of Colletotrichum spp. an Endophytic Fungi in a Medicinal Plant, Brazilian Pepper Tree. **ISRN Microbiology**, v. 2012, p. 1–7, 2012.

LINARES, J. F. et al. Antibiotics as intermicrobial signaling agents instead of weapons. **Proceedings of the National Academy of Sciences**, v. 103, n. 51, p. 19484–19489, 2006.

LIU, C. et al. Stimulation of nisin production from whey by a mixed culture of Lactococcus lactis and Saccharomyces cerevisiae. **Applied Biochemistry and Biotechnology**, v. 131, n. 1–3, p. 751–761, 2006.

LIU, W. C. et al. Production of polyketides with anthelmintic activity by the fungus Talaromyces wortmannii using one strain-many compounds (OSMAC) method. **Phytochemistry Letters**, v. 18, p. 157–161, 2016.

LIU, X. et al. Broad range chemical profiling of natural deep eutectic solvent extracts using a high performance thin layer chromatography–based method. **Journal of Chromatography A**, v. 1532, p. 198–207, 2018.

LOCEY, K. J.; LENNON, J. T. Scaling laws predict global microbial diversity. **Proceedings of the National Academy of Sciences**, v. 113, n. 21, p. 5970–5975, 2016.

LOPEZ-MEDINA, E. et al. Candida albicans Inhibits Pseudomonas aeruginosa Virulence through Suppression of Pyochelin and Pyoverdine Biosynthesis. **PLoS Pathogens**, v. 11, n. 8, p. 1–34, 2015.

LU, F. T. et al. Antitumour activity of 3-nitropropionic acid from Phomopsis sp. and optimization of fermentation conditions. **Letters in Applied Microbiology**, v. 61, n. 2, p. 165–170, 2015.

MAIER, A. et al. Actinomycetales bacteria from a spruce stand: Characterization and effects on growth of root symbiotic and plant parasitic soil fungi in dual culture. **Mycological Progress**, v. 3, n. 2, p. 129–136, 2004.

MALDONADO, A.; RUIZ-BARBA, J. L.; JIMÉNEZ-DÍAZ, R. Production of plantaricin NC8 by Lactobacillus plantarum NC8 is induced in the presence of different types of gram-positive bacteria. **Archives of Microbiology**, v. 181, n. 1, p. 8–16, 2004.

MALZ, F.; JANCKE, H. Validation of quantitative NMR. **Journal of Pharmaceutical and Biomedical Analysis**, v. 38, n. 5 SPEC. ISS., p. 813–823, 2005.

MAN, L. L.; MENG, X. C.; ZHAO, R. H. Induction of plantaricin MG under co-culture with certain lactic acid bacterial strains and identification of LuxS mediated quorum sensing system in Lactobacillus plantarum KLDS1.0391. **Food Control**, v. 23, n. 2, p. 462–469, 2012.

MANICI, L. M.; CAPUTO, F.; SACCÀ, M. L. Secondary metabolites released into the rhizosphere by Fusarium oxysporum and Fusarium spp. as underestimated component of nonspecific replant disease. **Plant and Soil**, v. 415, n. 1–2, p. 85–98, 2017.

MARKLEY, J. L. et al. The future of NMR-based metabolomics. **Current Opinion in Biotechnology**, v. 43, p. 34–40, 2017.

MARMANN, A. et al. Co-cultivation - A powerful emerging tool for enhancing the chemical diversity of microorganisms. **Marine Drugs**, v. 12, n. 2, p. 1043–1065, 2014.

MARSTON, A.; KISSLING, J.; HOSTETTMANN, K. A rapid TLC bioautographic method for the detection of acetylcholinesterase and butyrylcholinesterase inhibitors in plants. **Phytochemical Analysis**, v. 13, n. 1, p. 51–54, 2002.

MARTIN, N. et al. Aroma Compound Production in Cheese Curd by Coculturing with Selected Yeast and Bacteria. **Journal of Dairy Science**, v. 84, n. 10, p. 2125–2135, 2001.

MCALESTER, G.; O'GARA, F.; MORRISSEY, J. P. Signal-mediated interactions between Pseudomonas aeruginosa and Candida albicans. **Journal of Medical Microbiology**, v. 57, n. 5, p. 563–569, 2008.

MEARNS-SPRAGG, A. et al. Cross-species induction and enhancement of antimicrobial activity produced by epibiotic bacteria from marine algae and invertebrates, after exposure to terrestrial bacteria.

Letters in applied microbiology, v. 27, n. 3, p. 142–146, 1998.

MECA, G. et al. Antibacterial effect of the bioactive compound beauvericin produced by Fusarium proliferatum on solid medium of wheat. **Toxicon**, v. 56, n. 3, p. 349–354, 2010.

MESAK, L. R.; MIAO, V.; DAVIES, J. Effects of subinhibitory concentrations of antibiotics on SOS and DNA repair gene expression in Staphylococcus aureus. **Antimicrobial Agents and Chemotherapy**, v. 52, n. 9, p. 3394–3397, 2008.

MEYER, V.; STAHL, U. The influence of co-cultivation on expression of the antifungal protein in Aspergillus giganteus. **Journal of Basic Microbiology**, v. 43, n. 1, p. 68–74, 2003.

MICHIELSE, C. B.; REP, M. Pathogen profile update: Fusarium oxysporum. **Molecular Plant Pathology**, v. 10, n. 3, p. 311–324, 2009.

MILOJKOVIĆ-OPSENICA, D. et al. Planar chromatographic systems in pattern recognition and fingerprint analysis. **Chromatographia**, v. 76, n. 19–20, p. 1239–1247, 2013.

MINERDI, D. et al. Volatile organic compounds: A potential direct long-distance mechanism for antagonistic action of Fusarium oxysporum strain MSA 35. **Environmental Microbiology**, v. 11, n. 4, p. 844–854, 2009.

MOODY, S. C. Microbial co-culture: harnessing intermicrobial signaling for the production of novel antimicrobials. **Future Microbiology**, v. 9, n. 5, p. 575–8, 2014.

MOREE, W. J. et al. Interkingdom metabolic transformations captured by microbial imaging mass spectrometry. **Proceedings of the National Academy of Sciences**, v. 109, n. 34, p. 13811–13816, 2012.

MOREE, W. J. et al. Imaging Mass Spectrometry of a Coral Microbe Interaction with Fungi. **Journal of Chemical Ecology**, v. 39, n. 7, p. 1045–1054, 2013.

MORLOCK, G. E.; RISTIVOJEVIC, P.; CHERNETSOVA, E. S. Combined multivariate data analysis of high-performance thin-layer chromatography fingerprints and direct analysis in real time mass spectra for profiling of natural products like propolis. **Journal of Chromatography A**, v. 1328, p. 104–112, 2014.

MÜLLER, M. E. H. et al. Cocultivation of phytopathogenic Fusarium and Alternaria strains affects fungal growth and mycotoxin production. **Journal of Applied Microbiology**, v. 113, n. 4, p. 874–887, 2012.

MUSHTAQ, M. Y. et al. Extraction for metabolomics: Access to the metabolome. **Phytochemical Analysis**, v. 25, n. 4, p. 291–306, 2014.

NARVHUS, J. A.; GADAGA, T. H. file:///C:/Users/denis/Downloads/doi_10.1016_S0168-1605(03)00247-2.pdf. **International Journal of Food Microbiology**, v. 86, n. 1–2, p. 51–60, 2003.

NETT, M.; IKEDA, H.; MOORE, B. S. Genomic basis for natural product biosynthetic diversity in the actinomycetes. **Natural Product Reports**, v. 26, n. 11, p. 1362, 2009.

NETZKER, T. et al. Microbial communication leading to the activation of silent fungal secondary metabolite gene clusters. **Frontiers in Microbiology**, v. 6, p. 1–13, 2015.

NEWMAN, D. J.; CRAGG, G. M. Natural Products as Sources of New Drugs from 1981 to 2014. **Journal of Natural Products**, v. 79, n. 3, p. 629–661, 2016.

NG, J. et al. Dereplication and de novo sequencing of nonribosomal peptides. **Nature Methods Methods**, v. 6, n. 8, p. 569–599, 2009.

NICHOLSON, J. K.; LINDON, J. C. System Biology: Metabolomics. **The FEBS journal**, v. 455, p. 1054–1056, 2008.

NIELSEN, K. F. et al. Dereplication of microbial natural products by LC-DAD-TOFMS. **Journal of Natural Products**, v. 74, n. 11, p. 2338–2348, 2011.

NIELSEN, K. F.; LARSEN, T. O. The importance of mass spectrometric dereplication in fungal secondary metabolite analysis. **Frontiers in Microbiology**, v. 6, n. FEB, p. 1–15, 2015.

NONAKA, K. et al. Enhancement of metabolites productivity of Penicillium pinophilum FKI-5653, by co-culture with Trichoderma harzianum FKI-5655. **Journal of Antibiotics**, v. 64, n. 12, p. 769–774, 2011.

NOTZ, R.; MAURHOFER, M.; DUBACH, H. Fusaric acid-producing strains of Fusarium oxysporum alter 2, 4-diacetylphloroglucinol biosynthetic gene expression in Pseudomonas fluorescens CHA0 in vitro and. **Applied and Environmental Microbiology**, v. 68, n. 5, p. 2229–2235, 2002.

OH, D. C. et al. Induced production of emericellamides A and B from the marine-derived fungus Emericella sp. in competing co-culture. **Journal of Natural Products**, v. 70, n. 4, p. 515–520, 2007.

OHNISHI, Y. et al. Genome sequence of the streptomycin-producing microorganism Streptomyces griseus IFO 13350. **Journal of Bacteriology**, v. 190, n. 11, p. 4050–4060, 2008.

OJIKA, M. et al. The second Phytophthora mating hormone defines interspecies biosynthetic crosstalk. **Nature Chemical Biology**, v. 7, n. 9, p. 591–593, 2011.

OLA, A. R. B. et al. Inducing Secondary Metabolite Production by the Endophytic Fungus Fusarium tricinctum through Coculture with Bacillus subtilis. **Journal of Natural Products**, v. 76, n. 11, p. 2094–2099, 2013.

OLIVER, S. G. et al. Systematic functional analysis of the yeast genome. **Trends in Biotechnology**, v. 16, n. 9, p. 373–378, 1998.

OMURA, S. et al. Genome sequence of an industrial microorganism Streptomyces avermitilis: Deducing the ability of producing secondary metabolites. **Proceedings of the National Academy of Sciences**, v. 98, n. 21, p. 12215–12220, 2001.

ONAKA, H. et al. Goadsporin, a Chemical Substance which Promotes Secondary Metabolism and Morphogenesis in Streptomycetes. I. Purification and Characterization. **The Journal of Antibiotics**, v.

54, n. 12, p. 1036–1044, 2001.

ONAKA, H. et al. Mycolic acid-containing bacteria induce natural-product biosynthesis in Streptomyces species. **Applied and Environmental Microbiology**, v. 77, n. 2, p. 400–406, 2011.

ONAKA, H. Novel antibiotic screening methods to awaken silent or cryptic secondary metabolic pathways in actinomycetes. **The Journal of Antibiotics**, v. 70, p. 865–870, 2017.

OOIJKAAS, L. P. et al. Medium optimization for spore production of Coniothyrium minitans using statistically-based experimental designs. **Biotechnology and Bioengineering**, v. 64, n. 1, p. 92–100, 1999.

PANKEY, G. A.; SABATH, L. D. Clinical Relevance of Bacteriostatic versus Bactericidal Mechanisms of Action in the Treatment of Gram-Positive Bacterial Infections. **Clinical Infectious Diseases**, v. 38, n. 6, p. 864–870, 2004.

PARK, H. B. et al. Glionitrin A , an Antibiotic-Antitumor Metabolite Derived from Competitive Interaction. **Journal of Natural Products**, v. 72, p. 248–252, 2009.

PARKINSON, D.; THOMAS, A. A COMPARISON OF METHODS FOR THE ISOLATION OF FUNGI FROM RHIZOSPHERES. **Canadian Journal of Microbiology**, v. 11, n. 6, p. 1001–1007, 1965.

PAULI, G. F. et al. Quantitative 1H NMR. Development and potential of an analytical method: An update. **Journal of Natural Products**, v. 75, n. 4, p. 834–851, 2012.

PAULI, G. F. et al. Importance of purity evaluation and the potential of quantitative 1H NMR as a purity assay. **Journal of Medicinal Chemistry**, v. 57, n. 22, p. 9220–9231, 2014.

PAULI, G. F.; JAKI, B. U.; LANKIN, D. C. Quantitative 1H NMR: Development and Potential of a Method for Natural Products Analysis. **Journal of Natural Products**, v. 68, n. 1, p. 133–149, 2005.

PETERSON, S. B. et al. Peptidoglycan from Bacillus cereus mediates commensalism with rhizosphere bacteria from the Cytophaga-Flavobacterium group. **Applied and Environmental Microbiology**, v. 72, n. 8, p. 5421–5427, 2006.

PETTIT, R. K. Mixed fermentation for natural product drug discovery. **Applied Microbiology and Biotechnology**, v. 83, n. 1, p. 19–25, 2009.

PETTIT, R. K. et al. Isolation of human cancer cell growth inhibitory, antimicrobial lateritin from a mixed fungal culture. **Planta Medica**, v. 76, n. 5, p. 500–501, 2010.

PETTIT, R. K. Culturability and Secondary Metabolite Diversity of Extreme Microbes: Expanding Contribution of Deep Sea and Deep-Sea Vent Microbes to Natural Product Discovery. **Marine Biotechnology**, v. 13, n. 1, p. 1–11, 2011a.

PETTIT, R. K. Small-molecule elicitation of microbial secondary metabolites. **Microbial Biotechnology**, v. 4, n. 4, p. 471–478, 2011b.

PEZZUTO, J. M. **Plant-derived anticancer agentsBiochemical Pharmacology**, 1997.

PHANSALKAR, R. S. et al. Evolution of Quantitative Measures in NMR: Quantum Mechanical qHNMR Advances Chemical Standardization of a Red Clover (Trifolium pratense) Extract. **Journal of Natural Products**, v. 80, n. 3, p. 634–647, 2017.

PILATTI, F. K. et al. Metabolomics of Ulva lactuca Linnaeus (Chlorophyta) exposed to oil fuels: Fourier transform infrared spectroscopy and multivariate analysis as tools for metabolic fingerprint. **Marine Pollution Bulletin**, v. 114, n. 2, p. 831–836, 2017.

PIMENTA, E. F. et al. Use of experimental design for the optimization of the production of new secondary metabolites by two Penicillium species. **Journal of Natural Products**, v. 73, n. 11, p. 1821–1832, 2010.

POLONIO, J. C. et al. 3-Nitropropionic acid production by the endophytic Diaporthe citri: Molecular taxonomy, chemical characterization, and quantification under pH variation. **Fungal Biology**, v. 120, n. 12, p. 1600–1608, 2016.

PRADO, R. M. et al. Metabolomics and Agriculture : What Can Be Done ? **mSystems**, v. 3, n. 2, p. 2–4, 2018.

PRINCE, K. A. et al. Anti-Mycobacterium tuberculosis activity of fungus Phomopsis stipata. **Brazilian Journal of Microbiology**, v. 55, p. 224–229, 2012.

QUEIROZ, E. F.; WOLFENDER, J.-L.; HOSTETTMANN, K. Modern Approaches in the Search for New Lead Antiparasitic Compounds from Higher Plants. **Current Drug Targets**, v. 10, n. 3, p. 202–211, 2009.

RAFIEI, A.; SLENO, L. Comparison of peak-picking workflows for untargeted liquid chromatography/high-resolution mass spectrometry metabolomics data analysis. **Rapid Communications in Mass Spectrometry**, v. 29, n. 1, p. 119–127, 2014.

RATEB, M. E. et al. Diverse metabolic profiles of a Streptomyces strain isolated from a hyper-arid environment. **Journal of Natural Products**, v. 74, n. 9, p. 1965–1971, 2011.

RATEB, M. E. et al. Induction of diverse secondary metabolites in Aspergillus fumigatus by microbial co-culture. **RSC Advances**, v. 3, n. 34, p. 14444, 2013.

RENOUF, V. et al. Interactions between Brettanomyces bruxellensis and other yeast species during the initial stages of winemaking. **Journal of Applied Microbiology**, v. 100, n. 6, p. 1208–1219, 2006.

RIGALI, S. et al. Feast or famine: The global regulator DasR links nutrient stress to antibiotic production by Streptomyces. **EMBO Reports**, v. 9, n. 7, p. 670–675, 2008.

RIZZO, V.; PINCIROLI, V. Quantitative NMR in synthetic and combinatorial chemistry. **Journal of Pharmaceutical and Biomedical Analysis**, v. 38, n. 5 SPEC. ISS., p. 851–857, 2005.

ROJO-BEZARES, B. et al. Coculture-inducible bacteriocin activity of Lactobacillus plantarum strain J23

isolated from grape must. **Food Microbiology**, v. 24, n. 5, p. 482–491, 2007.

ROMANO, S. et al. Extending the “one strain many compounds” (OSMAC) principle to marine microorganisms. **Marine Drugs**, v. 16, n. 7, p. 1–29, 2018.

ROSS, C. et al. Biosynthesis of antifungal and antibacterial polyketides by Burkholderia gladioli in coculture with Rhizopus microsporus. **Mycoses**, v. 57, n. s3, p. 48–55, 2014.

ROZE, L. V et al. The initiation and pattern of spread of histone H4 acetylation parallel the order of transcriptional activation of genes in the aflatoxin cluster. **Molecular Microbiology**, v. 66, n. 3, p. 713–726, 2007.

RUNDLOF, T. et al. Survey and qualification of internal standards for quantification by 1H NMR spectroscopy. **Journal of Pharmaceutical and Biomedical Analysis**, v. 52, n. 5, p. 645–651, 2010.

RUTLEDGE, P. J.; CHALLIS, G. L. Discovery of microbial natural products by activation of silent biosynthetic gene clusters. **Nature Reviews Microbiology**, v. 13, n. 8, p. 509–523, 2015.

RYAN, R. P. et al. Interspecies signalling via the Stenotrophomonas maltophilia diffusible signal factor influences biofilm formation and polymyxin tolerance in Pseudomonas aeruginosa. **Molecular Microbiology**, v. 68, n. 1, p. 75–86, 2008.

SANGER, F.; NICKLEN, S.; COULSON, A. R. DNA sequencing with chain-terminating inhibitors. **Proceedings of the National Academy of Sciences**, v. 74, n. 12, p. 5463–5467, 1977.

SAVOIE, J. M.; MATA, G. The antagonistic action of Trichoderma sp. hyphae to Lentinula edodes hyphae changes lignocellulotytic activities during cultivation in wheat straw. **World Journal of Microbiology and Biotechnology**, v. 15, n. 3, p. 369–373, 1999.

SAVORANI, F.; TOMASI, G.; ENGELSEN, S. B. icoshift: A versatile tool for the rapid alignment of 1D NMR spectra. **Journal of Magnetic Resonance**, v. 202, n. 2, p. 190–202, 2010.

SCHAKER, P. D. C. et al. Metabolome Dynamics of Smutted Sugarcane Reveals Mechanisms Involved in Disease Progression and Whip Emission. **Frontiers in Plant Science**, v. 8, n. May, p. 1–17, 2017.

SCHERLACH, K.; HERTWECK, C. Triggering cryptic natural product biosynthesis in microorganisms. **Organic & Biomolecular Chemistry**, v. 7, n. 9, p. 1753, 2009.

SCHNEIDER, J. et al. Streptomycin-induced expression in Bacillus subtilis of YtnP, a lactonase-homologous protein that inhibits development and streptomycin production in Streptomyces griseus. **Applied and Environmental Microbiology**, v. 78, n. 2, p. 599–603, 2012.

SCHOUTEN, A. et al. Defense responses of Fusarium oxysporum to 2,4-diacetylphloroglucinol, a broad-spectrum antibiotic produced by Pseudomonas fluorescens. **Molecular plant-microbe interactions: MPMI**, v. 17, n. 11, p. 1201–1211, 2004.

SCHOUTEN, A. et al. Involvement of the ABC transporter BcAtrB and the laccase BcLCC2 in defence of Botrytis cinerea against the broad-spectrum antibiotic 2,4- diacetylphloroglucinol. **Environmental**

Microbiology, v. 10, n. 5, p. 1145–1157, 2008.

SCHROECKH, V. et al. Intimate bacterial-fungal interaction triggers biosynthesis of archetypal polyketides in Aspergillus nidulans. **Proceedings of the National Academy of Sciences**, v. 106, n. 34, p. 14558–14563, 2009.

SCHWARZ, M. et al. 3-Hydroxypropionic acid as a nematicidal principle in endophytic fungi. **Phytochemistry**, v. 65, n. 15, p. 2239–2245, 2004.

SCORE, A. J.; PALFREYMAN, J. W.; WHITE, N. A. Extracellular phenoloxidase and peroxidase enzyme production during interspecific fungal interactions. **International Biodeterioration and Biodegradation**, v. 39, n. 2–3, p. 225–233, 1997.

SCOTT, J. J. et al. Bacterial protection of beetle-fungus mutualism. **Science**, v. 322, n. 5898, p. 63, 2008.

SELEGATO, D. M. et al. New dereplication method applied to NMR-based metabolomics on different fusarium species isolated from Rhizosphere of Senna spectabilis. **Journal of the Brazilian Chemical Society**, v. 27, n. 8, 2016a.

SELEGATO, D. M. et al. New Dereplication Method Applied to NMR-Based Metabolomics on Different. **Journal of the Brazilian Chemical Society**, v. 0027, n. 008, p. 1–11, 2016b.

SELEGATO, D. M. et al. Update: Biological and chemical aspects of Senna spectabilis. **Journal of the Brazilian Chemical Society**, v. 28, n. 3, 2017.

SERRANO, R. et al. Co-culturing of fungal strains against Botrytis cinerea as a model for the induction of chemical diversity and therapeutic agents. **Frontiers in Microbiology**, v. 8, p. 649–664, 2017.

SHAH, I. M. et al. A Eukaryotic-like Ser/Thr Kinase Signals Bacteria to Exit Dormancy in Response to Peptidoglycan Fragments. **Cell**, v. 135, n. 3, p. 486–496, 2008.

SHANK, E. A.; KOLTER, R. New developments in microbial interspecies signaling. **Current Opinion in Microbiology**, v. 12, n. 2, p. 205–214, 2009.

SHIMIZU, H. et al. Nisin production by a mixed-culture system consisting of Lactococcus lactis and Kluyveromyces marxianus. **Applied and Environmental Microbiology**, v. 65, n. 7, p. 3134–3141, 1999.

SHWETA, S. et al. Endophytic fungal strains of Fusarium solani, from Apodytes dimidiata E. Mey. ex Arn (Icacinaceae) produce camptothecin, 10-hydroxycamptothecin and 9-methoxycamptothecin. **Phytochemistry**, v. 71, n. 1, p. 117–122, 2010.

SIMMLER, C. et al. Universal quantitative NMR analysis of complex natural samples. **Current Opinion in Biotechnology**, v. 25, p. 51–59, 2014.

SKINDERSOE, M. E. et al. Effects of antibiotics on quorum sensing in Pseudomonas aeruginosa. **Antimicrobial Agents and Chemotherapy**, v. 52, n. 10, p. 3648–3663, 2008.

SLATTERY, M.; RAJBHANDARI, I.; WESSON, K. Competition-Mediated Antibiotic Induction in the

Marine Bacterium Streptomyces tenjimariensis. **Microbial Ecology**, v. 41, p. 90–96, 2001.

SODINI, I.; LATRILLE, E.; CORRIEU, G. Identification of interacting mixed cultures of lactic acid bacteria by their exclusion from a model predicting the acidifying activity of non-interacting mixed cultures. **Applied microbiology and biotechnology**, v. 54, n. 5, p. 715–8, 2000.

SON, S. W. et al. Bikaverin and fusaric acid from Fusarium oxysporum show antioomycete activity against Phytophthora infestans. **Journal of Applied Microbiology**, v. 104, n. 3, p. 692–698, 2008.

SONDERGAARD, T. E. et al. Fast Screening of Antibacterial Compounds from Fusaria. **Toxins**, v. 8, p. 355–364, 2016.

SONG, J. J.; YEE, N. K. A Concise Synthesis of Fusaric Acid and (S)-(+)-Fusarinolic Acid. **The Journal of Organic Chemistry**, v. 66, n. 2, p. 605–608, 2001.

SONNENBICHLER, J.; DIETRICH, J.; PEIPP, H. Secondary Fungal Metabolites and Their Biological Activities, V. Investigations Concerning the Induction of the Biosynthesis of Toxic Secondary Metabolites in Basidiomycetes. **Biological Chemistry Hoppe-Seyler**, v. 375, n. 1, p. 71–80, 1994.

SOUKUP, A. A. et al. Overexpression of the Aspergillus nidulans histone 4 acetyltransferase EsaA increases activation of secondary metabolite production. **Molecular Microbiology**, v. 86, n. 2, p. 314–330, 2012.

STARNER, T. D. et al. Subinhibitory concentrations of azithromycin decrease nontypeable Haemophilus influenzae biofilm formation and diminish established biofilms. **Antimicrobial Agents and Chemotherapy**, v. 52, n. 1, p. 137–145, 2008.

STERMITZ, F. R. et al. Synergy in a medicinal plant: Antimicrobial action of berberine potentiated by 5'-methoxyhydnocarpin, a multidrug pump inhibitor. **Proceedings of the National Academy of Sciences**, v. 97, n. 4, p. 1433–1437, 2000.

STIERLE, A. A. et al. The Berkeleylactones, Antibiotic Macrolides from Fungal Coculture. **Journal of Natural Products**, v. 80, n. 4, p. 1150–1160, 2017.

STRAIGHT, P. D.; WILLEY, J. M.; KOLTER, R. Interactions between Streptomyces coelicolor and Bacillus subtilis: Role of surfactants in raising aerial structures. **Journal of Bacteriology**, v. 188, n. 13, p. 4918–4925, 2006.

SUD, M. et al. LIPID MAPS-Nature Lipidomics Gateway: An Online Resource for Students and Educators Interested in Lipids. **J Chem Educ**, v. 89, n. 2, p. 291–292, 2012.

SUNG, A. A.; GROMEK, S. M.; BALUNAS, M. J. Upregulation and identification of antibiotic activity of a marine-derived Streptomyces sp. via co-cultures with human pathogens. **Marine Drugs**, v. 15, n. 8, 2017.

TABASCO, R. et al. Lactobacillus acidophilus La-5 increases lactacin B production when it senses live target bacteria. **International Journal of Food Microbiology**, v. 132, n. 2–3, p. 109–116, 2009.

TADA, S. et al. Fed-batch coculture of Lactobacillus kefiranofaciens with Saccharomyces cerevisiae for effective production of kefiran. **Journal of Bioscience and Bioengineering**, v. 103, n. 6, p. 557–562, 2007.

TAO, K. et al. Biodegradation of crude oil by a defined co-culture of indigenous bacterial consortium and exogenous Bacillus subtilis. **Bioresource Technology**, v. 224, p. 327–332, 2017.

TARKKA, M. T.; SARNIGUET, A.; FREY-KLETT, P. Inter-kingdom encounters: Recent advances in molecular bacterium - Fungus interactions. **Current Genetics**, v. 55, n. 3, p. 233–243, 2009.

TESFAW, A.; ASSEFA, F. Co-culture: A great promising method in single cell protein production. **Biotechnology and Molecular Biology Reviews**, v. 9, n. 2, p. 12–20, 2014.

THOLL, D. et al. Practical approaches to plant volatile analysis. **Plant Journal**, v. 45, n. 4, p. 540–560, 2006.

TIAN, W. et al. Cytoskyrin C, an unusual asymmetric bisanthraquinone with cage-like skeleton from the endophytic fungus Diaporthe sp. **Fitoterapia**, v. 128, n. May, p. 253–257, 2018.

TODOROV, S. D. Bacteriocins from Lactobacillus plantarum production, genetic organization and mode of action: produção, organização genética e modo de ação. **Brazilian Journal of Microbiology**, v. 40, n. 2, p. 209–221, 2009.

TOMASI, G.; VAN DEN BERG, F.; ANDERSSON, C. Correlation optimized warping and dynamic time warping as preprocessing methods for chromatographic data. **Journal of Chemometrics**, v. 18, n. 5, p. 231–241, 2004.

TORRES, P. S. et al. Controlled synthesis of the DSF cell-cell signal is required for biofilm formation and virulence in Xanthomonas campestris. **Environmental Microbiology**, v. 9, n. 8, p. 2101–2109, 2007.

TRAXLER, M. F. et al. Interspecies interactions stimulate diversification of the Streptomyces coelicolor secreted metabolome. **mBio**, v. 4, n. 4, p. 459–13, 2013.

TRISCHMAN, J. A. et al. Competitive induction and enhancement of indole and a diketopiperazine in marine bacteria. **Marine Biotechnology**, v. 6, n. 3, p. 215–220, 2004.

TURPIN, P. E. et al. The effect of Streptomycetes species on the survival of Salmonella in soil. **FEMS Microbiology Ecology**, v. 101, p. 271–280, 1992.

UEDA, K.; BEPPU, T. Antibiotics in microbial coculture. **Journal of Antibiotics**, v. 70, n. 4, p. 361–365, 2017.

VALLIAPPAN, K.; SUN, W.; LI, Z. Marine actinobacteria associated with marine organisms and their potentials in producing pharmaceutical natural products. **Applied Microbiology and Biotechnology**, v. 98, n. 17, p. 7365–7377, 2014.

VAN DEN DOOL, H.; KRATZ, P. D. A generalization of the retention index system including linear temperature programmed gas—liquid partition chromatography. **Journal of Chromatography A**, v. 11,

n. 3, p. 463–471, 1963.

VAN RIJ, E. T. et al. Influence of fusaric acid on phenazine-1-carboxamide synthesis and gene expression of Pseudomonas chlororaphis strain PCL1391. **Microbiology**, v. 151, n. 8, p. 2805–2814, 2005.

VANDERMOLEN, K. M. et al. Evaluation of culture media for the production of secondary metabolites in a natural products screening program. **AMB Express**, v. 3, p. 1–7, 2013.

VENISETTY, R. K.; CIDDI, V. Application of Microbial Biotransformation for the New Drug Discovery Using Natural Drugs as Substrates. **Current Pharmaceutical Biotechnology**, v. 4, n. 3, p. 153–167, 2003.

VESSECCHI, R. et al. Aplicação da Química Quântica Computacional no Estudo de Processes Químicos Envolvidos em Espectrometria de Massas. **Quim. Nova**, v. 31, n. 4, p. 840–853, 2008.

VINALE, F. et al. Harzianic acid, an antifungal and plant growth promoting metabolite from Trichoderma harzianum. **Journal of Natural Products**, v. 72, n. 11, p. 2032–2035, 2009.

VINALE, F. et al. Co-Culture of Plant Beneficial Microbes as Source of Bioactive Metabolites. **Scientific Reports**, v. 7, n. 1, p. 1–12, 2017.

WAGENAAR, M. M. et al. Three new cytochalasins produced by an endophytic fungus in the genus Rhinocladiella. **Journal of Natural Products**, v. 63, n. 12, p. 1692–1695, 2000.

WAGNER, C.; SEFKOW, M.; KOPKA, J. Construction and application of a mass spectral and retention time index database generated from plant GC/EI-TOF-MS metabolite profiles. **Phytochemistry**, v. 62, n. 6, p. 887–900, 2003.

WAKEFIELD, J. et al. Dual induction of new microbial secondary metabolites by fungal bacterial co-cultivation. **Frontiers in Microbiology**, v. 8, p. 1284–1294, 2017.

WANG, J. et al. A New Polusubstituted Benzaldehyde from the co-culture broth of two marine fungi (strains Nos. E33 and K38). **Chemistry of Natural Compounds**, v. 49, n. 5, p. 689–691, 2013.

WANG, L. H. et al. A bacterial cell-cell communication signal with cross-kingdom structural analogues. **Molecular Microbiology**, v. 51, n. 3, p. 903–912, 2004.

WANG, M. et al. Sharing and community curation of mass spectrometry data with Global Natural Products Social Molecular Networking. **Nature Biotechnology**, v. 34, n. 8, p. 828–837, 2016.

WANG, Y. et al. Bioactive metabolites from the endophytic fungus Alternaria alternata. **Fitoterapia**, v. 99, n. 1, p. 153–158, 2014.

WATANABE, R. et al. Quantitative nuclear magnetic resonance spectroscopy based on PULCON methodology: Application to quantification of invaluable marine toxin, okadaic acid. **Toxins**, v. 8, n. 10, p. 1–9, 2016.

WATANABE, R.; SUZUKI, T.; OSHIMA, Y. Development of quantitative NMR method with internal standard for the standard solutions of paralytic shellfish toxins and characterisation of gonyautoxin-5 and gonyautoxin-6. **Toxicon**, v. 56, n. 4, p. 589–595, 2010.

WATANABE, T.; IZAKI, K.; TAKAHASHI, H. New Polyenic Antibiotics Against Gram-positive and -Negative Bacteria. **The Journal of Antibiotics**, v. 35, n. 9, p. 1141–1147, 1982.

WATROUS, J. et al. Mass spectral molecular networking of living microbial colonies. **Proceedings of the National Academy of Sciences**, v. 109, n. 26, p. E1743–E1752 PNAS, 2012.

WEGH, R. S. et al. Non-targeted workflow for identification of antimicrobial compounds in animal feed using bioassay-directed screening in combination with liquid chromatography-high resolution mass spectrometry. **Food Additives and Contaminants - Part A Chemistry, Analysis, Control, Exposure and Risk Assessment**, v. 34, n. 11, p. 1935–1947, 2017.

WEI, H. et al. OSMAC (One Strain Many Compounds) approach in the research of microbial metabolites--a review. **Wei Sheng Wu Xue Bao**, v. 50, n. 6, p. 701–709, 2010.

WEI, H. et al. Sesquiterpenes and other constituents of Xylaria sp. NC1214, a fungal endophyte of the moss Hypnum sp. **Phytochemistry**, v. 118, p. 102–108, 2015.

WHITT, J. et al. Tetramic acid analogues produced by coculture of saccharopolyspora erythraea with fusarium pallidoroseum. **Journal of Natural Products**, v. 77, n. 1, p. 173–177, 2014.

WIDER, G.; DREIER, L. Measuring protein concentrations by NMR spectroscopy. **Journal of the American Chemical Society**, v. 128, n. 8, p. 2571–2576, 2006.

WILLCOTT, M. R. **MestreNovaJournal of the American Chemical Society**Mestrelab Research, , 2009. Disponível em: <http://mestrelab.com/>

WILLIAMS, R. B. et al. Biomolecular Chemistry Dereplication of natural products using minimal NMR data inputs. **Org. Biomol. Chem.**, v. 13, p. 9957–9962, 2015.

WISHART, D. S. et al. HMDB: The human metabolome database. **Nucleic Acids Research**, v. 35, n. SUPPL. 1, p. 521–526, 2007.

WOLFENDER, J.-L. et al. MS-based plant metabolomic approaches for biomarker discovery. **Nat Prod Commun**, v. 4, n. 10, p. 1417–30, 2009.

WOLFENDER, J.-L. et al. Editorial on “Current approaches and challenges for the metabolite profiling of complex natural extracts”. **Journal of Chromatography A**, v. 1382, n. November 2014, p. 135, 2015.

WOLFENDER, J.-L.; QUEIROZ, E. F.; HOSTETTMANN, K. The importance of hyphenated techniques in the discovery of new lead compounds from nature. **Expert Opinion on Drug Discovery**, v. 1, n. 3, p. 237–260, 2006.

WORLEY, B.; POWERS, R. **Multivariate Analysis in MetabolomicsCurrent Metabolomics**, 2013. Disponível em: <http://www.eurekaselect.com/node/105190/article>

XU, Y. et al. Cytotoxic and antihaptotactic beauvericin analogues from precursor-directed biosynthesis with the insect pathogen Beauveria bassiana ATCC 7159. **Journal of Natural Products**, v. 70, n. 9, p. 1467–1471, 2007.

YAKOVLEVA, E. P.; BULGAKOVA, T. N. Formation of Amphotericin B in Mixed Cultures. **Pharmaceutical Chemistry Journal**, v. 12, n. 11, p. 1483–1488, 1978.

YAMANAKA, K. et al. Desferrioxamine E produced by Streptomyces griseus stimulates growth and development of Streptomyces tanashiensis. **Microbiology**, v. 151, n. 9, p. 2899–2905, 2005.

YANG, J. Y. et al. Molecular networking as a dereplication strategy. **Journal of Natural Products**, v. 76, n. 9, p. 1686–1699, 2013.

YAO, L. et al. Discovery of novel xylosides in co-culture of basidiomycetes Trametes versicolor and Ganoderma applanatum by integrated metabolomics and bioinformatics. **Scientific Reports**, v. 6, n. June, p. 1–13, 2016.

YULIANA, N. D. et al. Metabolomics for bioactivity assessment of natural products. **Phytotherapy Research**, v. 25, n. 2, p. 157–169, 2011.

ZHANG, A. et al. Modern analytical techniques in metabolomics analysis. **The Analyst**, v. 137, n. 2, p. 293–300, 2012.

ZHANG, H. et al. Isolation and identification of the antimicrobial agent beauvericin from the endophytic Fusarium oxysporum 5-19 with NMR and ESI-MS/MS. **BioMed Research International**, v. 2016, p. 1–4, 2016.

ZHANG, H.; STEPHANOPOULOS, G. Co-culture engineering for microbial biosynthesis of 3-amino-benzoic acid in Escherichia coli. **Biotechnology Journal**, v. 11, n. 7, p. 981–987, 2016.

ZHANG, Z. M.; CHEN, S.; LIANG, Y. Z. Baseline correction using adaptive iteratively reweighted penalized least squares. **The Analyst**, v. 135, n. 5, p. 1138, 2010.

ZHOU, B. et al. LC-MS-based metabolomics. **Mol Biosyst**, v. 8, n. 2, p. 470–481, 2012.

ZHU, F. et al. Aspergicin, a new antibacterial alkaloid produced by mixed fermentation of two marine-derived mangrove epiphytic fungi. **Chemistry of Natural Compounds**, v. 47, n. 5, p. 767–769, 2011.

ZHU, F. et al. Structure revision and cytotoxic activity of marinamide and its methyl ester, novel alkaloids produced by co-cultures of two marine-derived mangrove endophytic fungi. **Natural Product Research**, v. 27, n. 21, p. 1960–1964, 2013.

ZHU, F.; LIN, Y. Marinamide, a novel alkaloid and its methyl ester produced by the application of mixed fermentation technique to two mangrove endophytic fungi from the South China Sea. **Chinese Science Bulletin**, v. 51, n. 12, p. 1426–1430, 2006.

ZUCK, K. M.; SHIPLEY, S.; NEWMAN, D. J. Induced Production of N-Formyl Alkaloids from Aspergillus fumigatus by Co-culture with Streptomyces peucetius. **Journal of Natural Products**, v. 74,

p. 1653–1657, 2011.

UNIVERSIDADE ESTADUAL PAULISTA
"JÚLIO DE MESQUITA FILHO"

Nucleus of Bioassays, Biosynthesis and Ecophysiology of natural products

(NuBBE)

DENISE MEDEIROS SELEGATO

SUPPLEMENTARY MATERIAL

METABOLOMICS STUDIES OF PLANT-ASSOCIATED FUNGI – METHOD DEVELOPMENT FOR THE INCREASED PRODUCTION AND IDENTIFICATION OF MICROBIAL BIOACTIVE SECONDARY METABOLITES

Supervisor: Prof. Dr. Ian Castro-Gamboa

Co-supervisor: Dr. Rafael Teixeira Freire

Araraquara, 2019.

CHAPTER 1. DEREPLICATION OF MAJOR SECONDARY METABOLITES BY NUCLEAR MAGNETIC RESONANCE (NMR)

Article title: New dereplication methods applied to NMR-based metabolomics on different *Fusarium* species isolated from *Senna spectabilis*'s rhizosphere (http://dx.doi.org/10.5935/0103-5053.20160139).

Target Journal: Journal of the Brazilian Chemical Society (JBCS).

Status: Published.

Authors: Denise M. Selegato[a], Rafael T. Freire[b], Alberto Tannús[b], Ian Castro-Gamboa[a*]

Affiliations:

[a] Nuclei of Bioassays, Ecophysiology and Biosynthesis of Natural Products (NuBBE), Institute of Chemistry (ICAr) – São Paulo State University (UNESP) – Araraquara, SP**,** Brazil.

[b] Centro de Imagens e Espectroscopia in vivo por Ressonância Magnética (CIERMag), Instituto de Física de São Carlos (IFSC) – University of São Paulo (USP) – São Carlos, SP**,** Brazil.

Figure SM1. Tumor cell cytotoxicity assay of fungal extracts; Evaluation of HCT116 colorectal cancer cells after 72 hours of incubation by the MTT test. Subtitles: (5) *F. solani* CSP-5b, (10) *F. oxysporum* CSP-R18, (13) *F. oxysporum* CSP-19b.

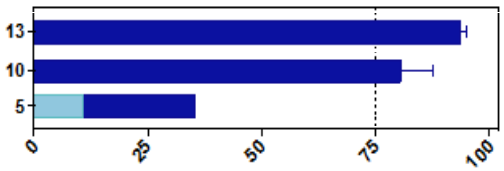

Table SM1. Preliminary Biological Assays of fungal extract of *Fusarium* species isolated from the rhizosphere of *S. spectabilis*. Bioautography of *Cladosporium cladosporioides* and *C. Sphaerospermum* and Acetylcholinesterase Inhibition assay.

Samples	**Antifungal Assay**		**Acetylcholinesterase Inhibition**
	C. cladosporioides	***C. sphaerospermum***	
CSP-R18-1	0.01-0.48*** 0.52-0.57** 0.67-0.74*	0.04-0.27** 0.34-0.43*	Origin-0.24*** 0.27-0.48* 0.66-0.78*
CSP-R18-2	Origin-0.48***	Origin-0.22** 0.22-0.33***	Origin-0.36***
CSP-19b	0.06-0.30*** 0.45-0.79**	0.07-0.26*** 0.31*; 0.43-0.54***	0.38-0.51*** 0.52-0.56*** 0.61-0.69***
CSP-5b	0.13-0.61*** 0.71-0.80**	0.23-0.37* 0.51-0.56*** 0.57-0.62*	0.06-0.30*** 0.61-0.69***
+ standard	origin ***	origin***	origin***

Legend: Samples *F. solani* CSP-5b and *F. oxysporum* CSP-R18 were eluted with $CHCl_3$:MeOH (90:5); Sample *F. oxysporum* CSP-19b was eluted with AcOET:Hex (90:10). Activities: *low, **moderate, *** high***.

Table SM2. Genetic sequences of *Fusarium* species isolated from the rhizosphere of *S. spectabilis*.

CSP	Sequence	Genetic identification	Identity (%)	Access number
5b	TCCCCCACTCCCACCACCACCCCAACGCCTCCACCCCTCTTCGCTT CCAACCCTCCGGAGGTGACCTGCGGACGAATATGATCAGAGGAA GATCTGTTTCTATAATGTTTTTTCTGAGTAAACAAGCAAATAAAT CAAAACTTTCAACAACGGATCTCTTGGCTCTGGCATCGATGAAGA ACGCAGCGAAATGCGATAAGTAATGTGAATTGCAGAATTCAGTG AATCATCGAATCTTTGAACGCACATTGCGCCCGCCAGTATTCTGG CGGGCATGCCTGTTCGAGCGTCATTACAACCCTCAGGCCCCCGGG TCTGGCGTTGGGGATCGGCGGAAGCCCCCTGTGGGCACAACGCC GTCCCCCAAATACAGTGGCGGTCCCGCCGCAGCTTCCATTGCGTA GTAGCTAACACCTCGCAACTGGAGAGCGGCGCGGCCACGCCGTA AAACACCCAACTTCTGAATGTTGACCTCGAATCAGGTAGGAATA CCCGCTGAACTTAAGCATATCATGAGCGGGGAAAGAAAGTATAT G	*Fusarium solani*	99	JX435189.1
R18	GAACCTCCATCAAACGGTAGGAGGTGACCTGCGGAGAATATCAA TCAGCGGAGGACCCGTCCCGAGGAAAACGGGACGGCCCGCCAGA GGACCCCTAAACTCTGTTTCTATATGTAACTTCTGAGTAAAACCA TAAATAAATCAAAACTTTCAACAACGGATCTCTTGGTTCTGGCAT CGATGAAGAACGCAGCAAAATGCGATAAGTAATGTGAATTGCAG AATTCAGTGAATCATCGAATCTTTGAACGCACATTGCGCCCGCCA GTATTCTGGCGGGCATGCCTGTTCGAGCGTCATTTCAACCCTCAA GCACAGCTTGGTGTTGGGACTCGCGTTAATTCGCGTTCCTCAAAT TGATTGGCGGTCACGTCGAGCTTCCATAGCGTAGTAGTAAAACCC TCGTTACTGGTAATCGTCGCGGCCACGCCGTTAAACCCCAACTTC TGAATGTTGACCTCGGATCAGGTAGGAATACCCGCTGAACTTAA GCATATCAATAAGGCGGAGGAA	*Fusarium oxysporum*	99	KP230811.1
19b	GCCAATGCGGTAAGTTCGTCGTAGGTGACCTGCGGAGGACATAT CAATAAGCGGAGGATCCGTCCGCGAGGTGACCTGACGGCCCCCC AGAGGACCCCTAAACTCTGTTTCTATATGTAACTTCTGAGTAAAA CCATAAATAAATCAAAACTTTCAACAACGGATCTCTTGGTTCTGG CATCGATGAAGAACGCAGCAAAATGCGATAAGTAATGTGAATTG CAGAATTCAGTGAATCATCGAATCTTTGAACGCACATTGCGCCCG CCAGTATTCTGGCGGGCATGCCTGTTCGAGCGTCATTTCAACCCT CAAGCACAGCTTGGTGTTGGGACTCGCGTTAATTCGCGTTCCTCA AATTGATTGGCGGTCACGTCGAGCTTCCATAGCGTAGTAGTAAAA CCCTCGTTACTGGTAATCGTCGCGGCCACGCCGTTAAACCCCAAC TTCTGAATGTTGACCTCGGATCAGGTAGGAATACCCGCTGAACTT AAGCATATCAATAAGCGGAGGAA	*Fusarium oxysporum* f. sp. melonis	99	LC055797.1

Figure SM2. One-dimensional TOCSY of *F. oxysporum* crude extract: (A) aliphatic fusaric acid chain, irradiation at δ0.86 (*t*, 3H, *J* 7.0 Hz); (B) aromatic portion of the methylphenylalanine residue of beauvericin, irradiation at δ7.16 (*m*); (C) hydroxy-isovalerate residue of beauvericin, irradiation at δ0.15 (*d*, 3H, *J* 6.9 Hz); (D) aliphatic portion of the methylphenylalanine of beauvericin, irradiation at δ 5.70 (*dd*, 1H, *J* 12.7 and 4.5 Hz).

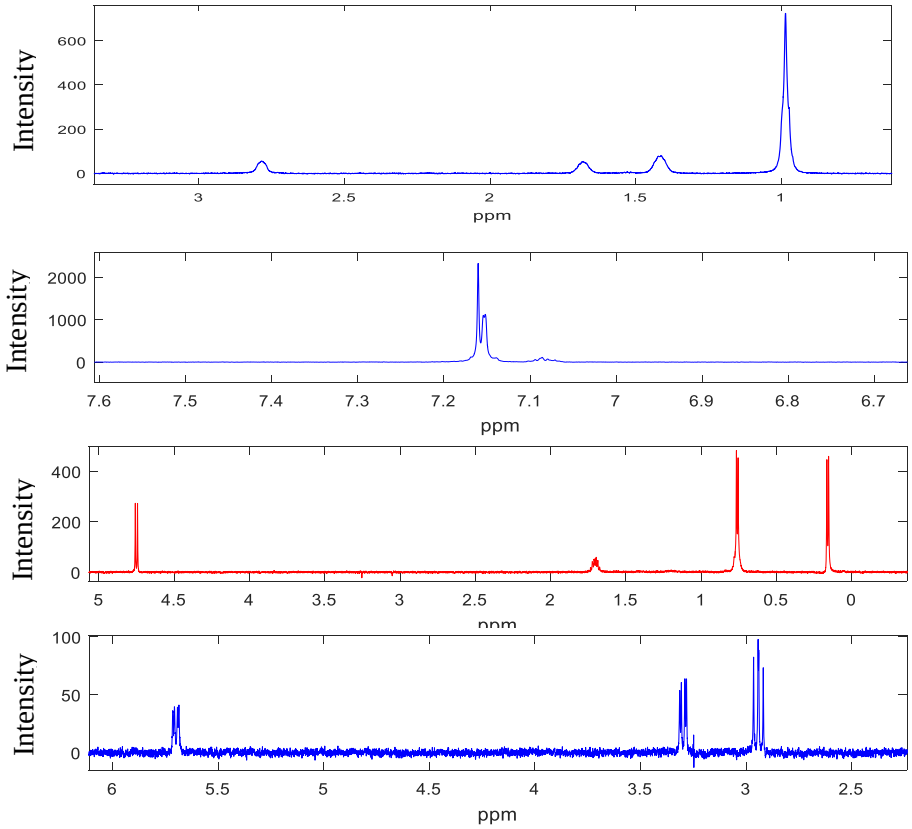

CHAPTER 2. DEREPLICATION OF MAJOR SECONDARY BY MASS SPECTOMETRY (MS)

Article title: Dereplication of Secondary metabolite from *Fusarium* species by mass-spectrometry.

Journal: Journal of the Brazilian Chemical Society (JBCS).

Status: Unpublished.

Authors: Denise M. Selegato[a] and Ian Castro-Gamboa[a*]

Affiliations:

[a] Nuclei of Bioassays, Ecophysiology and Biosynthesis of Natural Products (NuBBE), Institute of Chemistry (ICAr) – São Paulo State University (UNESP) – Araraquara, SP**,** Brazil.

Figure SM3. Chromatograms of *F. oxysporum* CSP-R18 at 254 nm. Experiments were carried out with the use of a basic modifier (0.1% of triethylamine). For this four experiments, we have varied the flow of the mobile phase and the organic solvent gradient.

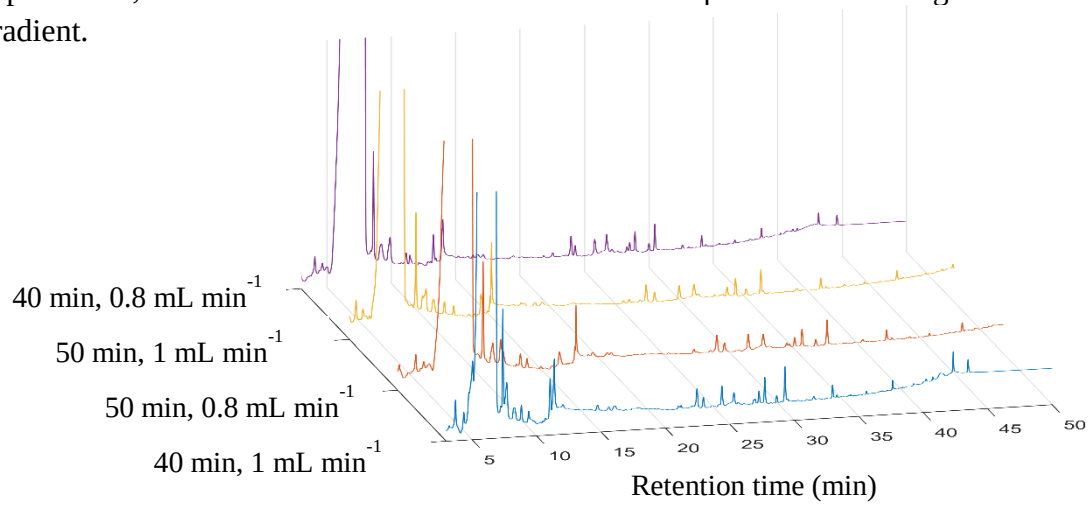

Figure SM4. Linear Regression graph of **(A)** Carbon number x Retention time (min); **(B)** Retention time (min) x Linear retention indices (LRI). Figure SM4 A shows the plot of retention times for all injected hydrocarbons, while Figure SM4 B shows retention times (TR) versus LRI. Both display a satisfactory linear response (R2 of 0.9851 and 0.9845, respectively).

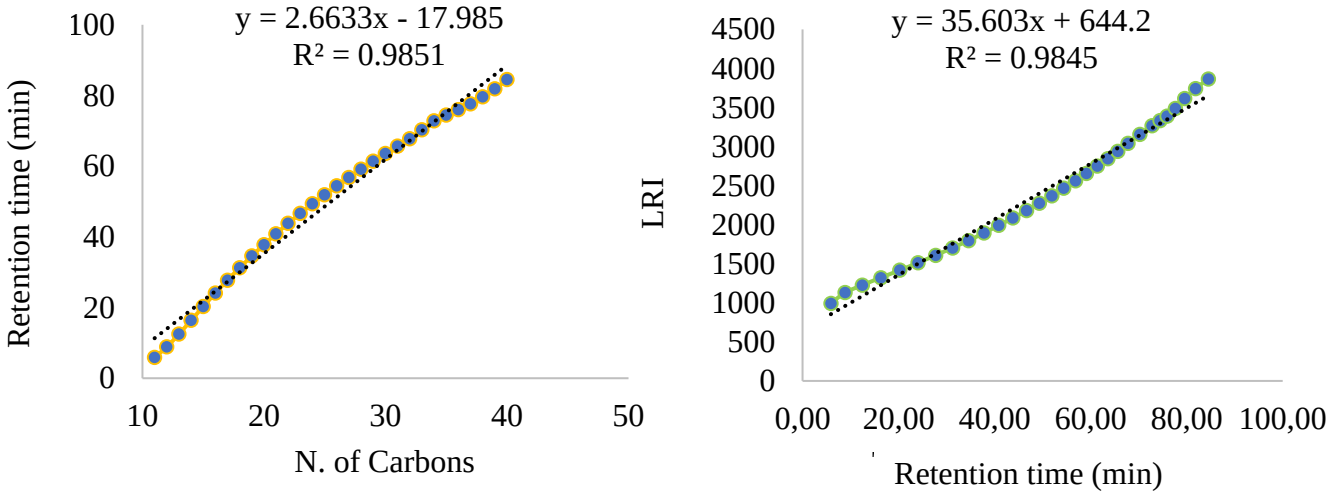

CHAPTER 3. DEREPLICATION BY MS/MS MOLECULAR NETWORING - SELECTION OF BIOLOGICALLY PROMISING FRACTIONS AND IDENTIFICATION OF MAJOR AND MINOR SECONDARY METABOLITES

Article title: MS/MS Molecular Networking Analysis of *Fusarium* species – evaluation of metabolic dynamics and dereplication of bioactive secondary metabolites

Authors: Denise M. Selegato[a], Ian Castro-Gamboa[a*]

Journal: Planta Medica.

Status: Unpublished.

Affiliations:

[a] Nuclei of Bioassays, Ecophysiology and Biosynthesis of Natural Products (NuBBE), São Paulo State University (UNESP) – Araraquara, SP**,** Brazil.

[b] NPPNS, Faculdade de Ciências Farmacêuticas de Ribeirão Preto, Universidade de São Paulo (USP), Ribeirão Preto, São Preto, Brasil.

Figure SM5. Total Ion Chromatogram of fungal fractions from **(A)** *F. oxysporum* CSP-19b; (**B**) *F. solani* CSP-5b; **(C)** *F. oxysporum* CSP-R18.

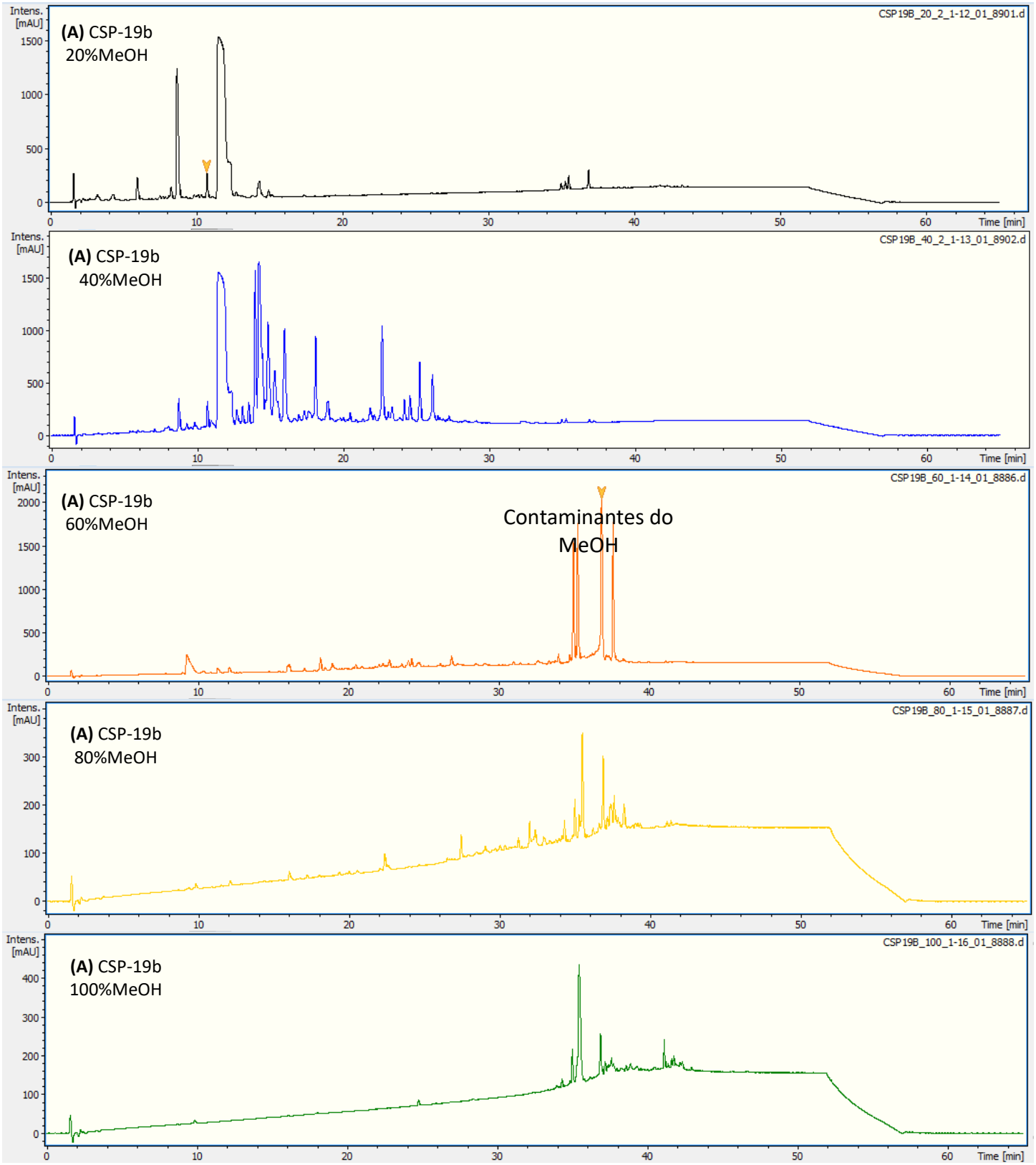

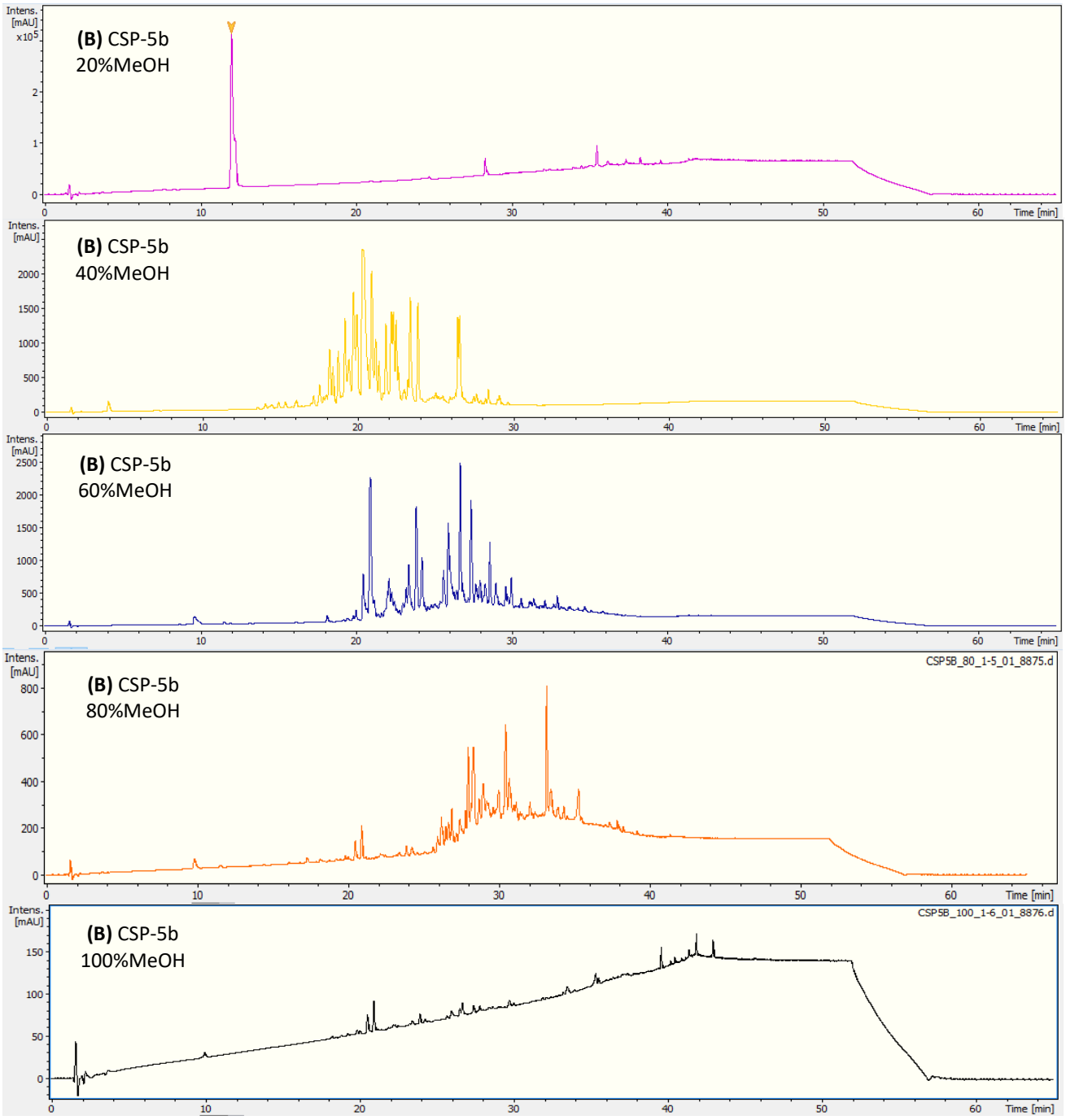
Intens. [mAU] x10^5
(B) CSP-5b
20%MeOH
Time [min]
Intens. [mAU]
(B) CSP-5b
40%MeOH
Time [min]
Intens. [mAU]
(B) CSP-5b
60%MeOH
Time [min]
Intens. [mAU]
CSP5B_80_1-5_01_8875.d
(B) CSP-5b
80%MeOH
Time [min]
Intens. [mAU]
CSP5B_100_1-6_01_8876.d
(B) CSP-5b
100%MeOH
Time [min]

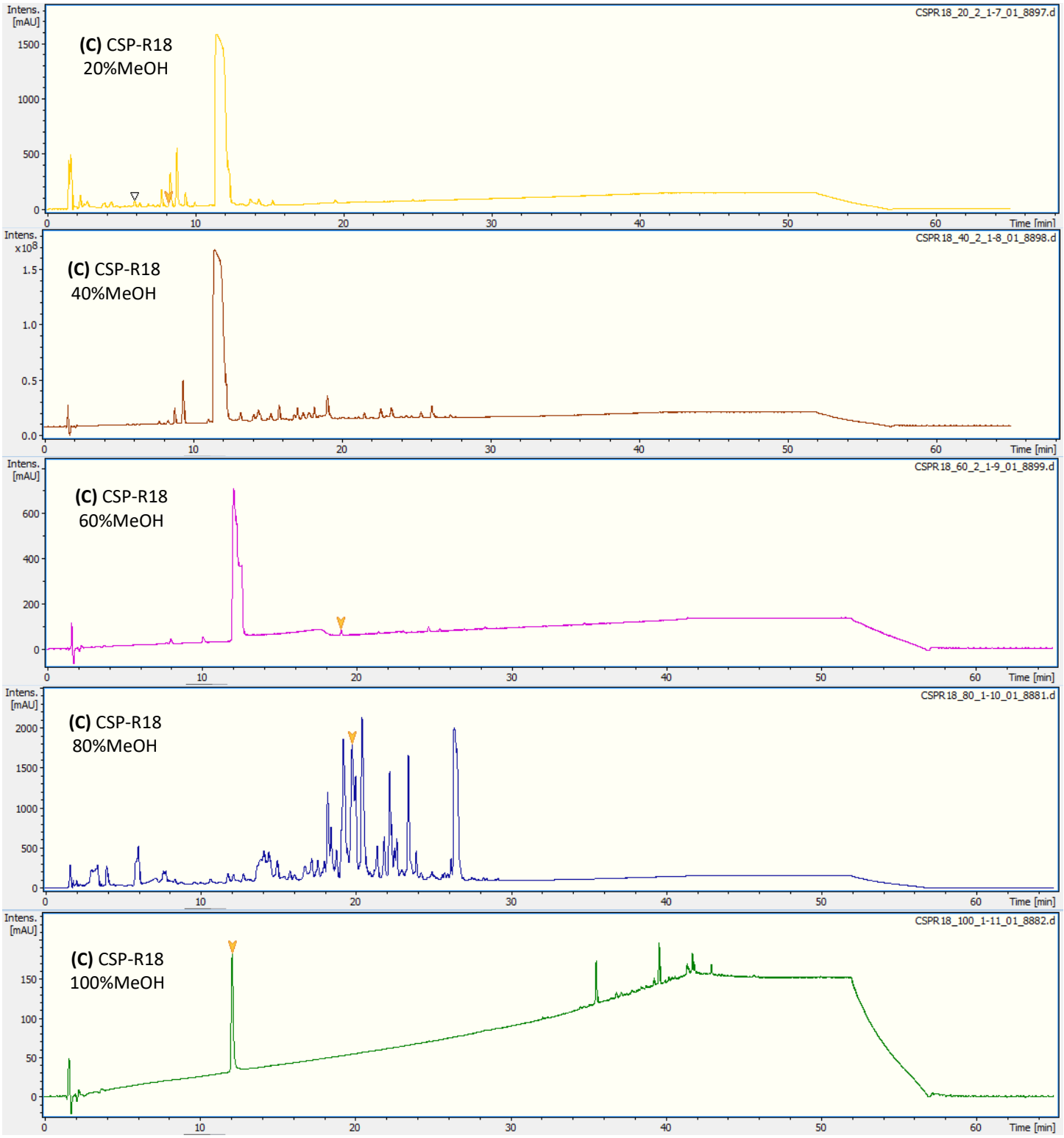
Intens. [mAU]
CSPR18_20_2_1-7_01_8897.d
(C) CSP-R18
20%MeOH
Time [min]
Intens. x10^8
CSPR18_40_2_1-8_01_8898.d
(C) CSP-R18
40%MeOH
Time [min]
Intens. [mAU]
CSPR18_60_2_1-9_01_8899.d
(C) CSP-R18
60%MeOH
Time [min]
Intens. [mAU]
CSPR18_80_1-10_01_8881.d
(C) CSP-R18
80%MeOH
Time [min]
Intens. [mAU]
CSPR18_100_1-11_01_8882.d
(C) CSP-R18
100%MeOH
Time [min]

Figure SM6. (A) TLC plate from fungal extracts after development in mobile phase AcOEt:Hex (9:1); **(B)** TLC plate from fungal extracts after development in mobile phase $CHCl_3$:MeOH (95:5). Selected fungi were coded as 5, 10 and 13 for *F. solani* CSP-5b, *F. oxysporum* CSP-R18 and *F. oxysporum* CSP-19b, respectively.

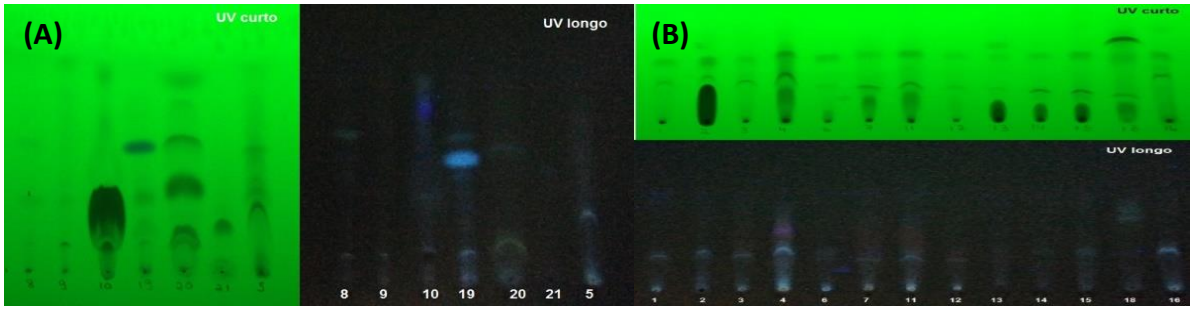

Figure SM7. TLC plate results for the bioautography of **(A)** *Cladosporium cladosporioides* and **(B)** *C. sphaerospermum;* and the TLC plate for the acetylcholinesterase inhibition assay. Fungal fractions are coded as (1) CSP-5b 20%, (2) CSP-5b 40%, (3) CSP-5b 60%, (4) CSP-5b 80%, (5) CSP-5b 100%; (6) CSP-19b 20%, (7) CSP-19b 40%, (8) CSP-19b 60%, (9) CSP-19b 80%, (10) CSP-19b 100%, (11) CSP-19b 20%, (12) CSP-19b 40%, (13) CSP-19b 60%, (14) CSP-19b 80%, (15) CSP-19b 100%, (F) Fisostigmin, (N) Nistatin.

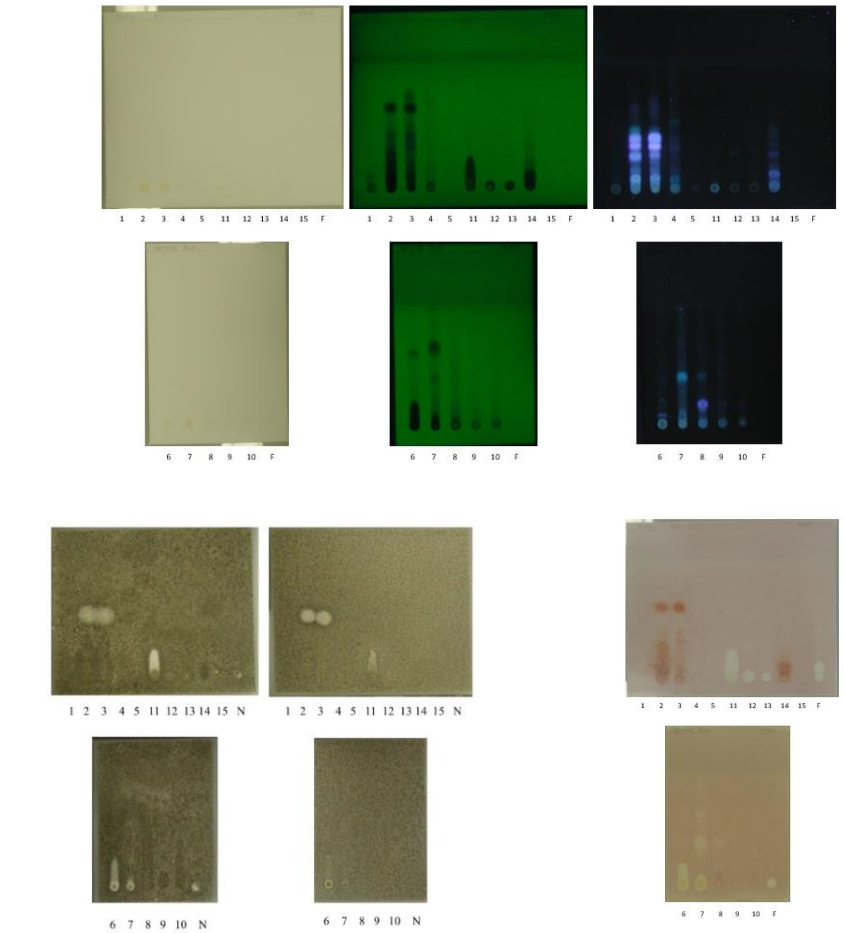

Figura SM8. Fragmentation mechanisms of beauvericin analogs found by MS/MS Molecular Networking; (A) MS1 spectra; *m/z* in red corresponds the ions selected for fragmentation; (B) Tandem mass spectra (MS2) of the selected ions. All the mechanisms were proposed by the author.

FOxy 01

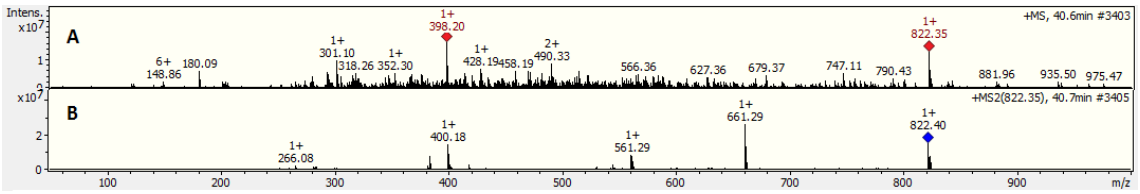

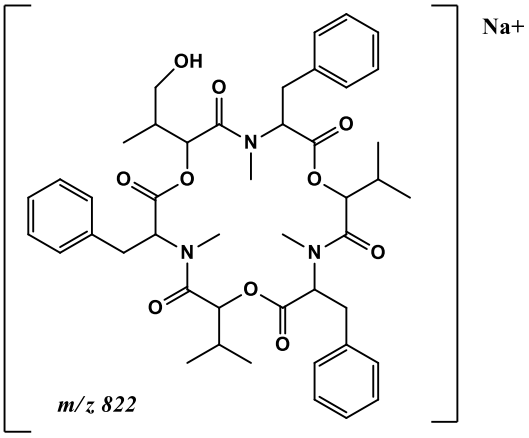

fragmentos b

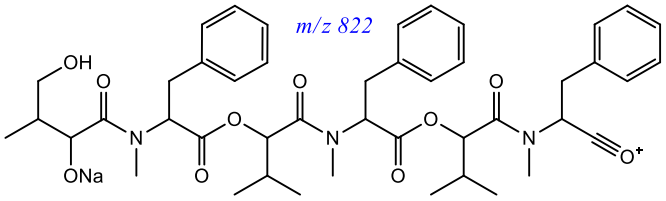

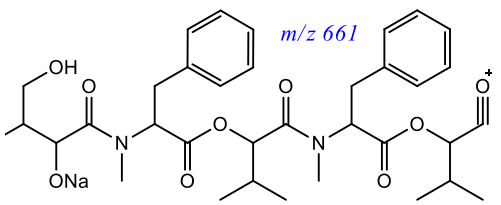

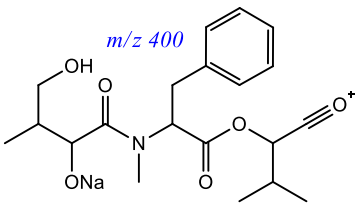

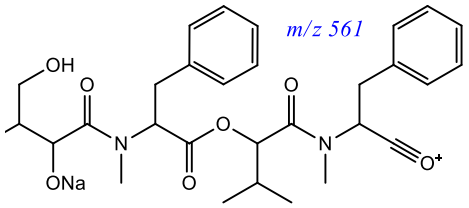

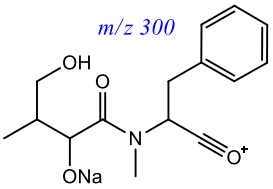

FOxy 02

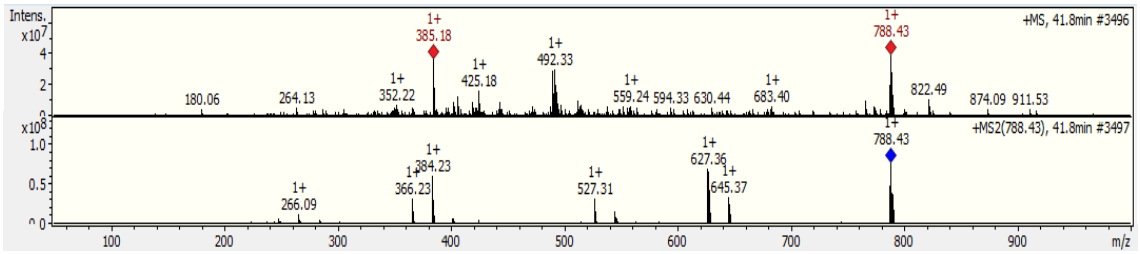

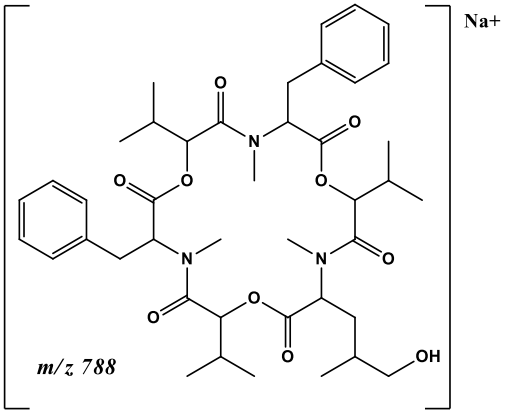

fragmentos b

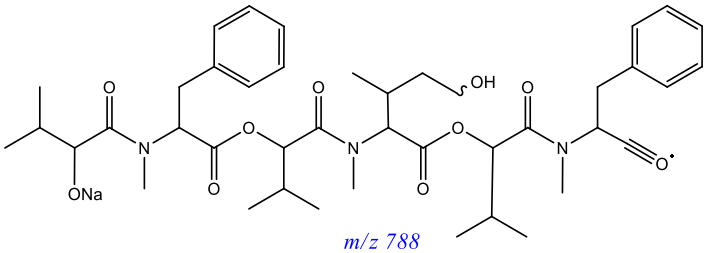

m/z 788

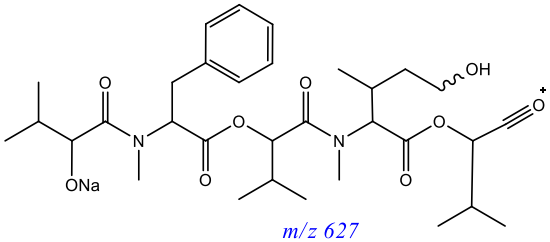

m/z 627

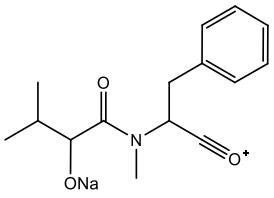

m/z 284

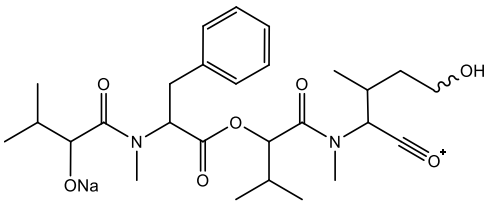

m/z 527

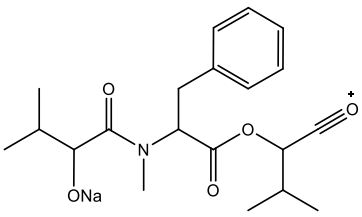

m/z 384

Beauvericin G2

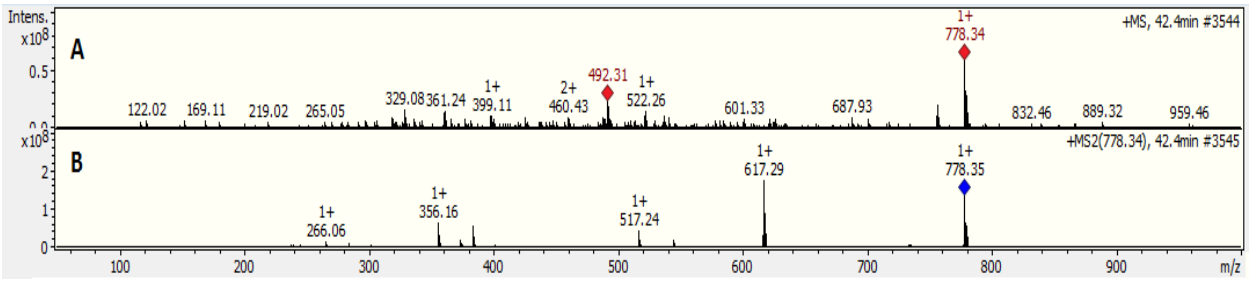

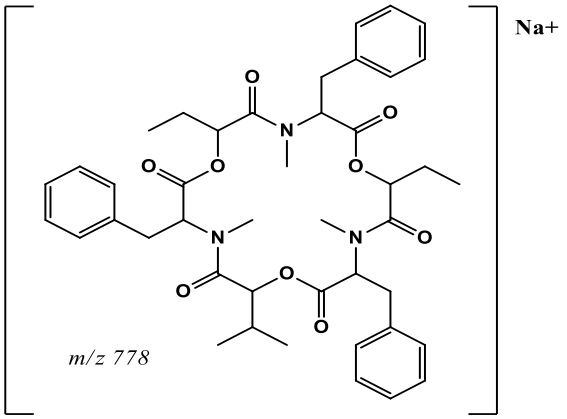

fragmentos b

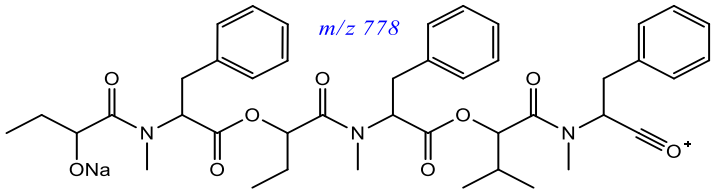

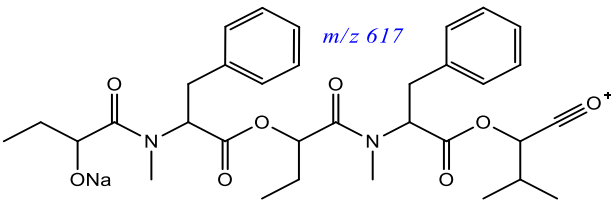

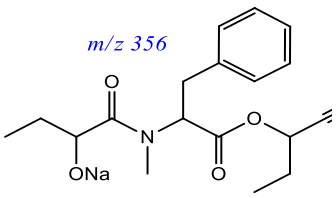

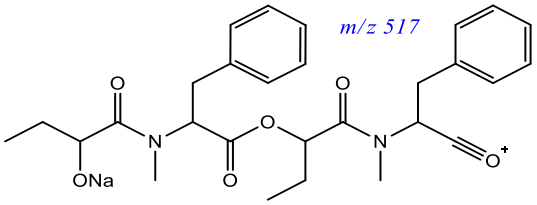

Beauvericin G1

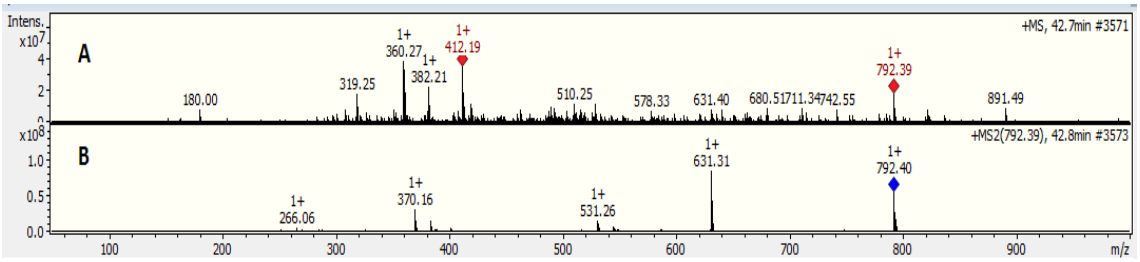

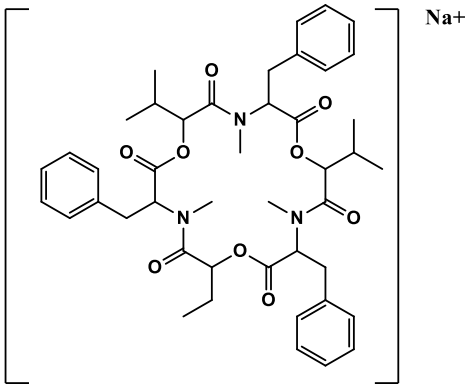

fragmentos b

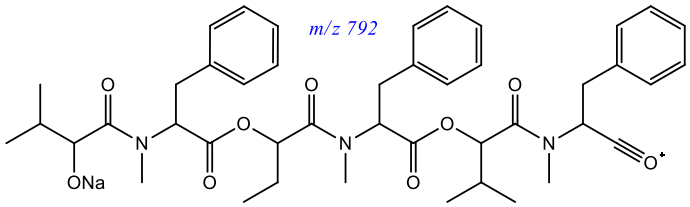

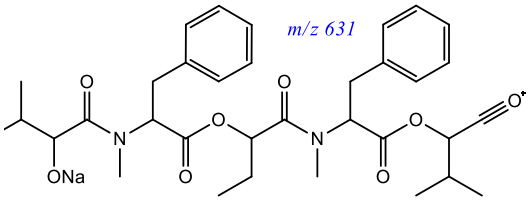

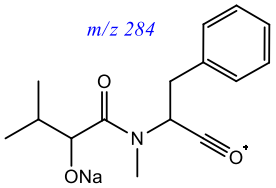

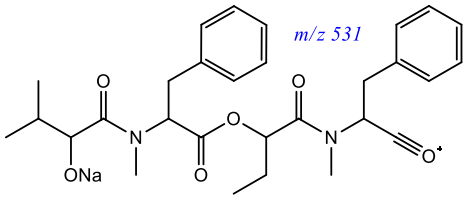

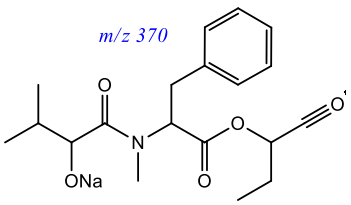

FOxy 3

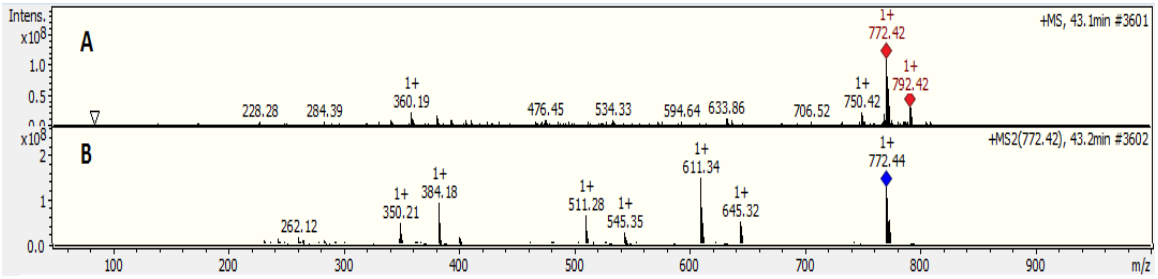

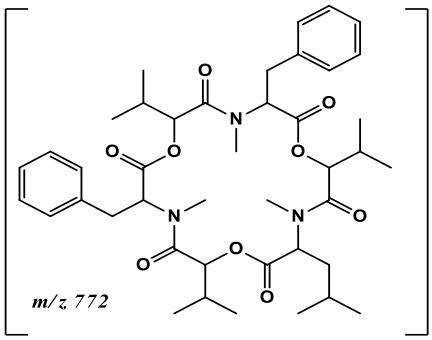

fragmentos b

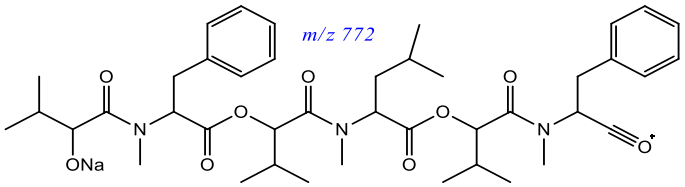

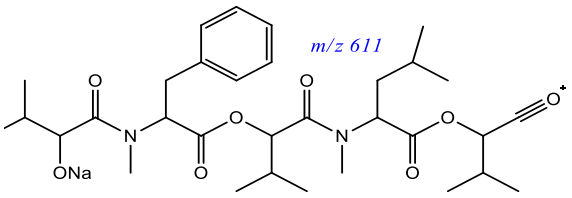

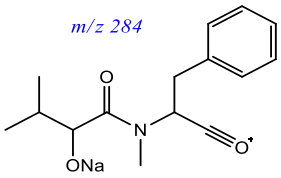

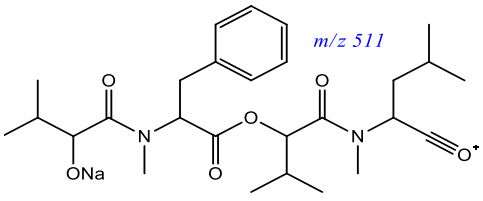

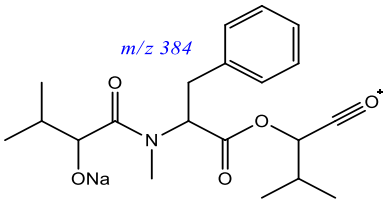

Beauvericin A

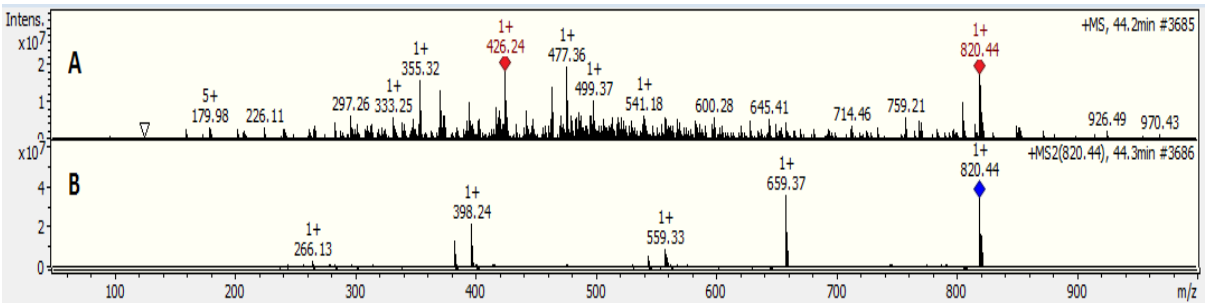

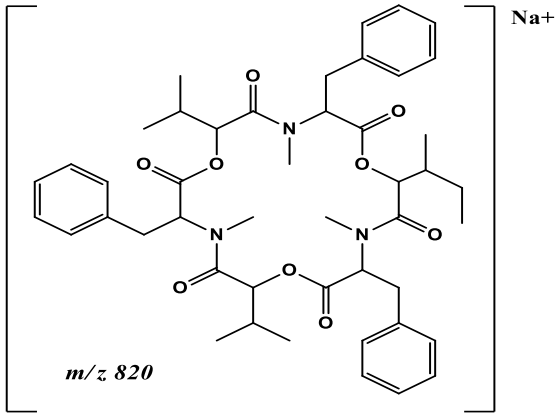

fragmentos b

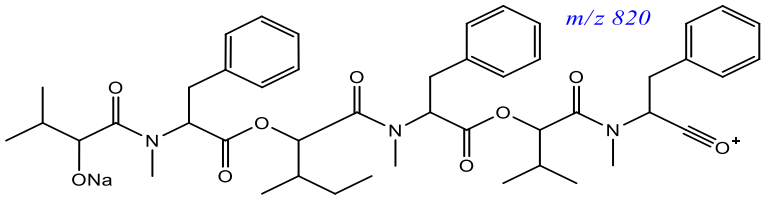

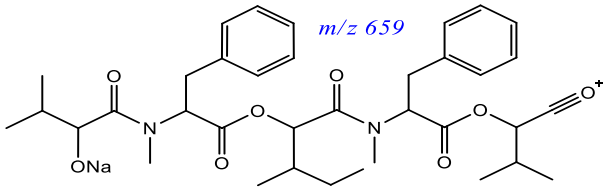

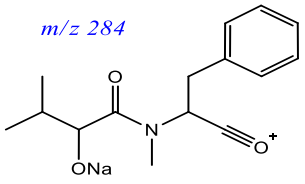

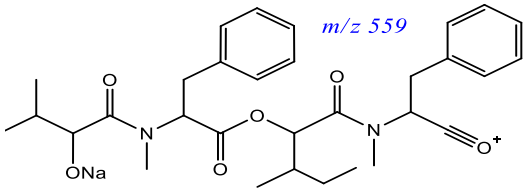

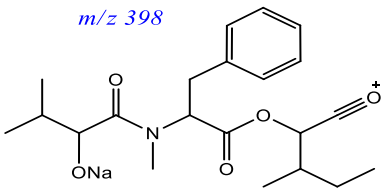

CHAPTER 4. REVIEW - ENHANCING CHEMICAL AND BIOLOGICAL DIVERSITY BY CO-CULTURE – WHAT WE KNOW AND WHERE DO WE GO

Article title: Enhancing Chemical And Biological Diversity By Co-Culture – What We Know And Where Do We Go

Journal: Applied Microbiology and Biotechnology.

Status: Submitted.

Authors: Denise M. Selegato[1,2], Ian Castro-Gamboa[2], Hye Kyong Kim [1], Young H. Choi[1, 3].

Affiliations:

[1] Natural Products Laboratory, Institute of Biology, Leiden University, Leiden, The Netherlands.

[2] Nucleus of Bioassays, Biosynthesis and Ecophysiology of natural products (NuBBE), Institute of Chemistry, São Paulo State University, Araraquara, Brazil.

[3] College of Pharmacy, Kyung Hee University, 02447, Seoul, Republic of Korea

References

Adnani N, Vazquez-Rivera E, Adibhatla SN, Ellis GA, Braun DR, Bugni TS (2015) Investigation of interspecies interactions within marine micromonosporaceae using an improved co-culture approach. Mar Drugs 13:6082–6098 . doi: 10.3390/md13106082

Akone SH, Mándi A, Kurtán T, Hartmann R, Lin W, Daletos G, Proksch P (2016) Inducing secondary metabolite production by the endophytic fungus Chaetomium sp . through fungal e bacterial co-culture and epigenetic modi fi cation. Tetrahedron 72:6340–6347 . doi: 10.1016/j.tet.2016.08.022

Angell S, Bench BJ, Williams H, Watanabe CMH (2006) Pyocyanin Isolated from a Marine Microbial Population: Synergistic Production between Two Distinct Bacterial Species and Mode of Action. Chem Biol 13:1349–1359 . doi: 10.1016/j.chembiol.2006.10.012

Araújo WL, Creason AL, Mano ET, Camargo-Neves AA, Minami SN, Chang JH, Loper JE (2016) Genome Sequencing and Transposon Mutagenesis of Burkholderia seminalis TC3.4.2R3 Identify Genes Contributing to Suppression of Orchid Necrosis Caused by B. gladioli. Mol Plant Microbe Interact 29:MPMI02160047R . doi: 10.1094/MPMI-02-16-0047-R

Ariana M, Hamedi J (2017) Enhanced production of nisin by co-culture of Lactococcus lactis sub sp. lactis and Yarrowia lipolytica in molasses based medium. J Biotechnol 256:21–26 . doi: 10.1016/j.jbiotec.2017.07.009

Baldrian P (2004) Increase of laccase activity during interspecific interactions of white-rot fungi. FEMS Microbiol Ecol 50:245–253 . doi: 10.1016/j.femsec.2004.07.005

Barefoot SF, Chen Y, Hughes TA, Bodine AB, Shearer MY, Hughes MD (1994) Identification and Purification of a Protein That Induces Production of the Lactobacillus acidophilus Bacteriocin Lactacin Bt. Appl Environ Microbiol 60:3522–3528

Benitez L, Correa A, Daroit D, Brandelli A (2011) Antimicrobial activity of Bacillus amyloliquefaciens LBM 5006 is enhanced in the presence of Escherichia coli. Curr Microbiol 62:1017–1022 . doi: 10.1007/s00284-010-9814-z

Berleman JE, Chumley T, Cheung P, Kirby JR (2006) Rippling is a predatory behavior in Myxococcus xanthus. J Bacteriol 188:5888–5895 . doi: 10.1128/JB.00559-06

Bertrand S, Schumpp O, Bohni N, Monod M, Gindro K, Wolfender J-L (2013) De novo production of metabolites by fungal co-culture of Trichophyton rubrum and Bionectria ochroleuca. J Nat Prod 76:1157–1165 . doi: 10.1021/np400258f

Bohni N, Hofstetter V, Gindro K, Buyck B, Schumpp O, Bertrand S, Monod M, Wolfender J-L (2016) Production of fusaric acid by Fusarium spp. in pure culture and in solid medium co-cultures. Molecules 21:370–386 . doi: 10.3390/molecules21030370

Boon C, Deng Y, Wang LH, He Y, Xu JL, Fan Y, Pan SQ, Zhang LH (2008) A novel DSF-like signal from Burkholderia cenocepacia interferes with Candida albicans morphological transition. ISME J 2:27–36 . doi: 10.1038/ismej.2007.76

Brasch J, Horter F, Fritsch D, Beck-Jendroschek V, Troger A, Francke W (2014) Acyclic sesquiterpenes released by Candida albicans inhibit growth of dermatophytes. Med Mycol 52:48–55 . doi: 10.3109/13693786.2013.814174

Butcher RA, Schroeder FC, Fischbach MA, Straight PD, Kolter R, Walsh CT, Clardy J (2007) The identification of bacillaene, the product of the PksX megacomplex in Bacillus subtilis. Proc Natl Acad Sci 104:1506–1509 . doi: 10.1073/pnas.0610503104

Carlson S, Tanouye U, Omarsdottir S, Murphy BT (2015) Phylum-specific regulation of resistomycin production in a streptomyces sp. via microbial coculture. J Nat Prod 78:381–387 . doi: 10.1021/np500767u
Chagas FO, Dias LG, Pupo MT (2013) A Mixed Culture of Endophytic Fungi Increases Production of Antifungal Polyketides. J Chem Ecol 39:1335–1342 . doi: 10.1007/s10886-013-0351-7
Chang JY, Lee HJ, Chang HC (2007) Identification of the agent from Lactobacillus plantarum KFRI464 that enhances bacteriocin production by Leuconostoc citreum GJ7. J Appl Microbiol 103:2504–2515 . doi: 10.1111/j.1365-2672.2007.03543.x
Chanos P, Mygind T (2016) Co-culture-inducible bacteriocin production in lactic acid bacteria. Appl Microbiol Biotechnol 100:4297–4308 . doi: 10.1007/s00253-016-7486-8
Cheirsilp B, Shimizu H, Shioya S (2003) Enhanced kefiran production by mixed culture of and. J Biotechnol 100:43–53 . doi: 10.1016/S0168-1656(02)00228-6
Chi Y, Hatakka A, Maijala P (2007) Can co-culturing of two white-rot fungi increase lignin degradation and the production of lignin-degrading enzymes? Int Biodeterior Biodegrad 59:32–39 . doi: 10.1016/j.ibiod.2006.06.025
Cho JY, Kim MS (2012) Induction of Antifouling Diterpene Production by Streptomyces cinnabarinus PK209 in Co-Culture with Marine-Derived Alteromonas sp. KNS-16. Biosci Biotechnol Biochem 76:1849–1854 . doi: 10.1271/bbb.120221
Cook LC, LaSarre B, Federle MJ (2013) Interspecies communication among commensal and pathogenic streptococci. MBio 4:1–11 . doi: 10.1128/mBio.00382-13
Cueto M, Jensen PR, Kauffman C, Fenical W, Lobkovsky E, Clardy J (2001) Pestalone, a New Antibiotic Produced by a Marine Fungus in Response to Bacterial Challenge. J Nat Prod 64:1444–1446
Cugini C, Calfee MW, Farrow JM, Morales DK, Pesci EC, Hogan DA (2007) Farnesol, a common sesquiterpene, inhibits PQS production in Pseudomonas aeruginosa. Mol Microbiol 65:896–906 . doi: 10.1111/j.1365-2958.2007.05840.x
Dashti Y, Grkovic T, Abdelmohsen UR, Hentschel U, Quinn RJ (2014) Production of induced secondary metabolites by a co-culture of sponge-associated actinomycetes, Actinokineospora sp. EG49 and Nocardiopsis sp. RV163. Mar Drugs 12:3046–3059 . doi: 10.3390/md12053046
Davies DG, Marques CNH (2009) A fatty acid messenger is responsible for inducing dispersion in microbial biofilms. J Bacteriol 191:1393–1403 . doi: 10.1128/JB.01214-08
Degenkolb T, Heinze S, Schlegel B, Strobel G, Gräfe U (2002) Formation of new lipoaminopeptides, acremostatins A, B, and C, by co-cultivation of Acremonium sp. Tbp-5 and Mycogone rosea DSM 12973. Biosci Biotechnol Biochem 66:883–886 . doi: 10.1271/bbb.66.883
Di Cagno R, De Angelis M, Coda R, Minervini F, Gobbetti M (2009) Molecular adaptation of sourdough Lactobacillus plantarum DC400 under co-cultivation with other lactobacilli. Res Microbiol 160:358–366 . doi: 10.1016/j.resmic.2009.04.006
Dourado MN, Santos DS, Nunes LR, Costa de Oliveira RLB, de Oliveira M V, Araújo WL (2015) Differential gene expression in Xylella fastidiosa 9a5c during co-cultivation with the endophytic bacterium Methylobacterium mesophilicum SR1.6/6. J Basic Microbiol 55:1357–1366 . doi: 10.1002/jobm.201400916
Dusane DH, Matkar P, Venugopalan VP, Kumar AR, Zinjarde SS (2011) Cross-species induction of antimicrobial compounds, biosurfactants and quorum-sensing

inhibitors in tropical marine epibiotic bacteria by pathogens and biofouling microorganisms. Curr Microbiol 62:974–980 . doi: 10.1007/s00284-010-9812-1
Ebrahim W, El-Neketi M, Lewald LI, Orfali RS, Lin W, Rehberg N, Kalscheuer R, Daletos G, Proksch P (2016) Metabolites from the Fungal Endophyte Aspergillus austroafricanus in Axenic Culture and in Fungal-Bacterial Mixed Cultures. J Nat Prod 79:914–922 . doi: 10.1021/acs.jnatprod.5b00975
Ferreira Gregorio AP, Da Silva IR, Sedarati MR, Hedger JN (2006) Changes in production of lignin degrading enzymes during interactions between mycelia of the tropical decomposer basidiomycetes Marasmiellus troyanus and Marasmius pallescens. Mycol Res 110:161–168 . doi: 10.1016/j.mycres.2005.10.002
Fouhy Y, Scanlon K, Schouest K, Spillane C, Crossman L, Avison MB, Ryan RP, Dow JM (2007) Diffusible signal factor-dependent cell-cell signaling and virulence in the nosocomial pathogen Stenotrophomonas maltophilia. J Bacteriol 189:4964–4968 . doi: 10.1128/JB.00310-07
Freitag M, Morrell JJ (1992) Changes in selected enzyme activities during growth of pure and mixed cultures of the white-rot decay fungus Trametes versicolor and the potential biocontrol fungus Trichoderma harzianum. Can J Microbiol 38:317–23 . doi: 10.1139/m92-053
Ge J, Fang B, Wang Y, Song G, Ping W (2014) Bacillus subtilis enhances production of Paracin1.7, a bacteriocin produced by Lactobacillus paracasei HD1-7, isolated from Chinese fermented cabbage. Ann Microbiol 64:1735–1743 . doi: 10.1007/s13213-014-0817-z
Gibson J, Sood A, Hogan DA (2009) Pseudomonas aeruginosa-Candida albicans interactions: Localization and fungal toxicity of a phenazine derivative. Appl Environ Microbiol 75:504–513 . doi: 10.1128/AEM.01037-08
Glauser G, Gindro K, Fringeli J, De Joffrey JP, Rudaz S, Wolfender J-L (2009) Differential Analysis of Mycoalexins in Confrontation Zones of Grapevine Fungal Pathogens by Ultrahigh Pressure Liquid Chromatography / Time-of-Flight Mass Spectrometry and Capillary Nuclear Magnetic Resonance. J Agric Food Chem 57:1127–1134 . doi: 10.1021/jf8033539
Hiscox J, Baldrian P, Rogers HJ, Boddy L (2010) Changes in oxidative enzyme activity during interspecific mycelial interactions involving the white-rot fungus Trametes versicolor. Fungal Genet Biol 47:562–571 . doi: 10.1016/j.fgb.2010.03.007
Hoefler BC, Gorzelnik K V, Yang JY, Hendricks N, Dorrestein PC, Straight PD (2012) Enzymatic resistance to the lipopeptide surfactin as identified through imaging mass spectrometry of bacterial competition. Proc Natl Acad Sci 109:13082–13087 . doi: 10.1073/pnas.1205586109
Hoffman LR, Deziel E, D'Argenio DA, Lepine F, Emerson J, McNamara S, Gibson RL, Ramsey BW, Miller SI (2006) Selection for Staphylococcus aureus small-colony variants due to growth in the presence of Pseudomonas aeruginosa. Proc Natl Acad Sci 103:19890–19895 . doi: 10.1073/pnas.0606756104
Hoshino S, Okada M, Wakimoto T, Zhang H, Hayashi F, Onaka H, Abe I (2015a) Niizalactams A-C, Multicyclic Macrolactams Isolated from Combined Culture of Streptomyces with Mycolic Acid-Containing Bacterium. J Nat Prod 78:3011–3017 . doi: 10.1021/acs.jnatprod.5b00804
Hoshino S, Wakimoto T, Onaka H, Abe I (2015b) Chojalactones A-C, cytotoxic butanolides isolated from streptomyces sp. cultivated with mycolic acid containing bacterium. Org Lett 17:1501–1504 . doi: 10.1021/acs.orglett.5b00385
Hoshino S, Zhang L, Awakawa T, Wakimoto T, Onaka H, Abe I (2015c) Arcyriaflavin E, a new cytotoxic indolocarbazole alkaloid isolated by combined-culture of

mycolic acid-containing bacteria and Streptomyces cinnamoneus NBRC 13823. J Antibiot (Tokyo) 68:342–344
Huang S, Ding W, Li C, Cox DG (2014) Two new cyclopeptides from the co-culture broth of two marine mangrove fungi and their antifungal activity. Pharmacogn Mag 10:410–414 . doi: 10.4103/0973-1296.141781
Iakovlev A, Stenlid J (2000) Spatiotemporal Patterns of Laccase Activity in Interacting Mycelia of Wood-Decaying Basidiomycete Fungi. Microb Ecol 39:236–245 . doi: 10.1007/s002480000022
Joint I, Tait K, Callow ME, Callow JA, Milton D, Williams P, Cámara M (2002) Cell-to-cell communication across the prokaryote-eukaryote boundary. Science (80-) 298:1207 . doi: 10.1126/science.1077075
König CC, Scherlach K, Schroeckh V, Horn F, Nietzsche S, Brakhage AA, Hertweck C (2013) Bacterium Induces Cryptic Meroterpenoid Pathway in the Pathogenic Fungus Aspergillus fumigatus. ChemBioChem 14:938–942 . doi: 10.1002/cbic.201300070
Kos B, Beganović J, Jurašić L, Švađumović M (2011) Coculture-inducible bacteriocin biosynthesis of different probiotic strains by dairy starter culture Lactococcus lactis. Mljekarstvo 61:273–282
Kreth J, Merritt J, Shi W, Qi F (2005) Competition and Coexistence between Streptococcus mutans and Streptococcus sanguinis in the Dental Biofilm Competition and Coexistence between Streptococcus mutans and Streptococcus sanguinis in the Dental Biofilm. J Bacteriol 187:7193–7203 . doi: 10.1128/JB.187.21.7193
Kurosawa K, Ghiviriga I, Sambandan TG, Lessard PA, Barbara JE, Rha C, Sinskey AJ (2008) Rhodostreptomycins, antibiotics biosynthesized following horizontal gene transfer from Streptomyces padanus to Rhodococcus fascians. J Am Chem Soc 130:1126–1127 . doi: 10.1021/ja077821p
Li C, Wang J, Luo C, Ding W, Cox DG (2014) A new cyclopeptide with antifungal activity from the co-culture broth of two marine mangrove fungi. Nat Prod Res 28:616–621 . doi: 10.1080/14786419.2014.887074
Li C, Zhang J, Shao C, Ding W, She Z, Lin J (2011) A New Xanthone Derivative from the co-culture broth of two marine fungi (strain No. E33 and K38). Chem Nat Compd 47:342–344
Li CY, Ding WJ, Shao CL, She ZG, Lin Y-C (2010) A new diimide derivative from the co-culture broth of two mangrove fungi (strain (strains nos. E33 and K38). J Asian Nat Prod Res 12:809–813 . doi: 10.1007/s10600-013-0751-5
Liu C, Hu B, Liu Y, Chen S (2006) Stimulation of nisin production from whey by a mixed culture of Lactococcus lactis and Saccharomyces cerevisiae. Appl Biochem Biotechnol 131:751–761 . doi: 10.1385/ABAB:131:1:751
Long RA, Azam F (2001) Antagonistic interactions among marine pelagic bacteria. Appl Environ Microbiol 67:4975 . doi: 10.1128/AEM.67.11.4975
Lopez-Medina E, Fan D, Coughlin LA, Ho EX, Lamont IL, Reimmann C, Hooper L V, Koh AY (2015) Candida albicans Inhibits Pseudomonas aeruginosa Virulence through Suppression of Pyochelin and Pyoverdine Biosynthesis. PLoS Pathog 11:1–34 . doi: 10.1371/journal.ppat.1005129
Maldonado A, Ruiz-Barba JL, Jiménez-Díaz R (2004) Production of plantaricin NC8 by Lactobacillus plantarum NC8 is induced in the presence of different types of gram-positive bacteria. Arch Microbiol 181:8–16 . doi: 10.1007/s00203-003-0606-8
Man LL, Meng XC, Zhao RH (2012) Induction of plantaricin MG under co-culture with certain lactic acid bacterial strains and identification of LuxS mediated quorum

sensing system in Lactobacillus plantarum KLDS1.0391. Food Control 23:462–469 . doi: 10.1016/j.foodcont.2011.08.015
McAlester G, O'Gara F, Morrissey JP (2008) Signal-mediated interactions between Pseudomonas aeruginosa and Candida albicans. J Med Microbiol 57:563–569 . doi: 10.1099/jmm.0.47705-0
Mearns-Spragg A, Bregu M, Boyd KG, Burgess JG (1998) Cross-species induction and enhancement of antimicrobial activity produced by epibiotic bacteria from marine algae and invertebrates, after exposure to terrestrial bacteria. Lett Appl Microbiol 27:142–146 . doi: 10.1046/j.1472-765X.1998.00416.x
Menezes RC, Kai M, Krause K, Matthäus C, Svatoš A, Popp J, Kothe E (2015) Monitoring metabolites from Schizophyllum commune interacting with Hypholoma fasciculare combining LESA-HR mass spectrometry and Raman microscopy. Anal Bioanal Chem 407:2273–2282 . doi: 10.1007/s00216-014-8383-6
Meng LH, Liu Y, Li XM, Xu GM, Ji NY, Wang BG (2015) Citrifelins A and B, Citrinin Adducts with a Tetracyclic Framework from Cocultures of Marine-Derived Isolates of Penicillium citrinum and Beauveria felina. J Nat Prod 78:2301–2305 . doi: 10.1021/acs.jnatprod.5b00450
Meyer V, Stahl U (2003) The influence of co-cultivation on expression of the antifungal protein in Aspergillus giganteus. J Basic Microbiol 43:68–74 . doi: 10.1002/jobm.200390007
Minerdi D, Bossi S, Gullino ML, Garibaldi A (2009) Volatile organic compounds: A potential direct long-distance mechanism for antagonistic action of Fusarium oxysporum strain MSA 35. Environ Microbiol 11:844–854 . doi: 10.1111/j.1462-2920.2008.01805.x
Moree WJ, Phelan V V, Wu C-H, Bandeira N, Cornett DS, Duggan BM, Dorrestein PC (2012) Interkingdom metabolic transformations captured by microbial imaging mass spectrometry. Proc Natl Acad Sci 109:13811–13816 . doi: 10.1073/pnas.1206855109
Moree WJ, Yang JY, Zhao X, Liu WT, Aparicio M, Atencio L, Ballesteros J, Sánchez J, Gavilán RG, Gutiérrez M, Dorrestein PC (2013) Imaging Mass Spectrometry of a Coral Microbe Interaction with Fungi. J Chem Ecol 39:1045–1054 . doi: 10.1007/s10886-013-0320-1
Müller MEH, Steier I, Köppen R, Siegel D, Proske M, Korn U, Koch M (2012) Cocultivation of phytopathogenic Fusarium and Alternaria strains affects fungal growth and mycotoxin production. J Appl Microbiol 113:874–887 . doi: 10.1111/j.1365-2672.2012.05388.x
Nonaka K, Abe T, Iwatsuki M, Mori M, Yamamoto T, Shiomi K, Ômura S, Masuma R (2011) Enhancement of metabolites productivity of Penicillium pinophilum FKI-5653, by co-culture with Trichoderma harzianum FKI-5655. J Antibiot (Tokyo) 64:769–774 . doi: 10.1038/ja.2011.91
Notz R, Maurhofer M, Dubach H (2002) Fusaric acid-producing strains of Fusarium oxysporum alter 2, 4-diacetylphloroglucinol biosynthetic gene expression in Pseudomonas fluorescens CHA0 in vitro and. Appl Environ Microbiol 68:2229–2235 . doi: 10.1128/AEM.68.5.2229
Oh DC, Jensen PR, Kauffman CA, Fenical W (2005) Libertellenones A-D: Induction of cytotoxic diterpenoid biosynthesis by marine microbial competition. Bioorganic Med Chem 13:5267–5273 . doi: 10.1016/j.bmc.2005.05.068
Oh DC, Kauffman CA, Jensen PR, Fenical W (2007) Induced production of emericellamides A and B from the marine-derived fungus Emericella sp. in

competing co-culture. J Nat Prod 70:515–520 . doi: 10.1021/np060381f
Ojika M, Molli SD, Kanazawa H, Yajima A, Toda K, Nukada T, Mao H, Murata R, Asano T, Qi J, Sakagami Y (2011) The second Phytophthora mating hormone defines interspecies biosynthetic crosstalk. Nat Chem Biol 7:591–593 . doi: 10.1038/nchembio.617
Ola ARB, Thomy D, Lai D, Brötz-Oesterhelt H, Proksch P (2013) Inducing Secondary Metabolite Production by the Endophytic Fungus Fusarium tricinctum through Coculture with Bacillus subtilis. J Nat Prod 76:2094–2099 . doi: 10.1021/np400589h
Onaka H, Mori Y, Igarashi Y, Furumai T (2011) Mycolic acid-containing bacteria induce natural-product biosynthesis in Streptomyces species. Appl Environ Microbiol 77:400–406 . doi: 10.1128/AEM.01337-10
Park HB, Kwon HC, Lee CH, Yang HO (2009) Glionitrin A , an Antibiotic-Antitumor Metabolite Derived from Competitive Interaction. J Nat Prod 72:248–252 . doi: 10.1021/np800606e
Peterson SB, Dunn AK, Klimowicz AK, Handelsman J (2006) Peptidoglycan from Bacillus cereus mediates commensalism with rhizosphere bacteria from the Cytophaga-Flavobacterium group. Appl Environ Microbiol 72:5421–5427 . doi: 10.1128/AEM.02928-05
Pettit RK, Pettit GR, Xu JP, Weber CA, Richert LA (2010) Isolation of human cancer cell growth inhibitory, antimicrobial lateritin from a mixed fungal culture. Planta Med 76:500–501 . doi: 10.1055/s-0029-1240617
Rateb ME, Hallyburton I, Houssen WE, Bull AT, Goodfellow M, Santhanam R, Jaspars M, Ebel R (2013) Induction of diverse secondary metabolites in Aspergillus fumigatus by microbial co-culture. RSC Adv 3:14444 . doi: 10.1039/c3ra42378f
Rickard AH, Palmer RJ, Blehert DS, Campagna SR, Semmelhack MF, Egland PG, Bassler BL, Kolenbrander PE (2006) Autoinducer 2: A concentration-dependent signal for mutualistic bacterial biofilm growth. Mol Microbiol 60:1446–1456 . doi: 10.1111/j.1365-2958.2006.05202.x
Rojo-Bezares B, Sáenz Y, Navarro L, Zarazaga M, Ruiz-Larrea F, Torres C (2007) Coculture-inducible bacteriocin activity of Lactobacillus plantarum strain J23 isolated from grape must. Food Microbiol 24:482–491 . doi: 10.1016/j.fm.2006.09.003
Ross C, Opel V, Scherlach K, Hertweck C (2014) Biosynthesis of antifungal and antibacterial polyketides by Burkholderia gladioli in coculture with Rhizopus microsporus. Mycoses 57:48–55 . doi: 10.1111/myc.12246
Ryan RP, Fouhy Y, Garcia BF, Watt SA, Niehaus K, Yang L, Tolker-Nielsen T, Dow JM (2008) Interspecies signalling via the Stenotrophomonas maltophilia diffusible signal factor influences biofilm formation and polymyxin tolerance in Pseudomonas aeruginosa. Mol Microbiol 68:75–86 . doi: 10.1111/j.1365-2958.2008.06132.x
Salas-Marina MA, Silva-Flores MA, Uresti-Rivera EE, Castro-Longoria E, Herrera-Estrella A, Casas-Flores S (2011) Colonization of Arabidopsis roots by Trichoderma atroviride promotes growth and enhances systemic disease resistance through jasmonic acid/ethylene and salicylic acid pathways. Eur J Plant Pathol 131:15–26 . doi: 10.1007/s10658-011-9782-6
Savoie JM, Mata G (1999) The antagonistic action of Trichoderma sp. hyphae to Lentinula edodes hyphae changes lignocellulotytic activities during cultivation in wheat straw. World J Microbiol Biotechnol 15:369–373 . doi: 10.1023/A:1008979701853

Schneider J, Yepes A, Garcia-Betancur JC, Westedt I, Mielich B, López D (2012) Streptomycin-induced expression in Bacillus subtilis of YtnP, a lactonase-homologous protein that inhibits development and streptomycin production in Streptomyces griseus. Appl Environ Microbiol 78:599–603 . doi: 10.1128/AEM.06992-11

Schouten A, van den Berg G, Edel-Hermann V, Steinberg C, Gautheron N, Alabouvette C, de Vos CH, Lemanceau P, Raaijmakers JM (2004) Defense responses of Fusarium oxysporum to 2,4-diacetylphloroglucinol, a broad-spectrum antibiotic produced by Pseudomonas fluorescens. Mol plant-microbe Interact MPMI 17:1201–1211 . doi: 10.1094/MPMI.2004.17.11.1201

Schroeckh V, Scherlach K, Nutzmann HW, Shelest E, Schmidt-Heck W, Schuemann J, Martin K, Hertweck C, Brakhage AA (2009) Intimate bacterial-fungal interaction triggers biosynthesis of archetypal polyketides in Aspergillus nidulans. Proc Natl Acad Sci 106:14558–14563 . doi: 10.1073/pnas.0901870106

Score AJ, Palfreyman JW, White NA (1997) Extracellular phenoloxidase and peroxidase enzyme production during interspecific fungal interactions. Int Biodeterior Biodegrad 39:225–233 . doi: 10.1016/S0964-8305(97)00012-7

Serrano R, González-Menéndez V, Rodríguez L, Martín J, Tormo JR, Genilloud O (2017) Co-culturing of fungal strains against Botrytis cinerea as a model for the induction of chemical diversity and therapeutic agents. Front Microbiol 8:649–664 . doi: 10.3389/fmicb.2017.00649

Shah IM, Laaberki MH, Popham DL, Dworkin J (2008) A Eukaryotic-like Ser/Thr Kinase Signals Bacteria to Exit Dormancy in Response to Peptidoglycan Fragments. Cell 135:486–496 . doi: 10.1016/j.cell.2008.08.039

Sher D, Thompson JW, Kashtan N, Croal L, Chisholm SW (2011) Response of Prochlorococcus ecotypes to co-culture with diverse marine bacteria. ISME J 5:1125–1132 . doi: 10.1038/ismej.2011.1

Shimizu H, Mizuguchi T, Tanaka E, Shioya S (1999) Nisin production by a mixed-culture system consisting of Lactococcus lactis and Kluyveromyces marxianus. Appl Environ Microbiol 65:3134–3141

Shin CS, Kim HJ, Kim MJ, Ju JY (1998) Morphological change and enhanced pigment production of Monascus when cocultured with Saccharomyces cerevisiae or Aspergillus oryzae. Biotechnol Bioeng 59:576–581 . doi: 10.1002/(SICI)1097-0290(19980905)59:5<576::AID-BIT7>3.0.CO;2-7

Slattery M, Rajbhandari I, Wesson K (2001) Competition-Mediated Antibiotic Induction in the Marine Bacterium Streptomyces tenjimariensis. Microb Ecol 41:90–96 . doi: 10.1007/978-1-60327-140-0_4

Soliman SSM, Raizada MN (2013) Interactions between co-habitating fungi elicit synthesis of Taxol from an endophytic fungus in host Taxus plants. Front Microbiol 4:1–14 . doi: 10.3389/fmicb.2013.00003

Sonnenbichler J, Dietrich J, Peipp H (1994) Secondary Fungal Metabolites and Their Biological Activities, V. Investigations Concerning the Induction of the Biosynthesis of Toxic Secondary Metabolites in Basidiomycetes. Biol Chem Hoppe Seyler 375:71–80 . doi: 10.1515/bchm3.1994.375.1.71

Stierle AA, Stierle DB, Decato D, Priestley ND, Alverson JB, Hoody J, McGrath K, Klepacki D (2017) The Berkeleylactones, Antibiotic Macrolides from Fungal Coculture. J Nat Prod 80:1150–1160 . doi: 10.1021/acs.jnatprod.7b00133

Straight PD, Willey JM, Kolter R (2006) Interactions between Streptomyces coelicolor and Bacillus subtilis: Role of surfactants in raising aerial structures. J Bacteriol 188:4918–4925 . doi: 10.1128/JB.00162-06

Sung AA, Gromek SM, Balunas MJ (2017) Upregulation and identification of antibiotic activity of a marine-derived Streptomyces sp. via co-cultures with human pathogens. Mar Drugs 15: . doi: 10.3390/md15080250
Tabasco R, García-Cayuela T, Peláez C, Requena T (2009) Lactobacillus acidophilus La-5 increases lactacin B production when it senses live target bacteria. Int J Food Microbiol 132:109–116 . doi: 10.1016/j.ijfoodmicro.2009.04.004
Tada S, Katakura Y, Ninomiya K, Shioya S (2007) Fed-batch coculture of Lactobacillus kefiranofaciens with Saccharomyces cerevisiae for effective production of kefiran. J Biosci Bioeng 103:557–562 . doi: 10.1263/jbb.103.557
Tata A, Perez C, Campos ML, Bayfield MA, Eberlin MN, Ifa DR (2015) Imprint Desorption Electrospray Ionization Mass Spectrometry Imaging for Monitoring Secondary Metabolites Production during Antagonistic Interaction of Fungi. Anal Chem 87:12298–12305 . doi: 10.1021/acs.analchem.5b03614
Tong H, Chen W, Merritt J, Qi F, Shi W, Dong X (2007) Streptococcus oligofermentans inhibits Streptococcus mutans through conversion of lactic acid into inhibitory H2O2: A possible counteroffensive strategy for interspecies competition. Mol Microbiol 63:872–880 . doi: 10.1111/j.1365-2958.2006.05546.x
Traxler MF, Watrous JD, Alexandrov T, Dorrestein PC, Kolter R (2013) Interspecies interactions stimulate diversification of the Streptomyces coelicolor secreted metabolome. MBio 4:459–13 . doi: 10.1128/mBio.00459-13
Trischman JA, Oeffner RE, De Luna MG, Kazaoka M (2004) Competitive induction and enhancement of indole and a diketopiperazine in marine bacteria. Mar Biotechnol 6:215–220 . doi: 10.1007/s10126-003-0010-z
Turpin PE, Dhir VK, Maycroft KA, Rowland C, Wllington EMH (1992) The effect of Streptomycetes species on the survival of Salmonella in soil. FEMS Microbiol Ecol 101:271–280
Ueda K, Kawai S, Ogawa H, Kiyama A, Kubota T, Kawanobe H, Beppu T (2000) Wide Distribution of Interspecific Stimulatory Events on Antibiotic Production and Sporulation among Streptomyces species. J Antibiot (Tokyo) 53:979–982 . doi: 11099234
van Rij ET, Girard G, Lugtenberg BJJ, Bloemberg G V (2005) Influence of fusaric acid on phenazine-1-carboxamide synthesis and gene expression of Pseudomonas chlororaphis strain PCL1391. Microbiology 151:2805–2814 . doi: 10.1099/mic.0.28063-0
Vega NM, Allison KR, Samuels AN, Klempner MS, Collins JJ (2013) Salmonella typhimurium intercepts Escherichia coli signaling to enhance antibiotic tolerance. Proc Natl Acad Sci 110:14420–14425 . doi: 10.1073/pnas.1308085110
Vinale F, Nicoletti R, Borrelli F, Mangoni A, Parisi OA, Marra R, Lombardi N, Lacatena F, Grauso L, Finizio S, Lorito M, Woo SL (2017) Co-Culture of Plant Beneficial Microbes as Source of Bioactive Metabolites. Sci Rep 7:1–12 . doi: 10.1038/s41598-017-14569-5
Wang J, Ding W, Li C, Huang S, She Z, Lin Y (2013a) A New Polusubstituted Benzaldehyde from the co-culture broth of two marine fungi (strains Nos. E33 and K38). Chem Nat Compd 49:689–691
Wang J, Lin W, Wray V, Lai D, Proksch P (2013b) Induced production of depsipeptides by co-culturing Fusarium tricinctum and Fusarium begoniae. Tetrahedron Lett 54:2492–2496 . doi: 10.1016/j.tetlet.2013.03.005
Wang LH, He Y, Gao Y, Wu JE, Dong YH, He C, Wang SX, Weng LX, Xu JL, Tay L, Fang RX, Zhang LH (2004) A bacterial cell-cell communication signal with cross-kingdom structural analogues. Mol Microbiol 51:903–912 . doi: 10.1046/j.1365-

2958.2003.03883.x
Watanabe T, Izaki K, Takahashi H (1982) New Polyenic Antibiotics Against Gram-positive and -Negative Bacteria. J Antibiot (Tokyo) 35:1141–1147
Watsuji T, Yamada S, Yamabe T, Watanabe Y, Kato T, Saito T, Ueda K, Beppu T (2007) Identification of indole derivatives as self-growth inhibitors of Symbiobacterium thermophilum, a unique bacterium whose growth depends on coculture with a Bacillus sp. Appl Environ Microbiol 73:6159–6165 . doi: 10.1128/AEM.02835-06
White N, Boddy L (1992) Extracellular enzyme localization during interspecific fungal interactions. FEMS Microbiol Lett 98:75–80 . doi: 10.1111/j.1574-6968.1992.tb05493.x
Whitt J, Shipley SM, Newman DJ, Zuck KM (2014) Tetramic acid analogues produced by coculture of saccharopolyspora erythraea with fusarium pallidoroseum. J Nat Prod 77:173–177 . doi: 10.1021/np400761g
Xu XL, Lee RTH, Fang HM, Wang YM, Li R, Zou H, Zhu Y, Wang Y (2008) Bacterial Peptidoglycan Triggers Candida albicans Hyphal Growth by Directly Activating the Adenylyl Cyclase Cyr1p. Cell Host Microbe 4:28–39 . doi: 10.1016/j.chom.2008.05.014
Yakovleva EP, Bulgakova TN (1978) Formation of Amphotericin B in Mixed Cultures. Pharm Chem J 12:1483–1488
Yao L, Zhu LP, Xu XY, Tan LL, Sadilek M, Fan H, Hu B, Shen XT, Yang J, Qiao B, Yang S (2016) Discovery of novel xylosides in co-culture of basidiomycetes Trametes versicolor and Ganoderma applanatum by integrated metabolomics and bioinformatics. Sci Rep 6:1–13 . doi: 10.1038/srep33237
Yu L, Ding W, Wang Q, Ma Z, Xu X, Zhao X, Chen Z (2017) Induction of cryptic bioactive 2,5-diketopiperazines in fungus Penicillium sp. DT-F29 by microbial co-culture. Tetrahedron 73:907–914 . doi: 10.1016/j.tet.2016.12.077
Zhang H, Stephanopoulos G (2016) Co-culture engineering for microbial biosynthesis of 3-amino-benzoic acid in Escherichia coli. Biotechnol J 11:981–987 . doi: 10.1002/biot.201600013
Zhu F, Chen G, Chen X, Huang M, Wan X (2011) Aspergicin, a new antibacterial alkaloid produced by mixed fermentation of two marine-derived mangrove epiphytic fungi. Chem Nat Compd 47:767–769 . doi: 10.1007/s10600-011-0053-8
Zhu F, Chen GY, Wu JS, Pan JH (2013) Structure revision and cytotoxic activity of marinamide and its methyl ester, novel alkaloids produced by co-cultures of two marine-derived mangrove endophytic fungi. Nat Prod Res 27:1960–1964 . doi: 10.1080/14786419.2013.800980
Zhu F, Lin Y, Ding J, Wang X, Huang L (2007) Secondary metabolites of two marine-derived mangrove endophytic fungi (strain nos. 1924# and 3893#) by mixed fermentation. Chem Ind For Prod 27:8–20
Zuck KM, Shipley S, Newman DJ (2011) Induced Production of N-Formyl Alkaloids from Aspergillus fumigatus by Co-culture with Streptomyces peucetius. J Nat Prod 74:1653–1657 . doi: 10.1021/np200255f

CHAPTER 5. EXPANSION OF THE MICROBIAL METABOLOME - INDUCING CRYPTIC ANTIMICROBIAL SECONDARY METABOLITES BY CO-CULTURE

Article title: Enhancement of microbial chemical diversity – Inducing cryptic antimicrobial secondary metabolites by co-culture.

Journal: RSC Advances.

Status: Unpublished.

Authors: Denise Medeiros Selegato[1,2], Özlem Erol[1], Rafael Teixeira Freire[3], Ian Castro-Gamboa[2], Young Hae Choi[1]

Affiliations:

[1] Natural Products Laboratory, Institute of Biology, Leiden University, Leiden, The Netherlands.

[2] Nucleus of Bioassays, Biosynthesis and Ecophysiology of natural products (NuBBE), Institute of Chemistry, São Paulo State University, Araraquara, Brazil.

[3] Medway Metabonomics Research Group, University of Greenwich, Chatham Maritime, Kent, UK.

Figure SM9. Co-culture experiments of **(A)** *A. alternata*/*F. oxysporum* and **(B)** *D. eres/F. oxysporum* on day 4 and day 12. On day 4, *A. alternata*/*F. oxysporum* displayed a distance-inhibition while *D. eres/F. oxysporum* showed a zone line. On day 12, however, *F. oxysporum* overcame the inhibition barrier, growing over the challenge fungi in a overgrowth interaction.

(A)

(B)

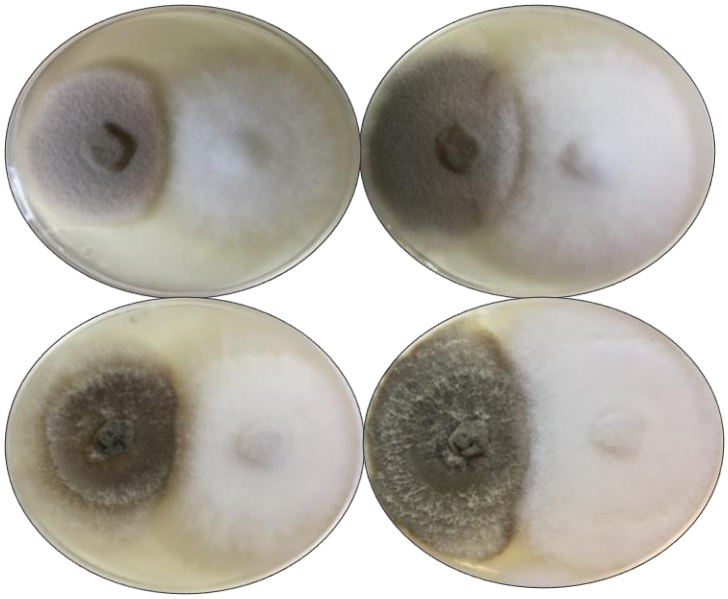

LC-MS Analysis

Automated MS/AutoMS mode is commonly prioritized in the analysis of molecular networking since it provides the simultaneous fragmentation of several ions in an extract. In practice, this process ensures that most of the metabolites in a extract are detected and fragmented in one single injection, decreasing the use of solvent and the analysis time.

LC-MS analysis was performed for all samples, including co-cultures, monocultures and blank. LC analysis was carried out in a Shimadzo Class-LC 10 and Diodes Array Detectors (DAD) with wavelength from 190 to 800 nm using the optimized method described in Chapter 2. The column eluent was divided using a 5:1 splitter, with the largest flow being directed to the DAD detector and the remainder to the mass spectrometer. The MS/AutoMS mode was acquired in a Bruker AmaZon Speed at the following parameters: nebulizer pressure 70 psi, drying gas flow 12.0 L min^{-1}, drying gas temperature 350 °C. The automatic mode was carried out with cycles for positive MS1 acquisition, followed by fragmentation of the two most intense ions (above > 1000 counts). Calibration was performed through addition of trifluoroacetic acid solution (Na-TFA, 10 mg mL^{-1}) at the beginning and end of each chromatographic analysis.

Figure SM10. (A) HPLC-DAD Data of single and monoculture of selected fungi. Identification of induced secondary metabolites in *Fusarium* co-cultures. **(B)** HPLC-DAD Data of single and monoculture of selected fungi. Identification of induced secondary metabolites in *Diaporthe* co-cultures.

(A) *m/z* 180 (fusaric acid); *m/z* 806 (beauvericin); *m/z* 360 (beauvericin monomers).

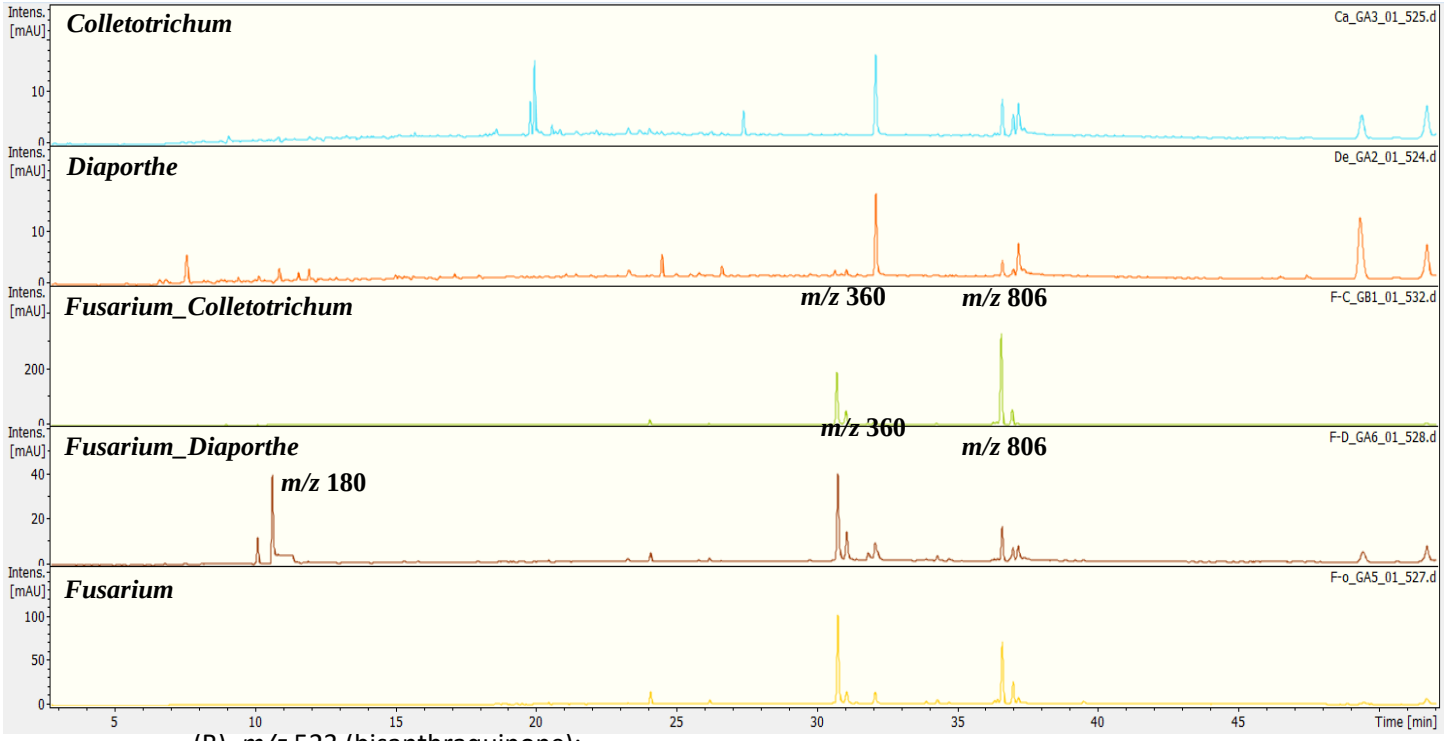

(B) *m/z* 523 (bisanthraquinone);

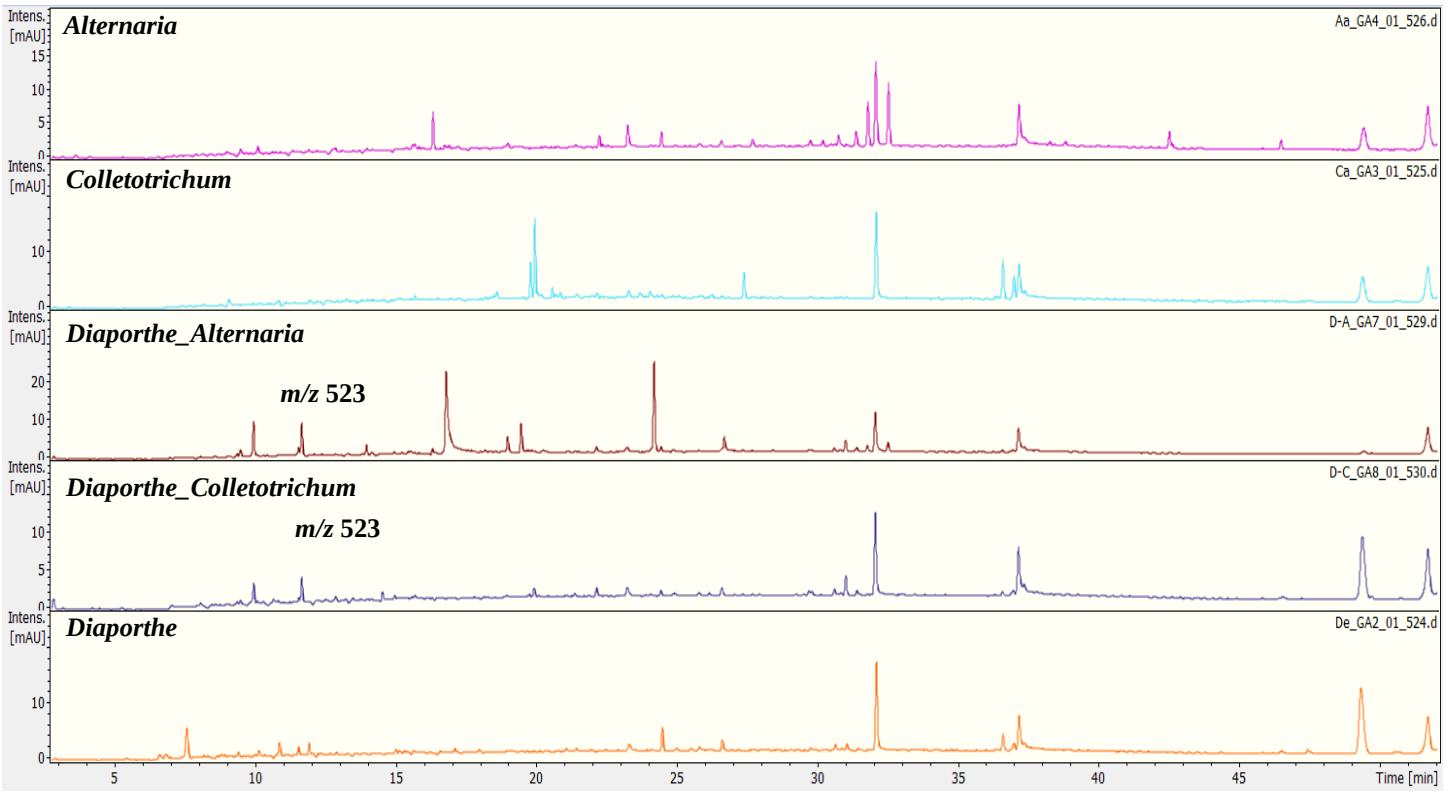

Figure SM11. Stacked plot of ^{1}H Spectra of Czapek and fungal cultures. Signals from two compounds were identified from the Czapek medium: Metabolite 1 at [δ5.37 (*m*), δ2.27 (*t*, *J* 7.4 Hz), δ2.02 (*d*, *J* 5.8 Hz), δ1.60 (*dt*, *J* 14.5 and 7.2 Hz)] ; Metabolite 2 at [δ7.45 (*dd*, *J* 8.2 and 2.2 Hz), δ7.22 (*d*, *J* 2.4 Hz, 1H), δ6.95 (*s*), δ5.80 (*ddt*, *J* 17.0, and 3.3 Hz), δ4.99 (*dd*, *J* 3.7 and 1.8 Hz), δ4.96 (*dd*, *J* 3.7 and 1.8 Hz) , δ4.02 (*t*, *J* 6.6 Hz), δ2.81 (*t*, *J* 7.4 Hz), δ2.56 (*t*, *J* 7.4 Hz), δ2.04 (*d*, *J* 7.4 Hz), δ0.89 (*t*, *J* 6.9 Hz).

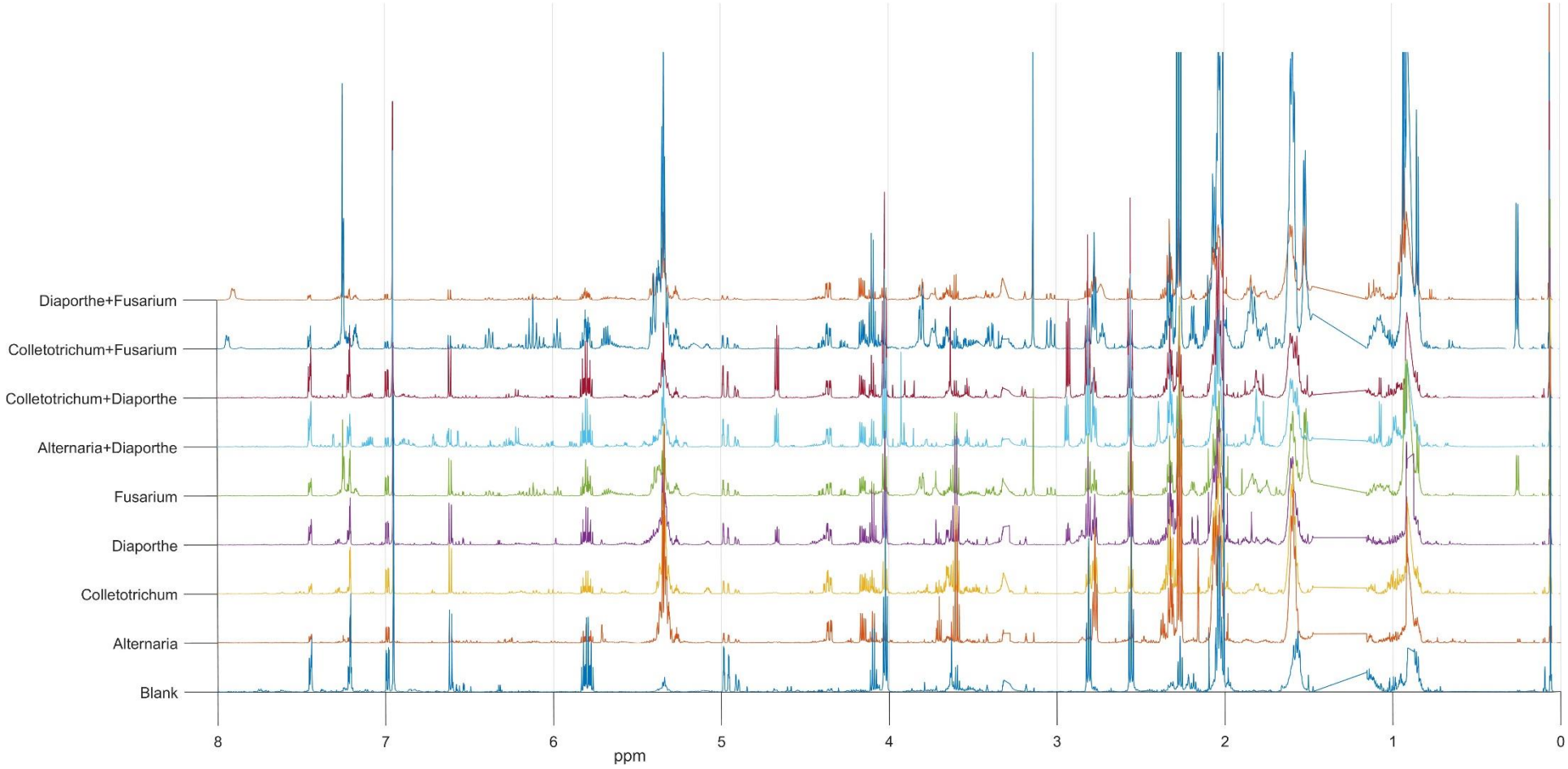

CHAPTER 6. EXPANSION OF THE MICROBIAL METABOLOME - A SYSTEMS APPROACH TO IMPROVE BIOACTIVE METABOLITE PRODUCTION BY OSMAC AND ^{1}HqNMR

Article title: Improvement of Bioactive Metabolite Production in Microbial Cultures - A systems approach by OSMAC and ^{1}HqNMR.

Journal: Magnetic Resonance in Chemistry.

Status: Accepted.

Authors: Denise Medeiros Selegato[a], Rafael Teixeira Freire[b], Alan César Pilon[c], Carolina Rabal Biasetto[a], Haroldo Cesar de Oliveira[d], Lucas Magalhães de Abreu[e], Angela Regina Araujo[a], Vanderlan da Silva Bolzani[a], Ian Castro-Gamboa[a*]

Affiliations:

[a] *Nucleus of Bioassays, Biosynthesis and Ecophysiology of natural products (NuBBE), Organic Chemistry Depart., Institute of Chemistry, São Paulo State University (UNESP), St. Prof. Francisco Degni, 55, Quitandinha, Post code 14800-060, Araraquara, SP, Brazil.*

[b] *Medway Metabonomics Research Group, University of Greenwich, Post Code ME4 4TB, Chatham Maritime, Kent, UK.*

c Núcleo de Pesquisa em Produtos Naturais e Sintéticos (NPPNS), Faculdade de Ciências Farmacêuticas, São Paulo University (USP), Avenida do Café s/n, Monte Alegre, Post Code 14040-903, Ribeirão Preto, SP, Brazil.

[d] *Laboratório de Micologia Clínica, Núcleo de Proteômica, Faculdade de Ciências Farmacêuticas de Araraquara, São Paulo State University (UNESP), Rodovia Araraquara Jaú, Km 01 - s/n, Campos Ville, Post Code 14800-903, Araraquara, SP, Brazil.*

[e] *Departamento de Fisiopatologia, Universidade de Viçosa (UFV), Campus Universitário, s/n, Post Code 36570 000, Viçosa, MG, Brazil.*

Fungi Genetic Identification

Table SM3. Gene sequence obtained from the genetic identification of endophytic and rhizosphere fungi.

Samples	DNA Sequence	Access number
Fusarium oxysporum	GAACCTCCATCAAACGGTAGGAGGTGACCTGCGG AGAATATCAATCAGCGGAGGACCCGTCCCGAGGA AAACGGGACGGCCCGCCAGAGGACCCCTAAACTC TGTTTCTATATGTAACTTCTGAGTAAAACCATAAA TAAATCAAAACTTTCAACAACGGATCTCTTGGTTC TGGCATCGATGAAGAACGCAGCAAAATGCGATAA GTAATGTGAATTGCAGAATTCAGTGAATCATCGA ATCTTTGAACGCACATTGCGCCCGCCAGTATTCTG GCGGGCATGCCTGTTCGAGCGTCATTTCAACCCTC AAGCACAGCTTGGTGTTGGGACTCGCGTTAATTCG CGTTCCTCAAATTGATTGGCGGTCACGTCGAGCTT CCATAGCGTAGTAGTAAAACCCTCGTTACTGGTAA TCGTCGCGGCCACGCCGTTAAACCCCAACTTCTGA ATGTTGACCTCGGATCAGGTAGGAATACCCGCTG AACTTAAGCATATCAATAAGGCGGAGGAA	KP230811.1
Diaporthe anacardii	GAAGTAAAARTCGTAACAAGGTCTCCGTTGGTGA ACCAGCGGAGGGATCATTGCTGGAACGCGCCCCT GGCGCACCCAGAAACCCTTTGTGAACTTATACCTT ACTGTTGCCTCGGCGCAGGCCGTCCCCTATGGGGT CCCTTGGAGACAAGGAGCAGCCGGCCGGTGGCCA AATTAACTCTGTTTTTACACTGTAACTCTGAGTAT AAAACATAAATGAATCAAAACTTTCAACAACGGA TCTCTTGGTTCTGGCATCGATGAAGAACGCAGCGA AATGCGATAAGTAATGTGAATTGCAGAATTCAGT GAATCATCGAATCTTTGAACGCACATTGCGCCCTC TGGTATTCCGGAGGGCATGCCTGTTCGAGCGTCAT TTCAACCCTCAAGCCTGGCTTGGTGTTGGGGCACT GCCTGTAAAAGGGCAGGCCCTGAAATATAGTGGC GAGCTCGCCAGGACTCCGAGCGTAGTAGTTAAAC CCTCGCTTTGGAAGGCCTGGCGGTGCCCTGCCGTT AAACCCCAACTTTTGAAAATTTGACCTCGGATCAG GTAGGAATACCCGCTGAACTTAAGCATATC	NR_111841.1
Xylaria cubensis strain CML 2843 alpha-actin gene, partial cds	ACGAGTCCTTCTGGCCCATACCGATCATGA TACTGAGGGGCACAAGTTAATCGACGGGCG CCCATGGTCGCAGAGATAGCGATCAATGCA TGCAGCAGGCACAAACTTACCCATGATGAC GGGGACGACCGACAATGGACGCTATGAGCA AAGGTCAGAAGACAAGTTGATGACGATGCA ACGAGCCGCATCTTGGCGAGGCACAAGCGG GGCTATCCGTTGGGCAAGGCTAGGGAGATA AGACTTACGGAAAACAGCTCGGGGAGCATC ATCACCGGCGAAACCGG	KY006658

Bioactive metabolite elucidation

The elucidation of the selected bioactive metabolites fusaric acid, cytochalasin D and nitropropionic acid from, respectively, *F. oxysporum*, *X. cubensis* and *D. anacardii* were conducted by one and two-dimensional NMR on a Bruker Ascend III of 14.09 Tesla (600.12 MHz to hydrogen frequency) spectrometer with cryo-probe technology (Bruker, USA).

For ^{1}H NMR acquisition, analysis parameters were TD 65k, NS 20, d1 2.00 s, SW 13 ppm, DS 4; and temperature: 295.2K. Saturation on the residual deuterated water signal, at δ4.902 (*s*, 2H) was performed by pre-saturation pulse sequence using composite pulse (zgcppr, Bruker).

For HMBC and HSQC acquisition, analysis parameters were, respectively for ^{1}H (f2) and ^{13}C (f1), spectrometer frequency 600.13 and 150.91 MHz; TD 512 and 512; SW 13 and 230 ppm; NS 32; d1 2.0 s and temperature 295.2K. The long-range coupling constant used for HMBC was 8.0 Hz. Pulse sequences used on 2D NMR analysis were (i) phase-sensitive ge-2D multiplicity edited HSQC using PEP and adiabatic pulses with gradients in back-inept (hsqcedetgpsisp2.4, Bruker) for ^{1}H-^{13}C HSQC and (ii) phase-sensitive ge-2D HMBC using a two-fold low-pass J-filter (hmbcetgpl3nd 2D, Bruker) for ^{1}H-^{13}C HMBC.

Figure SM12. Proton NMR Spectra of all factorial planning experiments of (A) *F. oxysporum*, (B) *X. cubensis* and (C) *D. anacardii*.

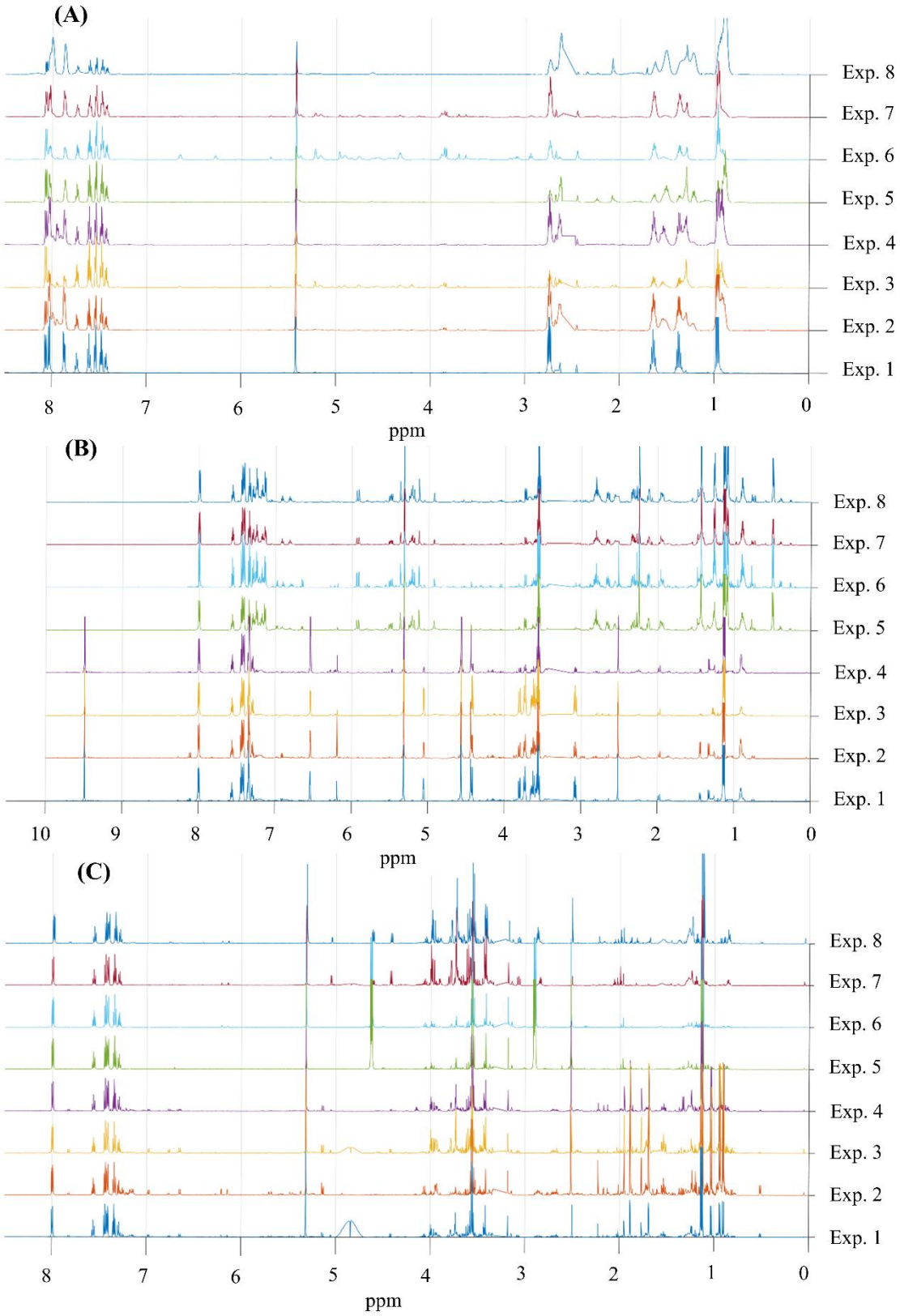

Fusaric acid elucidation in F. oxysporum

^{1}H-NMR spectrum of *F. oxysporum* (600MHz) suggested the presence of seven peaks (Table S2), displayed in the aromatic and aliphatic region. 1D-TOCSY revealed a linear alkyl chain from H7 to H10, as well as an aromatic spin system at H3-H4, indicating para-substituents in a pyridine ring. ^{1}H-^{13}C-HMBC showed correlation between H7 and the aromatic carbons C4, C5 and C6, indicating the presence of the previously determined alkyl group in C-4.

Figure SM13. ^{1}HNMR Spectra of *F. oxysporum* extract in DMSO-d_6. Chemical shift at δ5.42 (*s*, 2H, CH_2, H-8) refers to IS benzyl benzoate.

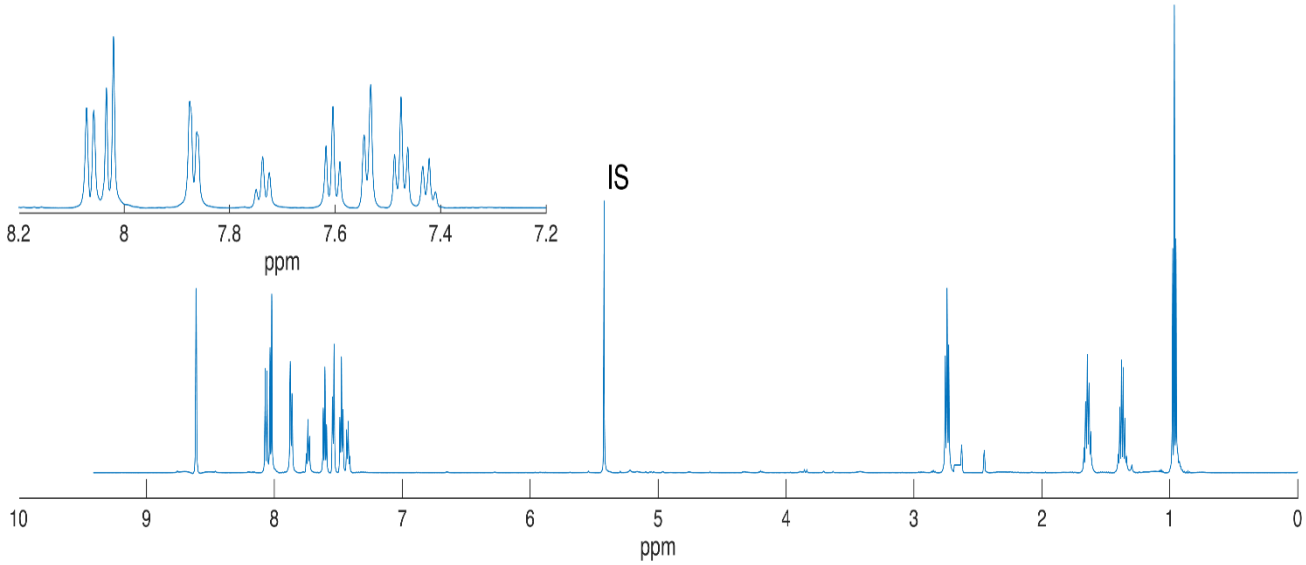

Table SM4. ^{1}H e ^{13}C chemical shifts, ^{1}H-^{1}H-COSY and ^{1}H-^{13}C HMBC correlation of fusaric acid identified and quantified from *F. oxysporum*.

	δ^{1}H (600 MHz, DMSO)	**δ^{13}C (150 MHz)**	**HMBC**	**COSY**
2	-	δ144.60	-	-
3	δ8.01 (*dd*, *J* 8.1 21.9 Hz, 1H, CH)	δ124.72	C5	H4
4	δ7.80 (*dd*, *J* 8.1 2.3 Hz, 1H, CH)	δ138.78	C1, C6	H3
5	-	δ143.07	-	-
6	δ8.61 (*s*, 1H, CH)	δ147.86	C1, C4	-
7	δ2.74 (*t*, *J* 8.1 Hz, 2H, CH_2),	δ77.38	C3, C4, C5, C8, C9	H8
8	δ1.38 (*m*, 2H, *J* 8.1 14.7, CH_2),	δ32.76	C9, C10	H7, H9
9	δ1.64 (*m*, *J* 7.714.7, 2H, CH_2),	δ21.62	C8, C10	H8, H10
10	δ0.96 (*t*, *J* 7.7 Hz, 3H CH_3)	δ12.92	C8, C9	H9

Nitropropionic acid elucidation in D. anacardii extract

Nitropropionic acid displays only two ^{1}H-NMR signals at δ2,92 (*t*, *J* 6.0 Hz, 2H, CH_2) and δ4.67 (*t*, *J* 6.0 Hz, 2H, CH_2), that correlated among themselves and the sp^2 carbon on C-1 (Table S3).

Figure SM14. *D. anacardii* extract in MeOD-*d*$_4$. Chemical shift at δ5.316 (*s*, 2H, CH_2, H-8) refers to IS benzyl benzoate.

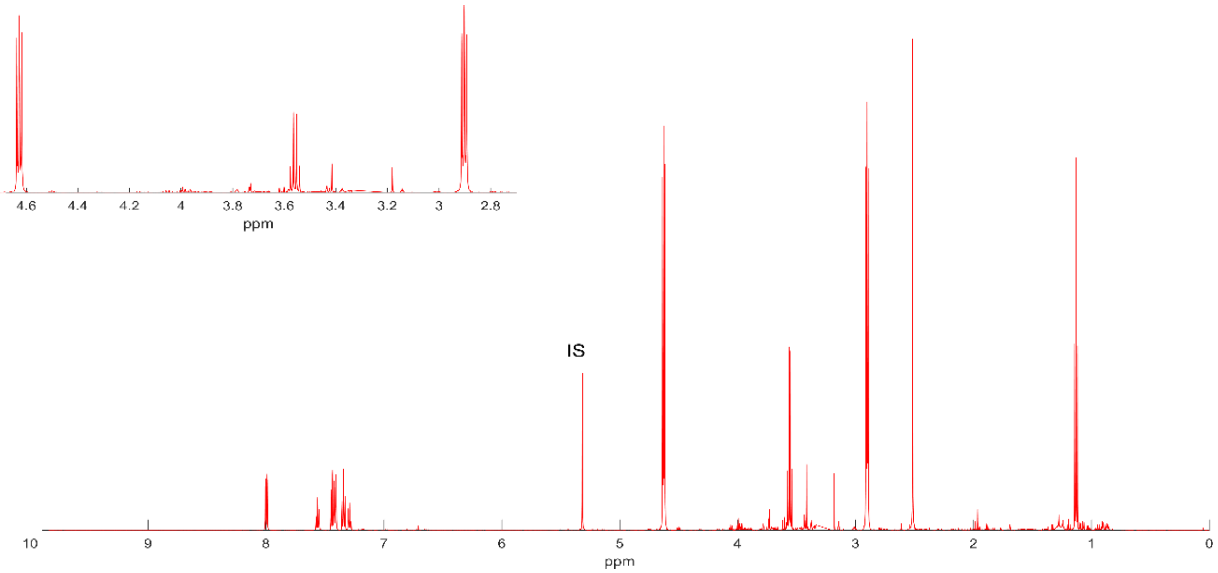

Table SM5. ^{1}H e ^{13}C chemical shifts, ^{1}H-^{1}H-COSY and ^{1}H-^{13}C HMBC correlation of nitropropionic acid identified and quantified from *D. anacardii*.

	δ^{1}H (600 MHz, DMSO)	**δ^{13}C (150 MHz, DMSO)**	**HMBC**	**COSY**
1	-	δ174.31	-	-
2	δ2.92 (*t*, *J* 6.0 Hz, 2H, CH_2)	δ30.20	C1, C3	C3
3	δ 4.67 (*t*, *J* 6.0 Hz, 2H, CH_2)	δ69.55	C1; C2	C2

Cytochalasin D elucidation in X. cubenses and D. anacardii extract

Cytochalasin D ^{1}H-NMR spectrum (600MHz) revealed peaks at the aromatic, olefinic and aliphatic NMR regions, with several second order signals. HMBC correlation showed a benzyl group correlated to H3 and H6 signals from olefinic hydrogens bonded in a macrocycle, as well as several other correlations displayed at Table S4.

Table SM6. ^{1}H e ^{13}C Chemical shifts, ^{1}H-^{1}H-COSY and ^{1}H-^{13}C HMBC correlation of cytochalasin D identified and quantified from *X. cubensis* and *D. anacardii*.

	$\delta^{1}H$ (600 MHz, MeOD)	**$\delta^{13}C$ (150 MHz, MeOD)**	**HMBC**	**COSY**
1	-	δ176.6	-	-
2	-	-	-	-
3	δ3.28 (*m*)	δ55.2	C1; C5; C4; C1’	H4
4	δ2.17 (*m*)	δ49.6	C1; C5; C10; C3; C6	H3; H5
5	δ2.61 (*m*)	δ33.4	C4; C11; C12	H4
6	-	δ150.9	-	-
7	δ3.70 (*d*; 10.4 Hz)	δ72.3	C5; C12; C13	H8
8	δ2.86 (*m*)	δ47.8	C1; C6; C7; C21	H7; H13
9	-	δ54.9	-	-
10α	δ2.71 (*m*)	δ44.9	C2’e 6’; C1’; C4; C3	H3
10β	δ2.88 (*m*)			
11	δ0.50 (*d*; 6.8 Hz)	δ13.5	C5; C4; C6	H5
12α	δ4.93 (*s*)	δ113.7	C5; C6; C7	H5
12β	δ5.12 (*s*)			
13	δ5.49 (*dd*; 9.8; 15.7 Hz)	δ131.8	C15; C8; C7	H8
14	δ5.23 (*m*)	δ134.5	C15; C8	H15β
15α	δ2.33 (*dd*; 5.0; 13.0 Hz)	δ39.4	C22; C16; C13; C17	H14
15β	δ2.37 (*m*)		C16; C13; C17	H16; H14
16	δ2.82 (*m*)	δ43.4	C15; C17	H22; H15β
17	-	δ211.7	-	-
18	-	δ79.3	-	-
19	δ5.18 (*d*; 2.5 Hz)	δ128.9	C20; C21	*
20	δ5.92 (*dd*; 2.5; 5.9 Hz)	δ133.4	C21; C18; C19	H19
21	δ5.37 (*t*; 2.5 Hz)	δ78.2	C4; C3; C19; C20; C24	*
22	δ1.26 (*d*; 6.8 Hz)	δ19.7	C15; C16; C17	H16
23	δ1.43 (*s*)	δ24.6	C19; C17	*
24	-	δ171.8	-	-
25	δ2.24 (*s*)	δ20.6	C21; C24	-
1’	-	δ138.4	-	-
2’ e 6’	δ7.14 (*d*; 8.1 Hz)	δ130.9	C10; C4’	H3’/H5’
3’ e 5’	δ7.56 (*t*; 7.5 Hz, 1H, CH)	δ129.6	C1’	H2’/H6’
4’	δ7.34 (*t*; 7.5 Hz, 1H, CH)	δ127.9	C2’/C6’	*

Figure SM15. NMR Spectrum of *X. cubensis* extract in MeOD-d_4. Chemical shift at δ5.31(*s*, 2H, CH_2, H-8) refers to IS benzyl benzoate.

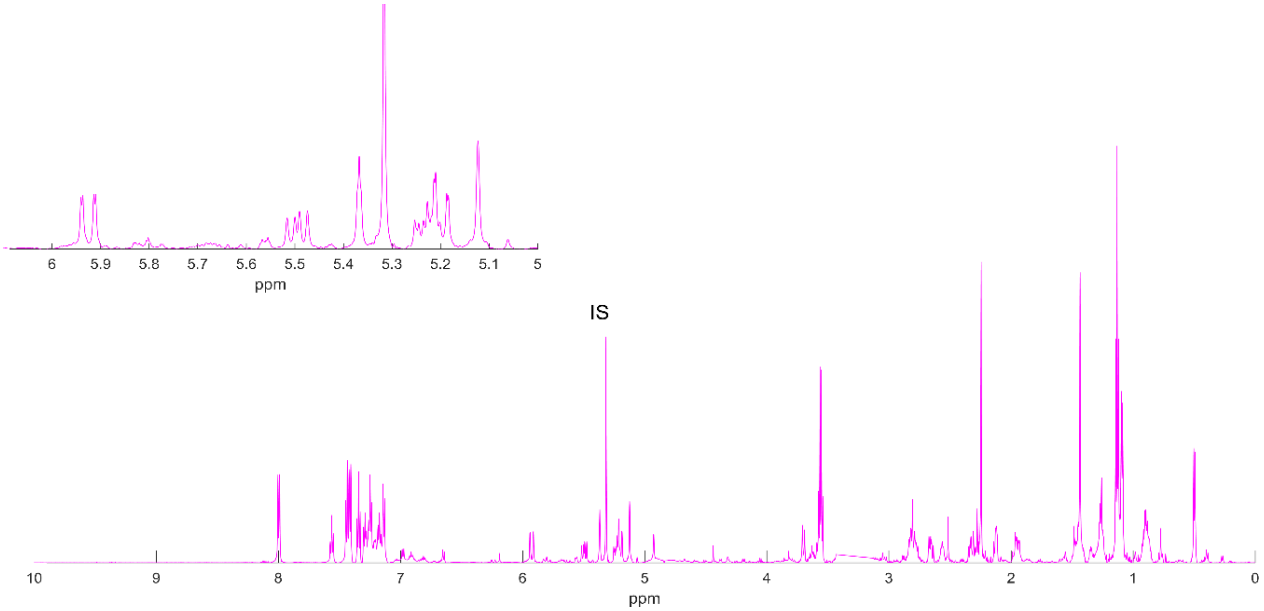

GSD Deconvolution of ^{1}HqNMR data

Figure SM16. Individual GSD-deconvoluted peaks superimposed with the experimental spectrum of all factorial planning experiments from *F. oxysporum* (Exp. 1-8).

Exp.1

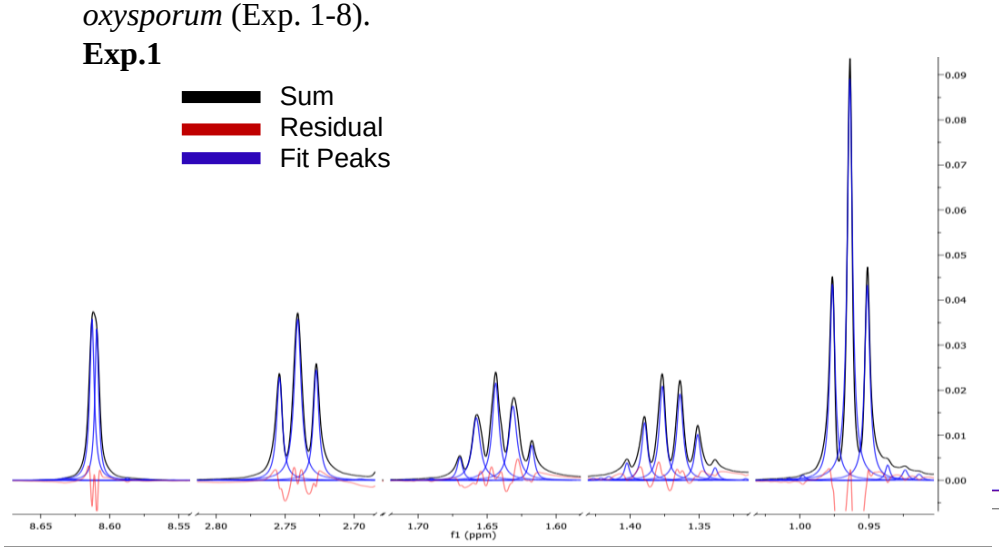

Exp.3

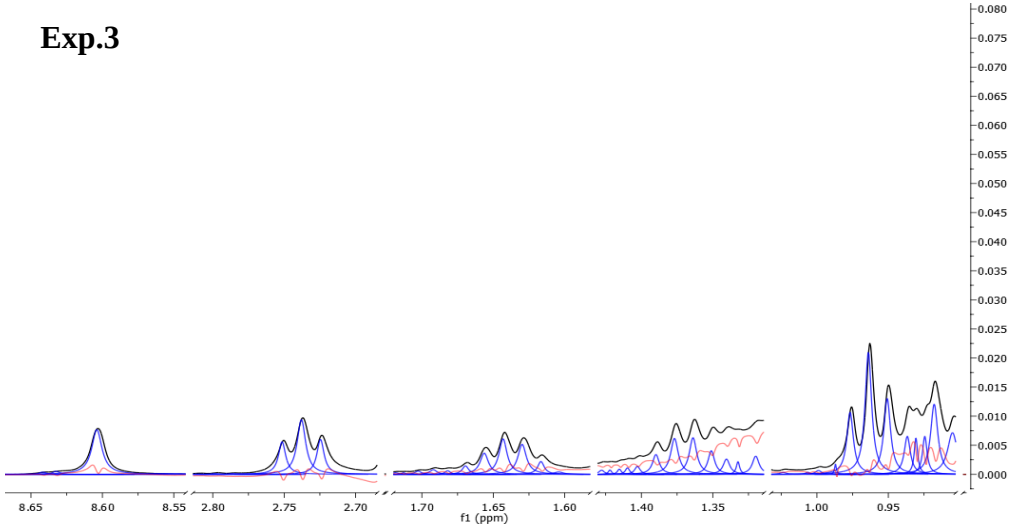

Exp.2

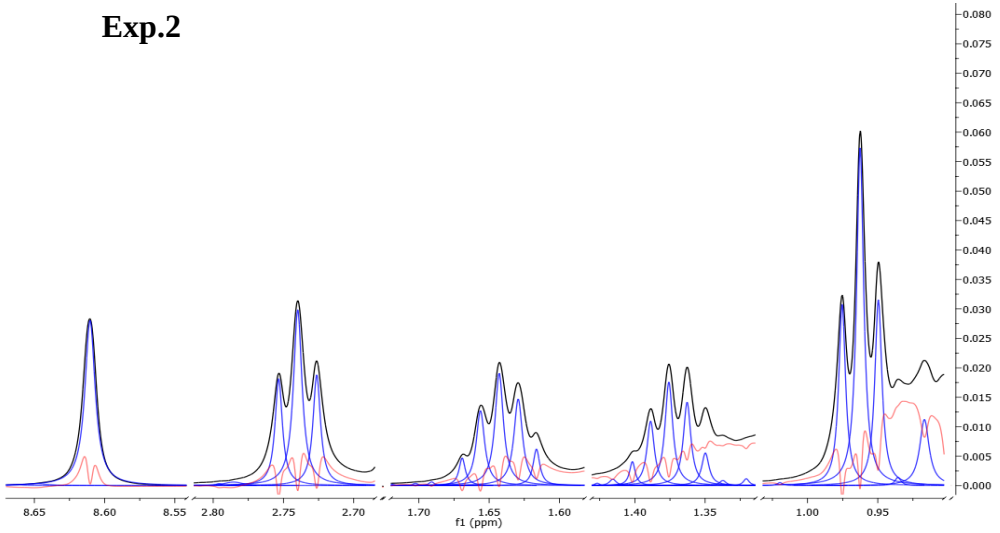

Exp.4

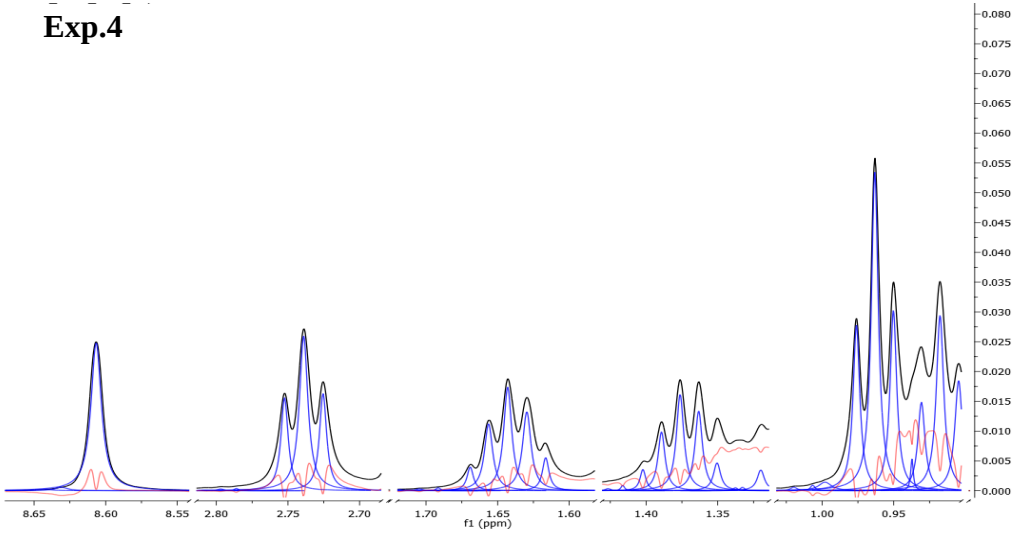

Exp.5

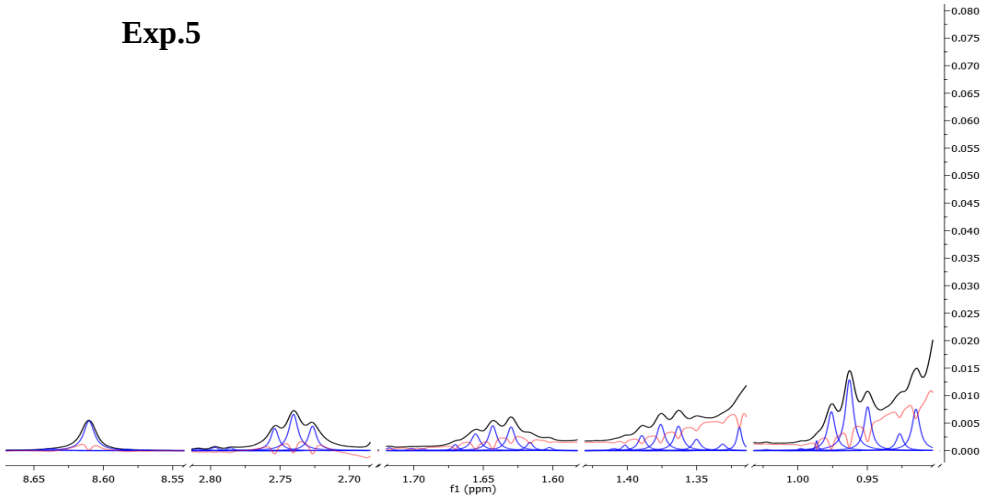

Exp.7

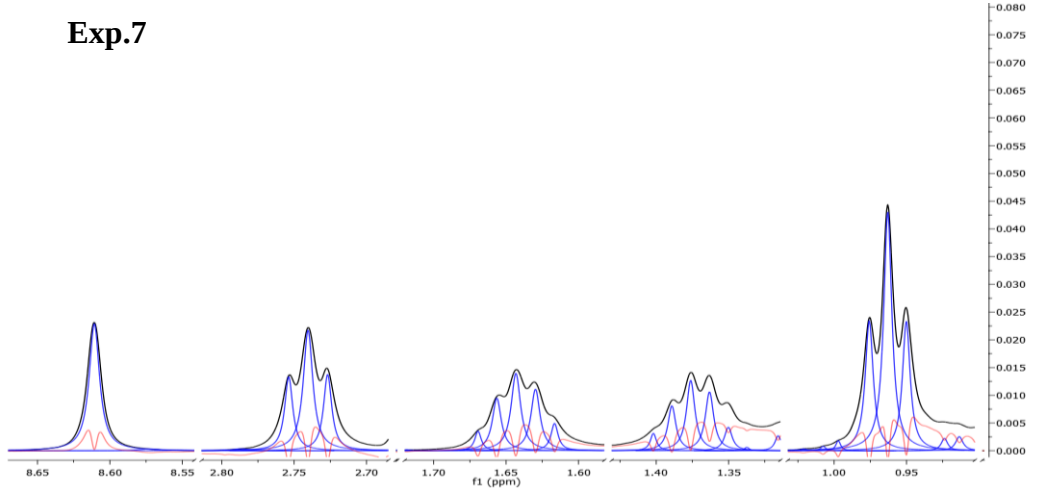

E xp.6

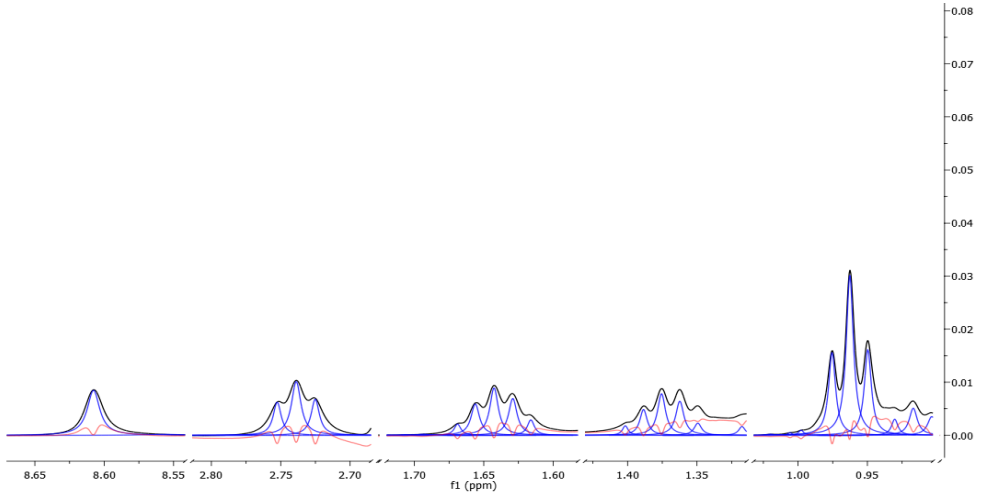

Exp.8

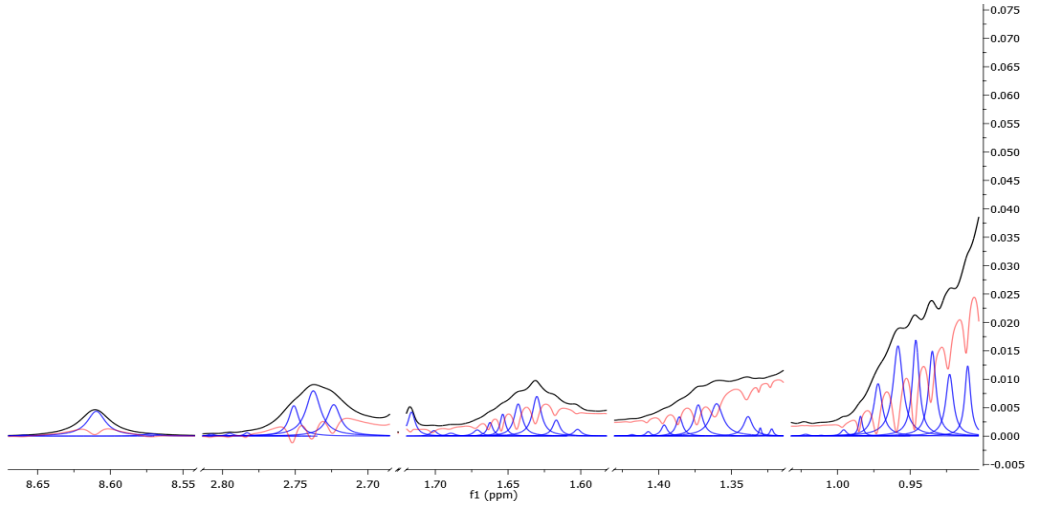

Figure SM17. Individual GSD-deconvoluted peaks superimposed with the experimental spectrum of all factorial planning experiments from *X. cubensis* (Exp. 1-8).

Exp.1

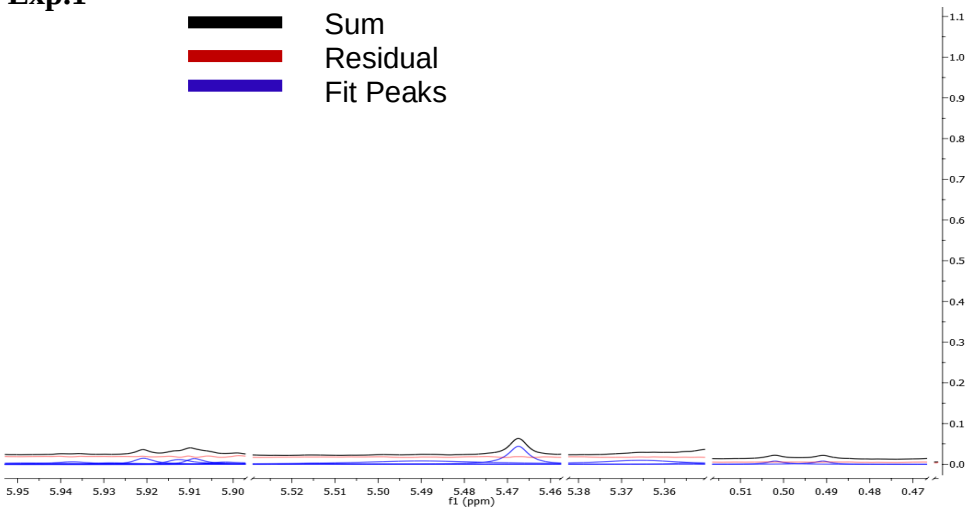

Exp.3

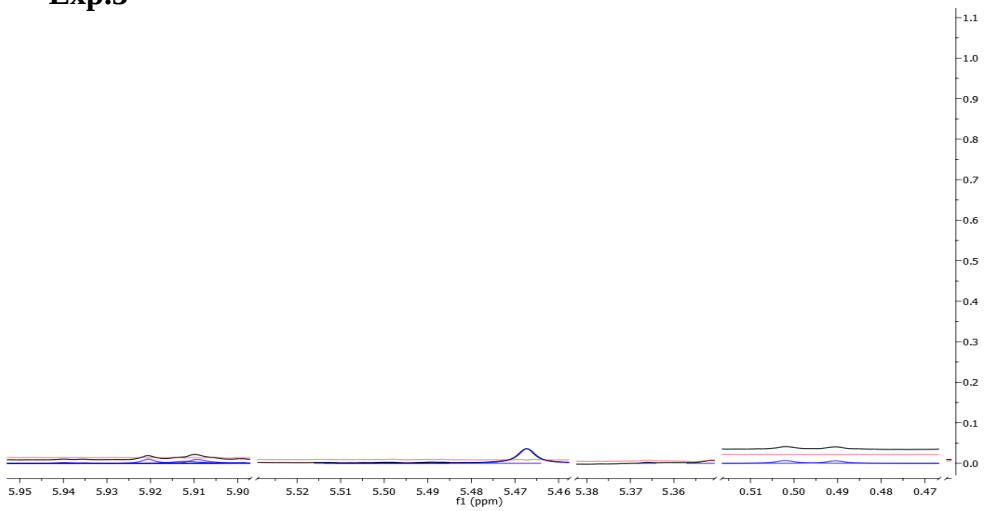

Exp.2

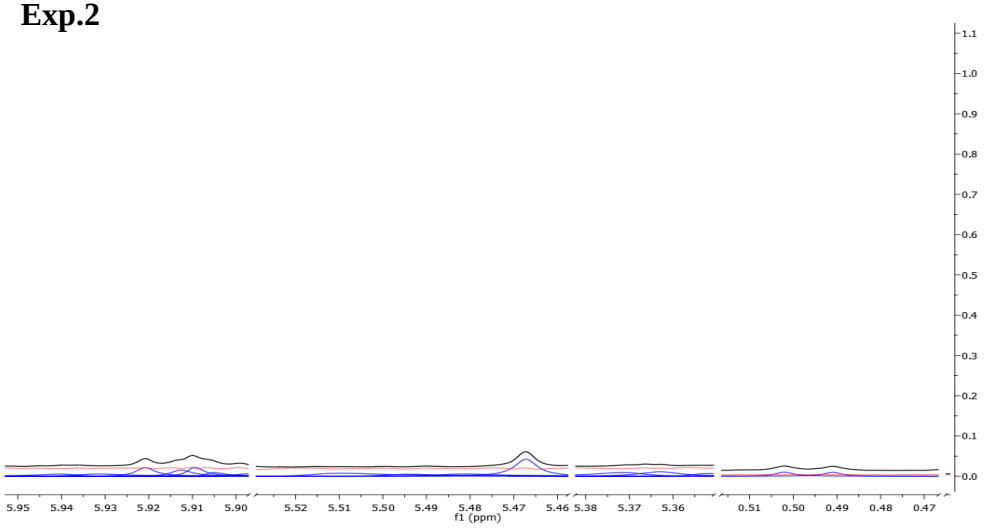

Exp.4

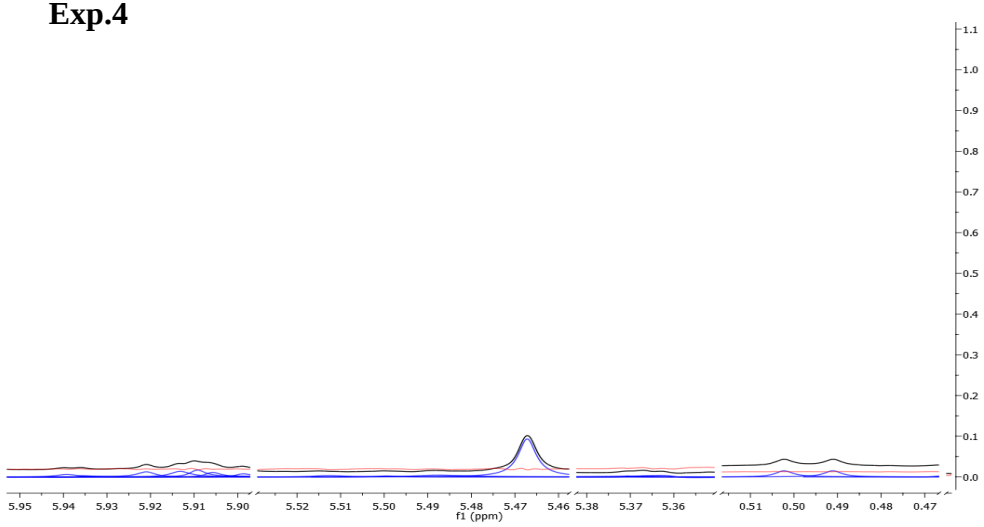

Exp.5

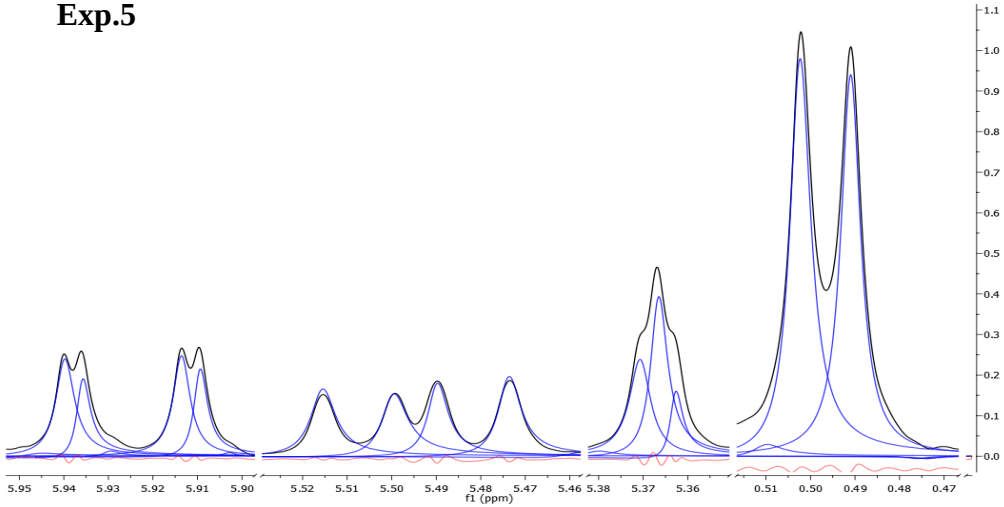

Exp.7

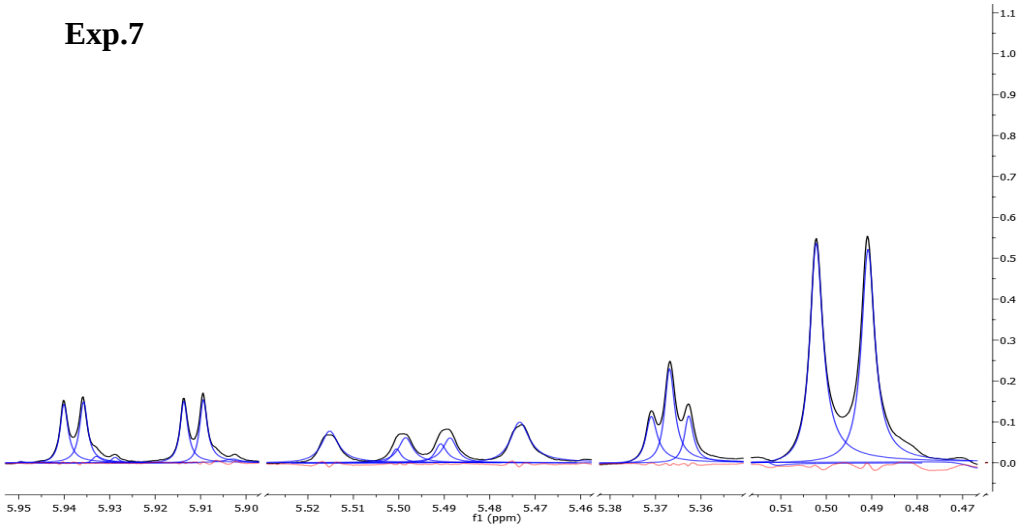

Exp.6

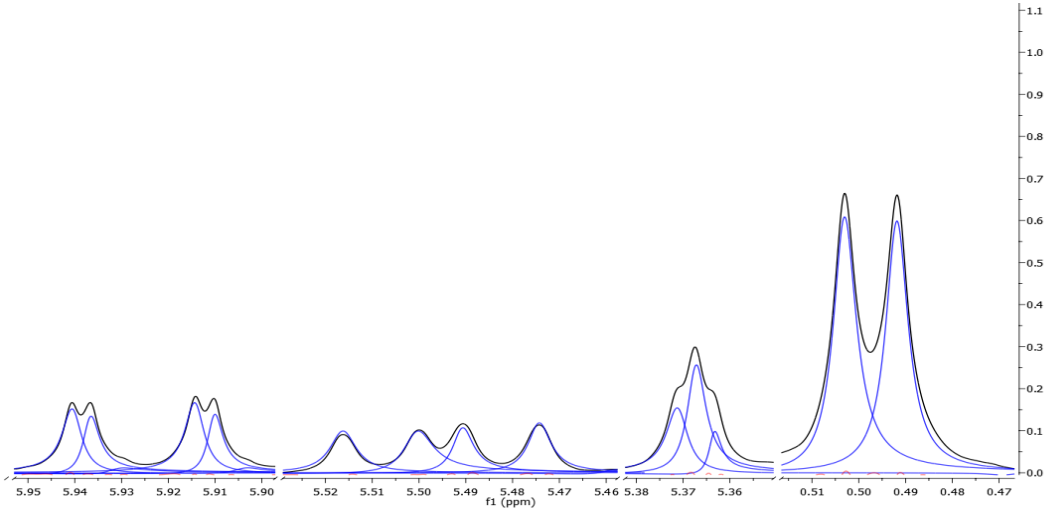

Exp.8

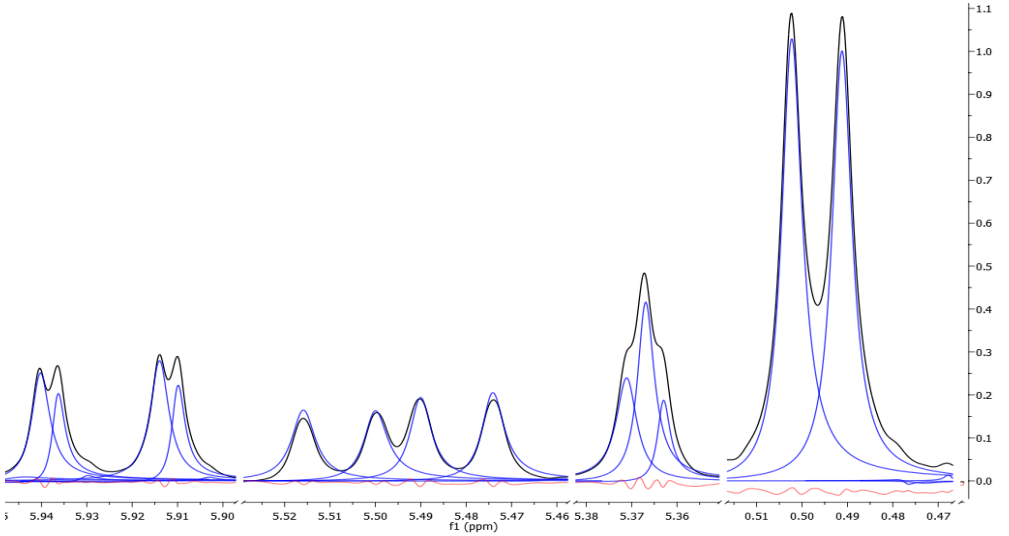

Figure SM18. Individual GSD-deconvoluted peaks superimposed with the experimental spectrum of all factorial planning experiments from *D. anacardii* (Exp. 1-8).

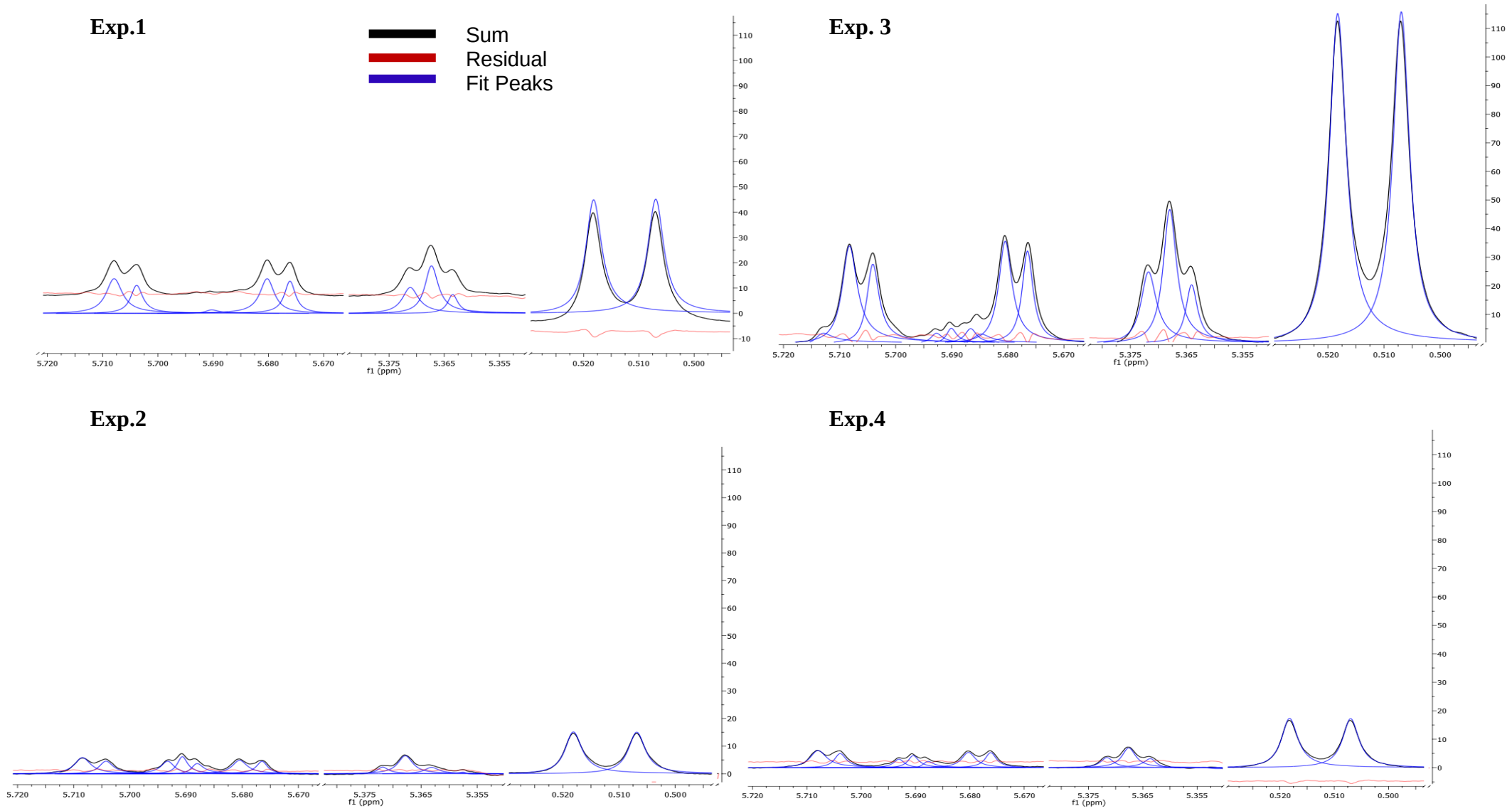

Exp.5

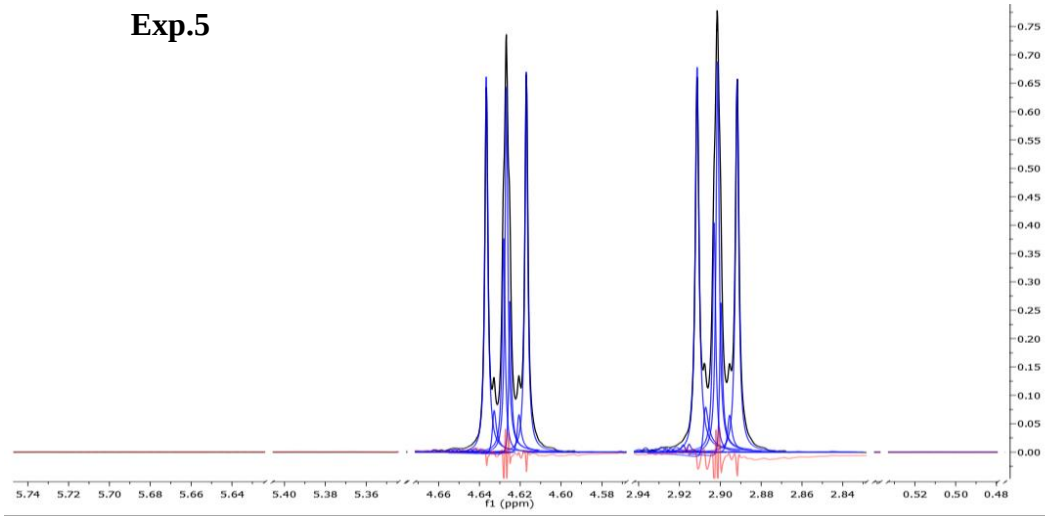

Exp.7

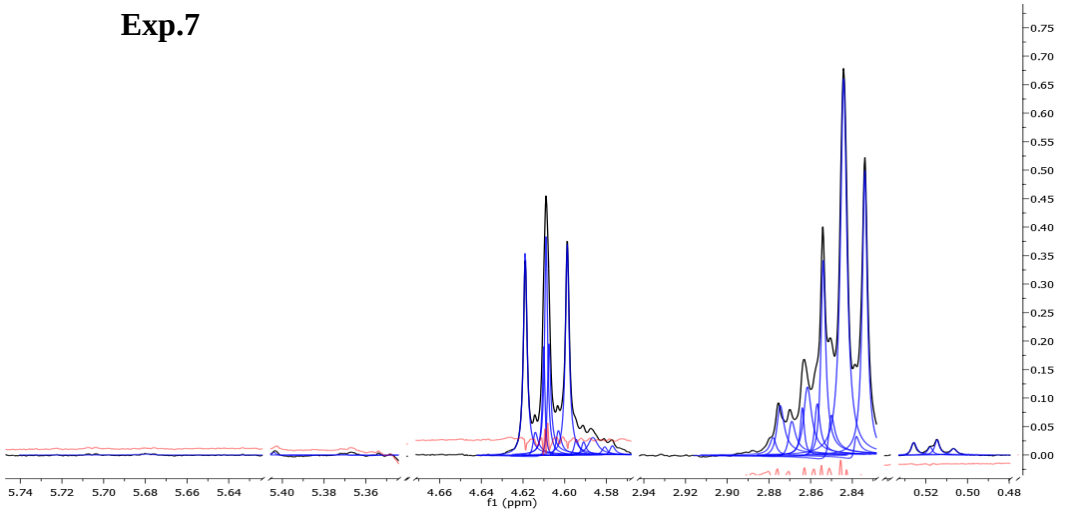

Exp.6

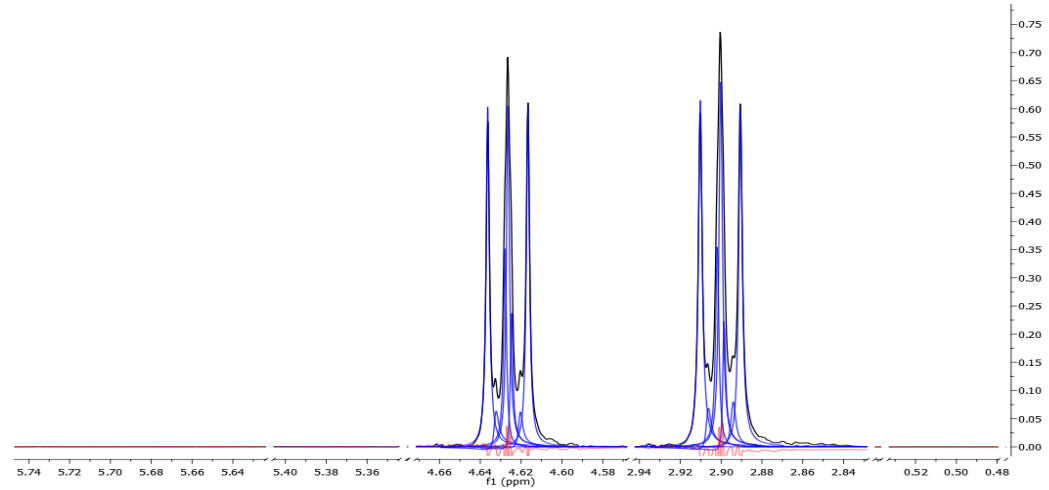

Exp.8

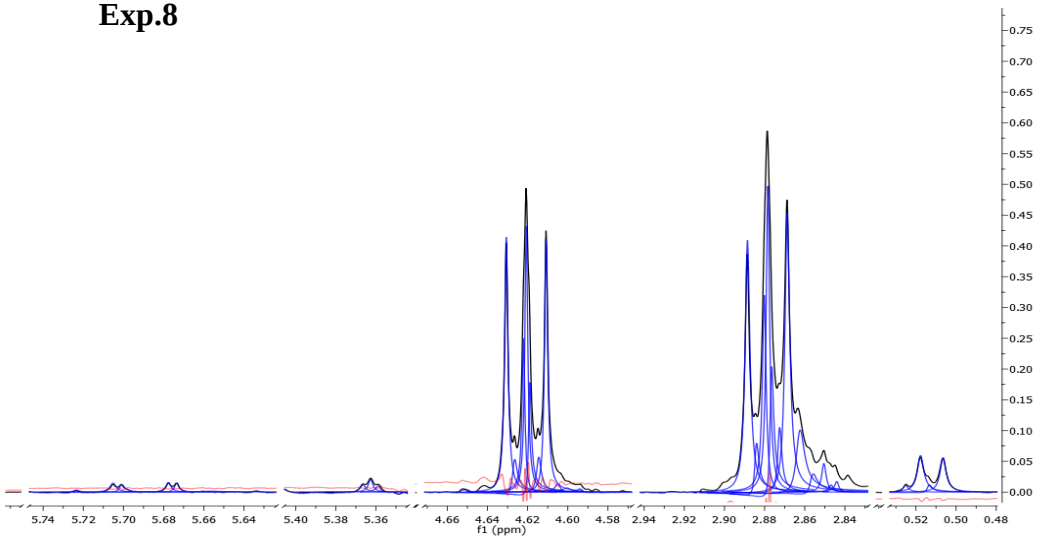

[1]HNMR Quantification

Table SM7. GSD-[1]HqNMR results of fusaric acid found in *F. oxysporum* extracts.

Exp.	ppm	Area	No. H.	Fusaric acid per tube (mg)	Average (mg)	SD	Purity %	Fusaric acid/extract (mg)
1	8.613	2.130	1	1.184	1.069	0.195	40.560	26.486
	5.421	2.153	2	-				
	1.644	3.412	2	0.948				
	1.377	3.108	2	0.863				
	0.976	6.909	3	1.280				
2	8.613	2.115	1	1.415	1.220	0.214	27.096	35.361
	5.421	1.909	2	-				
	1.644	3.390	2	1.134				
	1.377	2.864	2	0.958				
	0.976	6.154	3	1.372				
3	8.613	0.569	1	0.251	0.272	0.031	15.699	15.452
	5.421	2.744	2	-				
	1.644	1.116	2	0.246				
	1.377	1.266	2	0.279				
	0.976	2.128	3	0.313				
4	8.613	1.870	1	1.015	0.872	0.162	26.641	42.439
	5.421	2.303	2					
	1.644	2.935	2	0.797				
	1.377	2.502	2	0.679				
	0.976	5.511	3	0.997				
5	8.613	0.432	1	0.265	0.287	0.032	7.491	2.412
	5.421	2.188	2	-				
	1.644	0.888	2	0.273				
	1.370	0.909	3	0.279				
	0.976	1.580	3	0.324				
6	8.613	0.786	1	0.483	0.516	0.109	13.782	2.426
	5.421	1.948	2					
	1.644	1.652	2	0.507				
	1.377	1.329	2	0.408				
	0.976	3.258	3	0.667				
7	8.613	1.692	1	1.156	1.159	0.005	30.818	4.869
	5.421	1.791	2	-				
	1.644	2.660		0.908				
	1.377	2.217	2	0.757				
	0.976	5.109	3	1.163				
8	8.613	0.570	1	0.819	0.933	0.095	7.679	3.486
	5.421	0.861	2					

1.644	1.262	2	0.906
1.377	1.337	2	0.960
0.976	2.183	3	1.045

* No. H. = number of hydrogen.

Table SM8. IS-^{1}HqNMR results of fusaric acid found in *F. oxysporum* extracts.

Exp.	ppm	Area	N. H.	Fusaric acid per tube (mg)	Average (mg)	SD	Purity %	Fusaric acid/extract (mg)
1	0.96	5.630	3	1.213	1.266	0.071	48.084	31.399
	1.38	3.882	2	1.254				
	1.64	3.83	2	1.228				
	5.42	1.852	2	-				
	8.61	2.124	1	1.370				
2	0.96	7.883	3	2.008	1.898	0.154	42.186	55.052
	5.42	1.678	2	-				
	8.61	2.348	1	1.789				
3	5.42	2.487	2	-	0.331	-	19.133	18.832
	8.61	0.681	1	0.331				
4	0.96	6.262	3	1.284	1.257	0.038	38.424	23.879
	2.74	4.144	2	1.274				
	5.42	2.036	2	-				
	8.61	1.976	1	1.213				
5	5.42	1.982	2	-	0.400	-	10.446	3.363
	8.61	0.595	1	0.400				
6	0.96	3.442	3	0.788	0.697	0.070	18.614	3.276
	1.64	2.033	2	0.697				
	2.74	1.793	2	0.615				
	5.42	1.740	2	-				
	8.61	1.000	1	0.687				
7	1.64	3.578	2	1.223	1.282	0.059	34.094	5.386
	2.74	3.678	2	1.282				
	5.42	1.759	2	-				
	8.61	1.926	1	1.341				
8	5.42	0.746	2	-	1.487	-	12.247	5.560
	8.61	0.898	1	1.487				

* No. H. = number of hydrogen.

Table SM9. ERETIC2-^{1}HqNMR results of fusaric acid found in *F. oxysporum* extracts.

Exp.	ppm	N. H.	Fusaric acid per tube (mg)	Average (mg)	SD	Purity %	Fusaric acid/extract (mg)
1	8.612	1	0.770	0.730	0.050	27.705	18.092
	2.754	2	0.732				
	1.643	2	0.675				
	1.382	2	0.685				
	0.959	3	0.787				
2	8.613	1	1.081	1.131	0.068	25.136	32.802
	2.740	2	1.143				
	1.647	2	1.056				
	1.378	2	1.231				
	0.972	3	1.147				
3	8.548	1	0.242	0.234	0.016	13.487	13.275
	2.680	2	0.210				
	1.585	2	0.238				
	0.918	3	0.245				
4	8.557	1	0.722	0.692	0.026	21.151	33.693
	2.685	2	0.683				
	1.586	2	0.663				
	1.322	2	0.676				
	0.914	3	0.717				
5	8.622	1	0.273	0.291	0.025	7.587	2.443
	2.739	2	0.308				
6	8.615	1	0.491	0.474	0.033	12.662	2.228
	1.644	2	0.431				
	1.381	2	0.468				
	0.977	3	0.507				
7	8.617	1	0.835	0.813	0.060	21.617	3.415
	2.750	2	0.740				
	1.644	2	0.770				
	1.386	2	0.829				
	0.976	3	0.892				
8	8.486	1	0.773	0.773	-	6.367	2.891

*No. H. = number of hydrogen.

Table SM10. GSD-^{1}HqNMR results of cytochalasin D found in *X. cubensis* extracts.

Exp.	ppm	Area	N. H	Cytochalasin D per tube (mg)	Average (mg)	SD	Purity (%)	Cytochalasin D/experiment (mg)
1	5.316	53.629	2	0.000	0.000		0.000	0.000
2	5.316	56.262	2	0.000	0.000		0.000	0.000
3	5.316	52.678	2	0.000	0.000		0.000	0.000
4	5.316	55.689	2	0.000	0.000		0.000	0.000
	0.500	72.786	3	0.816				
	5.316	63.399	2	-				
5	5.360	25.775	1	0.867	0.900	0.087	20.051	31.921
	5.490	30.340	1	1.020				
	5.920	26.628	1	0.895				
	0.500	25.453	3	0.285				
	5.316	63.503	2	-				
6	5.360	8.372	1	0.281	0.287	0.009	8.255	20.440
	5.490	8.957	1	0.301				
	5.920	8.420	1	0.283				
	0.500	48.699	3	0.554				
	5.316	62.444	2	-				
7	5.360	16.633	1	0.568	0.602	0.047	17.285	53.099
	5.490	18.730	1	0.639				
	5.920	18.885	1	0.645				
	0.500	75.631	3	0.861				
	5.316	62.444	2	-				
8	5.360	22.604	1	0.772	0.906	0.114	26.020	85.449
	5.490	30.261	1	1.033				
	5.920	28.023	1	0.957				

*No. H. = number of hydrogen.

Table SM11. IS-^{1}HqNMR results of cytochalasin D found in *X. cubensis* extracts.

Exp	ppm	Area	N. H	Cytochalasin D per tube (mg)	Average (mg)	SD	Purity %	Cytochalasin D/experiment (mg)
1	-	-	-	-	-	-	-	-
2	-	-	-	-	-	-	-	-
3	-	-	-	-	-	-	-	-
4	-	-	-	-	-	-	-	-
5	0.500	74.990	3	0.936	0.890	0.039	25.579	40.721
	5.316	56.940	2	-				
	5.360	22.610	1	0.847				
	5.490	23.300	1	0.872				
	5.920	24.200	1	0.906				
6	0.500	24.750	3	0.312	0.313	0.019	8.993	22.267
	5.316	56.450	2	-				
	5.360	7.580	1	0.286				
	5.490	8.610	1	0.325				
	5.920	8.710	1	0.329				
7	0.500	48.900	3	0.579	0.572	0.056	16.421	50.446
	5.316	59.970	2	-				
	5.360	15.850	1	0.563				
	5.490	14.630	1	0.520				
	5.920	17.750	1	0.631				
8	0.500	70.680	3	0.900	0.881	0.054	25.324	83.162
	5.316	55.780	2	-				
	5.360	21.970	1	0.840				
	5.490	21.880	1	0.836				
	5.920	24.830	1	0.949				

*No. H. = number of hydrogen.

Table SM12. ERETIC2-^{1}HqNMR results of cytochalasin D found in *X. cubensis* extracts.

Exp.	ppm	Cytochalasin D/tube (Mm)	N. of H	Average (mM)	Cytochalasin D/tube (mg)	SD	Purity %	Cytochalasin D/experiment (mg)
1	-	-	-	-	-	-	-	-
2	-	-	-	-	-	-	-	-
3	-	-	-	-	-	-	-	-
4	-	-	-	-	-	-	-	-
	0.500	1.390	3					
	5.316	1.621	2					
5	5.360	1.331	1	1.301	0.462	0.074	13.279	21.140
	5.490	1.223	1					
	5.920	1.264	1					
	0.500	1.155	3					
	5.316	1.815	2					
6	5.360	1.067	1	1.109	0.394	0.036	11.324	28.038
	5.490	1.108	1					
	5.920	1.123	1					
	0.500	1.794	3					
	5.316	2.252	2					
7	5.360	1.745	1	1.814	0.645	0.202	18.521	56.897
	5.490	1.873	1					
	5.920	1.843	1					
	0.500	2.866	3					
	5.316	3.646	2					
8	5.360	2.632	1	4.517	0.952	0.252	27.361	89.853
	5.490	2.329	1					
	5.920	2.854	1					

*No. H. = number of hydrogen.

Table SM13. GSD-^{1}HqNMR results of target metabolites found in *D. anacardii* extracts. Exp. 1- 4 for cytochalasin D and Exp. 5-10 for nitropropionic acid.

Exp	ppm	Area	N. of H	Metabolite /tube (mg)	Average (mg)	SD	Purity %	Metabolite /experiment (mg)
1	5.367	1.060	1	0.078	0.077	0.0005	2.231	1.499
	5.316	28.972	2	-				
	0.5125	3.153	3	0.077				
2	5.367	2.750	1	0.202	0.206	0.005	5.923	3.139
	5.316	28.990	2	-				
	0.5125	8.554	3	0.209				
3	5.367	0.340	1	0.025	0.026	0.001	0.770	0.125
	5.316	28.729	2	-				
	0.5125	1.136	3	0.028				
4	5.367	0.412	1	0.030	0.030	0.0009	0.885	0.220
	5.316	29.104	2	-				
	0.5125	1.2904	3	0.031				
5	5.316	28.201	2	-	1.158	0.049	33.296	20.877
	2.901	126.724	2	1.194				
	4.627	134.65	2	1.123				
6	5.316	28.881	2	-	0.693	0.001	19.925	14.346
	2.901	80.213	2	0.692				
	4.627	80.000	2	0.694				
7	5.316	27.459	2	-	0.057	0.004	1.661	0.285
	2.901	6.738	2	0.061				
	4.627	5.962	2	0.054				
8	5.316	28.396	2	-	0.108	0.015	3.109	0.208
	2.901	11.057	2	0.097				
	4.627	13.519	2	0.119				

*No. H. = number of hydrogen.

Table SM14. IS-^{1}HqNMR results of target metabolites found in *D. anacardii* extracts. Exp. 1- 4 for cytochalasin D and Exp. 5-10 for nitropropionic acid.

Exp.	ppm	Area	N. H	Metabolite per tube (mg)	Average (mg)	SD	Purity %	Metabolite /experiment (mg)
1	5.370	2.964	3	0.089	0.086	0.003	2.480	1.666
	5.316	23.782	2	-				
	0.513	0.937	1	0.084				
2	5.370	7.781	3	0.243	0.233	0.015	6.682	3.541
	5.316	22.756	2	-				
	0.513	2.371	1	0.222				
3	5.370	0.974	3	0.024	0.023	0.001	0.659	0.107
	5.316	28.890	2	-				
	0.513	0.297	1	0.022				
4	5.370	1.110	3	0.027	0.026	0.002	0.745	0.186
	5.316	29.164	2	-				
	0.513	0.340	1	0.025				
5	5.316	180.851	2	-	3.539	-	101.690	63.759
	2.901	28.669	2	3.539				
6	5.316	106.028	2	-	2.451		70.425	50.706
	2.901	24.270	2	2.451				
7	5.316	7.092	2	-	0.174	-	5.005	0.861
	2.901	22.841	2	0.174				
8	5.316	14.193	2	-	0.336	-	9.668	0.648
	2.901	23.665	2	0.336				

*No. H. = number of hydrogen.

Table SM15. ERETIC2-[1]HqNMR results of target metabolites found in *D. anacardii* extracts. Exp. 1- 4 for cytochalasin D and Exp. 5-10 for nitropropionic acid.

Exp.	ppm	N. H	Metabolite per tube (mg)	Average (mg)	SD	Purity %	Metabolite /experiment (mg)
1	-	-	-	-	-	-	-
2	-	-	-	-	-	-	-
3	-	-	-	-	-	-	-
4	-	-	-	-	-	-	-
5	5.316	2	-	3.539	-	77.347	48.497
	2.901	2	3.539				
6	5.316	2	-	2.451		41.316	29.748
	2.901	2	2.451				
7	5.316	2	-	0.174	-	5.9476	1.023
	2.901	2	0.174				
8	5.316	2	-	0.336	-	6.283	0.421
	2.901	2	0.336				

*No. H. = number of hydrogen.

[1]HqNMR Validation

Selectivity

All samples of *F. oxysporum* and *X. cubensis* showed at least one isolated signal on the ^{13}C-HSQC spectra, allowing the selective evaluation of compound concentration by manual integration (IS-[1]HqNMR) and Electronic Reference To access *In vivo* Concentrations 2 (ERETIC2) approaches. On the other hand, for *D. eres*, all quantified signals were overlapped and did not present the required selectivity, exhibiting over-adjusted quantification results on both comparative methods. Isolated peaks selected for IS-[1]HqNMR and ERETIC2-[1]HqNMR analysis for fusaric acid and cytochalasin D were δ 8.61 (*s*, 1H, H-6) and δ 5.92 (*dd*, *J* 2.5, 5.9 Hz, 1H, H-20), respectively.

For GSD-based [1]HNMR quantification strategy, regardless of the species, all metabolite signals were "selective" for quantification due to previous signal deconvolution, emerging as a more advantageous and attractive methodology in analysis of microbial complex matrices. All the samples of *F. oxysporum*, *D. eres* and *X. cubensis* from the DoE-experiments were submitted to ^{13}C-HSQC analysis and Figure S8 illustrates the samples that shows the most convoluted chemical shifts.

Figure SM19. ^{13}C HSQC NMR spectra from raw extract of (A) *F. oxysporum*; (B) *X. cubensis*; (C) *D. anacardii*.

(A)

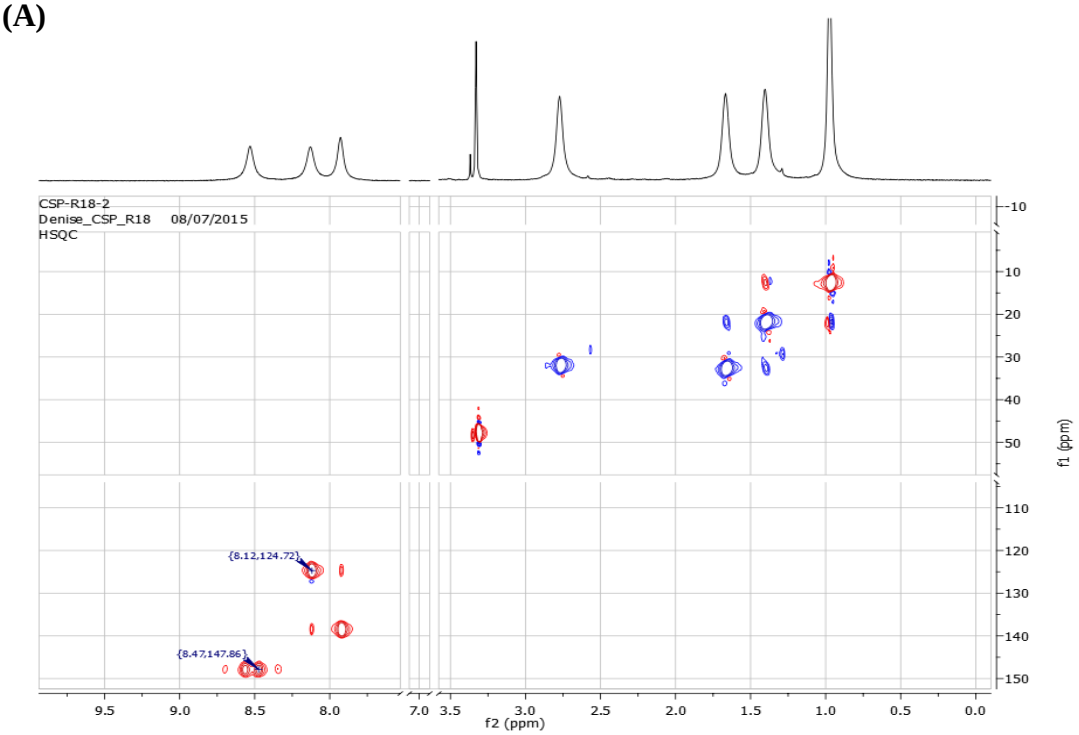

(B)

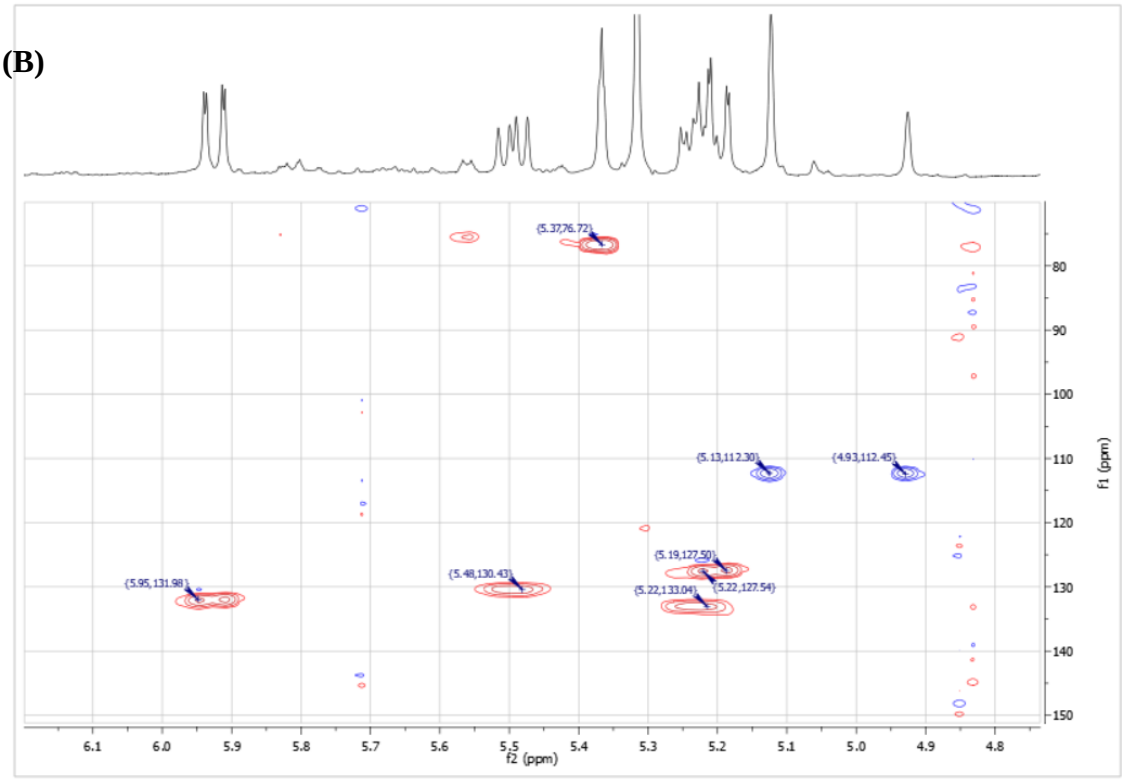

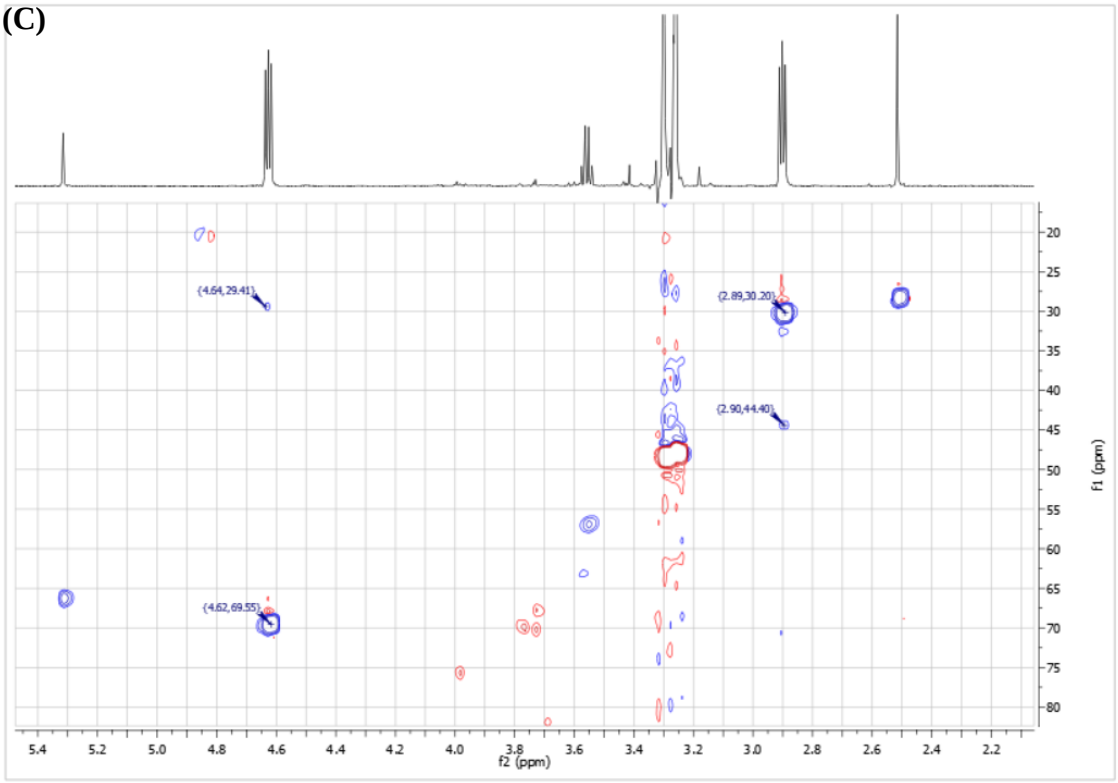

Stability

Stability measurements were performed by systematically repeating ^{1}HNMR acquisition every 2 hours, to determine loss by degradation. Acquisitions were performed with the least concentrated sample for each fungi (*F. oxysporum* Exp. 4, *X. cubensis* Exp. 6, *D. anacardii* Exp. 9) and the GSD-area values at δ 8.61 (*s*, 1H, H-6), δ 5.92 (*dd*, *J* 2.5, 5.9 Hz, 1H, H-20) and δ 2.90 (*t*, *J* 6.0 Hz, 2H, H-2), attributed to of fusaric acid, cytochalasin D and 3-NPA, were quantified by ^{1}HNMR.

Fusaric acid, cytochalasin D and 3-NPA were found to be stable for over 48 hours, demonstrating low differences in concentration (standard deviation of ± 0.02, 0.01 and 0.01 in the concentration values, respectively). The area values for each chemical shifts from the targeted metabolites in different times are displayed on Figure S9 of the Supplementary Material.

Precision

Precision was assessed by repetitive ^{1}HNMR acquisition of fusaric acid, cytochalasin D and nitropropionic acid in a short period of time, systematically changing operator, automation and time of day. Acquisitions were performed with the least concentrated sample for each fungi (*F. oxysporum* Exp. 4, *X. cubensis* Exp. 6, *D. anacardii* Exp. 9) and the GSD-area values at δ 8.61 (*s*, 1H, H-6), δ 5.92 (*dd*, *J* 2.5, 5.9 Hz, 1H, H-20) and δ 2.90 (*t*, *J* 6.0 Hz, 2H, H-2), attributed to of fusaric acid, cytochalasin D and 3-NPA, were quantified by ^{1}HNMR.

The concentration for each targeted metabolites display small overall differences and a standard deviation of ± 0.02, 0.02 and 0.01 mg for fusaric acid, cytochalasin D and

3-NPA, respectively. The area values for each chemical shifts from the targeted metabolites of all precision measurements are displayed on Figure S9 of the Supplementary Material

Figure SM20. Stability and precision measurements of target signals from ^{1}HNMR data of bioactive secondary metabolites.

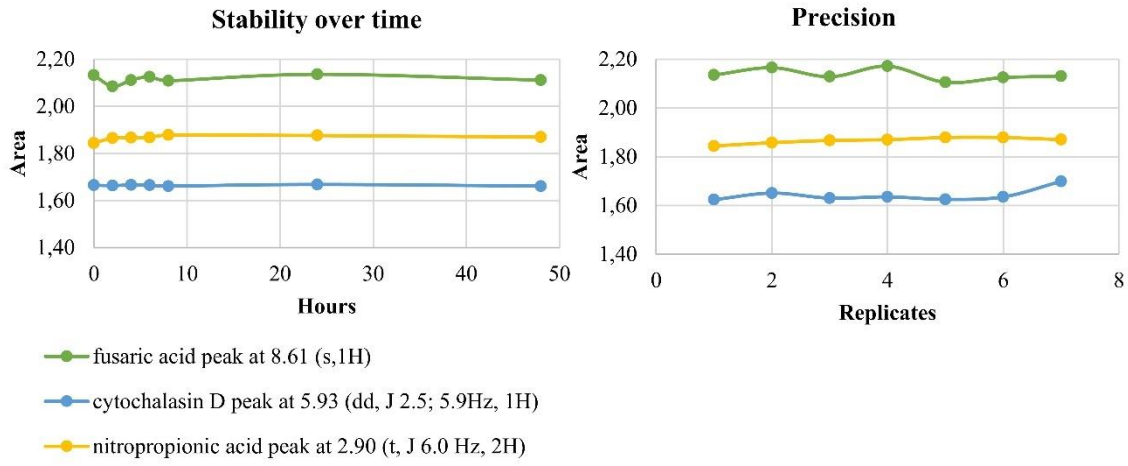

Limit of Detection (LoD)

Determination of S/N was performed by comparing quantified chemical shifts from the lowest concentration samples of each species with baseline intensity, targeting to establish LoD. All quantified peaks showed a S/N > 250 and a response within the quantification limits set on the calibration curve.

Accuracy

Accuracy was assessed by quantification of the chemical shift at δ 5.31 (*s*, 2H), from the internal standard benzyl benzoate, by different quantification methodologies. For this, we used standard samples of the IS (1, 2, 4, 10 and 20 m). The quantification methodologies used for comparison were gravimetric, ERETIC2-^{1}HqNMR, IS-^{1}HqNMR and GSD-based ^{1}HNMR quantification.

The strategies displayed low overall standard deviation (< ± 0.2 mg) for the signal area of benzyl benzoate at all quantified samples, as displayed on the Supplementary Material as Table S14.

Table SM16. Accuracy assay for internal standard ^{1}H-NMR peak; Comparison between Gravimetric, ERETIC2-^{1}HqNMR, classical ^{1}HqNMR and GSD-based ^{1}HNMR quantification.

Sample	Classical ^{1}H-qNMR	GSD-^{1}HqNMR	Gravimetric	ERETIC2-^{1}HqNMR	SD
Standard 1mM	0.956	0.832	1.00	1.201	0.152
Standard 2 mM	1.946	1.770	2.00	2.190	0.172
Standard 3 mM	4.201	3.866	4.00	4.229	0.172
Standard 10 mM	10.966	10.353	10.00	10.692	0.418
Standard 20 mM	20.466	20.040	20.00	20.384	0.237

Linearity of the calibration curves

A calibration curve was used to determine the linear response of the internal standard in a specific concentration range (1, 2, 4, 10 and 20 mM). The IS benzyl benzoate was prepared in triplicate for each selected concentration and acquired with optimized parameters. The chosen concentrations covered the working range of the method.

Linearity was evaluated by calculation of a regression line by the method of least squares. A correlation coefficient (R^2) of 0.9993 was determined, confirming highly linear behavior between peak integral and concentration, which means reliable estimation of the concentration across this range. The linear relation of the signal versus concentration is displayed on the Supplementary Material as Figure S10.

Figure SM21. Calibration curve of internal standard peak at δ5.316 (s, 2H).